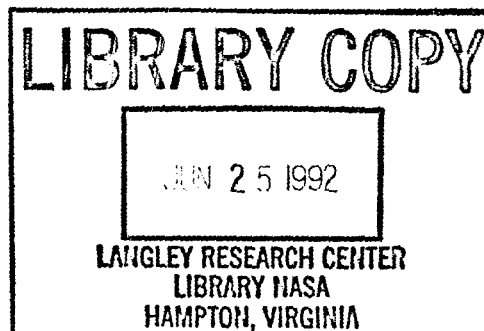


NASA-CR-177.8

NASA-CR-177855
19860014155

A Reproduced Copy

Reproduced for NASA
by the
Center for AeroSpace Information



3 1176 01355 6213

NASA CR-177855

CSC/TM-85/6119

NAVIGATION STUDY FOR LOW-ALTITUDE EARTH SATELLITES

(NASA-CR-177855) NAVIGATION STUDY FOR LOW-ALTITUDE EARTH SATELLITES (Computer Sciences Corp.) 171 p HC A08/MF A01

N86-23626

CSSL 22A

Unclas

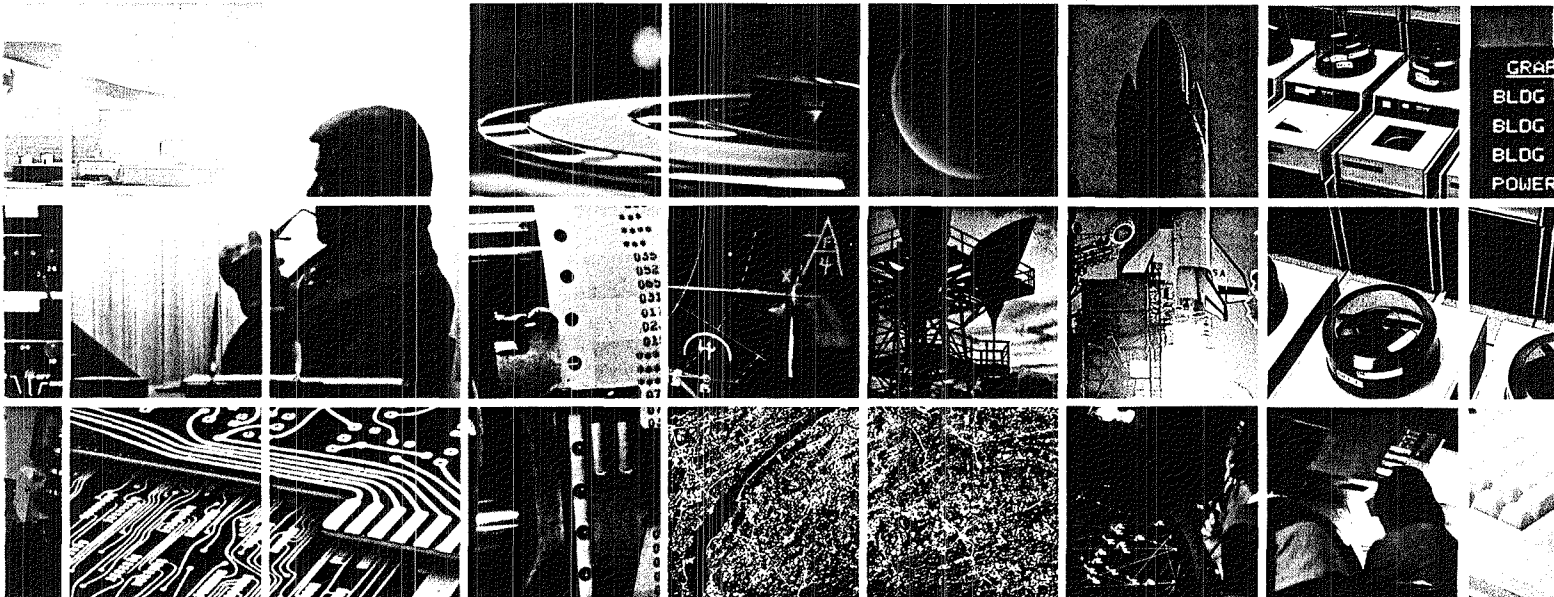
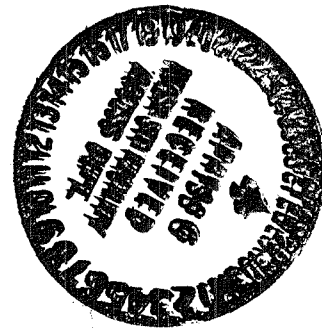
G3/18

09118

Prepared for
NATIONAL AERONAUTICS AND SPACE ADMINISTRATION
Goddard Space Flight Center
Greenbelt, Maryland

CONTRACT NAS 5-27888
Task Assignment 44500

DECEMBER 1985



CSC

COMPUTER SCIENCES CORPORATION

NAVIGATION STUDY FOR LOW-ALTITUDE EARTH SATELLITES

Prepared for
GODDARD SPACE FLIGHT CENTER

By
COMPUTER SCIENCES CORPORATION

Under
Contract NAS 5-27888
Task Assignment 44500

Prepared by:

PR Pastor 12/26/85
F. R. Pastor Date

E. T. Fang
C. P. Yee

Approved by:

Charles L Berry 12/26/85
C. Berry Date
Functional Area Manager

M. Plett for 12/27/85
M. Plett Date
Project Manager

This Page Intentionally Left Blank

ABSTRACT

This document describes several navigation studies for low-altitude Earth satellites. The use of Global Positioning System Navigation Package data for Landsat-5 orbit determination is evaluated. In addition, a navigation analysis for the proposed Tracking and Data Acquisition System is presented. This analysis, based on simulations employing one-way Doppler data, is used to determine the agreement between the Research and Development Goddard Trajectory Determination System and the Sequential Error Analysis Program results. Properties of several geopotential error models are studied as they apply to orbit navigation error analysis, and an exploratory study of orbit smoother process noise is presented.

PRECEDING PAGE BLANK NOT FILMED

PAGE _____ **INTENTIONALLY BLANK**

This Page Intentionally Left Blank

TABLE OF CONTENTS

<u>Section 1 - Introduction</u>	1-1
<u>Section 2 - Landsat-5 Orbit Determination Using GPSPAC</u> <u>Data</u>	2-1
2.1 Overview of Study Data.	2-2
2.2 Analysis of Landsat-5 GPSPAC Data Orbits.	2-3
2.3 Orbit Solutions Using Data From Single GPS Satellites.	2-7
2.4 Assessment of Landsat-5 Orbits Computed From GSTDN Data.	2-14
2.4.1 Comparison of Large Overlap Differences to Landsat-4 GSTDN Solutions	2-14
2.4.2 Analysis of Landsat-5 Larger-Than- Expected Overlap Ephemeris Differences.	2-17
2.4.3 Landsat-5 Solutions Involving Fewer Tracking Stations.	2-19
2.4.4 Analysis of Landsat-4 GSTDN Solutions With Reduced Number of Tracking Sta- tions.	2-21
2.5 Analysis of Possible Mismatches Between GLI and R&D GTDS.	2-27
2.6 Conclusions	2-34
2.7 References.	2-35
<u>Section 3 - Low-Altitude Satellite Navigation Using</u> <u>Simulated TDAS One-Way Doppler Data.</u>	3-1
3.1 Simulation Scenario	3-1
3.1.1 TDAS Configuration	3-1
3.1.2 User Satellite	3-3
3.1.3 Tracking Data.	3-3
3.2 Orbit Determination Scenario.	3-4
3.3 Simulation/Orbit Determination Error Results.	3-6
3.3.1 Geopotential Error	3-6
3.3.2 Clock Acceleration Error	3-11
3.3.3 TDAS Ephemeris Error	3-12
3.3.4 Error Results With Less Frequently Sampled Data	3-16
3.3.5 Comparison Between FLBT and FLST Tracking Modes	3-20

TABLE OF CONTENTS (Cont'd)

Section 3 (Cont'd)

3.4	Conclusions	3-20
3.5	References.	3-22

Section 4 - Lumped Geopotential Model for GEM-9. 4-1

4.1	The Lumped Error Model.	4-3
4.2	Global Distribution of Gravity Error for Dif- ferent Geopotential Error Models.	4-8
4.3	Navigation and Orbit Prediction Errors Intro- duced by Geopotential Uncertainty	4-32
4.4	Comparison With Landsat-5 Orbit Determination Results	4-33
4.5	Conclusions	4-35
4.6	References.	4-38

Section 5 - Orbit Smoother Process Noise Study 5-1

Section 6 - Conclusions. 6-1

Appendix A - Validation and Verification of the SEA
Smoother/TDAS Capability

Appendix B - Utilities for Geopotential Error Model
Studies

LIST OF ILLUSTRATIONS

Figure

2-1	Partial Observation Residual Report for GPSPAC Data Orbit Solution (Run G4B)	2-6
2-2	Representative Observation Residual Plots for GPSPAC Data Solutions Employing Com- posite and Single GPS Satellite Observa- tion Sets	2-13
2-3	Landsat-5 GSTDN Orbit Solution Overlap Ephemeris Comparison.	2-18
2-4	Plot of Ground Tracking Passes and Orbit Solution Arcs Involving April 1984 Landsat-5 GSTDN Data.	2-20
2-5	Plot of Ground Tracking Passes and Orbit Solution Arcs Involving October 1982 Landsat-4 GSTDN Data.	2-25
2-6	Ephemeris Comparison Between GPS Orbit (RUN G4A) Solutions With and Without Refer- ence Frame Mismatch Correction.	2-29
3-1	TDAS Configuration.	3-2
3-2	Geopotential (GEM-9/GEM-1 Difference Model) Error Projections in the User Orbit Plane as Determined From R&D GTDS FLBT Simula- tion.	3-8
3-3	User Clock Acceleration Error Projections in the User Orbit Plane as Determined From R&D GTDS FLBT Simulation.	3-13
3-4	TDAS Ephemeris Error Projections in the User Orbit Plane as Determined From R&D GTDS FLBT Simulation	3-17
4-1	Global Distribution of Gravitational Accelera- tion Uncertainties at an Altitude of 200 Kilometers, Computed From the Lumped Geo- potential Error Model Using GEM-9 Standard Deviations.	4-6
4-2	GEM-9/MD1 One-Half Difference Model, 200-Kilometer Altitude	4-10
4-3	GEM-9/MD1 One-Half Difference Model, 400-Kilometer Altitude	4-11
4-4	GEM-9/MD1 One-Half Difference Model, 600-Kilometer Altitude	4-12
4-5	GEM-9/SAO One-Half Difference Model, 200-Kilometer Altitude	4-13
4-6	GEM-9/SAO One-Half Difference Model, 400-Kilometer Altitude	4-14

LIST OF ILLUSTRATIONS (Cont'd)

Figure

4-7	GEM-9/SAO One-Half Difference Model, 600-Kilometer Altitude	4-15
4-8	GEM-9/GEM-5 Difference Model, 200-Kilometer Altitude	4-16
4-9	GEM-9/GEM-5 Difference Model, 400-Kilometer Altitude	4-17
4-10	GEM-9/GEM-5 Difference Model, 600-Kilometer Altitude	4-18
4-11	GEM-5/MD1 One-Half Difference Model, 200-Kilometer Altitude	4-19
4-12	GEM-5/MD1 One-Half Difference Model, 400-Kilometer Altitude	4-20
4-13	GEM-5/MD1 One-Half Difference Model, 600-Kilometer Altitude	4-21
4-14	GEM-9 Standard Deviation Model, 400-Kilometer Altitude	4-22
4-15	GEM-9 Standard Deviation Model, 600-Kilometer Altitude	4-23
4-16	GEM-9 Formal Uncertainties With Random Signs, 200-Kilometer Altitude.	4-24
4-17	GEM-9 Formal Uncertainties With Random Signs, 400-Kilometer Altitude.	4-25
4-18	GEM-9 Formal Uncertainties With Random Signs, 600-Kilometer Altitude.	4-26
4-19	GEM-9 Formal Uncertainties With Random Phase, 200-Kilometer Altitude.	4-27
4-20	GEM-9 Formal Uncertainties With Random Phase, 400-Kilometer Altitude.	4-28
4-21	GEM-9 Formal Uncertainties With Random Phase, 600-Kilometer Altitude.	4-29
4-22	GEM-9 Uncorrelated Standard Deviation Model, 200-Kilometer Altitude	4-30
4-23	Gravity Map at a 200-Kilometer Altitude for the Nonaxisymmetric Portion of GEM-9	4-31

LIST OF TABLES

Table

2-1	Landsat-5 GPSPAC Data Orbit Solution Characteristics and Comparisons With GSTDN Solutions	2-5
-----	---	-----

LIST OF TABLES (Cont'd)

Table

2-2	Landsat-5 GPSPAC Data Range-Rate and Evenly Weighted Orbit Solution Characteristics and Comparisons With GSTDN Solutions.	2-8
2-3	Characteristics of GPSPAC Data Solutions Using Observations From Single GPS Satellites	2-10
2-4	Intercomparisons of GPSPAC Data Solutions Using Single and Composite GPS Observation Sets.	2-11
2-5	1984 GSTDN Data Orbit Solution Characteristics.	2-15
2-6	1985 GSTDN Data Orbit Solution Characteristics.	2-16
2-7	Additional Landsat-5 GSTDN Data Orbit Solution Characteristics.	2-22
2-8	Summary of Landsat-4 GSTDN Solutions With Reduced Number of Tracking Stations	2-23
2-9	Reference Rotated GPSPAC Data Orbit Solution Characteristics and Comparisons With Non-rotated Solutions	2-32
3-1	Tracking Schedules for 600-Kilometer-Altitude, 28-Degree-Inclination User Satellite	3-5
3-2	Navigation Error Comparison Between R&D GTDS Simulation and Previous SEA Error Analysis Results	3-21
4-1	Navigation Errors Resulting From Geopotential Uncertainties.	4-34
5-1	Orbit Smoother Performance for the TDAS Navigation Scenario	5-2
5-2	Landsat-5 Orbit Smoother Error Caused by One-Half GEM-9/SAO Differences.	5-3

SECTION 1 - INTRODUCTION

This document describes several studies performed for the National Aeronautics and Space Administration/Goddard Space Flight Center (NASA/GSFC) relating to low-altitude Earth satellite navigation analysis. The first two studies analyzed the accuracy of satellite orbit determination using advanced navigation systems: the Global Positioning System (GPS), currently under development, and the Tracking and Data Acquisition System (TDAS), under study as a successor to the Tracking and Data Relay Satellite System (TDRSS). The latter two studies analyzed lumped geopotential modeling and orbit smoother process noise, two major components associated with orbit determination error analysis.

The GPS navigation study analyzed the orbit determination capabilities of the Landsat-5 (705-kilometer (km) altitude, 98-degree (deg) inclination) satellite. Landsat-5 uses navigation messages from GPS satellites that are extracted by an onboard Global Positioning System Navigation Package (GPSPAC). This study extended the effort of a previous analysis¹ that considered Landsat-4 GPSPAC data. The results of the Landsat-5 study and its comparison with the Landsat-4 study are presented in Section 2.

The TDAS navigation study, presented in Section 3, analyzed the performance of a 600-km, 28-deg inclination satellite using simulated TDAS one-way Doppler data. The study used a

¹B. T. Fang and E. Seifert, "An Evaluation of Global Positioning System Data for Landsat-4 Orbit Determination," paper delivered at AIAA 23rd Aerospace Science Meeting, January 1985; also Computer Sciences Corporation, CSC/TM-84/6077, Tracking and Data Acquisition System/Global Positioning System (TDAS/GPS) Navigation Analysis, September 1984.

number of TDAS enhancements that have been made to the Research and Development Goddard Trajectory Determination System (R&D GTDS). It served as a verification of a previous study that considered the same satellite scenario but used the TDAS enhanced Sequential Error Analysis (SEA) program.

The analysis of lumped geopotential modeling, presented in Section 4, studied several error models. All models use spherical-harmonic representations but with different sets of coefficients representing the errors. Global gravity error maps and orbit propagation errors corresponding to different error models are presented.

The orbit_smoother process noise study investigated the new smoother capacity to the SEA program. Limited investigations using this capacity have been performed to further explore orbit smoothers and also to validate the fading memory process noise option of the SEA smoother capability. The results of this study are presented in Section 5.

Appendix A describes the validation of the SEA program smoother/TDAS capability used in the orbit smoother process noise study. Appendix B describes utilities used in conjunction with the lumped geopotential error model study.

SECTION 2 - LANDSAT-5 ORBIT DETERMINATION USING GPSPAC DATA

This section discusses the accuracies of GPSPAC data for computing Landsat-5 orbits. The GPSPAC data were extracted from telemetry and processed by a large, sophisticated, batch orbit determination program (R&D GTDS) to produce 16-hour arc orbit solutions. The accuracies of the GPSPAC data and the orbit solutions were inferred from the following:

- Observation residuals
- Overlap ephemeris comparisons
- Comparisons with independent solutions derived from ground tracking data

As with the Landsat-4 GPSPAC data, it was found that pseudorange data appear inferior to delta pseudorange (Doppler) data. Efforts were made to determine whether pseudorange data are corrupted by several possible preprocessing sources of errors or whether data from individual GPS satellites may be defective. The latter effort involved computing Landsat-5 orbits from data from a single GPS satellite and was also a subject of interest by itself.

Section 2.1 presents an overview of the data studied and the orbit determination scenarios used. Section 2.2 describes Landsat-5 orbit solutions computed from GPSPAC data; Section 2.3, solutions based on data originating from single GPS satellites; and Section 2.4, solutions obtained from ground tracking data and inquiries into their accuracy degradation in comparison with Landsat-4 solutions. Section 2.5 investigates several possible sources of preprocessing errors and Section 2.6 summarizes the conclusions of the study.

2.1 OVERVIEW OF STUDY DATA

The Landsat-4 spacecraft (705-km altitude, 98-deg inclination orbit), launched in July 1982, carried an experimental NAVSTAR (Reference 2-1) GPSPAC and was the first satellite to use the GPS. The GPSPAC has a receiver/processor assembly that receives and decodes GPS tracking measurements and estimates the Landsat-4 position and velocity by using an onboard Kalman filter. The tracking measurements provided by GPSPAC are called pseudoranges and delta-pseudoranges. The former are decoded from pseudorandom noise ranging code and represent measured signal transit times from the GPS satellites to Landsat-4. The latter are computed from Doppler shifts of carrier signals, integrated over a nominal interval of 0.6 second. The term "pseudo" is used because these measurements were derived from the Landsat clock, which was not synchronized with the GPS clocks. The quoted precisions of these data are 1.5 meters (m) for the pseudorange and 2 centimeters (cm) for the delta pseudorange.

Landsat-5, launched in July 1984, is a replacement for the disabled Landsat-4 spacecraft. It has similar mission objectives and orbit characteristics. It also carries a GPSPAC with minor software modifications to avoid some known anomalies (Reference 2-2) that occurred in the Landsat-4 GPSPAC.

During the previous task assignment (42100), an investigation of the Landsat-4 GPSPAC data quality (Reference 2-3) was undertaken. The present study extended that effort to Landsat-5 GPSPAC data. As in the Landsat-4 study, the R&D GTDS batch orbit determination differential correction (DC) program was used to process both the GPSPAC telemetry to the ground and Ground Spaceflight Tracking and Data Network

(GSTDN) data. R&D GTDS allows extensive force modeling that is unavailable in the onboard GPSPAC Kalman filter.

The data in this study were obtained over four separate time periods: in April and August of 1984, and in May and July of 1985. The baseline force model and the orbit determination scenario used for the GSTDN and GPSPAC data solutions are as follows:

<u>GPSPAC data solutions</u>	<u>GSTDN data solutions</u>
21-by-21 Goddard Earth Model (GEM)-9 geopotential model	21-by-21 GEM-9 geopotential model
Jacchia-Roberts atmospheric density model	Jacchia-Roberts atmospheric density model
Cowell integrator	Cowell integrator
16-hour data arc length	30-hour data arc length
Solve for orbital elements, drag parameter, clock bias, clock drift	Solve for orbital elements, drag parameter
Select every 10th pair of observations	Select all observations
Use observation standard deviations = 1000 m (pseudorange) and 0.8 cm (δ pseudorange)	Use range-rate observations only for orbit solution

2.2 ANALYSIS OF LANDSAT-5 GPSPAC DATA ORBITS

Eight 16-hour data arcs using the NAVSTAR system's GPS data, as received by Landsat-5 GPSPAC, were processed with the R&D GTDS DC program and the same baseline force model employed in analyzing the Landsat-4 GPSPAC orbits. (These orbits will henceforth be referred to as the baseline set of GPSPAC data orbits.) As will be discussed in Section 2.4, the Landsat-5 GSTDN solutions displayed ephemeris overlap differences consistently larger than those observed for Landsat-4. In comparison, the Landsat-4 GSTDN solutions displayed enough accuracy to be used as definitive solutions. Because of this degradation, the Landsat-5 GSTDN

orbits could not be used as definitive solutions for comparison with corresponding GPSPAC solutions. Therefore, the present Landsat-5 analysis used the comparison among overlapping GPSPAC data orbit ephemerides and observation residuals to provide an idea of the GPSPAC accuracies.

The maximum ephemeris position differences for the four Landsat-5 GPSPAC data overlap periods vary from 64 to 19 m, compared to maxima with an average of 28 m, and a standard deviation of 14 m for six Landsat-4 GPSPAC overlap periods. As shown in Table 2-1, the 1984 GPSPAC overlap comparisons of 61 and 64 m are larger than the 1985 GPSPAC overlap comparisons of 19 and 32 m. (It is interesting to note that studied GPSPAC data solutions in 1985 involve six GPS satellites whereas those in 1984 involve five; nonetheless, reference to GPSPAC data solutions by the year of observation is for convenience only.) The improvement in the overlap comparisons for the 1985 GPSPAC data solutions, but no improvement in the corresponding 1985 GSTDN data (which is summarized in Section 2.4), appears to rule out the possibility that some unexplained dynamic errors common to GSTDN and GPSPAC data solutions are responsible for poor 1984 GPSPAC comparisons.

An examination of data residuals of the Landsat-5 GPSPAC orbit solutions shows that large pseudorange measurement residuals exist and vary substantially from GPS satellite to GPS satellite. These characteristics are in agreement with those observed in the Landsat-4 GPSPAC data solutions. Figure 2-1, which is a partial listing of a typical Landsat-5 GPSPAC observation residual report illustrating the large pseudorange residuals, displays no correlation between pseudorange residuals and delta-pseudorange measurements. This rules out systematic time tag errors as possible sources for the systematic GPSPAC range errors observed.

Table 2-1. Landsat-5 GPSPAC Data Orbit Solution Characteristics and Comparisons With GSTDN Solutions

RUN ID	ARC START TIME (date hour)	ARC LENGTH (hours)	NO OF OBSERVATIONS	SOLVE FOR PARAMETERS			RESIDUAL STATISTICS STANDARD DEVIATIONS		MAXIMUM POSITION DIFFERENCES OVER 4 HOUR OVERLAP OF ADJACENT ARCS (meters)				MAXIMUM POSITION DIFFERENCES FROM GSTDN ORBITS (meters)				REMARKS	
				e_1	B (10 ⁻³ sec)	\dot{B} (10 ⁻⁸ sec/sec)	RANGE (meters)	DELTA RANGE (cm)	RADIAL	C	ALONG TRACK	RSS	RADIAL	C	ALONG TRACK	RSS		
G4A	840413 2 h	16	1297	1 592	-3 127	-3 262	100 1	2 39										ONLY EVERY 10TH PAIR OF OBSERVATION DATA PROCESSED
G4B	840413 14 h	16	1192	2 900	-4 772	-3 257	71 50	2 27	5 69	14 4	61 0	61 3	13 4	30 6	45 1	54 3		
G8A	840807 3 h	16	1103	2 125	1 036	-2 283	84 25	2 25										
G8B	840807 15 h	16	1110	3 011	-0 197	-2 278	83 02	2 38	16 6	7 6	63 8	63 9	14 0	16 9	49 1	50 4		
G5A	850524 19 h	16	1190	4 913	-2 228	-0 6494	76 44	2 21										
G5B	850525 7 h	16	1146	-6 119	-2 508	-0 6467	66 33	2 19	4 94	7 67	17 9	19 4	13 5	11 9	52 2	53 3		
G7A	850726 0 h	16	1142	2 493	-0 6720	-0 3611	84 39	2 18										
G7B	850726 12 h	16	1000	-2 259	-0 8280	-0 3571	53 93	2 18	5 08	19 4	29 5	32 1	-	-	-	-		

2-5

0112 (76a*)/85

NOTES SATELLITE AND TIME PERIOD LANDSAT 5 APRIL 1984 - JULY 1985
 DATA GPS RANGE AND DELTA RANGE WITH RANGE WEIGHTED LIGHTLY
 FORCE MODEL BASELINE
 SOLVE FOR PARAMETERS DRAG SCALE FACTOR $e_1 = \Delta C_D / C_D$, CLOCK BIAS B AND DRIFT \dot{B} AT EPOCH
 C L AND RSS ARE THE ACROSS TRACK ALONG TRACK AND ROOT SUM SQUARED COMPARE DIFFERENCES RESPECTIVELY

GTDS DC PROGRAM
GIDS OBSERVATION RESIDUAL REPORT

TIME OF OBS				GPS NO	EDIT	OBS TYPE	END OF ITERATION NUMBER		5 RATIO TO SIGMA	C	ELV TO GPS	T A	OBS NO		
YYMMDD	HHMM	SS	SSSS				O	O-C							
840414	0335	31	3291	3		RGPS	20555	9966	57 7255	0 0577	20555	9389	26 47	0 0	1099
840414	0335	31	3291	3		DELR	0	1936	0 4729	0 5911	0	1936	26 47	0 0	1100
840414	0336	50	6492	3		RGPS	20608	7939	56 0749	0 0561	20608	7379	25 89	0 0	1101
840414	0336	50	6492	3		DELR	0	6073	0 5600	0 7000	0	6073	25 88	0 0	1102
840414	0337	56	6295	3		RGPS	20694	0352	56 7501	0 0568	20693	9784	24 99	0 0	1103
840414	0337	56	6295	3		DELR	0	9446	-0 8825	1 1031	0	9447	24 98	0 0	1104
840414	0339	11	4100	3		RGPS	20834	7875	54 9823	0 0550	20834	7325	23 54	0 0	1105
840414	0339	11	4100	3		DELR	1	3144	2 2863	2 8579	1	3144	23 53	0 0	1106
840414	0340	45	4795	2		RGPS	23799	3095	47 8019	0 0478	23799	2617	-1 31	0 0	1107
840414	0340	45	4795	2		DELR	4	3860	-1 3533	1 6916	4	3860	-1 34	0 0	1108
840414	0342	32	4520	3		RGPS	21428	8755	53 5017	0 0535	21428	8220	17 76	0 0	1109
840414	0342	32	4520	3		DELR	2	2053	-4 5615	5 7018	2	2053	17 74	0 0	1110
840414	0344	02	3532	3		RGPS	21784	7896	50 3040	0 0503	21784	7393	14 48	0 0	1111
840414	0344	02	3532	3		DELR	2	5404	-2 4399	3 0499	2	5404	14 45	0 0	1112
840414	0345	24	4544	3		RGPS	22150	9298	48 9816	0 0490	22150	8808	11 21	0 0	1113
840414	0345	24	4544	3		DELR	2	8066	-1 5124	1 8906	2	8066	11 18	0 0	1114
840414	0347	27	2582	4		RGPS	23359	5568	83 6347	0 0836	23359	4731	2 07	0 0	1115
840414	0347	27	2582	4		DELR	-3	0905	3 0651	3 8314	-3	0906	2 10	0 0	1116
840414	0348	47	4369	4		RGPS	22950	2739	85 5167	0 0855	22950	1884	5 46	0 0	1117
840414	0348	47	4369	4		DELR	-3	0316	-0 6679	0 8349	-3	0315	5 48	0 0	1118
840414	0350	08	2155	4		RGPS	22547	0940	85 9179	0 0859	22547	0081	8 86	0 0	1119
840414	0350	08	2155	4		DELR	-2	9541	4 6284	5 7855	-2	9542	8 89	0 0	1120
840414	0351	27	7209	3		RGPS	24098	2891	50 5839	0 0506	24098	2386	-4 98	0 0	1121
840414	0351	27	7209	3		DELR	3	4928	3 1373	3 9216	3	4928	-5 01	0 0	1122
840414	0352	53	9826	3		RGPS	24604	2494	51 4064	0 0514	24604	1980	-8 99	0 0	1123
840414	0352	53	9826	3		DELR	3	5391	1 8366	2 2958	3	5390	-9 02	0 0	1124
840414	0354	27	2715	4		RGPS	21344	9189	98 8276	0 0988	21344	8200	1 65	0 0	1125
840414	0354	27	2715	4		DELR	-2	5820	5 2484	6 5605	-2	5820	19 68	0 0	1126
840414	0355	33	2106	4		RGPS	21067	8473	105 3006	0 1053	21067	7472	22 32	0 0	1127
840414	0355	33	2106	4		DELR	-2	4572	1 9778	2 4722	-2	4572	22 34	0 0	1128
840414	0356	51	0495	4		RGPS	20759	3714	107 9952	0 1080	20759	2634	25 39	0 0	1129
840414	0356	51	0495	4		DELR	-2	2944	0 0562	0 0703	-2	2944	25 41	0 0	1130
840414	0357	58	3687	4		RGPS	20510	3762	108 7452	0 1087	20510	2674	27 97	0 0	1131
840414	0357	58	3687	4		DELR	-2	1406	4 0504	5 0629	-2	1407	27 99	0 0	1132
840414	0359	04	3080	4		RGPS	20283	8295	111 2355	0 1112	20283	7183	30 39	0 0	1133
840414	0359	04	3080	4		DELR	-1	9789	-0 1794	0 2243	-1	9789	30 41	0 0	1134
840414	0400	10	2473	4		RGPS	20075	8410	113 8694	0 1139	20075	5272	32 70	0 0	1135
840414	0400	10	2473	4		DELR	-1	8066	1 8112	2 2640	-1	8066	32 72	0 0	1136
840414	0401	16	2066	4		RGPS	19886	8684	112 9890	0 1130	19886	7554	34 88	0 0	1137
840414	0401	16	2066	4		DELR	-1	6245	-1 4928	1 8660	-1	6245	34 90	0 0	1138
840414	0402	35	4460	4		RGPS	19687	3051	114 0285	0 1140	19687	1911	37 26	0 0	1139
840414	0402	35	4460	4		DELR	-1	3939	1 7330	2 1662	-1	3939	37 28	0 0	1140
840414	0403	41	4255	4		RGPS	19544	8821	114 2552	0 1143	19544	7679	39 03	0 0	1141
840414	0403	41	4255	4		DELR	-1	1933	0 3029	0 3787	-1	1933	39 05	0 0	1142
840414	0404	47	3651	4		RGPS	19424	9645	119 1568	0 1192	19424	8453	40 57	0 0	1143
840414	0404	47	3651	4		DELR	-0	9862	1 3532	1 6915	-0	9862	40 58	0 0	1144
840414	0405	53	3248	4		RGPS	19328	0879	113 9587	0 1140	19328	9740	41 84	0 0	1145
840414	0405	53	3248	4		DELR	-0	7735	-0 7324	0 9154	-0	7735	41 85	0 0	1146
840414	0407	12	6445	4		RGPS	19242	9191	114 6570	0 1147	19242	8044	42 99	0 0	1147
840414	0407	12	6445	4		DELR	-0	5122	1 3105	1 6381	-0	5122	43 00	0 0	1148
840414	0408	18	6243	4		RGPS	19198	5680	114 0210	0 1140	19198	4540	43 61	0 0	1149
840414	0408	18	6243	4		DELR	-0	2921	0 6002	0 7503	-0	2921	43 61	0 0	1150
840414	0409	24	5443	4		RGPS	19178	5132	114 8783	0 1149	19178	3984	43 89	0 0	1151
840414	0409	24	5443	4		DELR	-0	0710	-1 7220	2 1525	-0	0709	43 89	0 0	1152
840414	0410	30	4643	4		RGPS	19182	7473	115 0050	0 1150	19182	6323	43 84	0 0	1153
840414	0410	30	4643	4		DELR	0	1498	-3 2074	4 0092	0	1499	43 84	0 0	1154
840414	0411	44	4827	5	...	RGPS	24689	3524	135 7784	0 1358	24689	2167	43 84	0 0	1155
840414	0411	44	4827	5	...	DELR	-3	8457	1 5200	1 9000	-3	8457	43 84	0 0	1156
840414	0413	50	2200	5		RGPS	23878	5729	137 8933	0 1379	23878	4350	0 37	0 0	1157
840414	0413	50	2200	5		DELR	-3	8836	0 7933	0 9917	-3	8836	0 40	0 0	1158
840414	0415	41	0254	4		RGPS	19525	7211	109 6832	0 1097	19525	6115	39 35	0 0	1159

ORIGINAL PAGE IS OF POOR QUALITY

2-6

OBSERVATIONS AND COMPUTED OBS

RANGES ARE IN KM
RATES AND RANGE DIFFERENCES ARE IN KM/SEC
ANGLES ARE IN DEGREES
DIR COSINES SCALED BY 1000
DTIC ARE IN MICROSECONDS

UNITS FOR INFORMATION RESIDUALS

RANGES ARE IN METERS
RATES AND RANGE DIFFRN ARE IN CM/SEC
ANGLES ARE IN SECONDS OF ARC
DIR COSINES SCALED BY 1000
DTIC ARE IN MICROSECONDS

EDIT FLAG

* = COMPUTE (O-C) (NOT IN NORMAL MATRIX)
... = EDIT BY ELEVATION ANGLE
... = EDIT BY 3 SIGMA CRITERIA
... = EDIT FROM SCOPE
\$ = EDIT BY ATMOSPHERIC INTERFERENCE

Figure 2-1. Partial Observation Residual Report for GPSPAC Data Orbit Solution (Run G4B)

Studies (discussed more fully in Section 2.5) that examine the effects of correcting assumed GPSPAC time tag errors give results that support this conclusion about no time tag errors. GPSPAC data observation residuals will be discussed further in Section 2.3.

In keeping with the methods employed in the Landsat-4 GPSPAC analysis, the baseline GPSPAC data orbit determination scenario was repeated with two different a priori observation weight specifications. When the weights were set to 10 m for pseudorange observations and 1000 cm for delta-pseudorange observations (effectively producing a range-only solution), the orbit comparison with the independent GSTDN data orbit produced larger differences than those seen in the baseline delta-range-only solutions in Table 2-1. When the weights were set to 1.5 m and 0.2 cm, respectively (in accordance with quoted data precision), the orbit solutions resulted in larger overlap differences than the baseline delta-range-only solutions but were typically smaller than the corresponding range-only solution. These trends in the variously weighted Landsat-5 GPSPAC solutions are in agreement with the trends observed in the Landsat-4 data. Table 2-2 summarizes the Landsat-5 results.

2.3 ORBIT SOLUTIONS USING DATA FROM SINGLE GPS SATELLITES

As discussed in Section 2.2, the observed large pseudorange residuals present in the GPSPAC data solutions do not appear to be specific to any single GPS satellite. Nevertheless, there was interest in whether intercomparisons of GPSPAC solutions, each using data from only a single GPS NAVSTAR satellite, would divulge erratic data associated with a GPS or would provide insight into the cause of the observed large pseudorange residuals. It was uncertain whether single GPS relay solutions would even converge because of the lack of

Table 2-2. Landsat-5 GPSPAC Data Range-Rate and Evenly Weighted Orbit Solution Characteristics and Comparisons With GSTDN Solutions

RUN ID	ARC START TIME (date, hour)	ARC LENGTH (hours)	NO OF OBSERVATIONS	SOLVE FOR PARAMETERS			RESIDUAL STATISTICS, STANDARD DEVIATIONS		MAXIMUM POSITION DIFFERENCES OVER 4 HOUR OVERLAP OF ADJACENT ARCS (meters)				MAXIMUM POSITION DIFFERENCES FROM GSTDN ORBITS (meters)				REMARKS
				e_1	B (10 ⁻³ sec)	\dot{B} (10 ⁻⁸ sec/sec)	RANGE (meters)	DELTA RANGE (cm)	RADIAL	C	ALONG TRACK	RSS	RADIAL	C	ALONG TRACK	RSS	
R4A	840413 2 h	16	1295	-0 209	-3 128	-3 261	41 85	2 66	7 2	18	48	51	25	25	70	73	RANGE SOLUTION ONLY EVERY 10TH PAIR OF OBSERVATION DATA PROCESSED
R4B	840413 14 h	16	1191	1 316	-4 772	-3 256	50 35	2 80					30	13	112	113	
R8A	840807 3 h	16	1102	19 757	1 036	-2 283	64 52	3 23	45	23	171	172	43	15	133	134	
R8B	840807 15 h	16	1109	15 56	-0 197	-2 278	68 52	3 12					31	16	99	101	
P4A	840413 2 h	16	1278	-0 867	-3 128	-3 261	36 79	2 62	2 9	14	36	39	24	28	64	68	EVENLY WEIGHTED SOLUTION ONLY EVERY 10TH PAIR OF OBSERVATION DATA PROCESSED
P4B	840413 14 h	16	1183	0 969	-4 772	-3 256	48 01	2 62					26	18	101	103	
P8A	840807 3 h	16	665	67 56	1 035	-2 283	55 26	3 08	48	24	177	178	49	33	188	191	
P8B	840807 15 h	16	1103	36 79	-0 197	-2 277	63 93	3 13					32	21	122	125	

NOTES SATELLITE AND TIME PERIOD LANDSAT 5 APRIL - AUGUST 1984
FORCE MODEL BASELINE

SOLVE FOR PARAMETERS DRAG SCALE FACTOR $e_1 = \Delta C_D / C_D$ CLOCK BIAS B AND DRIFT \dot{B} AT EPOCH
C L AND RSS ARE THE ACROSS TRACK ALONG TRACK AND ROOT SUM SQUARED COMPARE DIFFERENCES RESPECTIVELY

sufficient geometry. First, all observations, except for those associated with the requested GPS satellite, were edited from the GPSPAC data. Next, the resulting single GPS satellite data were input into an unmodified R&D GTDS run to process GPSPAC data. These single relay orbit solutions--except as otherwise specified--used the same dynamics, modeling, etc., employed in the corresponding composite relay solutions.

Contrary to geometrical considerations, the single GPS satellite solutions displayed robustness in their ability to recover the clock parameters and to converge using very short observation arcs. The single GPS solutions can converge in as little as two Landsat orbital periods provided that the observation timespan's placement is chosen so as to minimize GPS-Landsat nonvisibility periods. Also, the single GPS satellite solutions, even those of short duration, can recover the clock parameters (clock bias and drift) when no a priori information is provided. Table 2-3 summarizes the characteristics of several single GPS satellite GPSPAC data solutions.

Recovery of the clock parameters to a high degree of agreement, together with the single relay solution's ability to converge even with no a priori clock information, indicates that the clocks in the GPSPAC data are highly observable. This high clock observability provides the ability to resolve small variations in the clock parameters. This clock variability is evident, in Table 2-3, between range and delta-range solutions over the same observation timespan. The clock parameters can be expressed in terms of their resulting corrections to pseudorange measurements to yield an effective range offset. Using this technique, the variability of the observed clock for the ensemble of single GPS satellite solutions over the same observation timespan is presented in Table 2-4.

Table 2-3. Characteristics of GPSPAC Data Solutions Using Observations From Single GPS Satellites

RUN ^a ID	OBSERVATIONS FROM GPS SATELLITE NO	ARC LENGTH (hours)	NO OF OBSERVA- TIONS	RESIDUAL STATISTICS, STANDARD DEVIATIONS		SOLVE-FOR PARAMETERS			COMMENTS ON RUN ^b
				RANGE (meters)	DELTA RANGE (cm)	e_1	B (10^{-3} sec)	\dot{B} (10^{-8} sec/ sec)	
G42A	2	3	577	2 35	2 01	-0 290	-3 1277	-3 2631	COMBINED SOLUTION
G42B	2	3	577	2 35	2 01	-0 290	-3 1277	-3 2631	COMBINED SOLUTION, ZERO A PRIORI CLOCK PARAMETERS
G43A	3	2 5	430	41 86	2 01	0 001	-3 1276	-3 2640	DELTA-RANGE SOLUTION
G43B	3	2 5	423	1 53	2 02	-0 145	-3 1280	-3 2606	COMBINED SOLUTION
G43C	3	3	592	12 91	2 80	0 007	-3 1269	-3 2668	RANGE SOLUTION
G43D	3	3	592	24 34	2 09	-0 003	-3 1279	-3 2615	DELTA-RANGE SOLUTION
G43E	3	3	585	2 12	2 11	0 557	-3 1276	-3 2631	COMBINED SOLUTION
G43F	3	3	585	2 12	2 11	0 557	-3 1276	-3 2631	COMBINED SOLUTION, ZERO A PRIORI CLOCK PARAMETERS

NOTES SATELLITE AND TIME PERIOD LANDSAT-5, APRIL 1984
 DATA ALL AVAILABLE PAIRS OF OBSERVATIONS PROCESSED
 FORCE MODEL BASELINE
 SOLVE-FOR PARAMETERS DRAG SCALE FACTOR $e_1 = \Delta C_D / C_D$, CLOCK BIAS B, AND DRIFT \dot{B} AT EPOCH

^aALL SOLUTION ARC TIMES START ON 840413, 2 HOURS

^bALL SOLUTIONS INVOLVE PAIRS OF GPS RANGE AND DELTA-RANGE OBSERVATIONS IN COMBINED SOLUTIONS, BOTH DATA TYPES HAVE COMPARABLE WEIGHTINGS IN DELTA-RANGE SOLUTIONS, RANGE IS WEIGHTED LIGHTLY, IN RANGE SOLUTIONS, DELTA-RANGE IS WEIGHTED LIGHTLY

2-10

Table 2-4. Intercomparisons of GPSPAC Data Solutions Using Single and Composite GPS Observation Sets

RUN ^a ID	OBSERVATIONS FROM GPS SATELLITE NO	NO OF OBSERVA- TIONS ^b	RESIDUAL STATISTICS, STANDARD DEVIATIONS		SOLVE-FOR PARAMETERS			RANGE EQUIVALENT CLOCK DIFFERENCE ^c FROM COMPOSITE ^c (meters)
			RANGE (meters)	DELTA RANGE (cm)	ρ_1	B (10^{-3} sec)	\dot{B} (10^{-8} sec/ sec)	
G4A	ALL GPSs-COMPOSITE	1297	100 1	2 39	1 591	-3 12752	-3 26234	-
G41	1	2650	67 0	2 20	-3 280	-3 12855	-3 25963	76
G42	2	2446	152 6	2 20	0 487	-3 12708	-3 26375	-10
G43	3	2581	185 3	2 27	1 621	-3 12681	-3 26434	-38
G44	4	3000	180 4	2 49	9 872	-3 12924	-3 25785	130
G45	5	2080	55 4	2 29	-0 331	-3 12828	-3 26020	45

NOTES SATELLITE AND TIME PERIOD LANDSAT-5, APRIL 1984

DATA GPS RANGE AND DELTA-RANGE, WITH RANGE WEIGHTED LIGHTLY

FORCE MODEL BASELINE

SOLVE-FOR PARAMETERS DRAG SCALE FACTOR $\rho_1 = \Delta C_D / C_D$, CLOCK BIAS B, AND DRIFT \dot{B} AT EPOCH

^aALL SOLUTIONS HAVE DATA ARC LENGTHS OF 16 HOURS STARTING ON 840413, 2 HOURS

^bFOR COMPOSITE SOLUTION, ONLY EVERY 10TH PAIR OF OBSERVATION DATA IS PROCESSED, FOR SINGLE GPS SATELLITE SOLUTIONS, ALL PAIRS OF OBSERVATION DATA ARE PROCESSED

^cTHIS VALUE IS THE DIFFERENCE BETWEEN THE RANGE EQUIVALENT CLOCK ERROR FOR RUN ID G4A AND THE RANGE EQUIVALENT CLOCK ERROR FOR THE GPS SATELLITE SOLUTION CORRESPONDING TO THE TABLE ENTRY THE RANGE EQUIVALENT OF CLOCK ERROR IS CALCULATED AS $\delta R = (B + \dot{B} \Delta t) C$, WHERE Δt IS CHOSEN AS HALF THE SOLUTION ARC LENGTH, OR 8 HOURS, AND C IS THE SPEED OF LIGHT

Possibly related to the observed clock variations are characteristic gross structure signatures of the pseudorange residual in the GPSPAC solution plots. The typical pseudorange residual plots can be fit fairly well with a linear, nonzero slope function. This is most pronounced in single GPS satellite solutions but is also present in composite GPS solutions. Representative pseudorange residual plots for both single GPS satellite and composite GPS solutions are shown in Figure 2-2. One possible interpretation of the nonzero slope structure in the pseudorange residuals is that an inconsistency occurs in the observed clock drift rate between the pseudorange and delta-pseudorange GPSPAC data measurements.

In the search for information pertaining to the anomalous large pseudorange residuals, the inconsistency between pseudorange and delta-pseudorange measurements was rediscovered. This was previously discussed in connection with comparisons of GPSPAC data delta-range solutions to range solutions. In those instances, the inconsistency was most notable in the Landsat-4 analysis, when the delta-range solutions gave better comparison with GSTDN solutions than the corresponding range or evenly weighted solutions. In its present manifestation, the inconsistency can be interpreted as a mismatch between the observed clock parameters for delta pseudorange and pseudorange data. Alternately, the inconsistencies could be attributed to uncorrected signal propagation errors or difficulties with electronics.

Finally, intercomparisons between single GPS satellite solutions and between single satellite and composite solutions did not reveal any highly erratic single GPS satellite. All single satellite solutions agree within a maximum of ~ 80 m, and typically less than ~ 40 m. When observations corresponding to that GPS satellite for which single GPS satellite solution intercomparisons show the largest deviations

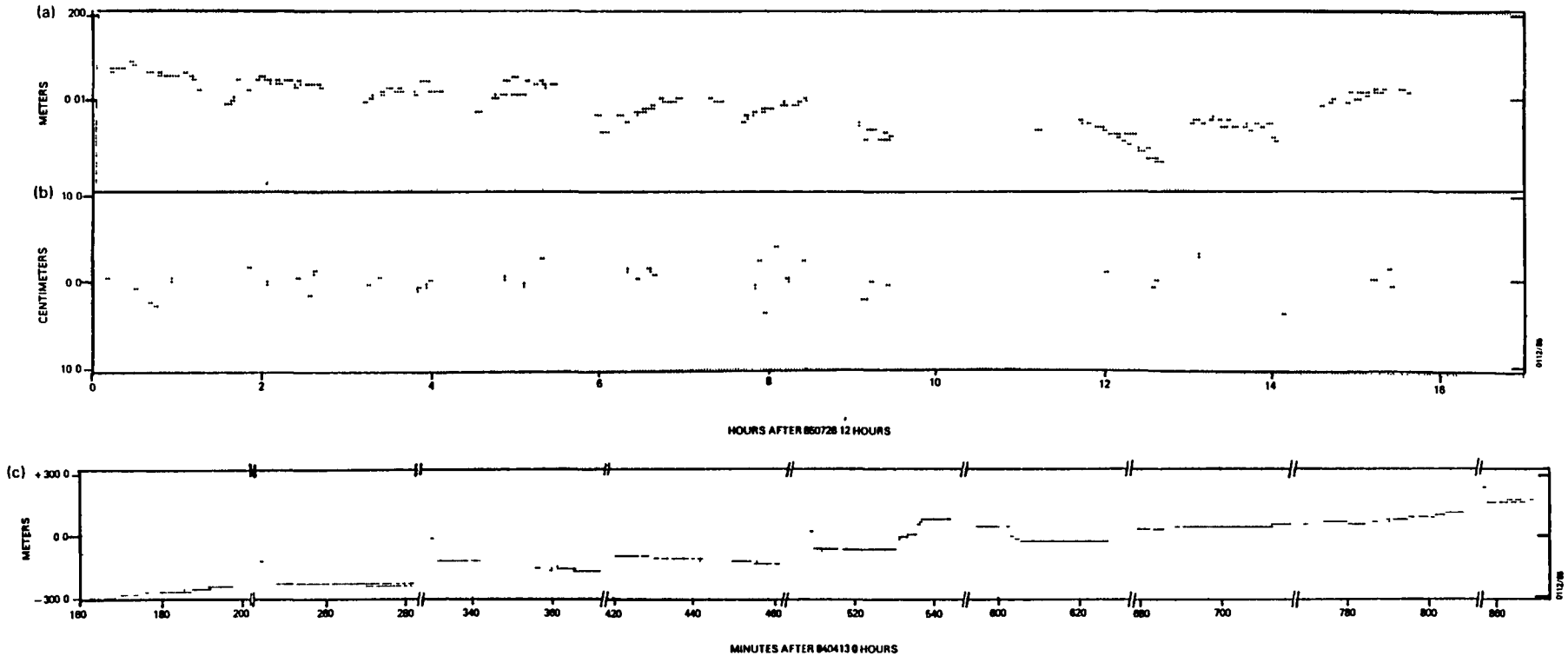


Figure 2-2. Representative Observation Residual Plots for GPSPAC Data Solutions Employing Composite and Single GPS Satellite Observation Sets

- (a) Range residuals for a solution that employs observations from all available GPS NAVSTAR satellites - a composite solution (Run G7B).
- (b) Composite solution's corresponding delta-range residuals. Delta-range residual plots for single GPS satellite solutions display similar signature and residuals.
- (c) Range residuals for a GPSPAC data solution using observations from a single GPS satellite (Run G-43).

were edited from a composite solution, the large pseudorange residuals are still seen.

2.4 ASSESSMENT OF LANDSAT-5 ORBITS COMPUTED FROM GSTDN DATA

2.4.1 COMPARISON OF LARGE OVERLAP DIFFERENCES TO LANDSAT-4 GSTDN SOLUTIONS

GSTDN data for this task were processed in 30-hour overlapping arcs, with overlap periods of 6 hours each. The difference between two adjacent orbital solutions in the overlap period serves as a measure of the GSTDN data-determined orbital accuracy. In this study, Landsat-5 GSTDN data from two different calendar years were processed. Overlapping arcs, sets of two runs each, were processed for April and August 1984 and for May 1985. The first two sets correspond to available GPSPAC data sets. The May 1985 GSTDN data were chosen, based on optimal GSTDN and GPSPAC data availability, from 13 timespans in 1985.

The maximum ephemeris position differences for the three overlapping periods were 106, 59, and 110 m. The root-mean-square (rms) ephemeris position differences for the two overlap periods were 64, 33, and 83 m. These differences are considerably greater than those in the Landsat-4 study. For Landsat-4, the maximum ephemeris position differences of seven overlap comparison periods averaged 29 m, with a standard deviation of 13 m. The rms ephemeris position differences for the Landsat-4 overlap periods averaged 18 m, with a standard deviation of 7 m. Tables 2-5 and 2-6 summarize the results of Landsat-5 GSTDN characteristics.

Although this study processed only a limited number of GSTDN tracking intervals, independent results indicate that 1984 and 1985 Landsat-5 solutions give consistently larger overlap differences when compared to the previous Landsat-4

Table 2-5. 1984 GSTDN Data Orbit Solution Characteristics

RUN ID	ARC START TIME (date, hour)	ARC LENGTH (hours)	NO OF TRACKING STATIONS INVOLVED	NO OF OBSERVATIONS	COMPUTED DRAG SCALE FACTOR $\rho_1 = \Delta C_D / C_D$	RESIDUAL STATISTICS, RANGE-RATE STANDARD DEVIATIONS (cm/sec)	MAXIMUM POSITION DIFFERENCES OVER 6-HOUR OVERLAP OF ADJACENT ARCS (meters)				REMARKS
							RADIAL	CROSS-TRACK	ALONG-TRACK	RSS TOTAL	
GDA	840413 0 h	30	3	507	-1 472	3 048	10 6	13 8	105 7	105 8	BASELINE MODEL JACCHIA ROBERTS ATMOSPHERIC DENSITY MODEL, A PRIORI DRAG COEFFICIENT $C_D = 2.0$, A DRAG SCALE FACTOR SOLVED FOR, 21×21 GEM 9 GEOPOTENTIAL MODEL
GDB	840414 0 h	30	5	702	-0 919	4 114					
GDM	840807 0 h	30	3	399	-8 833	3 478	8 1	8 7	58 4	59 2	
GDN	840808 0 h	30	4	444	-7 493	2 956					
S4A	840413 0 h	30	3	507	-1 965	3 035	10 2	13 8	101 1	101 3	HARRIS-PRIESTER F100 ATMOSPHERIC DENSITY MODEL, A PRIORI DRAG COEFFICIENT $C_D = 2.0$, A DRAG SCALE FACTOR SOLVED FOR, 21×21 GEM 9 GEOPOTENTIAL MODEL
S4B	840414 0 h	30	5	702	-0 674	4 100					
S8A	840807 0 h	30	3	399	-3 858	3 454	7 7	8 1	69 8	70 3	
S8B	840808 0 h	30	4	444	-4 348	2 960					
GMA	840413 0 h	30	3	507	-1 549	3 238	10 7	13 6	101 2	101 7	BASELINE ATMOSPHERE MODEL, WITH 36×36 GEM 10B GEOPOTENTIAL MODEL
GMB	840414 0 h	30	5	702	-1 092	3 860					
GMC	840413 0 h	30	3	507	-1 136	2 775	9 5	9 8	83 9	84 2	BASELINE MODEL WITH 36×36 GEM 10B GEOPOTENTIAL MODEL, MARSH STATION COORDINATES
GMD	840414 0 h	30	5	703	-0 959	2 822					

NOTES SATELLITE AND TIME PERIOD LANDSAT-5, APRIL-AUGUST 1984
 DATA GSTDN RANGE-RATE DATA
 RSS, ROOT-SUM-SQUARED

2-15

0112 (76*)/85

Table 2-6. 1985 GSTDN Data Orbit Solution Characteristics

RUN ID	ARC START TIME (date, hour)	ARC LENGTH (hours)	NO OF TRACKING STATIONS INVOLVED	NO OF OBSERVATIONS	COMPUTED DRAG SCALE FACTOR $q_1 = \Delta C_D / C_D$	RESIDUAL STATISTICS, STANDARD DEVIATIONS		MAXIMUM POSITION DIFFERENCES OVER 6-HOUR OVERLAP OF ADJACENT ARCS (meters)				REMARKS
						RANGE (meters)	DELTA RANGE (cm)	RADIAL	CROSS-TRACK	ALONG-TRACK	RSS TOTAL	
GS1	850524 6 h	30	3	239	- 11 07	-	1 319	11 1	26 4	107 3	110 2	BASELINE MODEL
GS2	850525 6 h	30	5	270	4 40	-	1 396					RANGE-RATE DATA ONLY
GSA	850524 6 h	30	4	400	- 8 97	10 47	5 361	16 2	19 7	69 0	69 1	NO OBSERVATION PROCESSING PERFORMED, BOTH RANGE AND RANGE-RATE DATA INCLUDED
GSB	850525 6 h	30	6	387	5 73	4 322	5 775					

NOTES SATELLITE AND TIME PERIOD LANDSAT-5, MAY 1985
 DATA GSTDN RANGE-RATE DATA
 RSS IS ROOT-SUM-SQUARED

GSTDN solutions. Tracking statistics do indicate an increasing amount of TDRS-East tracking data available for Landsat-5 in 1985. Overlap differences of TDRS-only solutions, associated with the single-TDRS S-band certification results, report 82, 71, 35, and 74 m (Reference 2-4). In addition, private conversations with investigators (Yuri Nakai, Computer Sciences Corporation) who are analyzing 1985 Landsat-5 orbit solution overlap differences using combinations of GSTDN, TDRSS, and Bilateral Ranging Transponder System (BRTS) data indicate ephemeris overlap differences consistently larger than the average 29 m observed for Landsat-4.

2.4.2 ANALYSIS OF LANDSAT-5 LARGER-THAN-EXPECTED OVERLAP EPHEMERIS DIFFERENCES

It was originally thought that these larger-than-expected overlap ephemeris differences could be attributed to inadequacies in atmospheric density modeling. Modeling error was suspected because the overlap comparison plot of the along-track difference, as shown in Figure 2-3, displays sinusoidally increasing differences that are generally typical of force modeling mismatch between the orbit solutions involved. No significant improvement was seen, however, when a different atmospheric model (Harris-Priester) was used.

In an attempt to reduce these ephemeris differences, the April 1984 GSTDN data arcs were again processed using the standard orbit determination scenario, but with two variations. First, orbits were obtained by using the 36-by-36 GEM-10B geopotential model. Second, a second set of orbits was obtained by using the Marsh tracking station position coordinates in addition to the GEM-10B model. As was also true in the Landsat-4 study, using these improved models did not result in substantial improvement in orbit determination performance. The results of the 1984 GSTDN orbit determination runs are summarized in Table 2-5.

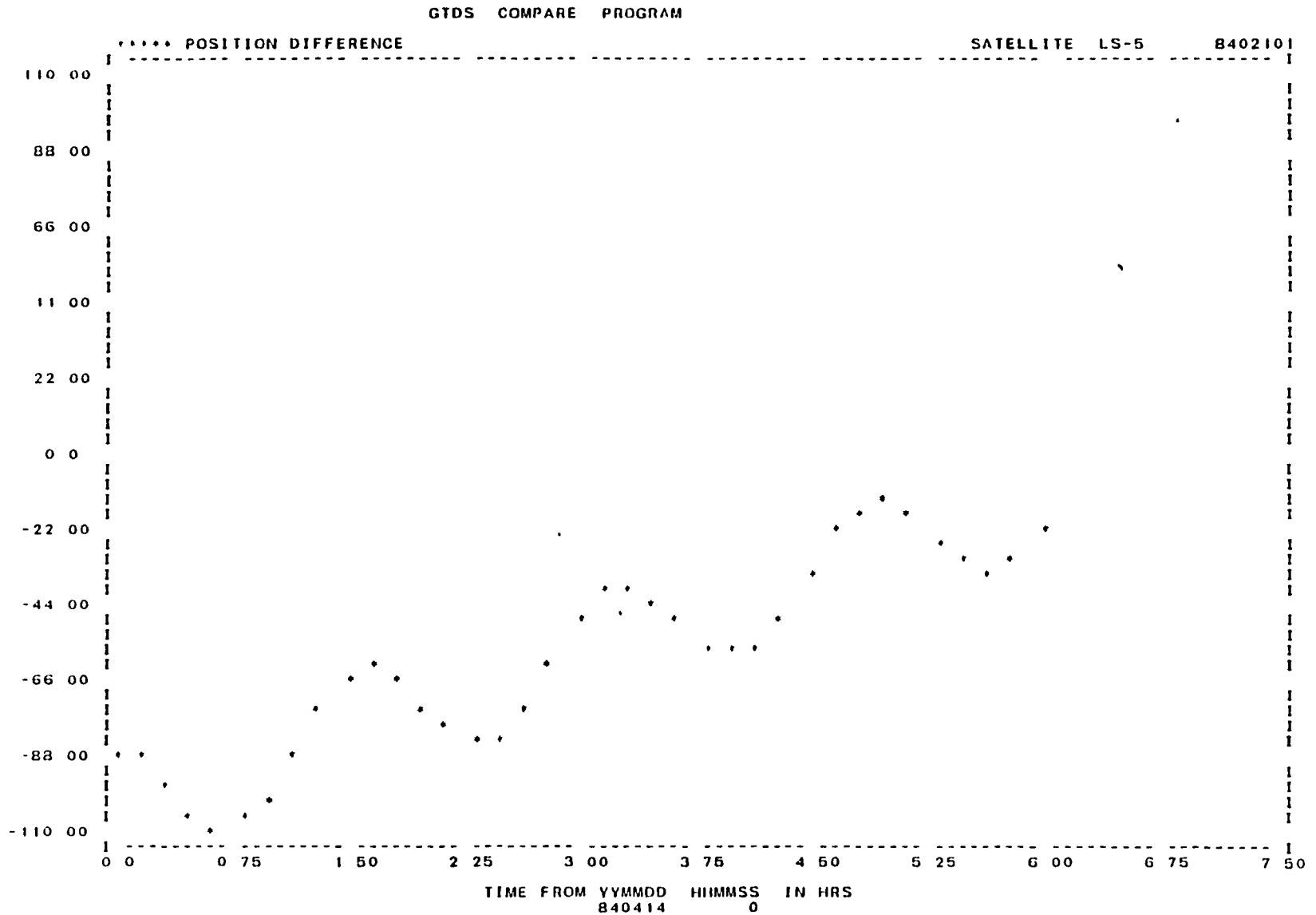


Figure 2-3. Landsat-5 GSTDN Orbit Solution Overlap Ephemeris Comparison

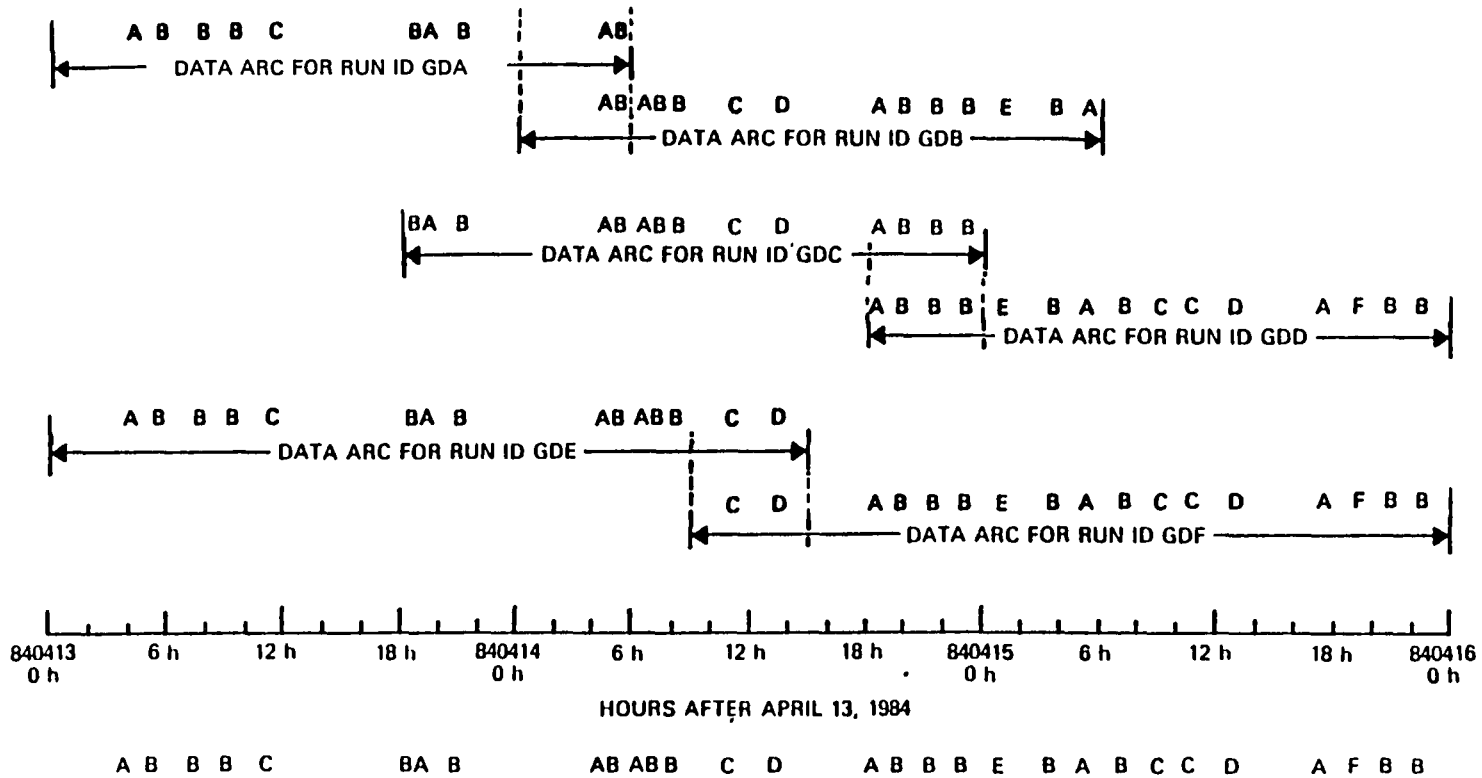
Although the previous Landsat-4 experience with unified S-band (USB) tracking data revealed systematic errors in the range observations, the May 1985 GSTDN data arcs were re-processed using both range and range-rate observations. This was done to determine if range errors were caused by redundant observation correction preprocessing in R&D GTDS. When the preprocessing was deleted, the resulting orbit solutions still displayed large range and range-rate residual statistics. Probably because of the greater observability afforded by the range observations, the maximum position difference was decreased from 110 to 69 m--still large in comparison with the Landsat-4 accuracies. The results of the 1985 GSTDN orbit determination runs are summarized in Table 2-6.

2.4.3 LANDSAT-5 SOLUTIONS INVOLVING FEWER TRACKING STATIONS

In comparison to previous Landsat-4 GSTDN data, the Landsat-5 solutions involved fewer ground tracking stations. In the typical Landsat-4 GSTDN 30-hour arc solutions, between 6 and 10 ground stations were involved in tracking. For the six baseline Landsat-5 GSTDN solutions in Tables 2-5 and 2-6, between three and five tracking stations were involved.

Irregularity of the Landsat-5 tracking passes may also contribute to the larger-than-expected overlap ephemeris differences. Figure 2-4 displays a plot of the ground tracking passes for Landsat-5 GSTDN data, beginning on April 13, 1984. This plot shows the 30-hour intervals for baseline run IDs GDA and GDB and their corresponding overlap interval extending from 0 hours to 6 hours on April 14 (840414).

Because it was suspected that the sparse tracking over the GDA-GDB 6-hour overlap contributed to its poor ephemeris overlap comparison (from Table 2-5, a maximum position difference rss of 106 m), alternate 30-hour arcs were chosen.



LEGEND

- A - GDS8
- B - ULA3
- C - MAD3
- D - AGO3
- E - GWM3
- F - GDS3

NOTES CAPITAL LETTERS INDICATE THE CORRESPONDENCE BETWEEN TRACKING PASSES (WITH A TYPICAL DURATION OF 10 MINUTES) AND THE TRACKING STATION FROM WHICH THE MEASUREMENT SIGNAL ORIGINATED
 THE TRACKING PASSES ABOVE THE TIME AXIS CONTRIBUTE TO THE ORBIT SOLUTION OVER THE DATA ARC
 THE TRACKING PASSES BELOW THE TIME AXIS ARE PRESENT IN THE GSTDN DATA BASE

0112/85

Figure 2-4. Plot of Ground Tracking Passes and Orbit Solution Arcs Involving April 1984 Landsat-5 GSTDN Data

These alternate arcs, labeled GDC and GDD, begin at 840413 18 hours and 840414 18 hours, respectively, and have a 6-hour overlap beginning at 840414 18 hours. As seen from the plot in Figure 2-4, this alternate overlap time includes more uniform tracking. This is reflected in the GDC-GDD overlap ephemeris comparison RSS of 44 m (from Table 2-7), which is a significant improvement over the GDA-GDB overlap (although it is still inferior to the Landsat-4 GSTDN overlap maxima, which have an RSS average of 28.8 m). Part of this improvement may also result because the alternate GDC and GDD arcs involve more tracking stations, four and six, respectively, compared to three and five for GDA and GDB.

A second set of GSTDN data orbit solutions were performed, using 39-hour arcs. These two arcs, labeled GDE and GDF, also have a 6-hour overlap, beginning at 840414 9 hours. The maximum position difference rss of this overlap is 72 m (Table 2-7). Although the number of tracking stations involved remained the same as in the GDC-GDD solutions, the larger orbit arcs resulted in a poorer overlap comparison. This suggests that the relatively small number of stations involved in Landsat-5 GSTDN data cannot be compensated for by extending orbit solutions over arcs of greater duration, thereby increasing the number of observations and possibly the number of tracking stations. Instead, the GDE-GDF overlap, when compared to GDC-GDD errors, indicates that the force modeling errors begin to increase at a greater rate than the observational benefits.

2.4.4 ANALYSIS OF LANDSAT-4 GSTDN SOLUTIONS WITH REDUCED NUMBER OF TRACKING STATIONS

To determine if poor Landsat-5 GSTDN solutions result from the small number of tracking stations involved, Landsat-4 GSTDN solutions with a reduced number of tracking stations were generated. The results of these solutions are summarized in Table 2-8. The first entry in the table, the

Table 2-7. Additional Landsat-5 GSTDN Data Orbit Solution Characteristics

RUN ID	ARC START TIME (date, hour)	ARC LENGTH (hours)	NO OF TRACKING STATIONS INVOLVED	NO OF OBSERVATIONS	COMPUTED DRAG SCALE FACTOR $\rho_1 = \Delta C_D / C_D$	RESIDUAL STATISTICS, RANGE-RATE STANDARD DEVIATIONS (cm/sec)	MAXIMUM POSITION DIFFERENCES OVER 6-HOUR OVERLAP OF ADJACENT ARCS (meters)				REMARKS
							RADIAL	CROSS-TRACK	ALONG-TRACK	RSS TOTAL	
GDC	840413 18 h	30	4	703	2 045	3 84	8 4	10 4	44 2	44 3	BASELINE MODEL
GDD	840414 18 h	30	6	723	0 065	3 54					
GDE	840413 0 h	39	4	767	-0 424	4 44	14 5	13 5	71 4	71 6	
GDF	840414 9 h	39	6	829	-0 390	4 31					

NOTES SATELLITE AND TIME PERIOD LANDSAT-5, APRIL 1984
 DATA GSTDN RANGE-RATE DATA
 RSS IS ROOT SUM SQUARED
 SEE FIGURE 2-4 FOR TRACKING PASSES AND ORBIT SOLUTION ARCS

2-22

0112 (76a*)/85

Table 2-8. Summary of Landsat-4 GSTDN Solutions With Reduced Number of Tracking Stations

RUN ID	ARC START TIME (date, hour)	NO OF TRACKING STATIONS ACCEPTED	NO OF TRACKING PASSES ACCEPTED	NO OF OBSERVATIONS	COMPUTED DRAG SCALE FACTOR $\epsilon_1 = \Delta C_D / C_D$	RESIDUAL STATISTICS, RANGE-RATE STANDARD DEVIATIONS (cm/sec)	MAXIMUM POSITION DIFFERENCES OVER 6-HOUR OVERLAP OF ADJACENT ARCS (meters)				REMARKS
							RADIAL	CROSS-TRACK	ALONG-TRACK	RSS TOTAL	
GL4	821001 0 h	10	16	145	-0.236	2.62	2.4	15.2	6.2	15.5	LANDSAT-4 BASELINE SOLUTION (PRESENTED FOR COMPARISON)
GL5	821002 0 h	6	16	116	-0.294	3.45					
GL41	821001 0 h	3	4	207	-0.779	3.17	10.3	23.1	155.2	155.4	LANDSAT-4 SOLUTIONS WITH REDUCED NO OF TRACKING STATIONS
GL51	821002 0 h	4	9	468	-0.347	2.94	6.5	8.2	25.6	25.7	
GL42	821001 0 h	4	9	453	-0.251	2.89					
GL43	821001 0 h	4	6	304	-0.286	2.99	11.7	13.7	30.5	33.3	
GL52	821002 0 h	2	7	367	-0.349	2.87	7.0	5.4	28.7	28.7	
GL44	821001 0 h	6	11	661	-0.268	2.60					

2-23

0112 (76a*)/85

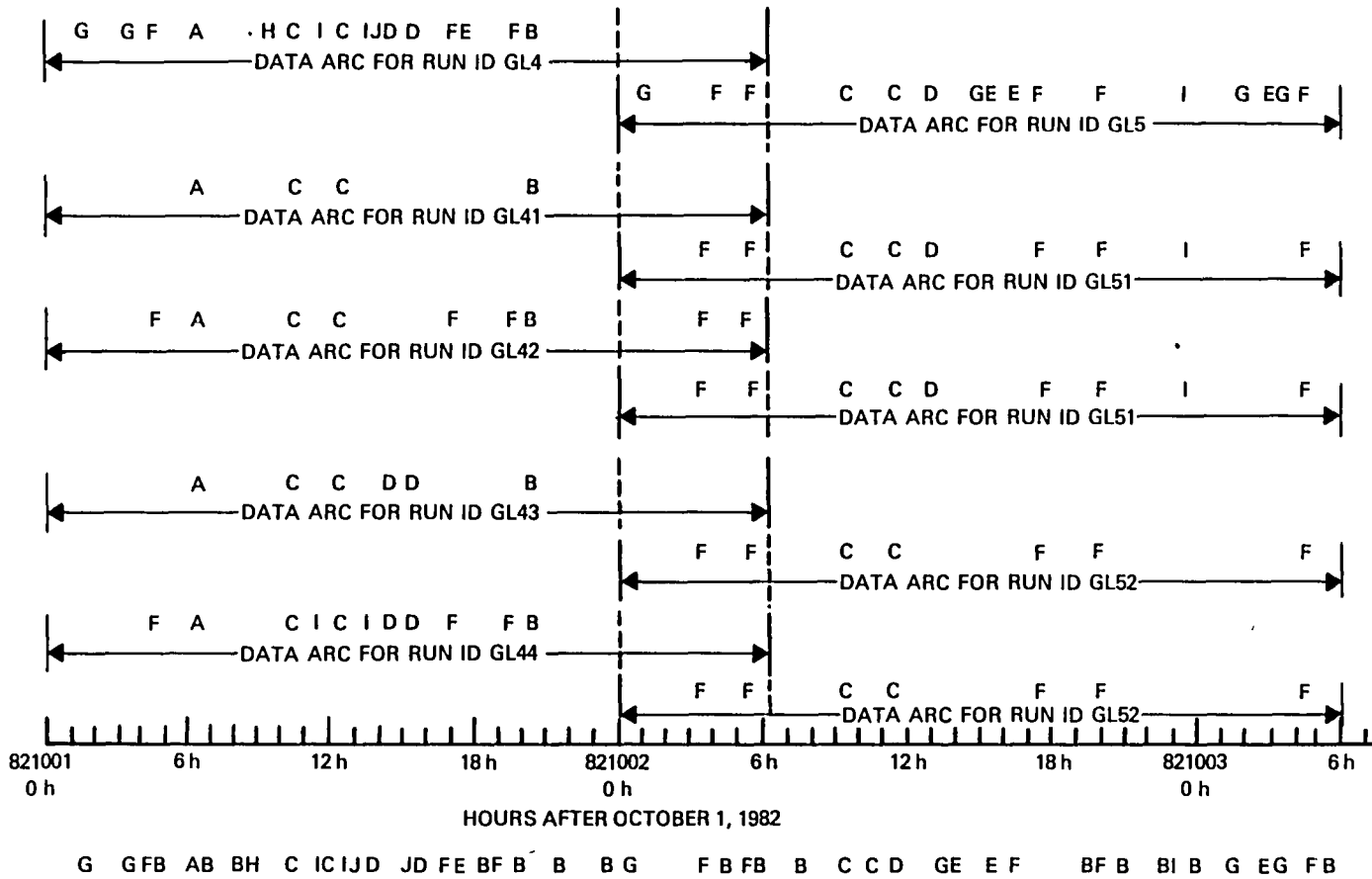
NOTES SATELLITE AND TIME PERIOD LANDSAT-4, OCTOBER 1982
 DATA GSTDN RANGE-RATE DATA
 RSS IS ROOT SUM SQUARED
 ALL SOLUTIONS HAVE DATA ARC LENGTHS OF 30 HOURS
 SEE FIGURE 2-5 FOR TRACKING PASSES AND ORBIT SOLUTION ARCS

overlap comparison between the nonreduced Landsat-4 arcs GL4 and GL5, is presented as the standard for comparison. The remaining entries in the table present comparative ephemeris overlap differences for orbits generated over the same time-spans as GL4 and GL5 but using different reduced sets of tracking stations.

The Landsat-4 GL4-GL5 set was chosen because it displays the smallest ephemeris overlap difference of all the Landsat-4 GSTDN comparisons. It was reasoned that the GL4-GL5 set would therefore produce the greatest range of sensitivity to reduced tracking station scenarios. In addition, because of the large number of stations involved, it was hoped that appropriate subsets of the GL4-GL5 tracking stations could be found to approximately reproduce the tracking geometries available in the Landsat-5 GSTDN solutions. Unfortunately, the latter purpose was frustrated by the absence of valid Landsat-4 observations corresponding to tracking stations in the Landsat-5 station set and the geometrical complications introduced in choosing substitution stations.

The reduced station results in Table 2-8 do produce poorer overlap comparisons. Specifically, as seen in set GL41-GL51 in comparison to set GL42-GL51, overlap comparisons deteriorate rapidly after some cutoff number of tracking station. As shown in the table, below this cutoff number the number of tracking passes involved begins to play an increasing importance in the overlap differences. As shown in Figure 2-5, which displays the tracking schedules for those runs summarized in Table 2-8, the number and duration of nontracking intervals also appears to affect the ephemeris differences.

Because of these complications introduced by station geometry, the number of tracking passes, and the amount and



LEGEND

- A - GDS8 F - GDS3
- B - ULA3 G - BLTA
- C - MAD3 H - MAD8
- D - AGO3 I - ORR3
- E - MIL3 J - BDA3

NOTES CAPITAL LETTERS INDICATE THE CORRESPONDENCE BETWEEN TRACKING PASSES (WITH A TYPICAL DURATION OF 10 MINUTES) AND THE TRACKING STATION FROM WHICH THE MEASUREMENT SIGNAL ORIGINATED
 THE TRACKING PASSES ABOVE THE TIME AXIS CONTRIBUTE TO THE ORBIT SOLUTION OVER THE DATA ARC
 THE TRACKING PASSES BELOW THE TIME AXIS ARE PRESENT IN THE GSTDN DATA BASE

0112/85

Figure 2-5. Plot of Ground Tracking Passes and Orbit Solution Arcs Involving October 1982 Landsat-4 GSTDN Data

duration of nontracking intervals, the reduced station results were inconclusive in determining the extent to which poor Landsat-5 GSTDN orbit solutions result solely from the small number of tracking stations. One very interesting statistic is that, for the Landsat-4 GSTDN tracking intervals (Figure 2-5), an average of 88 percent of the available stations and only 50 percent of the available tracking passes were accepted and thus contributed to the solution.¹ In contrast, for the Landsat-5 GSTDN tracking intervals (Figure 2-4), all the available stations and all the available tracking passes were accepted and thus contribute to the solution. This may indicate that the Landsat-5 solutions, because of the lower density of data, incorporated observations that would otherwise be edited out.

The present results and the previous Landsat-4 experiences lead to the conclusion that more stations, although each contains random errors and possibly even systematic errors, result not only in better observation geometry but also in a larger number of observations. A large amount of data is needed because many observations will be edited out because of validity, elevation, or 3σ editing. After this editing, if a sufficient amount of data remains, the remaining error sources can be averaged out in the orbit determination process to produce small ephemeris overlap differences. In short, more stations provide more measurements, more observability, and better statistics in dealing with existing observation error sources.

¹Available refers to observations--associated with a particular tracking pass or station--that are both present in the input data and not deleted by user observation accept/reject criteria; accepted data must meet the previous available criteria and must also not be edited out of the orbit solution due to either validity editing, elevation editing, or 3σ editing.

2.5 ANALYSIS OF POSSIBLE MISMATCHES BETWEEN GLI AND R&D GTDS

This section presents the results of an analysis to determine if possible inconsistencies or inaccuracies introduced in the R&D GTDS orbit determination processing cause the large pseudorange measurement residuals seen in both Landsat-4 and Landsat-5 GPSPAC data orbits (as described in Section 2.2). In the course of this analysis, the R&D GTDS code, which processes GPSPAC data, was investigated for correctness and consistency with the mathematical specifications of the GPSPAC/Landsat-D Interface System (GLI) (Reference 2-5). As noted in Section 2.1, the GPSPAC extracts GPS data from telemetry that is in turn preprocessed to transform it from Earth-fixed to inertial coordinates. In addition to other functions, GLI performs this preprocessing of the Landsat GPSPAC data for use in R&D GTDS.

This investigation verified the correctness of the R&D GTDS code that processes the GPSPAC data. However, a coordinate frame mismatch can occur when the coordinate reference frame of the R&D GTDS orbit integrator does not match the inertial frame of the GPSPAC data's internal state, which is included with the observations. For instance, in run ID G4A of Table 2-1, the Landsat-5 GPS orbit solution is integrated in a true-of-reference-date (TOR) coordinate frame (Reference 2-6) referenced to April 13, 1984. However, the observations' GPS inertial position and velocities are expressed in a coordinate frame referenced to April 8, 1984, the date EPOCH of the GPSPAC data observation file. Because the R&D GTDS does not check for reference frame inconsistency between the GPSPAC observations and the integration reference frame, it fails to take into account the Earth's precession and nutation effects (Reference 2-7) occurring in the 5 days between April 8 and April 13.

To correct this reference frame inconsistency, each GPS observation's position and velocity (the S and SDOT) vector (expressed in the GPSPAC EPDATE TOR frame) is rotated by a stand-alone routine to the reference date to be used by the R&D GTDS orbit integrator. For the G4A run, this rotation was from the April 8, 1984, to the April 13, 1984, TOR coordinate frame. This rotated GPSPAC data were then processed in an R&D GTDS DC run. The resultant Landsat-5 GPSPAC orbit solution still displays the same large pseudorange residuals previously observed. In fact, the converged orbit solution results in a state vector of the same magnitude as that generated in the nonrotated G4A run, except that it was rotated through a small angle. This result was to be expected because the reference frame rotation does not affect the individual GPSPAC pseudorange and delta-pseudorange measurements. Instead, it rotates the entire NAVSTAR GPS multi-satellite constellation through a fixed angle, which in this case corrects for the precession and nutation effects occurring between April 8 and April 13.

The comparison plot between the nonrotated G4A orbit and the G4A orbit with no reference frame inconsistency is shown in Figure 2-6. The comparison displays a constant difference in the spacecraft along-track direction. Because Landsat has a 98-deg-inclination orbit, this offset is due primarily to nutation effects. The difference in the cross-track direction, due primarily to precession effects, displays a sinusoidally varying function of period roughly equal to Landsat's own 98-minute period. The zeros in the difference function occur approximately over the poles while the extremes occur near the equatorial crossings.

Table 2-9 summarizes the characteristics of comparisons between nonrotated and reference rotated GPSPAC solutions for Landsat-4 and -5. The solutions were performed for Landsat-4 arcs to determine if reference rotation would

2-29

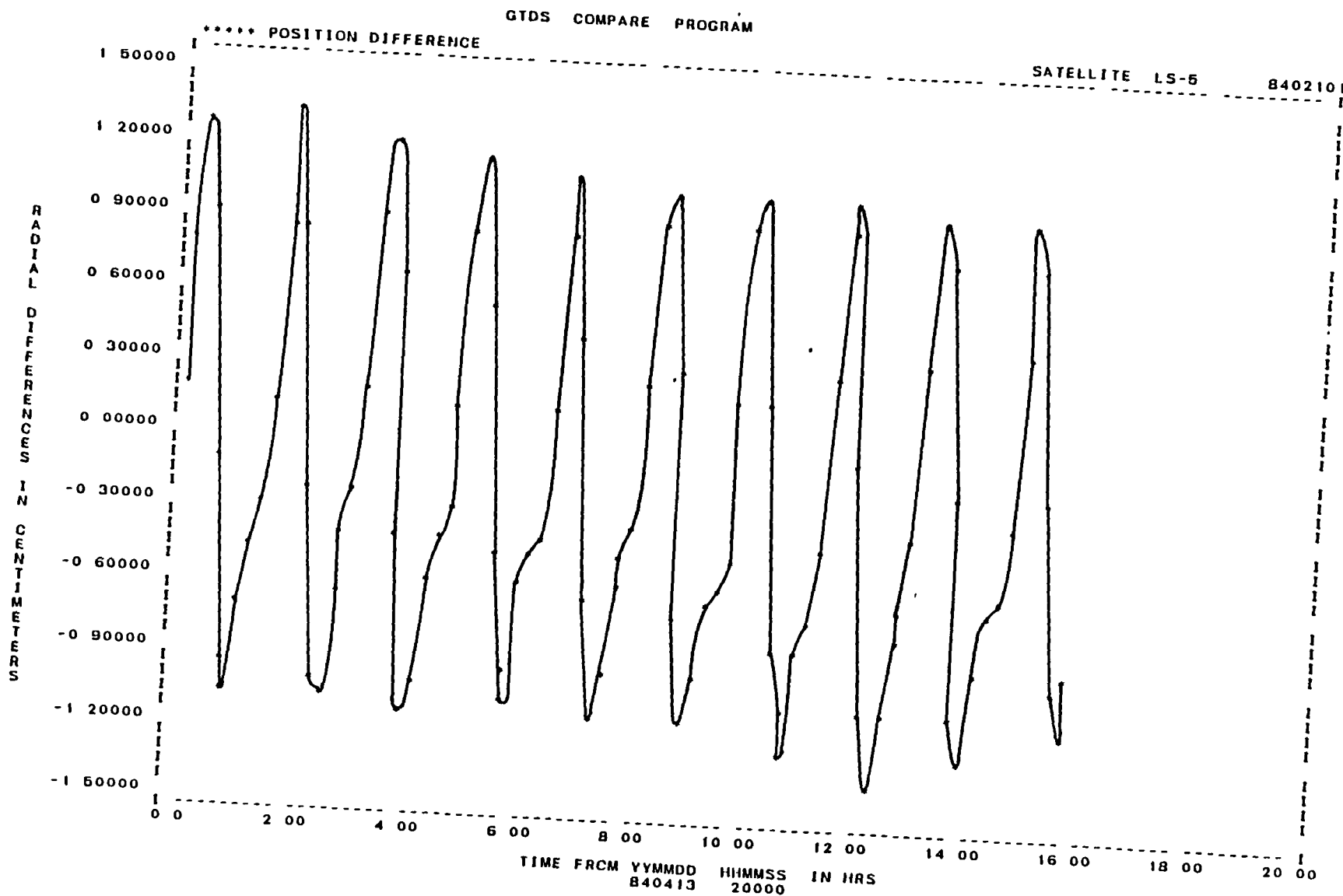


Figure 2-6. Ephemeris Comparison Between GPS Orbit (Run G4A) Solutions With and Without Reference Frame Mismatch Correction (1 of 3)

2-30

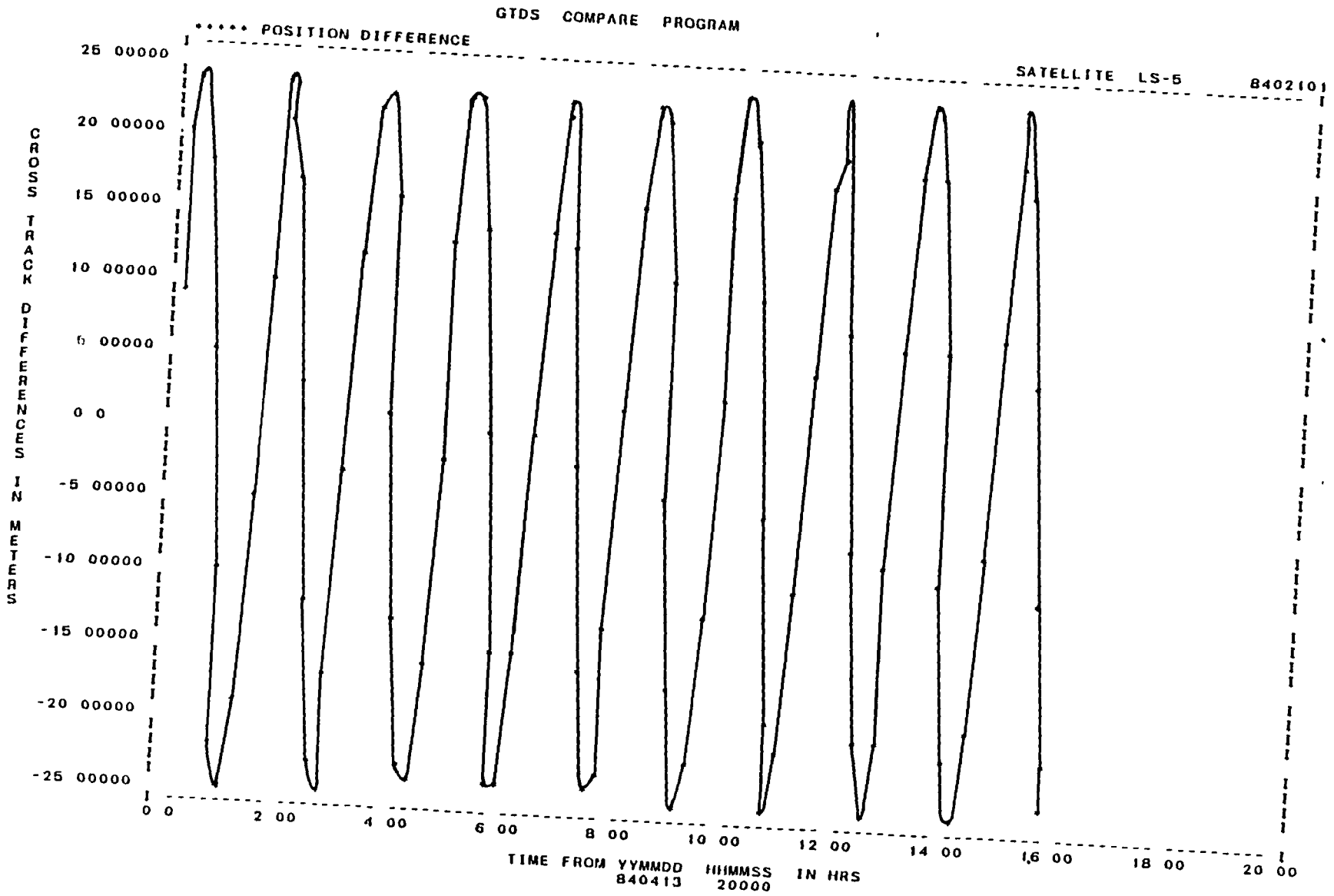
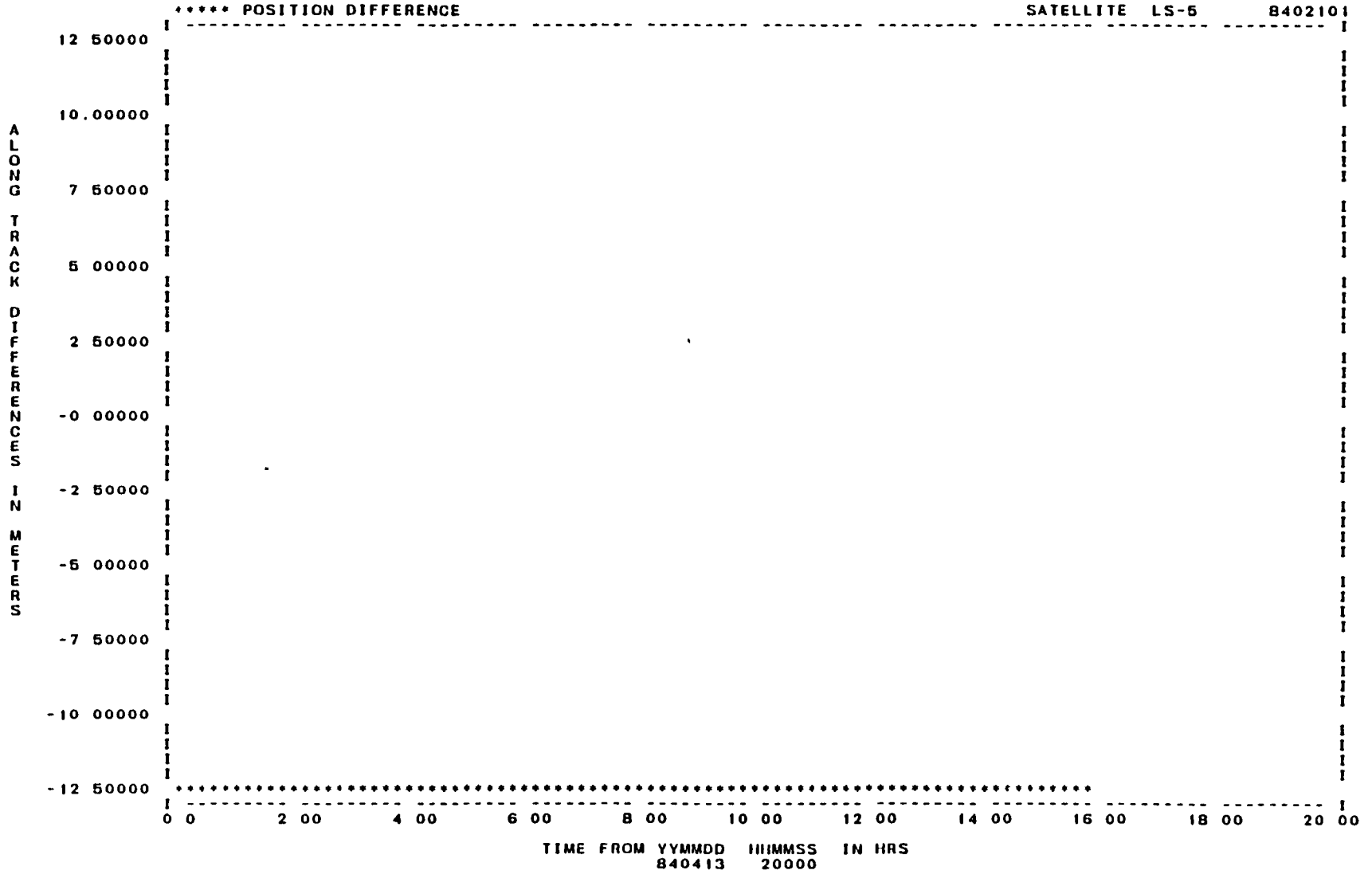


Figure 2-6. Ephemeris Comparison Between GPS Orbit (Run G4A) Solutions With and Without Reference Frame Mismatch Correction (2 of 3)

GTDS COMPARE PROGRAM



2-31

Figure 2-6. Ephemeris Comparison Between GPS Orbit (Run G4A) Solutions With and Without Reference Frame Mismatch Correction (3 of 3)

Table 2-9. Reference Rotated GPSPAC Data Orbit Solution Characteristics and Comparisons With Nonrotated Solutions

RUN ID	ARC START TIME (date hour)	ARC LENGTH (hours)	NO OF OBSERVATIONS	SOLVE FOR PARAMETERS			RESIDUAL STATISTICS, STANDARD DEVIATIONS		MAXIMUM POSITION DIFFERENCES OVER 4 HOUR OVERLAP OF ADJACENT ARCS (meters)					MAXIMUM POSITION DIFFERENCES FROM GSTDN ORBITS (meters)					REMARKS	
				e_1	B (10^{-3} sec)	\dot{B} (10^{-8} sec/sec)	RANGE (meters)	DELTA RANGE (cm)	RADIAL	C	ALONG TRACK	RSS	RSS ^a	RADIAL	C	ALONG TRACK	RSS	RSS ^a		
GP1R	820910 18 h	16	705	-0.305	-0.369	-0.786	132.5	2.53												SATELLITE LANDSAT 4
GP2R	820911 6 h	16	682	-1.107	-0.708	-0.785	246.9	2.79	2.5	15.8	13.0	18.5	20.5	11.1	44.4	31.7	49.7	46.5		
GP4R	821001 19 h	16	738	-0.230	-0.571	-0.704	312.8	3.59						12.2	61.9	32.1	64.9	48.1		
GP5R	821002 7 h	16	592	-0.610	-0.875	-0.702	294.2	3.43	10.2	34.4	47.3	54.0	53.8	6.3	55.2	37.2	65.4	63.3		
GP6R	821112 19 h	16	790	-0.277	-1.027	-0.546	1312.0	2.40						10.0	59.3	33.9	62.6	41.5		
GP7R	821113 7 h	16	795	-0.693	-1.264	-0.545	145.1	2.62	7.4	14.5	40.7	41.1	41.0	7.6	72.7	39.6	80.2	53.1		
G4AR	840413 2 h	16	1297	1.594	-3.127	-3.262	100.0	2.39						13.4	54.1	57.5	79.0	54.3	SATELLITE LANDSAT 5	

0112 (76-1)/84

NOTES FORCE MODEL BASELINE ONLY EVERY 10TH PAIR OF OBSERVATION DATA IS PROCESSED
 SOLVE FOR PARAMETERS DRAG SCALE FACTOR $e_1 = \Delta C_D / C_D$ CLOCK BIAS B AND DRIFT \dot{B} AT EPOCH
 C L AND RSS ARE THE ACROSS TRACK ALONG TRACK AND ROOT SUM SQUARED COMPARE DIFFERENCES RESPECTIVELY

^aFOR COMPARISON PURPOSES RSS CORRESPONDING TO PREVIOUSLY REPORTED NONROTATED GPSPAC DATA SOLUTIONS (FOR LANDSAT 4 FROM REFERENCE 2.3) ALL OTHER TABLE ENTRIES ARE FROM ROTATED SOLUTIONS

improve the GPSPAC-GSTDN ephemeris overlap compares. In most cases, very little difference is seen. Contrary to what was expected, in four instances, the reference frame rotation gives larger GPSPAC-GSTDN differences; although this may be caused by some geometric effect, these results are not fully understood and should be studied further. In any case, the rotation of the reference frame does not appear to cause, or affect, the large pseudorange residuals seen in any of the GPSPAC delta-range solutions.

A possible processing mismatch occurs if the GLI and R&D GTDS programs use different Greenwich hour angle (GHA) constants. To account for error on the order of 100 m, the GHA correction is estimated to be a rotation of roughly the same order of magnitude as that used to correct the coordinate reference frame inconsistency, that is, approximately 2×10^{-4} deg. As was expected, the correction of possible GHA errors resulted in comparison plots analogous to the reference frame rotation correction.

This study also considered other conceivable errors that can produce range error signatures on the order of 100 m and appear GPSPAC range-dependent, but are delta-range insensitive--in short, the range error signatures match the trend of the pseudorange residual errors seen in both the Landsat-4 and -5 GPSPAC solutions. Two possible error sources, which under certain scenarios meet this error signature and can be corrected for in the R&D GTDS processing, are time tag errors associated with a measurement or with the transformation from Earth-fixed to inertial coordinates. When these postulated errors were fixed, in isolation or in combination, the characteristic pseudorange residual errors in the R&D GTDS orbit solutions were increased or were only mildly affected, but they were still present.

2.6 CONCLUSIONS

The major conclusions concerning the accuracies of GPSPAC data for computing Landsat-5 orbits can be summarized as follows:

1. Landsat-5 orbit determination using GPSPAC data Landsat-5 orbit solutions computed from GPSPAC delta-pseudorange (Doppler) data are good. Maximum differences between GPSPAC and GSTDN solution are generally under 70 m. Maximum differences between partially overlapping GPSPAC solutions are even smaller. There is a good possibility that the GPSPAC solutions are superior to the GSTDN solutions in accuracy.

2. For orbit determination instead of real-time navigation, simultaneous data from four GPS satellites are not necessary. The results indicate that approximately 3 hours of data from a single GPS satellite are sufficient to resolve the Landsat-5 orbit and clock. A study of a randomly selected sample shows that the Landsat-5 orbit solutions based on individual GPS satellites agree to within 80 m, and typically less than 40 m.

3. As with the case of Landsat-4 GPSPAC data, there exist some inconsistencies between the Landsat-5 GPSPAC pseudorange and delta-pseudorange data. Landsat-5 solutions derived from pseudorange data generally differ from the GSTDN solutions by maximas over 100 m. Furthermore, large, GPS-independent, range observation residuals of over 100 m are seen in delta-pseudorange Landsat-5 GPSPAC data solutions. Based on these, it may be concluded that the pseudoranges have systematic errors on the order of 100 m in addition to the expected clock errors. The cause of these systematic errors has not been determined, although bad data

from an individual GPS satellite and several easily committed preprocessing errors have been eliminated as possible reasons.

4. In connection with the GPSPAC study, the computation of Landsat-5 orbits from GSTDN data was undertaken. Unfortunately, there are not as many ground tracking stations for Landsat-5 as for Landsat-4, and the accuracy of the resulting Landsat-5 orbit solutions is not as good as that of the corresponding Landsat-4 solutions. Investigation shows that this degradation cannot be attributed solely to dynamic modeling errors accentuated by the sparsity of tracking coverage.

2.7 REFERENCES

- 2-1. P. M. Jamiczek, editor, Global Positioning System Papers Published in Navigation. Washington, DC: Institute of Navigation, 1980
- 2-2. W. P. Birmingham, B. L. Miller, and W. L. Stein, "Experimental Results of Using the GPS for Landsat-4 On-board Navigation," paper presented at Institute of Navigation National Aerospace Meeting, March 1983
- 2-3. B. T. Fang and E. Seifert, "An Evaluation of Global Positioning System Data for Landsat-4 Orbit Determination," paper delivered at AIAA 23rd Aerospace Science Meeting, January 1985; also Computer Sciences Corporation, CSC/TM-84/6077, Tracking and Data Acquisition System/Global Positioning System (TDAS/GPS) Navigation Analysis, September 1984
- 2-4. Computer Sciences Corporation, CSC/TM-85/6731, Flight Dynamics Division (FDD) Single-TDRS S-Band Navigation Certification Results for Early Tracking and Data Relay Satellite System (TDRSS) Users, Part II - Certification Results, J. O. Cappellari, Jr., P. Y. Kay, and M. H. Nikonchuk, September 1985
- 2-5. National Aeronautics and Space Administration, STL-82-001, GPSPAC/Landsat-D Interface (GLI) System Description, J. B. Dunham, H. M. Silski, and W. T. Wallace, April 1982

- 2-6. Computer Sciences Corporation, CSC/TM-80/6028, Primary Coordinate Systems and Coordinate System Transformations in GTDS, R. L. Smith and M. J. Lucas, June 1980
- 2-7. Goddard Space Flight Center, X-582-76-77, Mathematical Theory of the Goddard Trajectory Determination System, J. O. Cappellari, Jr., C. E. Velez, and A. J. Fuchs (editors), April 1976

SECTION 3 - LOW-ALTITUDE SATELLITE NAVIGATION USING SIMULATED TDAS ONE-WAY DOPPLER DATA

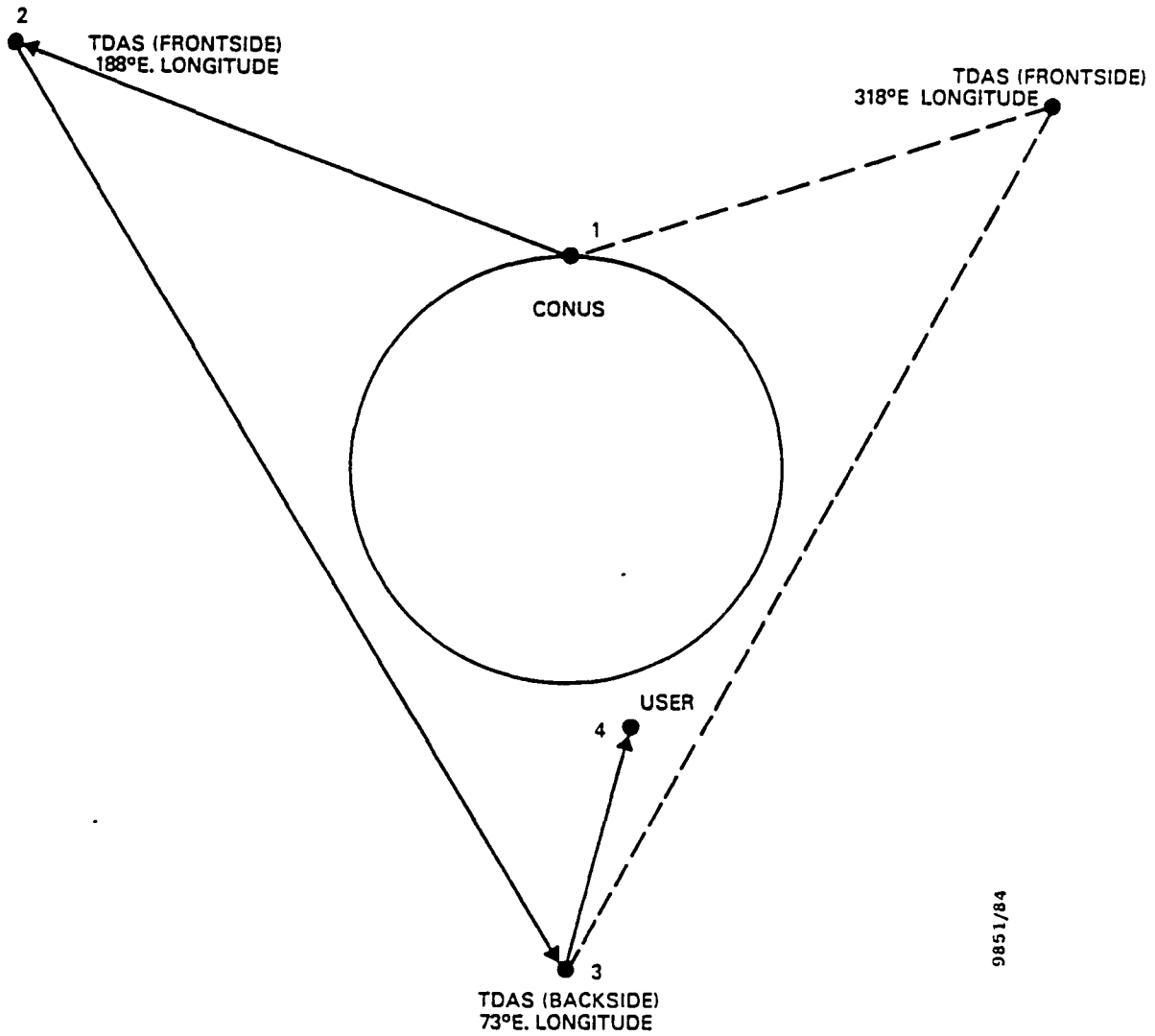
This study investigated the extent of agreement between orbit determination results using simulated TDAS one-way Doppler data and linear error analysis results from a previous study. The simulation and orbit determination results were obtained using the R&D GTDS TDAS enhancements described in Reference 3-1. These simulation/orbit determination results were compared, for an analogous satellite navigation scenario, with error analysis results presented in Reference 3-2 and produced using the TDAS-enhanced SEA program.

The scenario used to generate the R&D GTDS simulated data is presented in Section 3.1, and the corresponding orbit determination scenario, in Section 3.2. From the previous SEA error analysis results, the dominant orbit error sources for the satellite considered in this study were geopotential uncertainty, clock acceleration, and TDAS ephemeris errors. The contributions from these error sources, found using the R&D GTDS simulation/orbit determination results, and their comparison with the error analysis results are discussed in Section 3.3. Conclusions are presented in Section 3.4.

3.1 SIMULATION SCENARIO

3.1.1 TDAS CONFIGURATION

The present study considered a TDAS configuration identical to that used in the SEA error analysis study in Reference 3-2. The configuration consists of three geosynchronous satellites located at longitude 73 deg, 188 deg, and 318 deg east. These satellites are located relative to the continental United States as shown in Figure 3-1. Relay tracking of the user satellite occurs through either of the two frontside TDAS relays. In addition, tracking signals from the ground may be relayed through the 73-deg backside



9851/84

Figure 3-1. TDAS Configuration

TDAS via one of the frontside TDAS, when the target is not observable to the frontside TDASs.

3.1.2 USER SATELLITE

One user satellite at a 28.8-deg inclination and 600-km altitude was considered. The satellite is considered to have an area-to-mass ratio of 0.0027 meters² per kilogram (m²/kg). This spacecraft orbit scenario is similar to that planned for the Space Telescope mission. A nominal drag coefficient of $C_D = 2.0$ is assumed.

3.1.3 TRACKING DATA

The R&D GTDS one-way TDAS tracking data simulate tracking signals originating from the ground and relayed through the TDAS satellites to be received and decoded for range and Doppler information by the user satellite. In this simulation, range-rate Doppler data are modeled as the range difference between two consecutive integrated ranges, spaced 10 seconds (sec) apart. To reproduce the errors present in the previous error analysis study, the data simulated are corrupted by various systematic and random errors. The baseline truth model used in simulating the one-way TDAS data is as follows:

Description	Model
Geopotential	21-by-21 GEM-9
Solar flux/atmospheric density	Harris-Priester F150, $C_D = 2.0$
Random measurement error	
Range	5 m
Range-rate equivalent of Doppler noise	5 millimeters (mm)/sec
Measurement biases	
Range	10 m
Range-rate equivalent of Doppler bias	1 mm/sec
User clock error	
B	10^{-10} (sec/sec)/day

Description	Model
TDAS ephemeris error	
Height	25 m
Crosstrack	23 m
Alongtrack	40 m

Two alternate tracking schedules, similar to those used in Reference 3-3, were considered: the broadcast or beacon mode, in which continuous tracking is available, and the scheduled mode, in which tracking is scheduled for 30 minutes (min) every orbit, cycled through the three TDAS satellites with a 20- to 25-min data gap in between. For convenience, these will be referred to as the forward-link beacon tracking (FLBT) and forward-link scheduled tracking (FLST).

During the tracking periods, observations were simulated at a rate of one pair of range and range-rate measurements every 20-sec (although, in the orbit solutions, the observation weights were adjusted to result in a range-rate solution). The user satellite is sometimes visible to two TDAS satellites simultaneously. To be consistent with the error analysis study, it was assumed that the user satellite is tracked through one TDAS satellite and then switched to the next TDAS satellite when the first one leaves the user's field of view. In contrast with previous studies (References 3-1 and 3-4), no attempt was made to minimize tracking through the backside TDAS. The FLBT and FLST tracking schedules used are shown in Table 3-1; it is identical to that used in the error analysis study in Reference 3-2.

3.2 ORBIT DETERMINATION SCENARIO

An extended Kalman filter (EKF) orbit determination solution was used to reduce the simulated data discussed above. In this solution, the variables estimated were the position and velocity vectors, an effective atmospheric drag coefficient (ρ_1), and the bias and drift of the onboard clock (B and \dot{B}).

Table 3-1. Tracking Schedules for 600-Kilometer-Altitude, 28-Degree-Inclination User Satellite

FORWARD-LINK BEACON TRACKING			FORWARD-LINK SCHEDULED TRACKING		
TDAS1	TDAS2	TDAS3	TDAS1	TDAS2	TDAS3
0-3	64-95	3-64	100-110	65-75	5-15
95-132	166-200	132-166	205-215	170-180	135-145
200-236	269-305	236-269	305-315	270-280	240-250
305-340	372-408	340-372	410-420	375-385	340-350
408-444	475-510	444-475	510-520	480-490	445-455
510-547	580-612	547-580	615-625	580-590	550-560
612-650	684-715	650-684	720-730	685-695	655-665
715-753	788-819	753-788	820-830	790-800	755-765
819-856	890-924	856-890	925-935	895-905	860-870
924-960	993-1028	960-993	1030-1040	995-1005	960-970
1028-1064	1096-1131	1064-1096	1135-1145	1100-1110	1065-1075
1131-1168	1200-1234	1168-1200	1235-1245	1200-1210	1170-1180
1234-1271	1304-1336	1271-1304	1340-1350	1305-1315	1275-1285
1336-1375	1409-1439	1375-1409		1410-1420	1375-1385
1439-1440					

0112 (11/1)/85

The following state process noises were introduced: between measurements, the variances of the velocity components increase at a rate of 10^{-10} square meters per second cubed (m^2/sec^2)/sec; similarly, the clock drift rate variance increases at a rate of 10^{-6} nanoseconds (nsec) per second cubed (nsec/sec)²/sec between measurements. The complete baseline offset force model is summarized as follows:

<u>Description</u>	<u>Model</u>
Geopotential	21-by-21 GEM-7
Solar flux/atmospheric density	Harris-Priester F200, $C_D = 2.2$
User clock error	
B (clock bias)	10^{-2} sec
B (clock drift)	10^{-6} sec/sec
A priori offset in user satellite state (from truth model state)	300 m in x, y, z; (positions) 30 cm/sec in x, y, z (velocities)

The baseline a priori statistics are as follows:

<u>Description</u>	<u>Standard Deviation</u>
A priori state uncertainty	
User H, C, L	500 m
Orbit H, C, L	1 m/sec
User Bias	1 msec
Clock Drift	200 nsec/sec
Drag parameter	1
Gravitational constant, GM	0.25 parts per million (ppm)
Process noise	
Velocity variance growth rate	10^{-10} (m^2/sec^2)/sec
Clock drift rate variance	10^{-6} (nsec/sec) ² /sec

3.3 SIMULATION/ORBIT DETERMINATION ERROR RESULTS

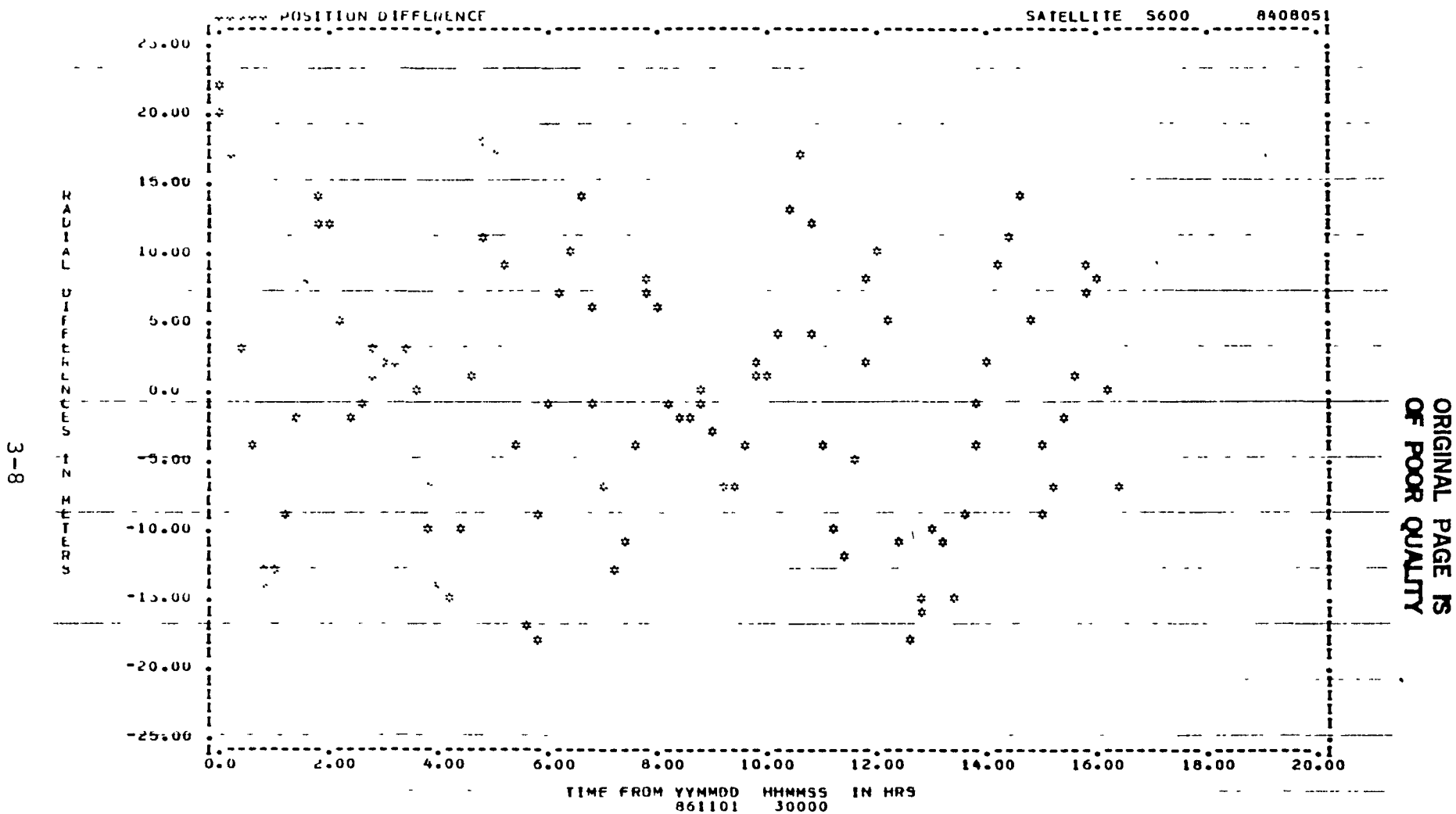
3.3.1 GEOPOTENTIAL ERROR

To compare the simulation results of this study with the error analysis results of the previous study, a common geopotential error model was chosen. The common error model, which can be accommodated using R&D GTDS, is the difference

between the 8-by-8 GEM-1 and the GEM-9 truncated to 15 by 15. In R&D GTDS, the contribution from the GEM-9/GEM-1 difference model was determined using the following method.

First, data were simulated using the baseline version of the truth model except that the geopotential model employed was the GEM-9 truncated to 15 by 15. These data were next reduced using two variations of the baseline force model. The first variation employed the same GEM-9 15-by-15 geopotential model used in simulating the data. In effect, this run incorporated no geopotential model mismatch. The second orbit determination run employed the 8-by-8 GEM-1, so that the run incorporated the GEM-9/GEM-1 model mismatch. Finally, the reduced ephemeris files of the two orbit solutions were compared, with statistics generated on the user's state vector differences over time. To the extent that nonlinear effects can be ignored, the differences in the ephemeris comparisons should arise solely from the GEM-9/GEM-1 model mismatch.

Very close agreement was seen between the R&D GTDS simulation and the previous SEA error analysis results for geopotential errors arising from the GEM-9/GEM-1 difference model. In the error analysis study, an FLBT maximum position error for the GEM-9/GEM-1 difference was reported as 38 m; in this study, 42 m was found using the simulation/orbit determination method discussed previously. As shown in Figure 3-2, the geopotential errors display the characteristic signature that the projections along the spacecraft H, C, and L directions are approximately the same, with the H projection being the smallest. In addition, the rss total geopotential error contribution is observed to be fairly constant in time. These observations are in agreement with the error signatures for the GEM-1/GEM-9 errors found from the SEA error analysis results.

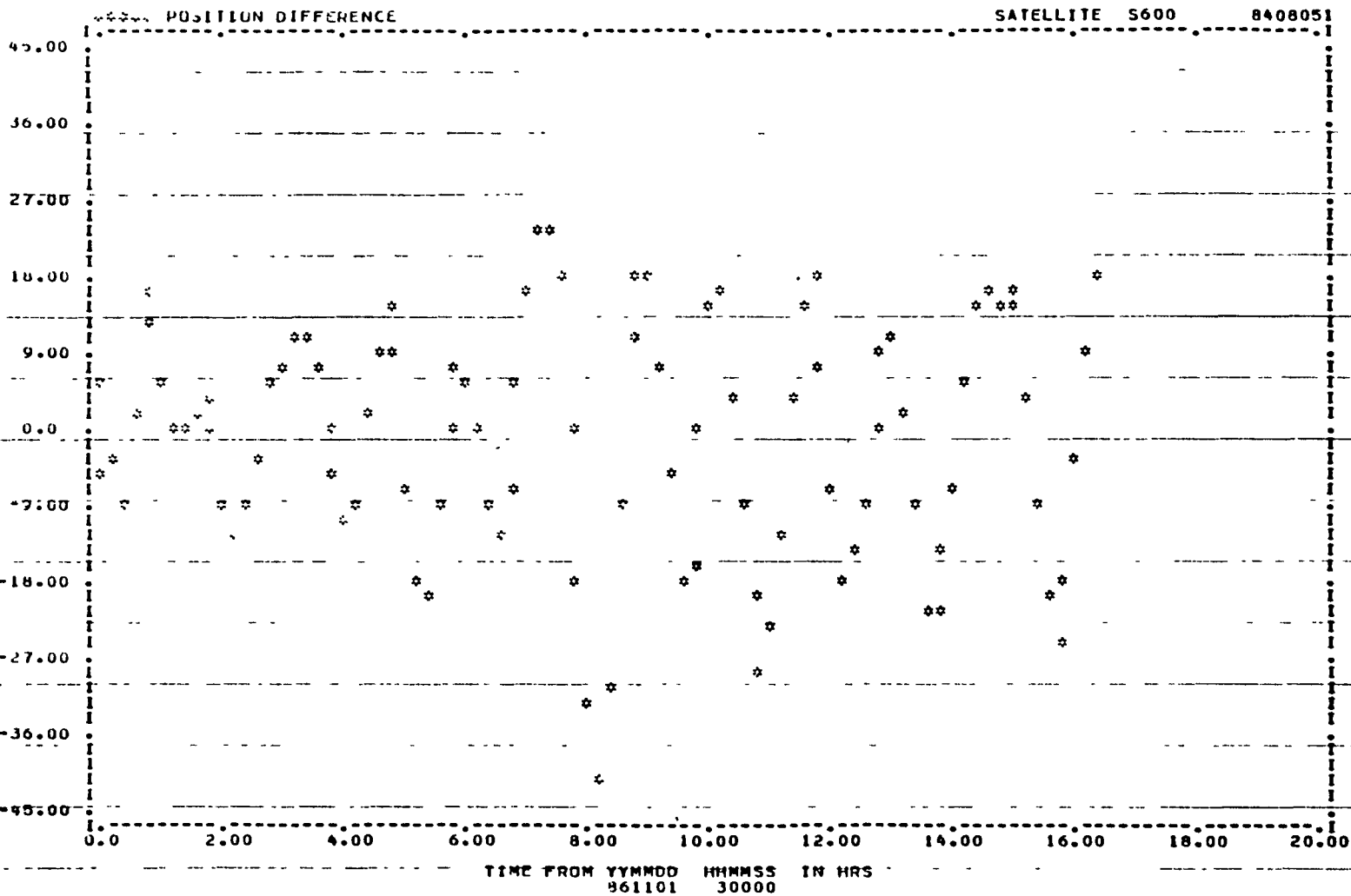


EPHEM FILE ON UNIT 24, DATA RECORDS START AT 861101 Q

EPHEM FILE ON UNIT 01, DATA RECORDS START AT 861101 0

USER'S NOTES.....

Figure 3-2. Geopotential (GEM-9/GEM-1 Difference Model) Error Projections in the User Orbit Plane as Determined From R&D GTDS FLBT Simulation (1 of 3)



3-9

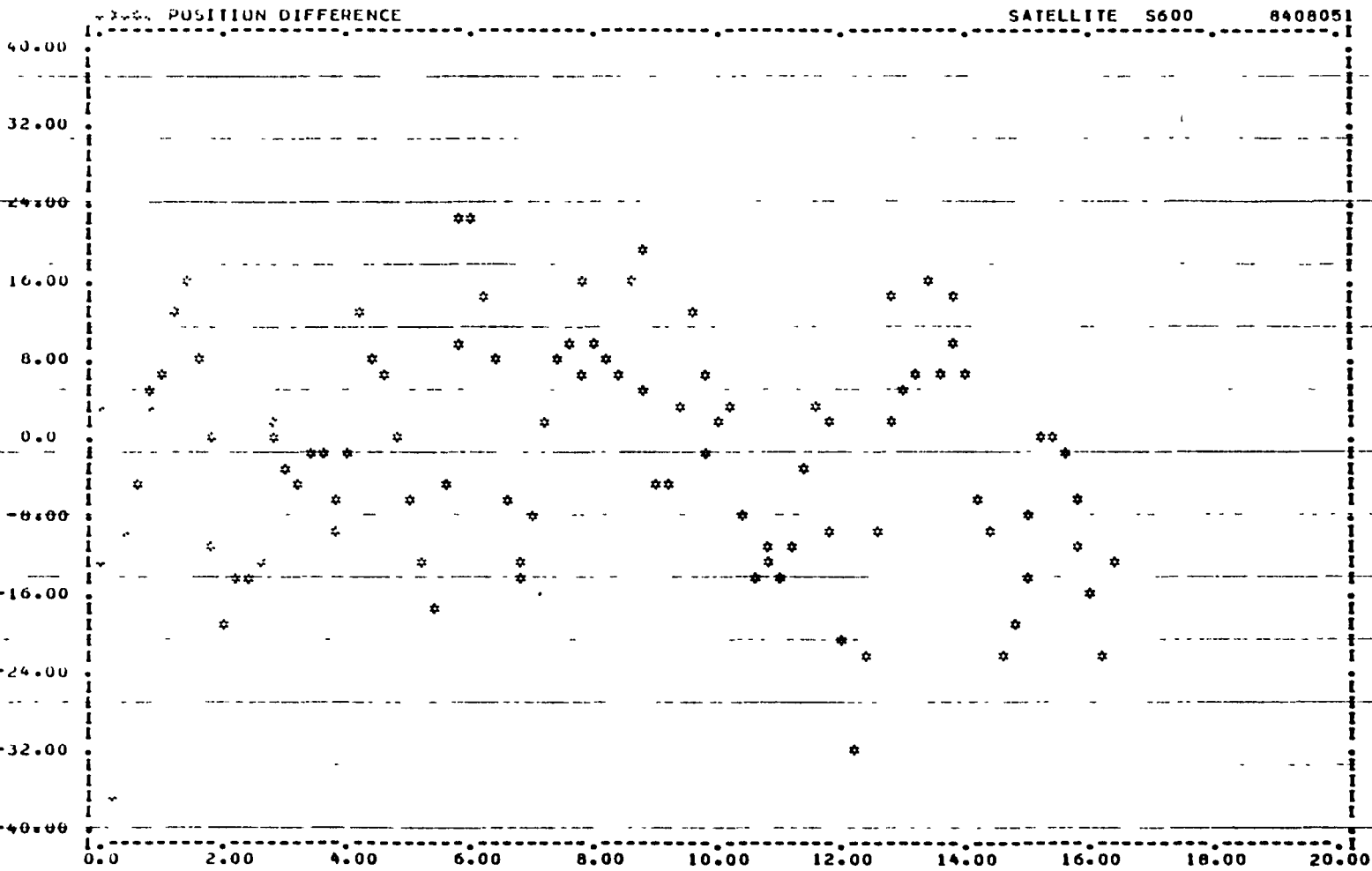
ORIGINAL PAGE IS OF POOR QUALITY

EPHEM FILE ON UNIT 24. DATA RECORDS START AT 861101 0

EPHEM FILE ON UNIT 81. DATA RECORDS START AT 861101 0

USER'S NOTES.....

Figure 3-2. Geopotential (GEM-9/GEM-1 Difference Model) Error Projections in the User Orbit Plane as Determined From R&D GTDS FLBT Simulation (2 of 3)



861101 30000

EPHEM FILE ON UNIT 24, DATA RECORDS START AT 861101 0

EPHEM FILE ON UNIT 81, DATA RECORDS START AT 861101 0

USER'S NOTES.....

Figure 3-2. Geopotential (GEM-9/GEM-1 Difference Model) Error Projections in the User Orbit Plane as Determined From R&D GTDS FLBT Simulation (3 of 3)

3-10

3.3.2 CLOCK ACCELERATION ERROR

The clock acceleration error was determined using the following method. Data were first simulated using the baseline truth model and reduced with the baseline force model; a converged user ephemeris file was then generated. Next, data were again simulated, using the same tracking schedule, but the baseline truth model was modified to exclude user clock acceleration offset. These simulated data were then reduced, using the same baseline force model as before, and a converged ephemeris file was generated. As the final step in determining the user clock acceleration error, the differences between these two user ephemeris files was calculated.

Very good agreement was found for the errors due to clock acceleration between R&D simulation and the SEA error analysis results of the previous study. In this study, a maximum clock acceleration error for FLBT tracking was 26 m; in the previous study, the maximum observed was 30 m. In the error analysis study, it was observed that the clock acceleration error contribution to the range-rate measurement error increases with elapsed time and is generally linear and in the spacecraft alongtrack direction. This study's simulation runs, which are range-rate solutions, are in agreement with those observations.

It should be noted that the present study's R&D solution used an EKF, whereas the previous study used a Kalman Filter (KF).¹ Even with this difference, the simulation and error analysis results show agreement in the interaction

¹The EKF, a variation to the KF, differs in that the solve-for state vector is corrected at each observation instead of waiting until the last observation. Descriptions of the EKF and KF in terms of their implementation in R&D GTDS are provided in Reference 3-5.

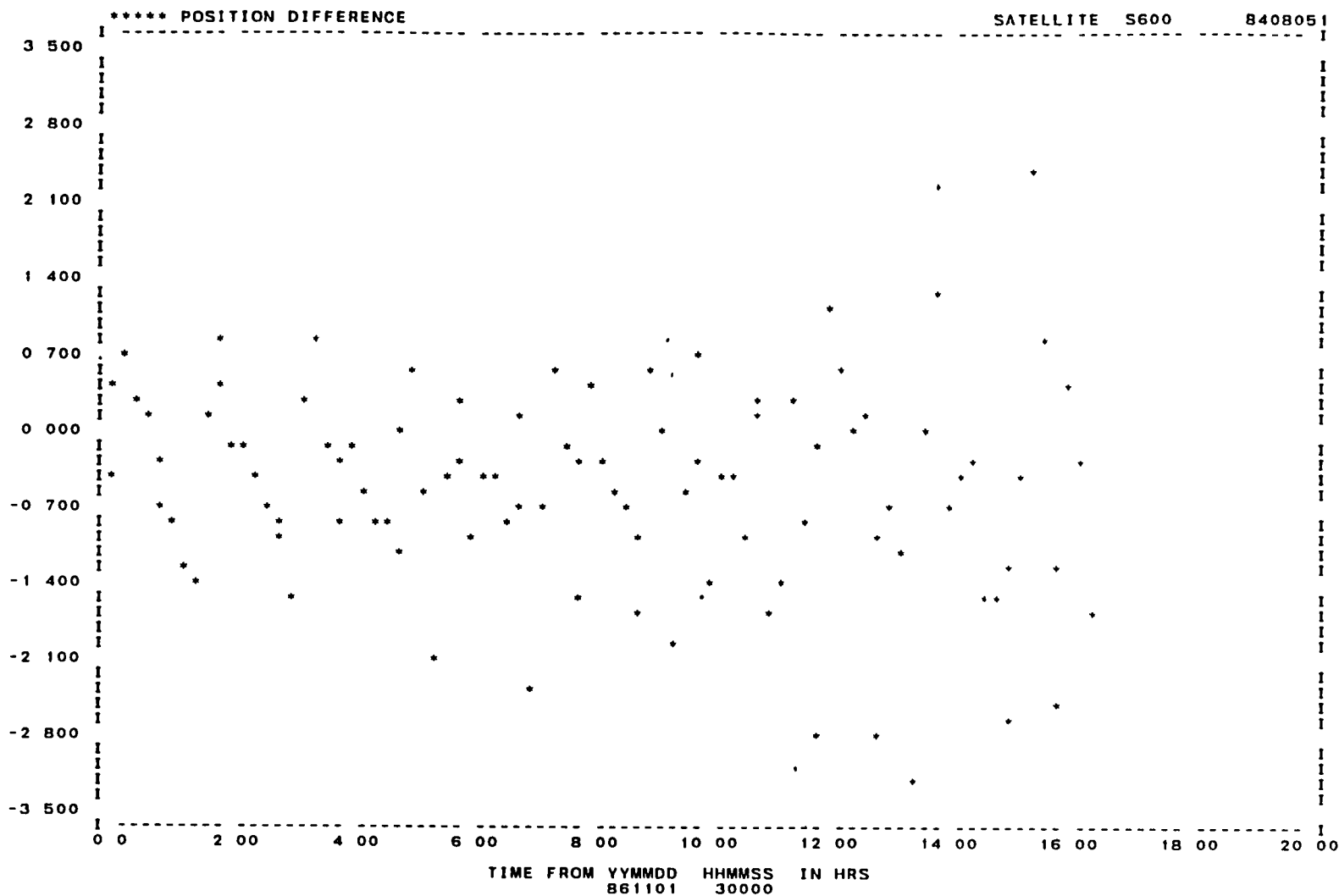
between clock process noise and clock acceleration error observed. The R&D GTDS FLBT results are 26 m compared with SEA's 30 m for clock acceleration error. Figure 3-3 displays ephemeris comparison plots of the contribution of acceleration error resulting from the R&D GTDS FLBT mode.

In addition, simulation and error analysis runs display consistent results if clock drift process noise is not used to compensate for clock errors in the filter. In SEA, when clock drift process noise is absent, clock acceleration causes an error reaching 200 m in an FLBT range-rate orbit solution after 24 hours. In R&D GTDS, simulations under the same scenario give a similarly inflated clock acceleration error of 132 m.

3.3.3 TDAS EPHEMERIS ERROR

R&D GTDS and SEA use slightly different TDAS ephemeris error modeling initialization. As described in Reference 3-1, the satellite ephemeris error model present in SEA is used in R&D GTDS for TDAS satellites. A description of this ephemeris error model and its input is presented in Reference 3-5. In the R&D GTDS implementation, to allow the greatest flexibility possible, the input phase angles θ and ϕ are specified separately for each TDAS relay. In contrast, in SEA, only a single seed--input into a random number generator--is used to specify the phase input initialization for the up to 18 GPS satellites possible. The output of the SEA random number generator has been determined, but because these numbers are real and the input phases into R&D GTDS are integers, an error of up to 0.5 deg can occur. This input mismatch can result in small inconsistencies between R&D GTDS and SEA ephemeris error contributions. In the case of small phase angles, this mismatch is enlarged because of the trigonometric functions involved. Nevertheless, close agreement is seen between the

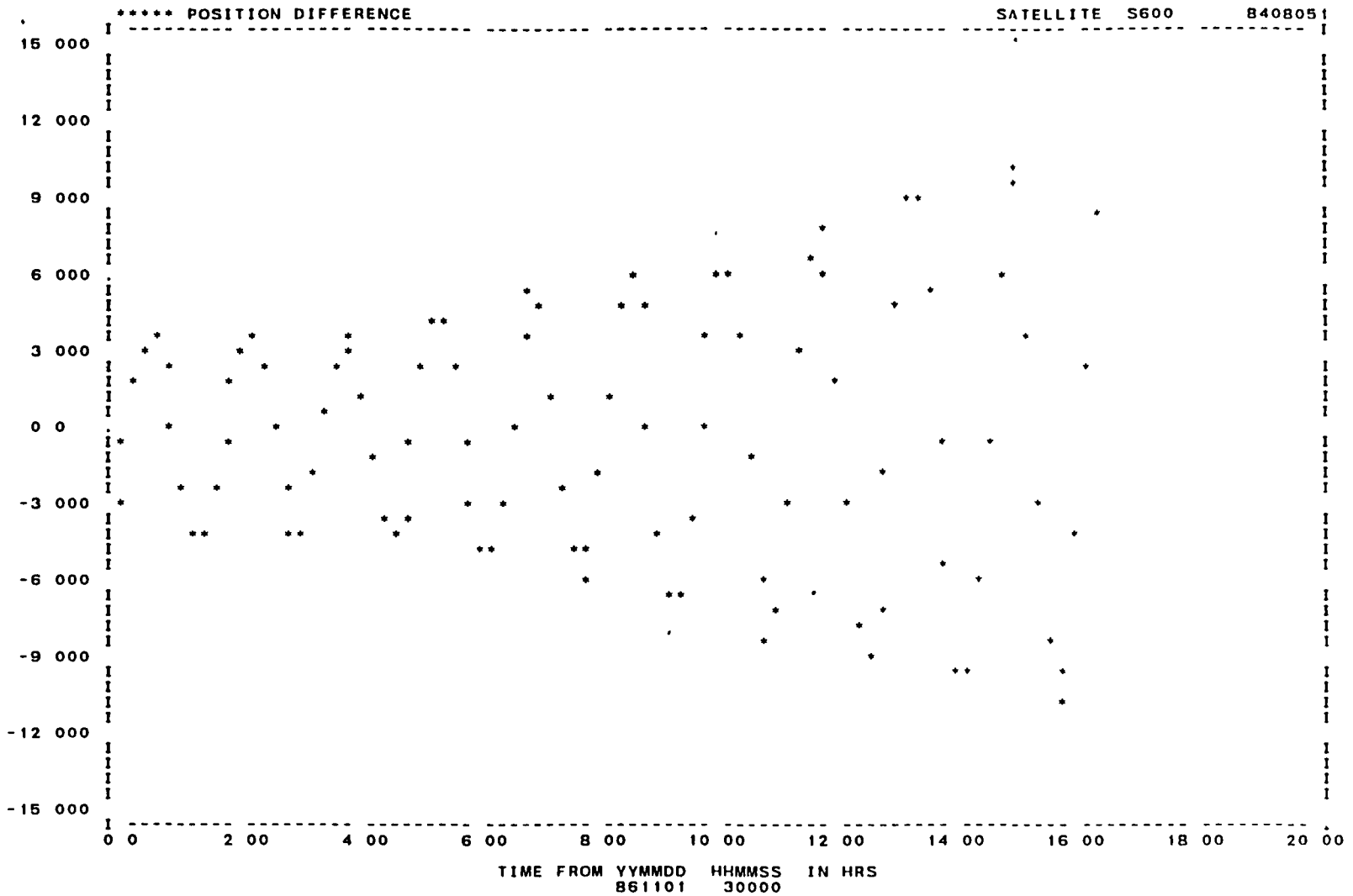
3-13
RADIAL DIFFERENCES IN METERS



EPHEM FILE ON UNIT 24, DATA RECORDS START AT 861101 0
 EPHEM FILE ON UNIT 81, DATA RECORDS START AT 861101 0

USER'S NOTES

Figure 3-3. User Clock Acceleration Error Projections in the User Orbit Plane as Determined From R&D GTDS FLBT Simulation (1 of 3)

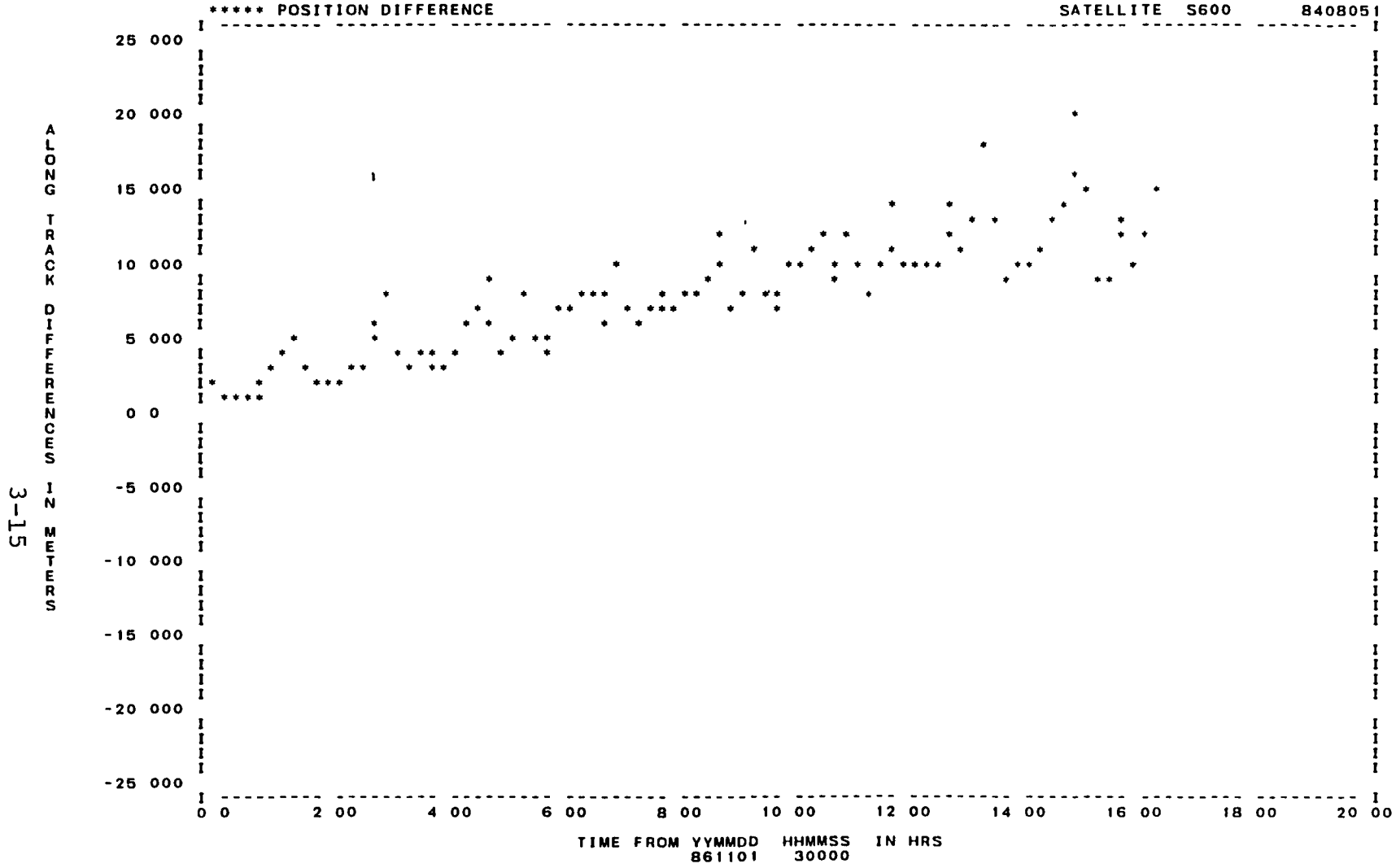


EPHEM FILE ON UNIT 24, DATA RECORDS START AT 861101 0
 EPHEM FILE ON UNIT 81, DATA RECORDS START AT 861101 0

USER'S NOTES

3-14

Figure 3-3. User Clock Acceleration Error Projections in the User Orbit Plane as Determined From R&D GTDS FLBT Simulation (2 of 3)



EPHEM FILE ON UNIT 24, DATA RECORDS START AT 861101 0
 EPHEM FILE ON UNIT 81, DATA RECORDS START AT 861101 0

USER'S NOTES

Figure 3-3. User Clock Acceleration Error Projections in the User Orbit Plane as Determined From R&D GTDS FLBT Simulation (3 of 3)

simulation and error analysis results for the contribution of TDAS ephemeris error.

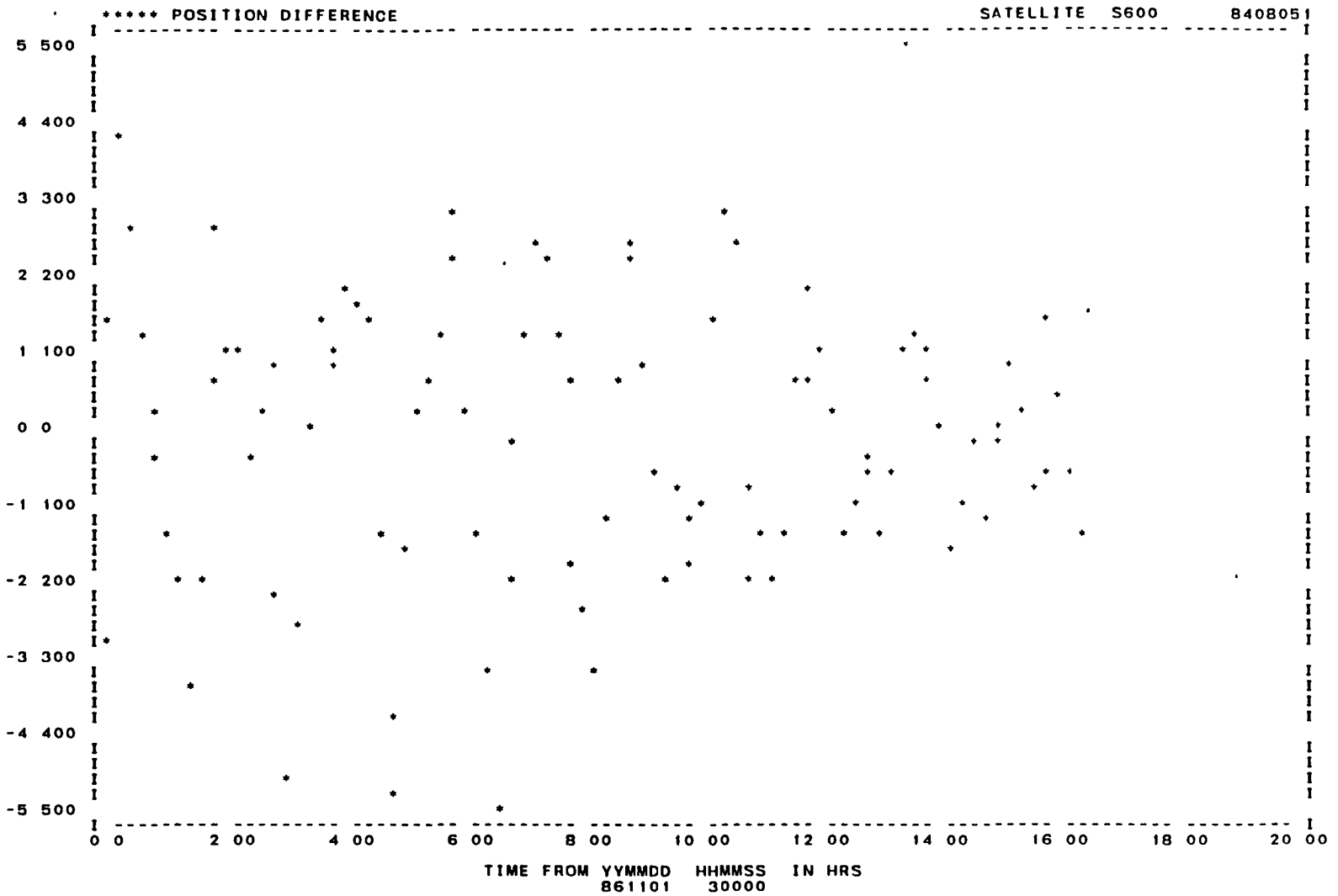
In R&D GTDS, the method of determining the contribution to TDAS ephemeris error is similar to that used in determining clock acceleration error. Specifically, instead of using the baseline truth model without clock acceleration, data are simulated without TDAS ephemeris error. The data are reduced using the baseline force model, and the converged ephemeris is then compared with an ephemeris generated using the baseline truth and force models.

From SEA, the contribution from TDAS ephemeris error is 23 m; from R&D GTDS simulation results for the FLBT mode, this error is 19 m. The ephemeris error, as shown in Figure 3-4, has its largest contribution in the alongtrack direction where it increases rapidly at first but then appears to saturate or display very slow growth. Similar signatures are seen in the SEA error analysis results.

3.3.4 ERROR RESULTS WITH LESS FREQUENTLY SAMPLED DATA

Previous error analysis results show that systematic error is the dominant error source. Little performance degradation would therefore be expected if the tracking data are reduced by sampling. Error analysis results also indicate that there is very little difference in navigation performance if tracking data are sampled and processed at 3-min intervals instead of the 20-sec intervals used in the baseline scenario. This observation is similarly verified in this study's simulation results. In varying the sample rate, the observation weights must, however, be properly scaled to offset the increase in the navigation error covariance resulting from the rarefied tracking data. Alternately, as employed in the SEA error analysis study, the change in sample rate may be compensated for through scaling the process noise.

SATELLITE S600 8408051

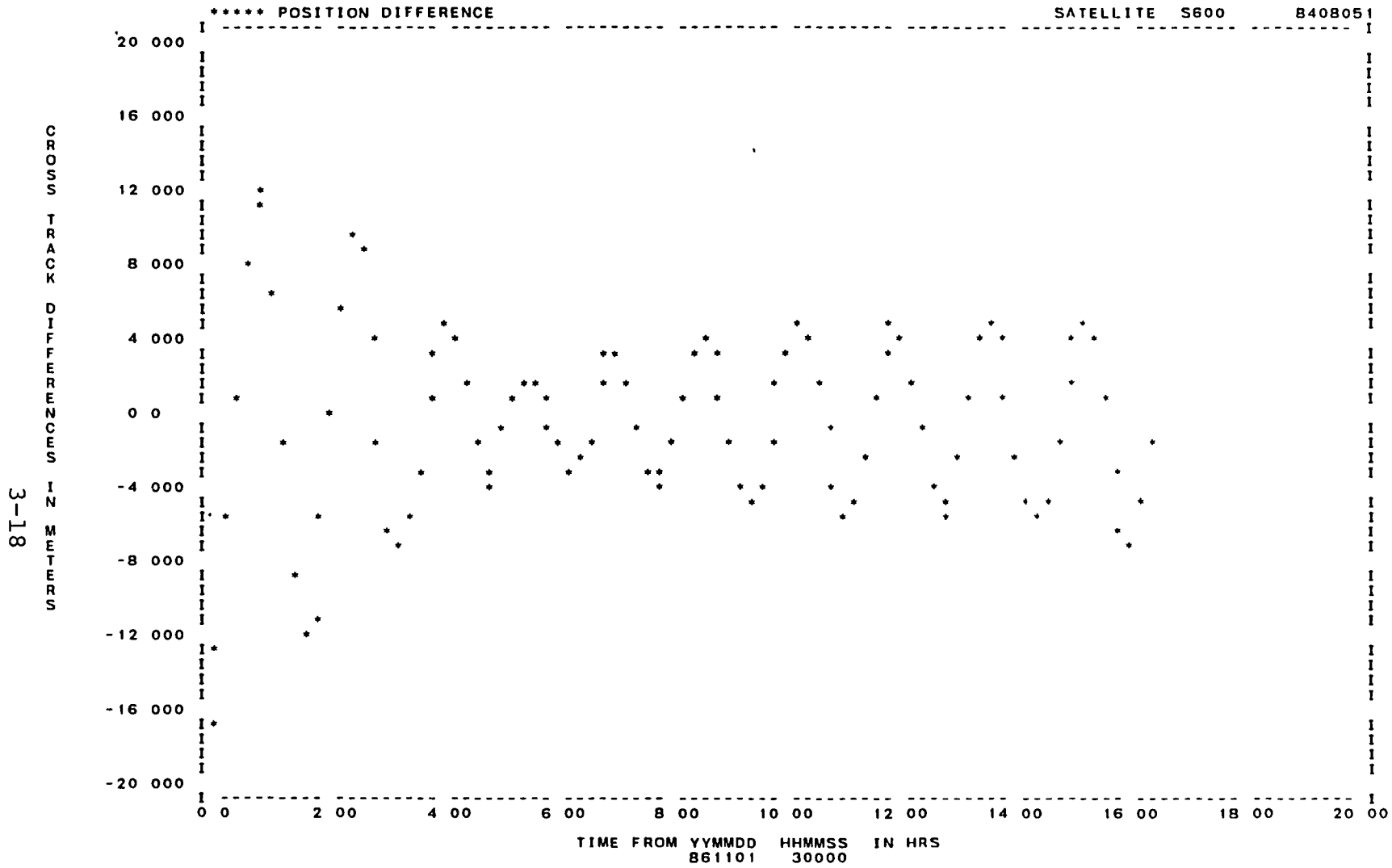


EPHEM FILE ON UNIT 24, DATA RECORDS START AT 861101 0

EPHEM FILE ON UNIT 81, DATA RECORDS START AT 861101 0

USER'S NOTES

Figure 3-4. TDAS Ephemeris Error Projections in the User Orbit Plane as Determined From R&D GTDS FLBT Simulation (1 of 3)



3-18
CROSS TRACK DIFFERENCES IN METERS

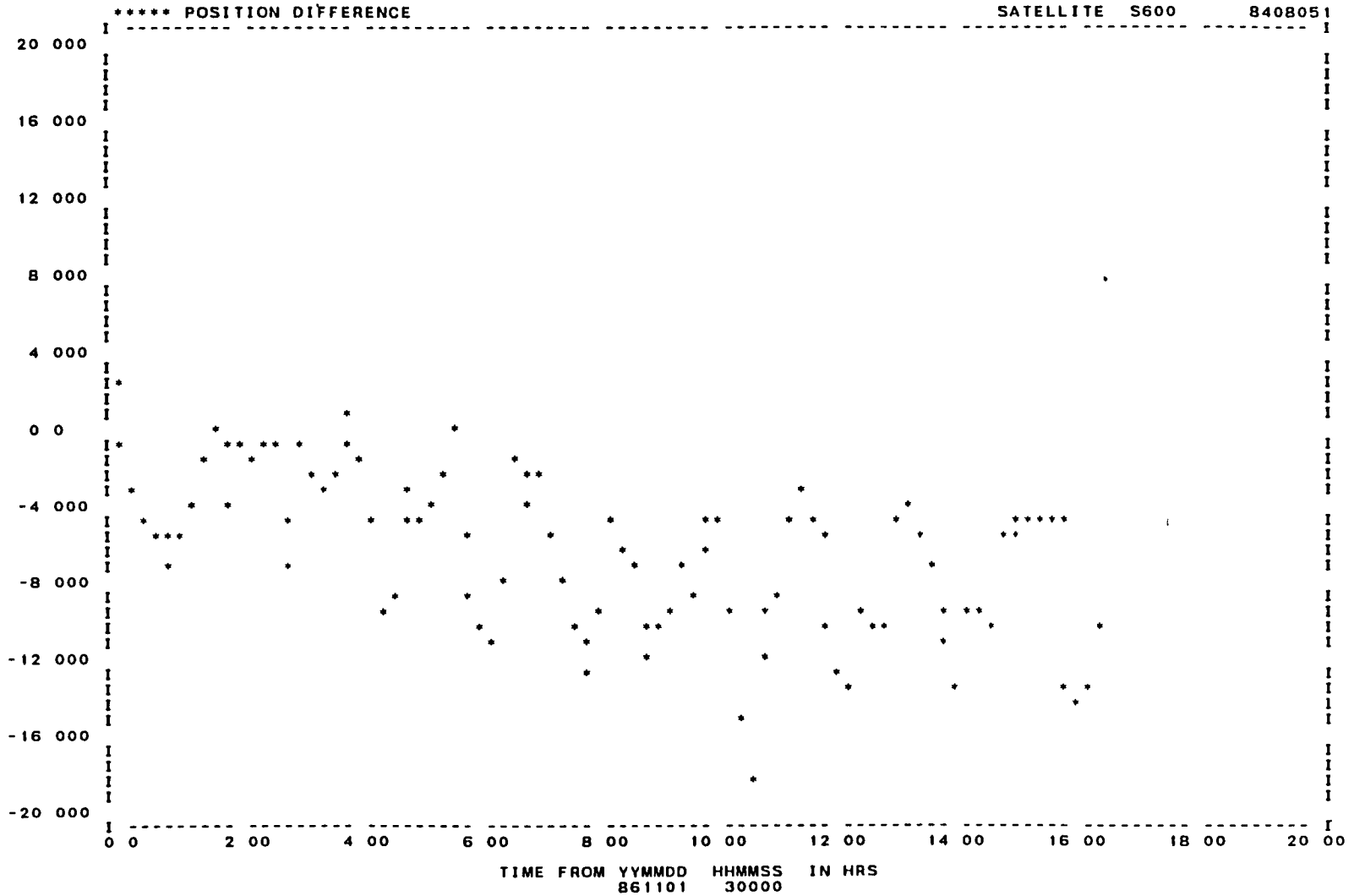
EPHEM FILE ON UNIT 24, DATA RECORDS START AT 861101 0

EPHEM FILE ON UNIT 81, DATA RECORDS START AT 861101 0

USER'S NOTES

Figure 3-4. TDAS Ephemeris Error Projections in the User Orbit Plane as Determined From R&D GTDS FLBT Simulation (2 of 3)

3-19
ALONG TRACK DIFFERENCES IN METERS



EPHEM FILE ON UNIT 24, DATA RECORDS START AT 861101 0

EPHEM FILE ON UNIT 81, DATA RECORDS START AT 861101 0

USER'S NOTES

Figure 3-4. TDAS Ephemeris Error Projections in the User Orbit Plane as Determined From R&D GTDS FLBT Simulation (3 of 3)

3.3.5 COMPARISON BETWEEN FLBT AND FLST TRACKING MODES

In agreement with the SEA error analysis results, this study's FLST simulation results displayed navigation performance inferior to that in the FLBT mode. Table 3-2 contrasts the error contributions in the two modes and their comparison with the results obtained from the SEA error analysis. The error analysis and simulation results display the same increasing trend in geopotential error contribution from FLBT to FLST mode. R&D and SEA results also show that clock acceleration error is reduced in the FLST mode.

As discussed in the error analysis study, caution must be exercised in comparing FLST and FLBT results directly because the two modes have different amounts of tracking but nonetheless use the same baseline process noise. In addition, in comparing R&D GTDS simulation results with the previous SEA error analysis results, a certain amount of caution must be exercised because R&D GTDS employs an EKF whereas SEA uses a KF. The difference in processing between the two types of filters may cause some of the differences between the error analysis and simulation results, specifically the errors seen for TDAS ephemeris.

3.4 CONCLUSIONS

Surprising agreement is seen between R&D GTDS simulation results and SEA error analysis results for a 600-km altitude and 28-deg-inclination spacecraft for both the FLST and FLBT modes. The agreement is a confirmation of the error analysis results and provides confidence in the methods used in the SEA error analysis program and the meaningfulness of its results. Because it directly parallels the actual orbit determination process, there is no direct substitution for the method of simulation and orbit determination used in this study. In comparison to SEA, simulation systems such as R&D GTDS are much larger and more environmentally

Table 3-2. Navigation Error Comparison Between R&D GTDS Simulation and Previous SEA Error Analysis Results

ERROR SOURCE	MAXIMUM POSITION ERROR (m) DURING 24 HOURS OF NAVIGATION FOR TWO TRACKING MODES					
	FLST			FLBT		
	SEA ^a	R&D GTDS		SEA ^a	R&D GTDS	
	20 SEC	180 SEC	20 SEC	20 SEC	180 SEC	20 SEC
GEPOTENTIAL (GEM-9/GEM-1 DIFFERENCE MODEL)	63	87.2	93.5	38	42.2	^b
CLOCK ACCELERATION	17	14.8	14.8	30	24.3	25.6
TDAS EPHEMERIS	23	20.8	21.4	23	15.5	18.6

0112 (131-a)/85

^aSEA RESULTS WERE REPORTED FOR ONLY THE 20-SEC OBSERVATION SAMPLING FREQUENCY

^bRUN WAS NOT PERFORMED

dependent, and so they are inherently more difficult to use and are computationally more expensive. The consistency of this study's simulation results with previous error analysis would therefore suggest that, after suitable calibration between simulation and error analysis has been ensured, efficiency of effort may be obtained in performing the majority of the navigation analysis with an error analysis program such as SEA.

3.5 REFERENCES

- 3-1. Computer Sciences Corporation, CSC/TM-84/6077, Tracking and Data Acquisition System/Global Positioning System (TDAS/GPS) Navigation Analysis, E. Seifert and P. R. Pastor, September 1984
- 3-2. --, CSC/TM-84/6161, Satellite Orbit Determination Using Tracking and Data Acquisition System/Global Positioning System, P. R. Pastor, December 1984
- 3-3. Stanford Telecommunications Inc., STI/E-TR-25066, Tracking and Data Acquisition System (TDAS) for the 1990's, B. Elrod, A. Jacobsen, R. Cook, and R. Singh, May 1983
- 3-4. Computer Sciences Corporation, CSC/TM-83/6138, Tracking and Data Relay Satellite System/Global Positioning System (TDRSS/GPS) Navigation Analysis, E. Seifert and M. Mallick, September 1983
- 3-5. --, CSC/SD-84/6057, Sequential Orbit-Determination Error Analysis Program (SEA) Programmer's Reference and User's Guide (Revision 1) Volume 1, P. R. Pastor, December 1984

SECTION 4 - LUMPED GEOPOTENTIAL MODEL FOR GEM-9

The following spherical harmonic representation of the geopotential is generally recognized as the most convenient for orbital analysis:

$$V = \frac{GM}{r} \left[1 + \sum_{\ell=2}^{\infty} \sum_{m=0}^{\ell} \frac{a_e}{r}{}^{\ell} P_{\ell m}(\sin \phi) (C_{\ell m} \cos m\lambda + S_{\ell m} \sin m\lambda) \right] \quad (4-1)$$

where GM = geocentric gravitational constant
a_e = mean equatorial radius of the Earth
P_{ℓm} = normalized associated Legendre function of degree ℓ and order m
r, φ, λ = distance to the center of the Earth, latitude, and longitude
C_{ℓm}, S_{ℓm} = normalized spherical harmonic coefficients

The quantity GM provides a scale for the whole field; a_e provides a scale for the altitude dependence, r; and C_{ℓm} and S_{ℓm} characterize the geographic, or nonspherical, variations. A geopotential model is defined by these parameters. Of necessity, the field is truncated at some finite degree and order. Over the years, NASA/GSFC has developed a series of progressively more accurate GEMs based on satellite tracking data, satellite-borne altimetry, and surface gravimetry. GEM-10B (Reference 4-1), complete to degree and order 36 by 36, is currently the most accurate model. The Goddard Trajectory Determination System (Reference 4-2), which is used for operational orbit determination at GSFC, has provisions for GEM-9 (Reference 4-3) further truncated to degree and order 21 by 21.

Even with accurate geopotential models such as GEM-9 and GEM-10B, the uncertainty in these models remains a major error source for low-altitude Earth satellite orbit determination. Geopotential error arises because of truncation (omission error) and because of errors in the spherical harmonic coefficients (commission error). Generally, with the derivation of a GEM, an error covariance matrix describing the uncertainties and correlations of the spherical harmonic coefficients is a standard byproduct. In principle, it would be straightforward to use this covariance matrix in linear error analysis to compute the effect of commission error on satellite orbit determination accuracy. However, the size of the covariance matrix makes this approach prohibitively expensive in computations.

As a simpler alternative, a so-called lumped geopotential error model was suggested (Reference 4-4) and implemented in orbit determination error analysis programs. Briefly, this approach takes the weighted differences of the geopotential coefficients of two independent geopotential models and computes the orbit determination error resulting from the lumped effect of these differences. Subsequently, standard deviations, which are the scaled-up formal uncertainties of GEM spherical harmonic coefficients, were used in place of the coefficient differences. The theoretical objection to the use of standard deviations was first raised in Reference 4-5. Its practical inadequacy was brought out in vivid graphical displays in Reference 4-6.

Section 4.1 describes the rationale of the lumped geopotential error model. Section 4.2 discusses the global distribution of gravity error for different geopotential error models. Section 4.3 discusses navigation and orbit prediction errors introduced by geopotential uncertainty. Section 4.4 compares results obtained using TDRS data with

those from the lumped geopotential error model for GEM-9. Section 4.5 presents conclusions.

4.1 THE LUMPED ERROR MODEL

The derivation of each GEM is always accompanied by a careful error analysis to assess its accuracy. Reference 4-7 on GEM-7 and GEM-8 is an outstanding example of the conscientiousness and thoroughness associated with such assessments. Analyses of GEM-9 and GEM-10 accuracies are available in References 4-3 and 4-1, respectively. Reference 4-8 contains a discussion of gravity model improvement and its implications for operational orbit determination.

As discussed before, each GEM is accompanied by an error covariance matrix associated with the geopotential coefficients. The covariance matrix is computed based on assumed precisions of tracking and other data from which the geopotential is derived. Because not all error sources in tracking data and in spherical harmonic coefficient estimation methods can be accounted for, the computed error covariance is not a true indication of the accuracy of the spherical harmonic coefficients. Part of the objective of geopotential model accuracy analysis is to derive a calibration factor, which is used to scale up the standard deviations from the error covariances to more realistic levels. The calibration factor is typically around 3.3.

One of the obvious methods of assessing a geopotential model is to compare it with other independently derived geopotential models. The lumped geopotential error model, first proposed by Martin and Roy (Reference 4-4), takes one-half the differences of two uncorrelated models of comparable accuracy as a measure of the accuracies of the individual models. The rationale can be explained as follows. Let $(C_{\ell m})_{\text{model A}}$ and $(C_{\ell m})_{\text{model B}}$ be the geopotential coefficients of the two models. If the two models are uncorrelated

but of comparable accuracy, their average is closer to the truth, i.e.,

$$(C_{\ell m})_{\text{truth}} \approx \frac{1}{2} \left[(C_{\ell m})_{\text{model A}} + (C_{\ell m})_{\text{model B}} \right] \quad (4-2)$$

and an estimate of the individual errors can be obtained as

$$\begin{aligned} (\Delta C_{\ell m})_{\text{model A}} &= (C_{\ell m})_{\text{model A}} - (C_{\ell m})_{\text{truth}} \\ &\approx \frac{1}{2} \left[(C_{\ell m})_{\text{model A}} - (C_{\ell m})_{\text{model B}} \right] \end{aligned} \quad (4-3)$$

Of course, an estimate using the sample mean based on only two samples, as in Equation (4-3), is not very reliable. The lumped model introduces additional samples or statistics by considering not a single $C_{\ell m}$ but the whole set of $C_{\ell m}$'s and $S_{\ell m}$'s in the geopotential model. In other words, it is not saying that $\Delta C_{\ell m}$ as given in Equation (4-3) is a good indicator of the accuracy of individual coefficients, but that the aggregate effect of all $\Delta C_{\ell m}$'s on the computed orbit is a reasonable representation of the effect of the geopotential uncertainty on orbit determination.

The key assumption of the lumped model is the requirement that the two models be uncorrelated. This generally means that the models be derived by two different organizations based on different data sets. It also implies that this lumped model does not adequately represent omission errors. The assumption that the two models are of equal accuracy is not essential, as the simple average in Equation (4-3) can be replaced by a weighted average. In the spirit of minimum variance estimators, the weights can be chosen to be inversely proportional to the variances of the individual

models. In practice, an educated guess or external calibration can be used to assign the weights.

The lumped model has been used in many orbit determination error analysis studies, perhaps not so much because it is a good model but because nothing better is available. Part of the difficulty of this approach is the availability of independent models. In a study (Reference 4-9) of onboard orbit determination using GEM-9 truncated to various degrees, it was suggested that the lumped model be used to represent the uncertainty in the truncated GEM-9 as follows: GEM-9 standard deviations would be used to represent the uncertainties of those spherical harmonic coefficients retained in the truncated model, and truncation errors would be represented by the truncated high degree and order GEM-9 spherical harmonic coefficients themselves. There are two theoretical objections (Reference 4-5) to the use of standard deviations instead of coefficient differences in the lumped model:

- The errors in the geopotential coefficients are likely to have both positive and negative signs, whereas the standard deviations are all positive.
- The standard deviations do not contain information about correlations among the coefficients.

It may be argued that, because the primary interest is in orbit determination errors, rather than in the errors in the geopotential coefficients, the use of the positive standard deviations may not be objectionable if the orbit error sensitivities to these coefficients are randomly distributed to serve to randomize their aggregate effect. Elrod, however, showed that this is not the case (Reference 4-6). Figure 4-1, reproduced from Reference 4-6, shows that the use of GEM-9 standard deviations results in a nonuniform global distribution of gravitational acceleration errors that is greater in the Northern Hemisphere with a singularity near

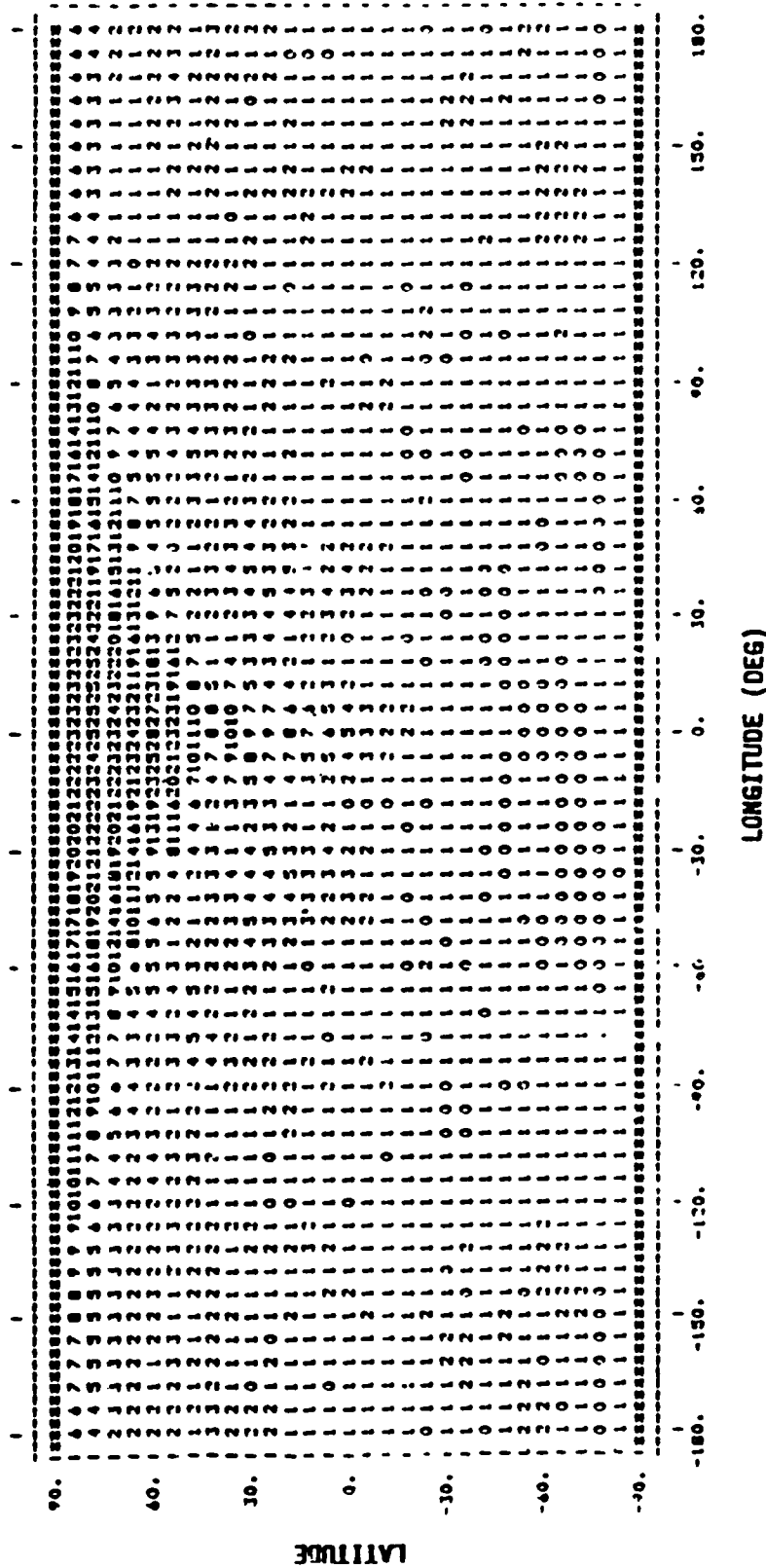


Figure 4-1. Global Distribution of Gravitational Acceleration Uncertainties at an Altitude of 200 Kilometers, Computed From the Lumped Geopotential Error Model Using GEM-9 Standard Deviations (Numbers on the map represent gravitational acceleration uncertainties in mgals (10^{-5} meter per second²) rounded to the nearest integer.)

0 deg longitude and 60 deg latitude. Such anomalous distribution is not supported by other evidence. Furthermore, Elrod showed that the anomaly does not occur if the rss result is obtained rather than the algebraic sum of the lumped error model. There is no question that the use of GEM-9 standard deviations in the lumped error model is faulty. The effect of false singularity is perhaps not serious for error analysis of the batch orbit determination method, but it can exaggerate local navigation errors in sequential navigation methods.

Because the standard deviations do not convey information about correlations, an obvious alternative is to assume that all errors in the spherical harmonic coefficients of a geopotential are uncorrelated. The total error of the geopotential model can thus be obtained as the rss of the error contribution of individual coefficients. Although it is known that certain geopotential coefficients are highly correlated, this model is perhaps as reasonable as any, short of having to consider the actual correlations. The major drawback of this model is the excessive amount of computation required to compute separately the error contributions of individual error coefficients, versus the spirit of the lumped error model. At best, only the level of orbit determination error resulting from geopotential uncertainty can be expected; therefore, the computationally expensive rss approach may not be justifiable, and simpler alternatives would be desirable. The following alternatives are proposed as candidates for study:

- Random-Sign Method--The lumped model will use the GEM-9 standard deviations, with positive and negative signs randomly assigned to them.

• Random-Phase Method--The terms involving the spherical harmonic coefficients in the geopotential representation, Equation (4-1), may be written as

$$C_{\ell m} \cos m\lambda + S_{\ell m} \sin m\lambda = \sqrt{C_{\ell m}^2 + S_{\ell m}^2} \cos (m\lambda - \phi_m) \quad (4-4)$$

In this method, the amplitudes

$$\sqrt{C_{\ell m}^2 + S_{\ell m}^2}$$

are computed from GEM-9 standard deviations, but the phase angles, ϕ_m , are selected from a uniform random distribution between 0 and 2π (for zonals, the phase is randomly chosen as 0 or π , i.e., random sign).

In addition to these models dependent on internal accuracy estimates, two geopotential models uncorrelated with GEM-9 are used in conjunction with GEM-9 to form geopotential difference error models. One of these is the 1969 Smithsonian Astrophysical Observatory (SAO) Standard Earth (Reference 4-10), referred to as the SAO model below. The other will be referred to as the MD1 model. One-half of the difference of this model and GEM-5 has been considered representative of the accuracy of GEM-5 (Reference 4-11). Both the SAO and MD1 models are inferior to GEM-9 in accuracy.

4.2 GLOBAL DISTRIBUTION OF GRAVITY ERROR FOR DIFFERENT GEOPOTENTIAL ERROR MODELS

The gravitational acceleration as specified by a geopotential model will have errors that vary with the geographical location (longitude and latitude) and decrease with the altitude. A gravity error map such as that illustrated in Figure 4-1 shows the magnitude (but not the direction) of

the gravitational acceleration error at a given altitude as a function of longitude and latitude, as predicted by a geopotential error model. Different error models give rise to different error characteristics. Of interest are orders of magnitude and geographical fluctuations of the errors. Figures 4-2 through 4-22 are gravity error maps at 200-, 400-, and 600-km altitudes for the following geopotential error models:

- GEM-9/MD1 one-half difference model
- GEM-9/SAO one-half difference model
- GEM-9/GEM-5 difference model
- GEM-5/MD-1 one-half difference model
- GEM-9 standard deviation model
- GEM-9 random sign model
- GEM-9 random-phase model
- GEM-9 uncorrelated model

The difference models, discussed in Section 4.1, are self-explanatory. The GEM-9 standard deviation model uses positive GEM-9 standard deviations as spherical harmonic error coefficients. The gravity error map for this model at 200-km altitude is shown in Figure 4-1, so only the maps at 400- and 600-km altitudes are shown here. The random-sign and random-phase models are also explained in Section 4.1. A number of variants of these models were also considered, but they did not show significant difference from those described here. The uncorrelated model is based on the rss of the contributions of individual coefficients; computing these errors is expensive, and the gravity error maps were taken from Reference 4-6. To provide a reference for gauging the magnitudes of gravity errors, Figure 4-23 shows a map representing the gravitational acceleration (not the error) resulting from the nonaxisymmetric (i.e., the nonzonal) portion

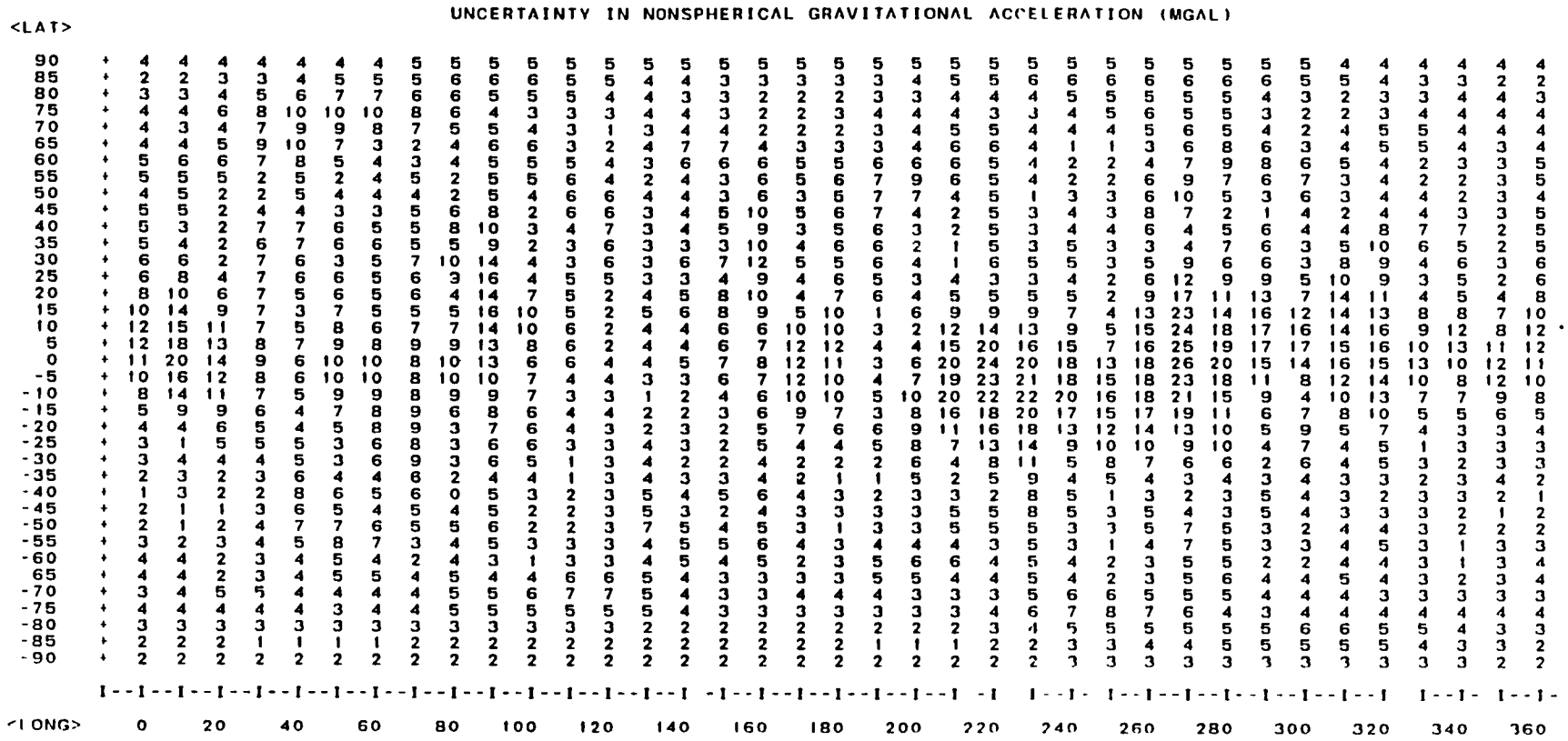


Figure 4-2. GEM-9/MD1 One-Half Difference Model, 200-Kilometer Altitude

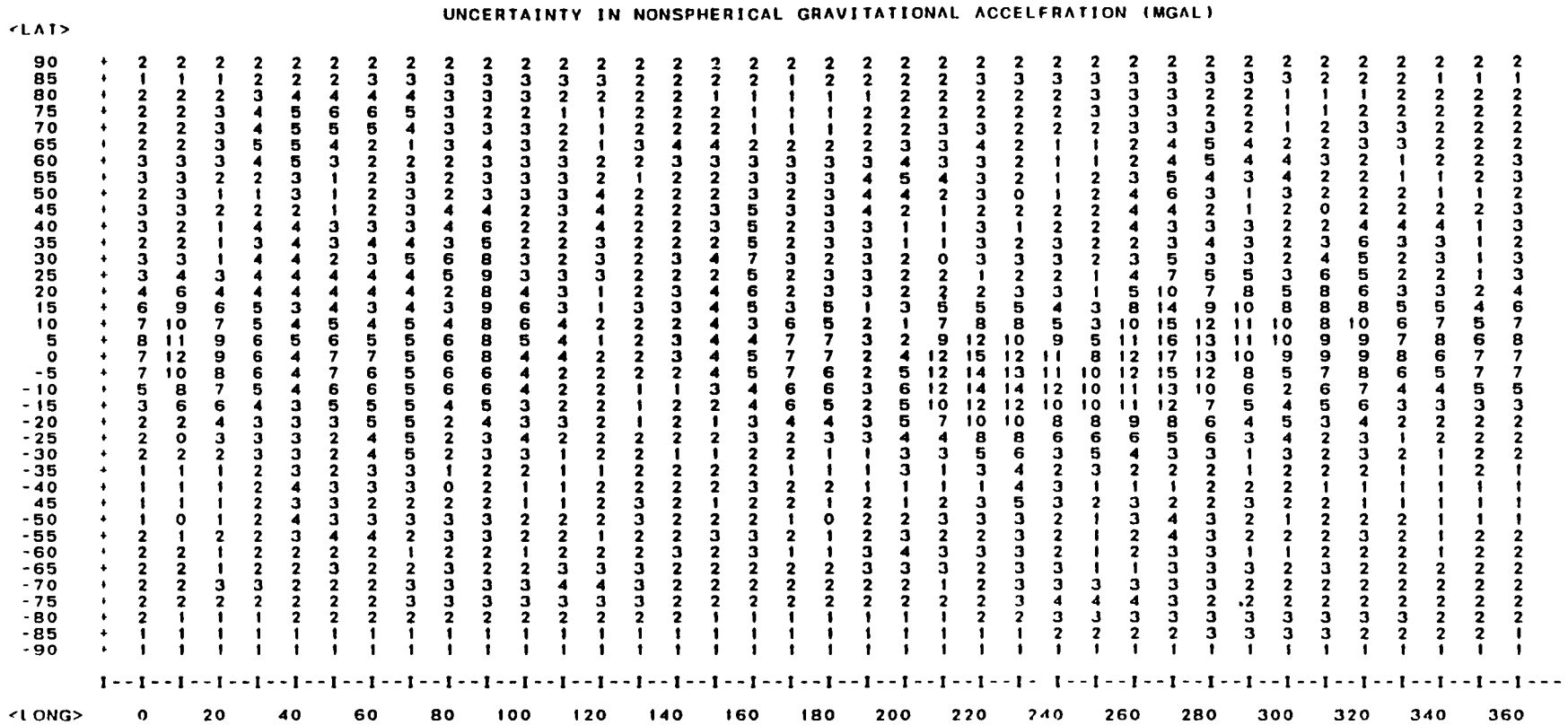


Figure 4-3. GEM-9/MD1 One-Half Difference Model, 400-Kilometer Altitude

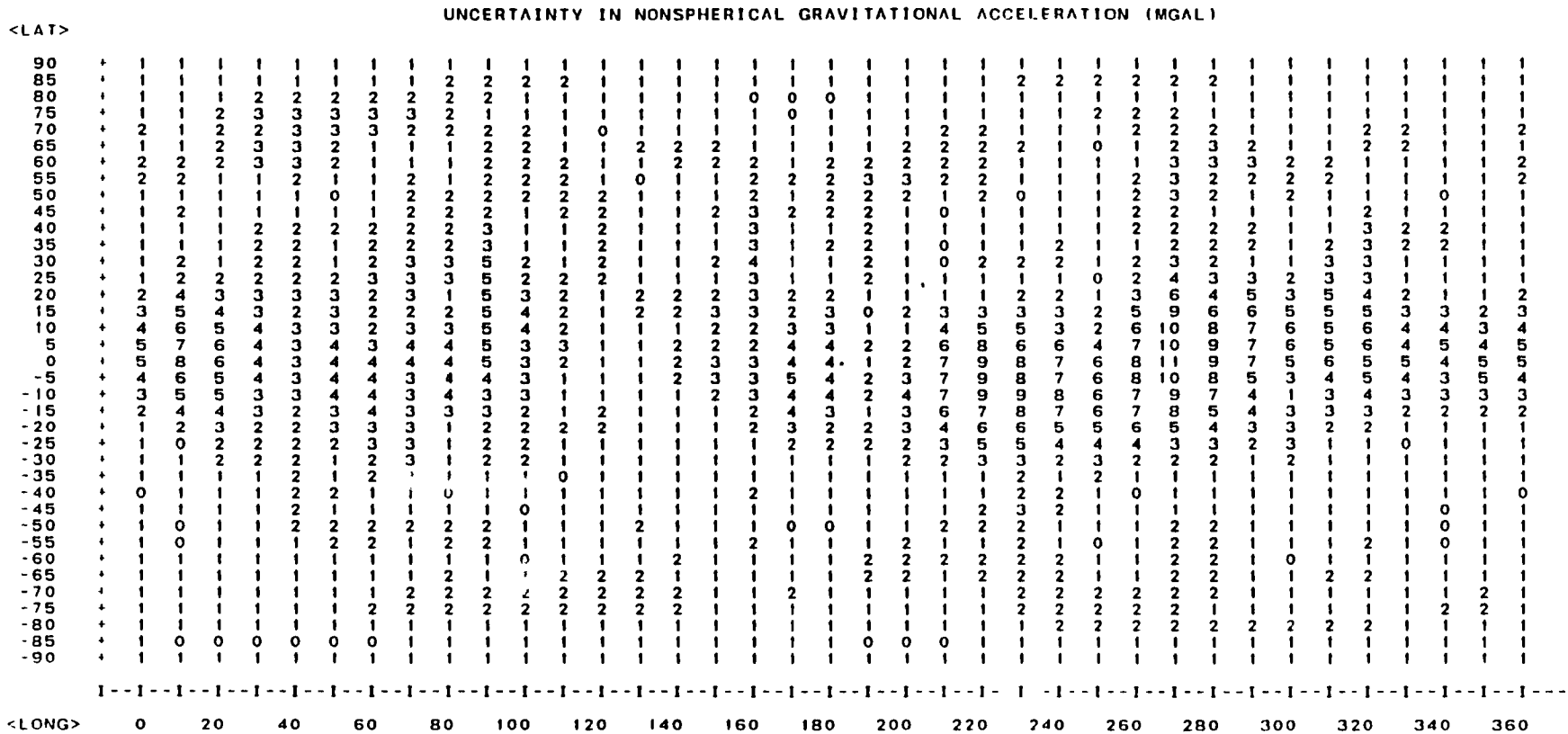
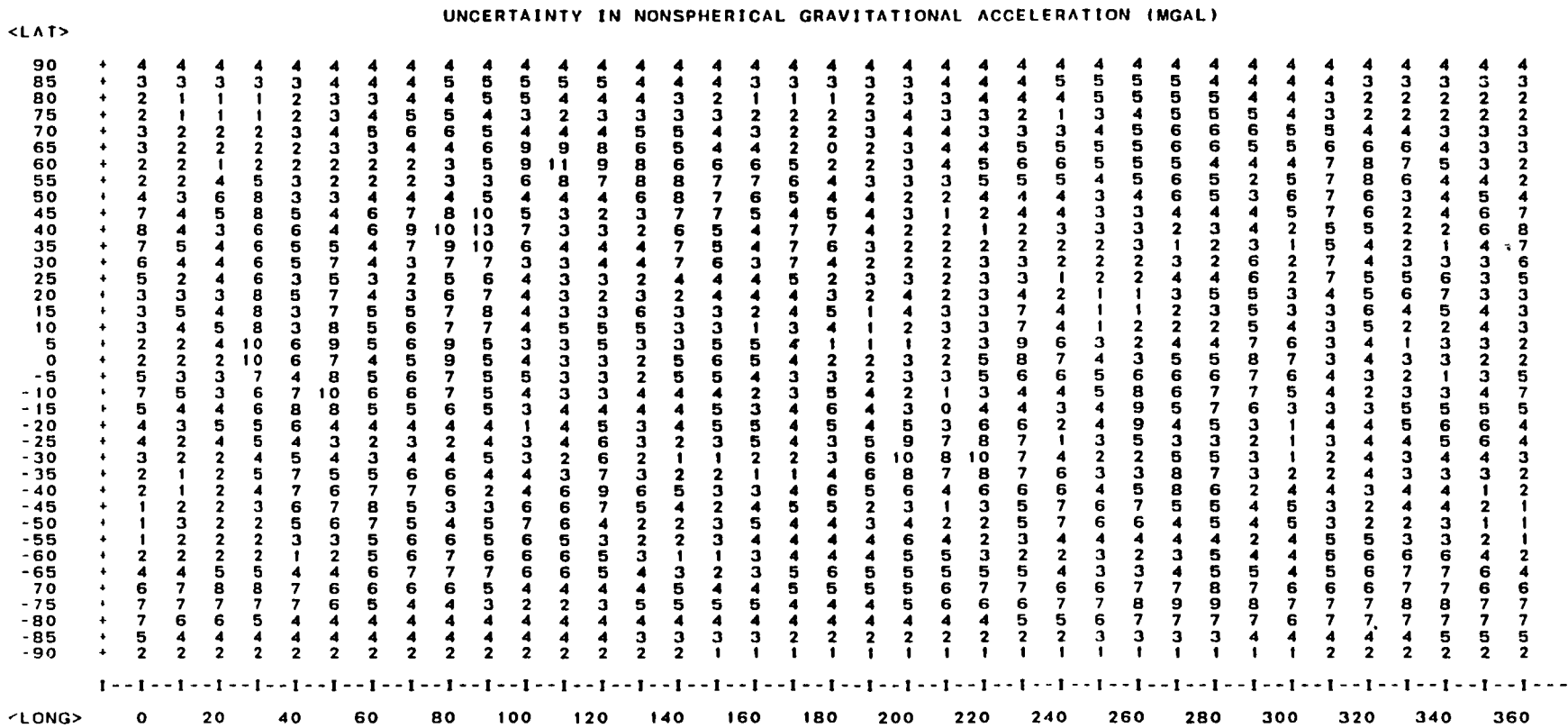


Figure 4-4. GEM-9/MD1 One-Half Difference Model, 600-Kilometer Altitude



ORIGINAL PAGE IS OF POOR QUALITY

Figure 4-5. GEM-9/SAO One-Half Difference Model, 200-Kilometer Altitude

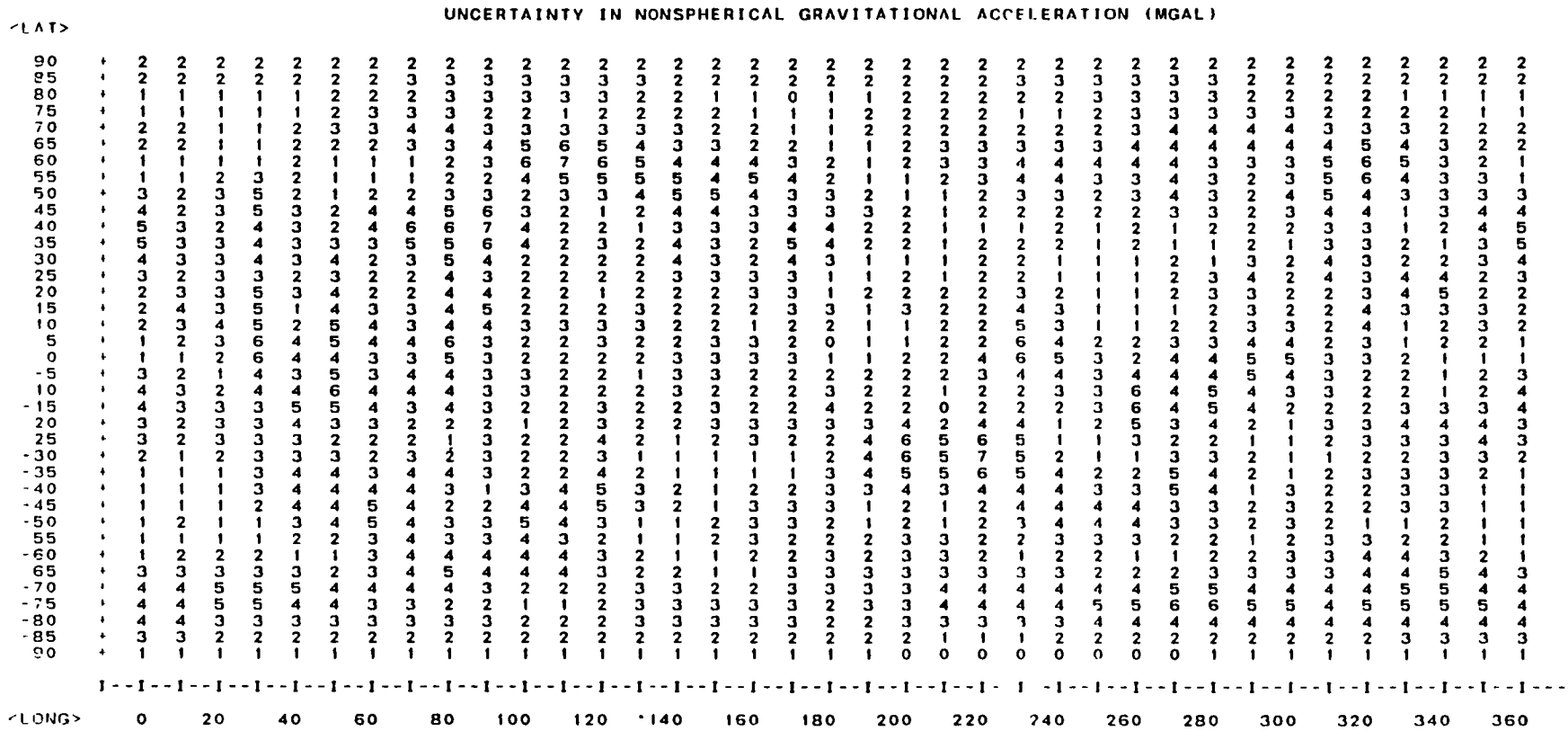


Figure 4-6. GEM-9/SAO One-Half Difference Model, 400-Kilometer Altitude

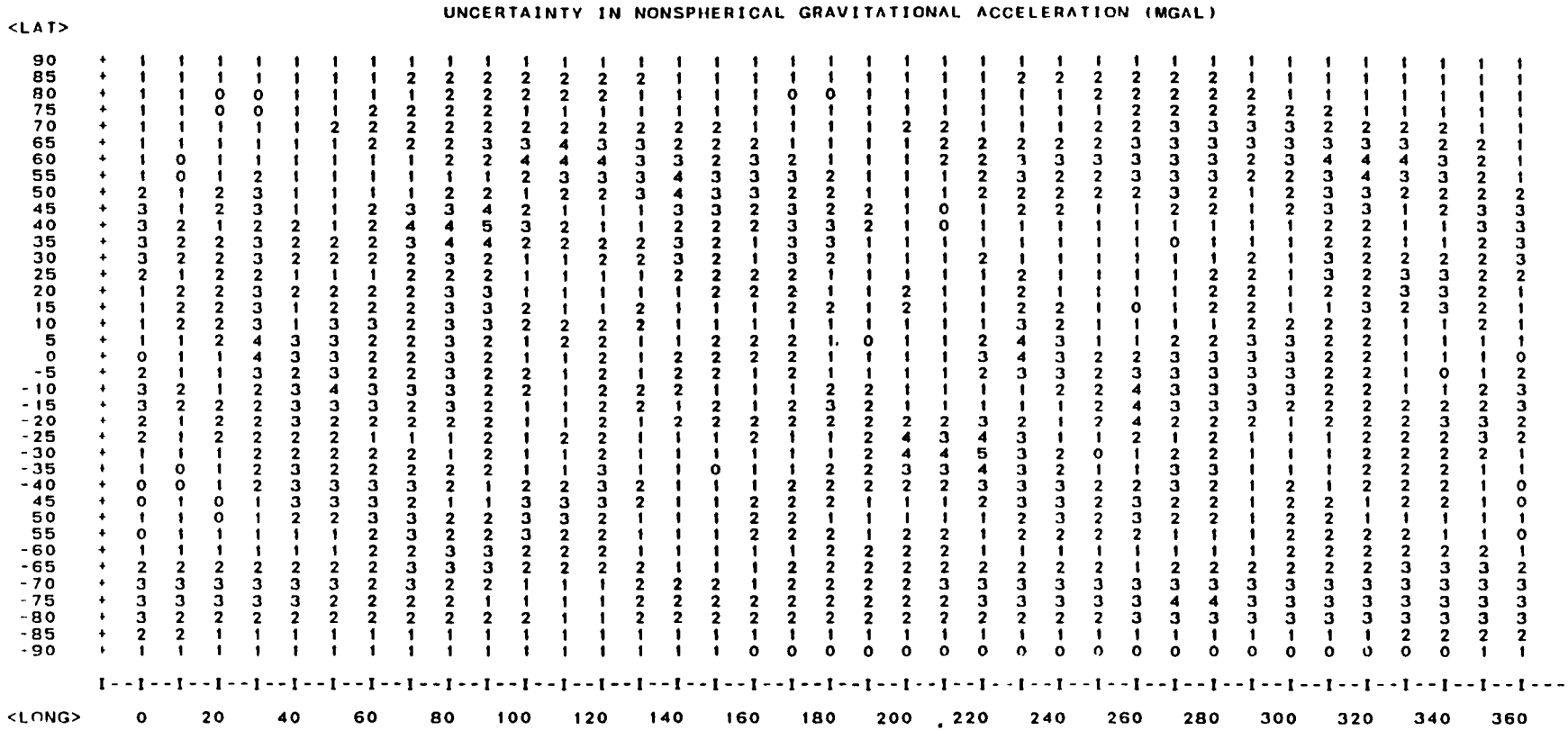


Figure 4-7. GEM-9/SAO One-Half Difference Model, 600-Kilometer Altitude

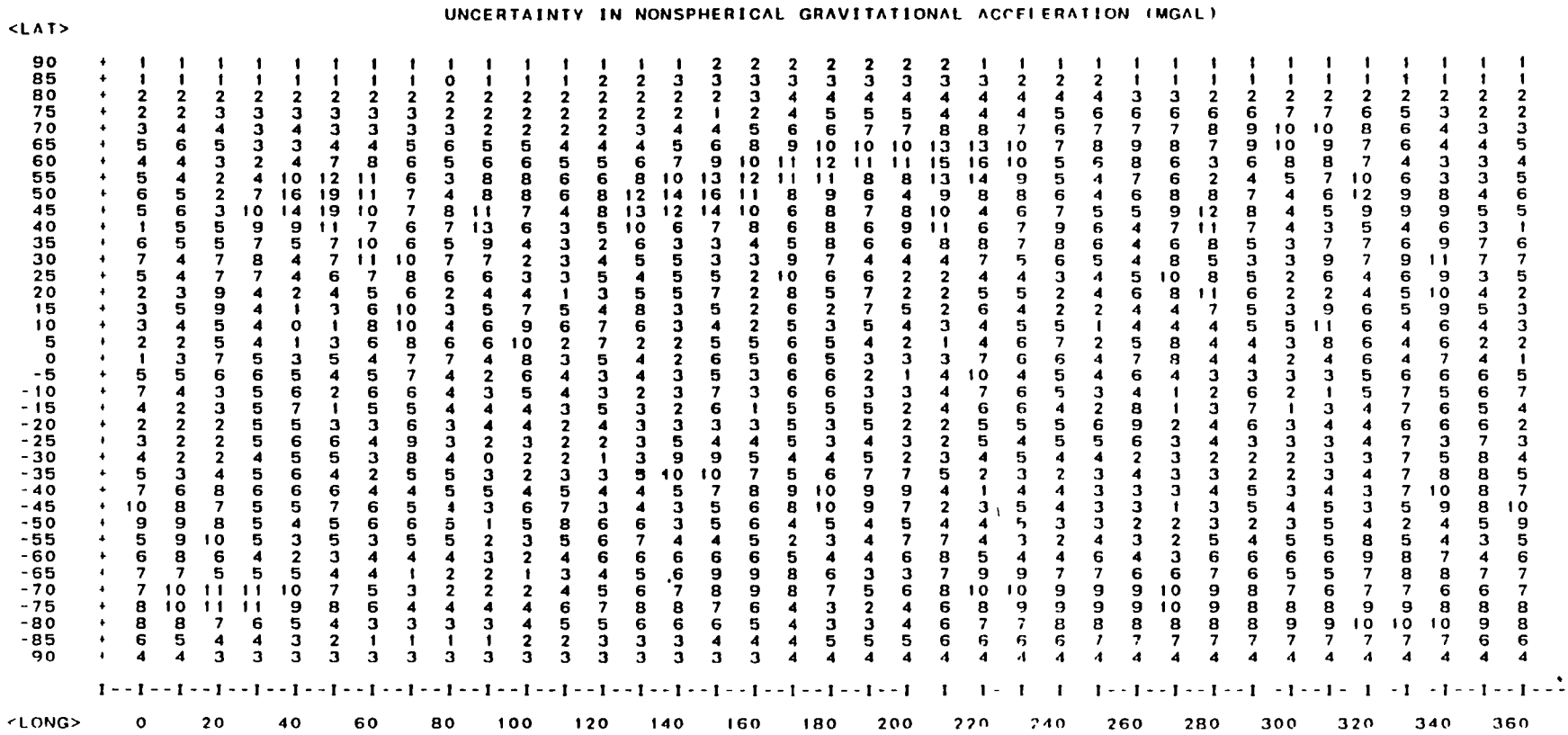


Figure 4-8. GEM-9/GEM-5 Difference Model, 200-Kilometer Altitude

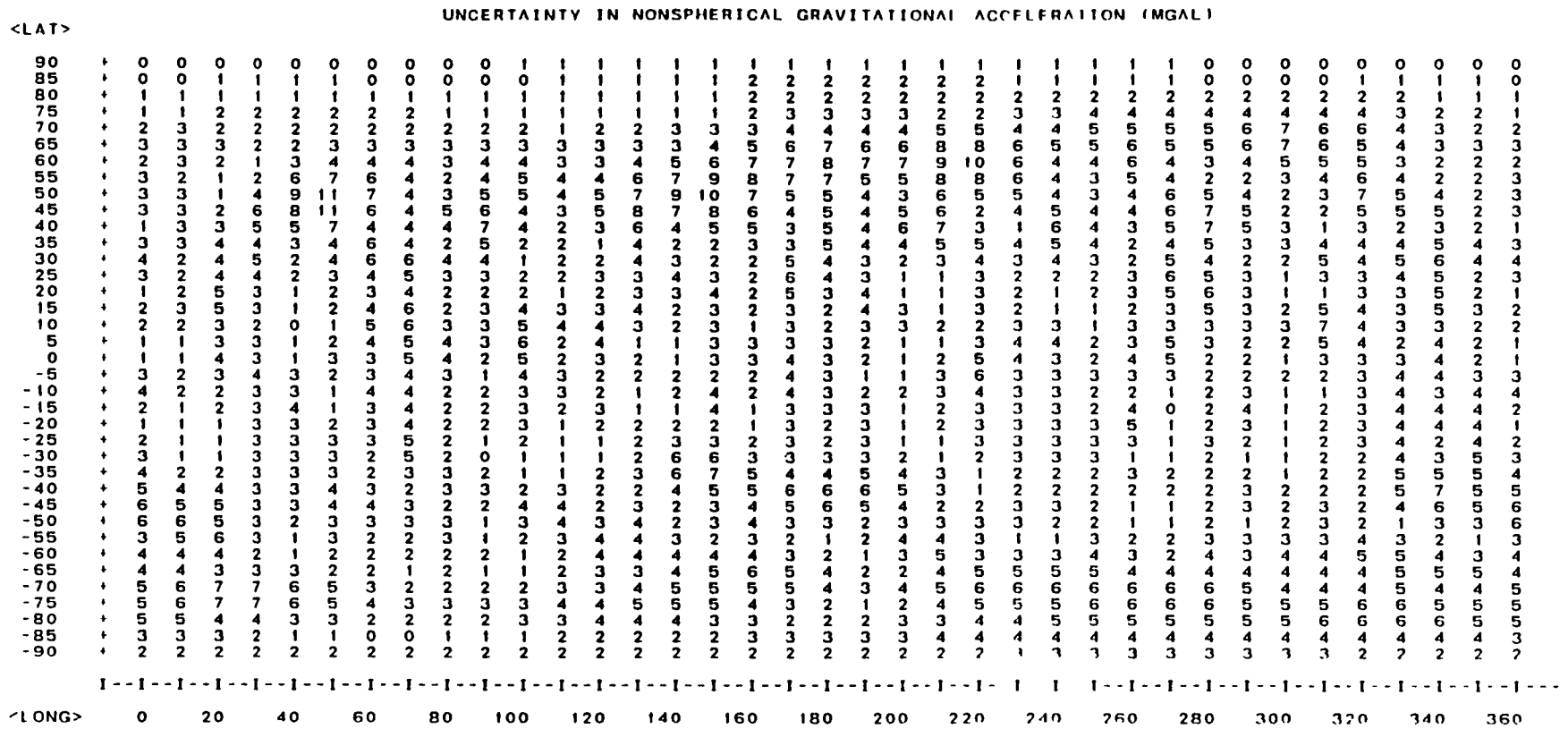


Figure 4-9. GEM-9/GEM-5 Different Model, 400-Kilometer Altitude

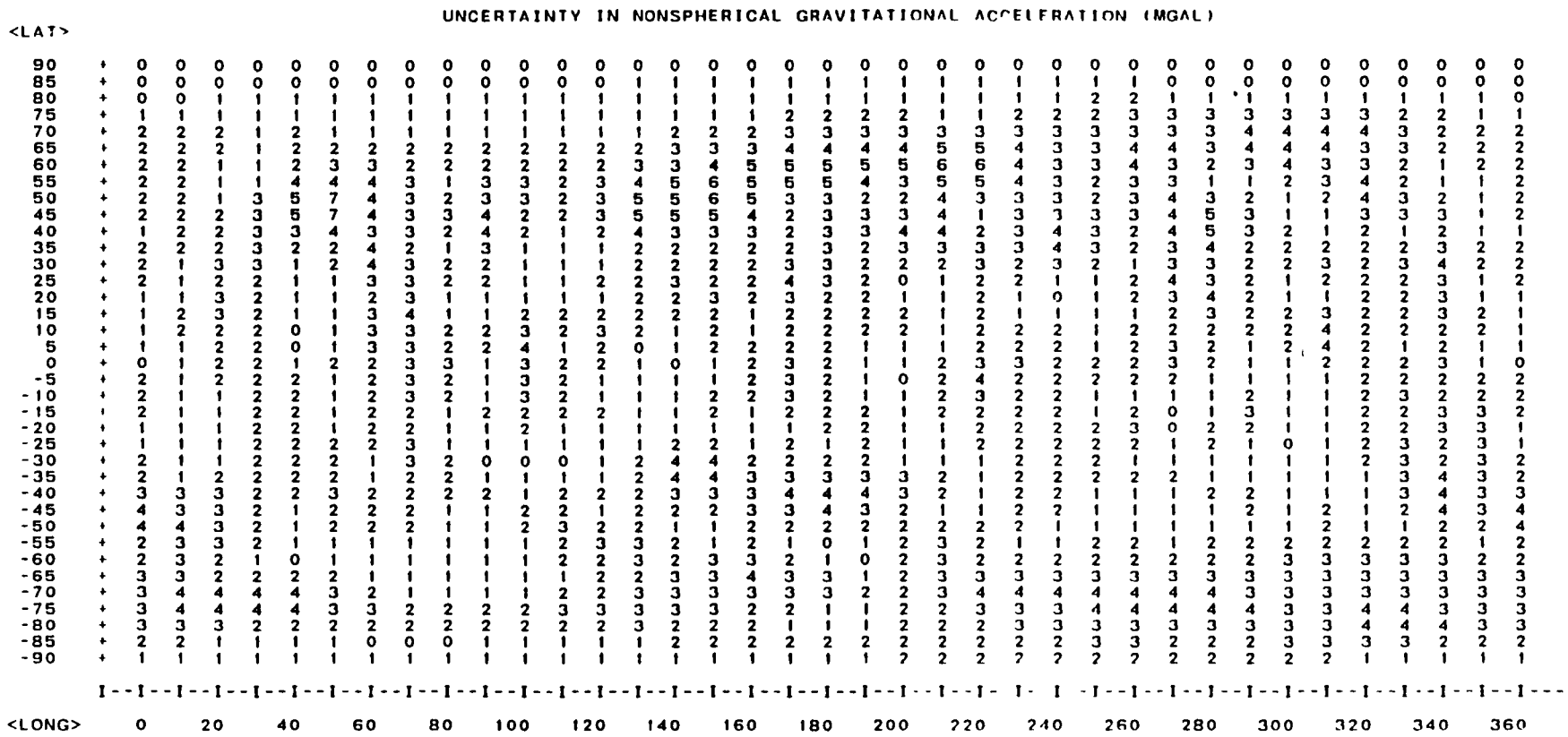


Figure 4-10. GEM-9/GEM-5 Difference Model, 600-Kilometer Altitude

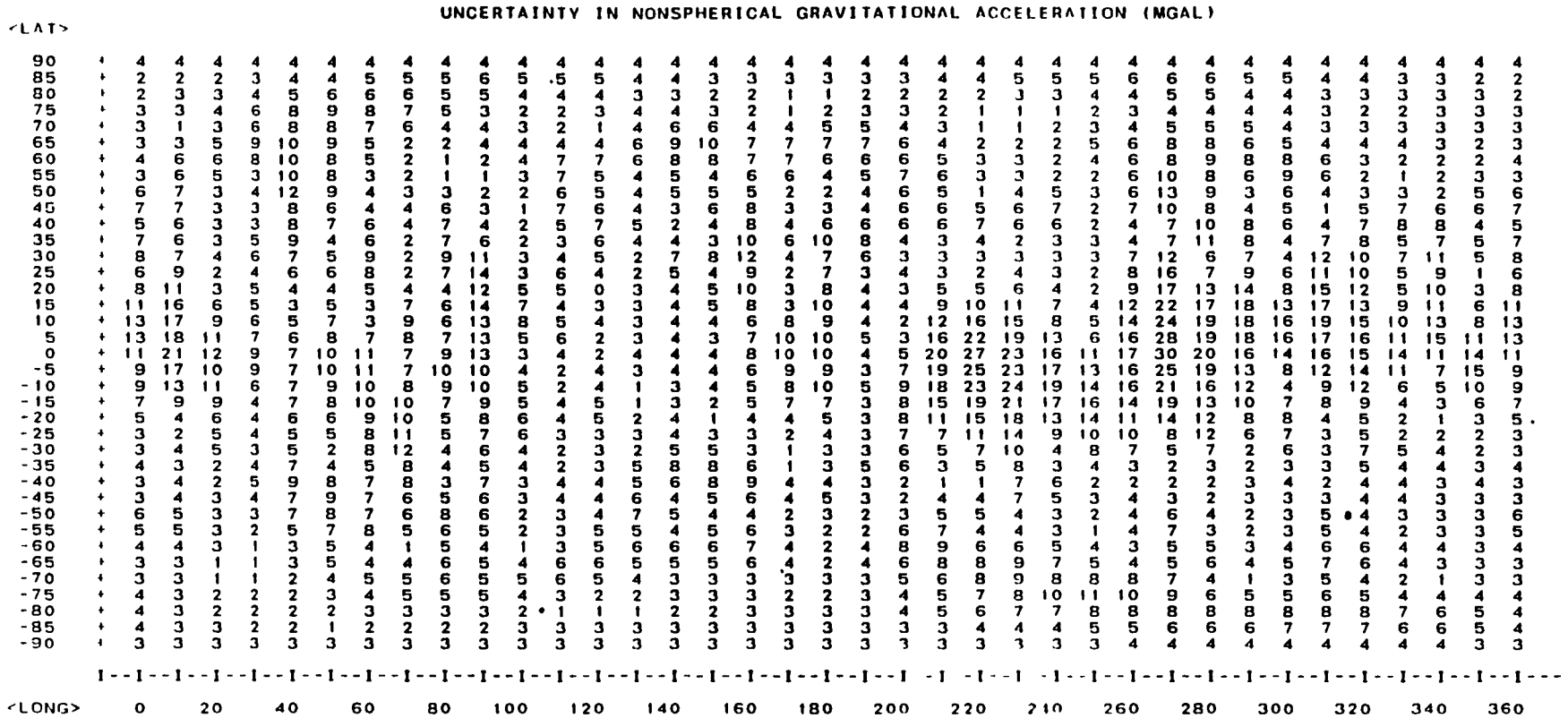


Figure 4-11. GEM-5/MD1 One-Half Difference Model, 200-Kilometer Altitude

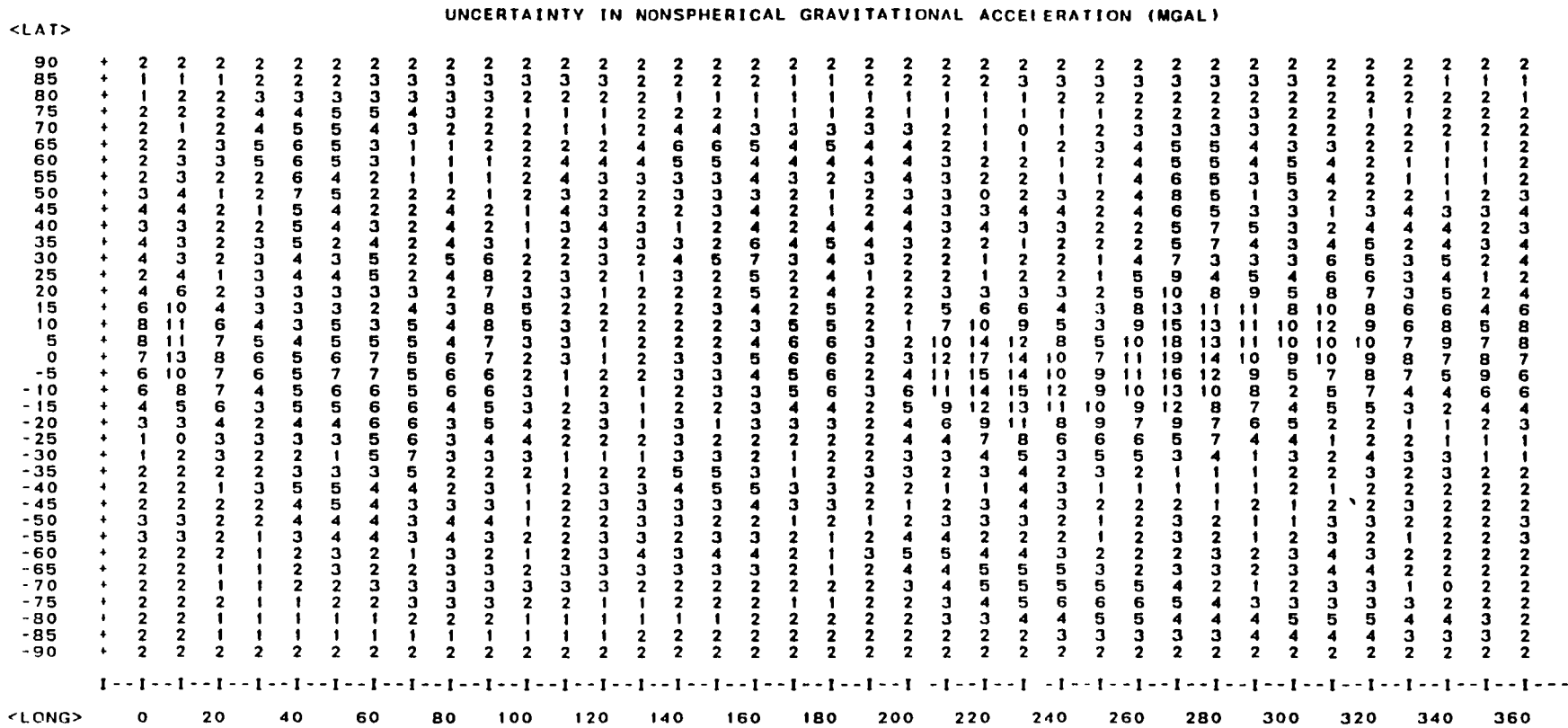


Figure 4-12. GEM-5/MD1 One-Half Difference Model, 400-Kilometer Altitude

UNCERTAINTY IN NONSPHERICAL GRAVITATIONAL ACCELERATION (MGAL)

<LAT>	0	20	40	60	80	100	120	140	160	180	200	220	240	260	280	300	320	340	360
90	+	1	1	1	1	1	1	1	1	1	1	1	1	1	1	1	1	1	1
85	+	1	0	1	1	1	1	1	1	1	1	1	1	1	1	1	1	1	1
80	+	1	1	1	1	1	1	1	1	1	1	1	1	1	1	1	1	1	1
75	+	1	1	1	1	2	2	3	3	3	3	3	3	3	3	3	3	3	3
70	+	1	1	1	1	2	3	3	3	3	3	3	3	3	3	3	3	3	3
65	+	1	1	1	2	3	3	3	3	3	3	3	3	3	3	3	3	3	3
60	+	1	2	2	3	3	3	3	3	3	3	3	3	3	3	3	3	3	3
55	+	1	2	2	3	3	3	3	3	3	3	3	3	3	3	3	3	3	3
50	+	2	2	1	1	1	1	1	1	1	1	1	1	1	1	1	1	1	1
45	+	2	2	1	1	1	1	1	1	1	1	1	1	1	1	1	1	1	1
40	+	2	2	1	1	1	1	1	1	1	1	1	1	1	1	1	1	1	1
35	+	2	2	1	1	1	1	1	1	1	1	1	1	1	1	1	1	1	1
30	+	2	2	1	1	1	1	1	1	1	1	1	1	1	1	1	1	1	1
25	+	1	2	2	2	2	2	2	2	2	2	2	2	2	2	2	2	2	2
20	+	2	4	2	2	2	2	2	2	2	2	2	2	2	2	2	2	2	2
15	+	4	6	3	3	2	2	2	2	2	2	2	2	2	2	2	2	2	2
10	+	5	7	4	3	3	3	3	3	3	3	3	3	3	3	3	3	3	3
5	+	5	7	4	3	3	3	3	3	3	3	3	3	3	3	3	3	3	3
0	+	4	8	5	4	4	4	4	4	4	4	4	4	4	4	4	4	4	4
-5	+	4	5	4	4	3	3	3	3	3	3	3	3	3	3	3	3	3	3
-10	+	4	5	4	4	3	3	3	3	3	3	3	3	3	3	3	3	3	3
-15	+	3	4	4	4	3	3	3	3	3	3	3	3	3	3	3	3	3	3
-20	+	2	2	2	2	2	2	2	2	2	2	2	2	2	2	2	2	2	2
-25	+	1	1	1	1	1	1	1	1	1	1	1	1	1	1	1	1	1	1
-30	+	1	1	1	1	1	1	1	1	1	1	1	1	1	1	1	1	1	1
-35	+	1	1	1	1	1	1	1	1	1	1	1	1	1	1	1	1	1	1
-40	+	1	1	1	1	2	3	3	3	3	3	3	3	3	3	3	3	3	3
-45	+	1	1	1	1	2	2	2	2	2	2	2	2	2	2	2	2	2	2
-50	+	2	2	1	1	2	2	2	2	2	2	2	2	2	2	2	2	2	2
-55	+	2	2	1	1	2	2	2	2	2	2	2	2	2	2	2	2	2	2
-60	+	2	2	1	1	2	2	2	2	2	2	2	2	2	2	2	2	2	2
-65	+	1	1	1	1	1	1	1	1	1	1	1	1	1	1	1	1	1	1
-70	+	1	1	1	1	1	1	1	1	1	1	1	1	1	1	1	1	1	1
-75	+	1	1	1	1	1	1	1	1	1	1	1	1	1	1	1	1	1	1
-80	+	1	1	1	1	1	1	1	1	1	1	1	1	1	1	1	1	1	1
-85	+	1	1	1	0	0	0	0	0	0	0	0	0	0	0	0	0	0	0
-90	+	1	1	1	1	1	1	1	1	1	1	1	1	1	1	1	1	1	1

ORIGINAL PAGE IS OF POOR QUALITY

Figure 4-13. GEM-5/MD1 One-Half Difference Model, 600-Kilometer Altitude

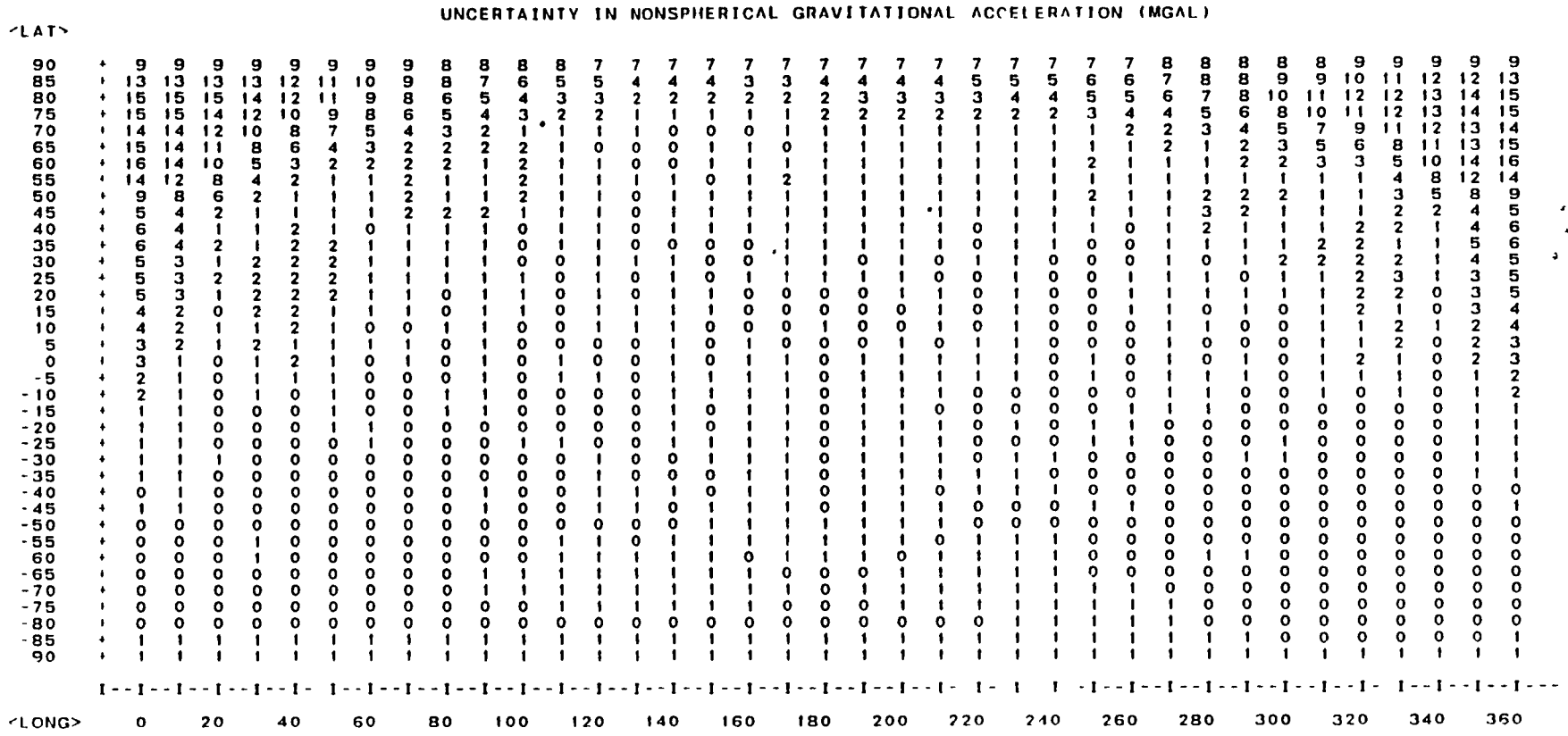
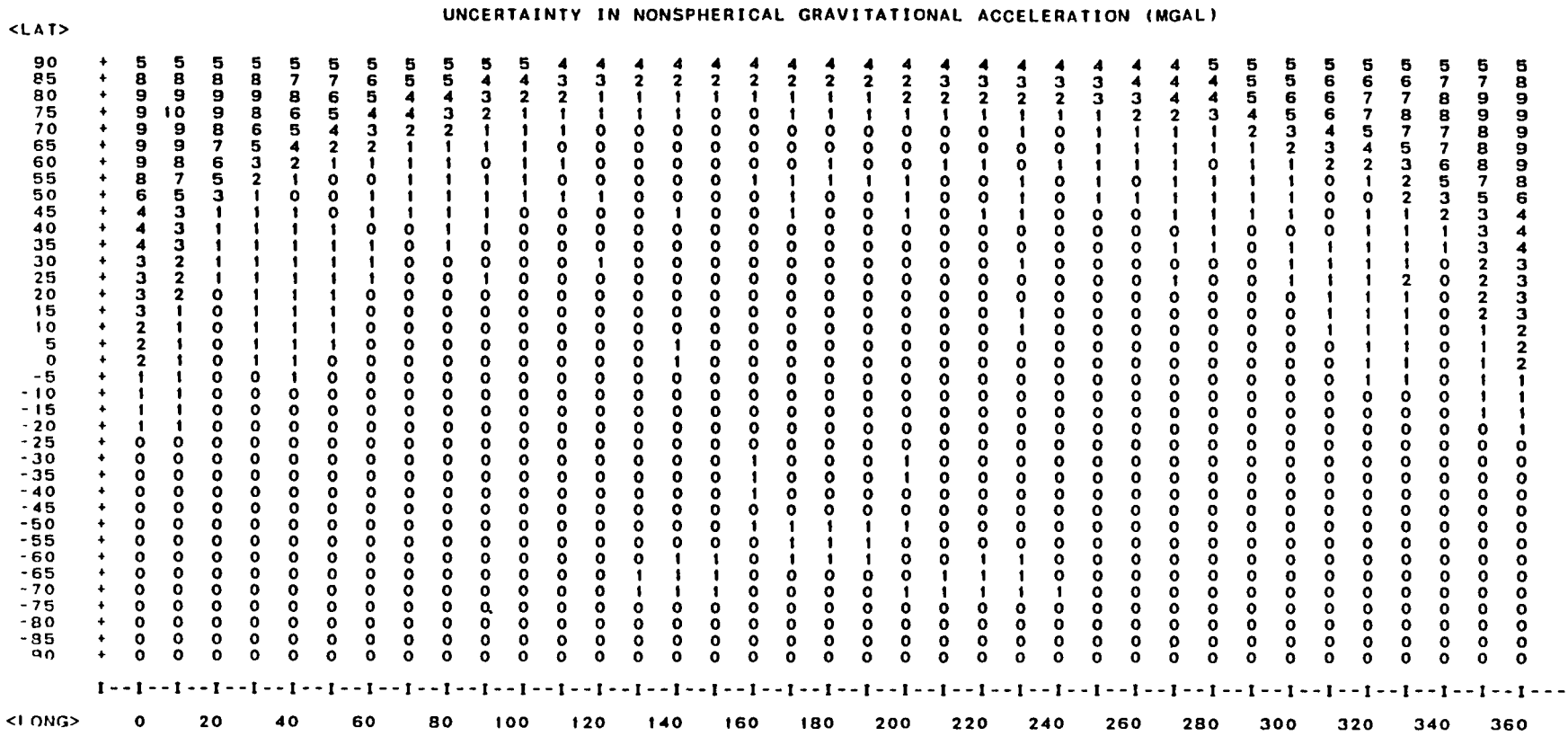


Figure 4-14. GEM-9 Standard Deviation Model, 400-Kilometer Altitude



4-23

Figure 4-15. GEM-9 Standard Deviation Model, 600-Kilometer Altitude

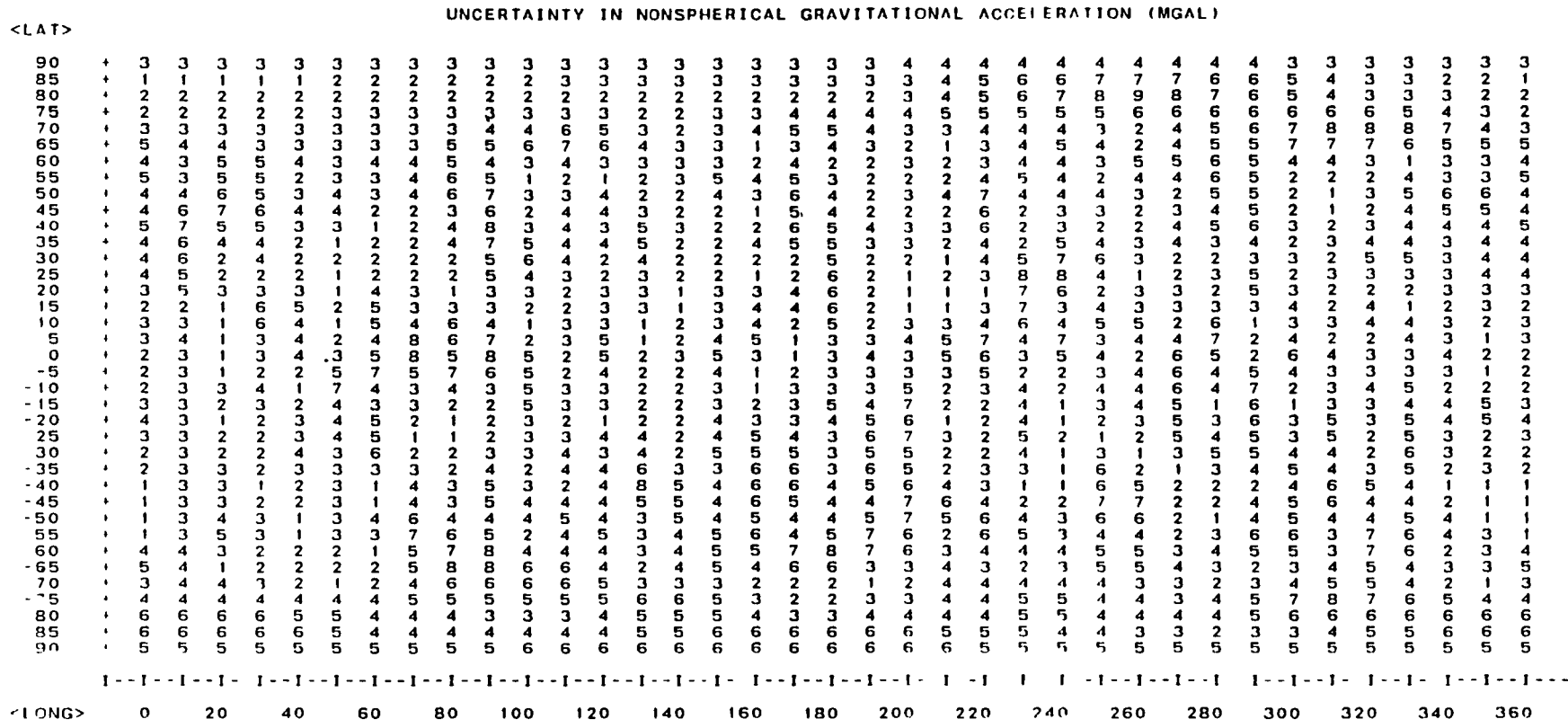


Figure 4-16. GEM-9 Formal Uncertainties With Random Signs, 200-Kilometer Altitude

		UNCERTAINTY IN NONSPHERICAL GRAVITATIONAL ACCELERATION (MGAL)																																																	
<LAT>		0	20	40	60	80	100	120	140	160	180	200	220	240	260	280	300	320	340	360	0	20	40	60	80	100	120	140	160	180	200	220	240	260	280	300	320	340	360												
90	+	2	2	2	2	2	2	2	2	2	2	2	2	2	2	2	2	2	2	2	2	2	2	2	2	2	2	2	2	2	2	2	2	2	2	2	2	2	2	2											
85	+	1	1	1	1	1	1	1	1	1	1	1	1	1	1	1	1	1	1	1	1	1	1	1	1	1	1	1	1	1	1	1	1	1	1	1	1	1	1	1	1										
80	+	1	1	1	1	1	1	1	1	1	1	1	1	1	1	1	1	1	1	1	1	1	1	1	1	1	1	1	1	1	1	1	1	1	1	1	1	1	1	1	1	1									
75	+	1	1	1	1	1	1	1	1	1	1	1	1	1	1	1	1	1	1	1	1	1	1	1	1	1	1	1	1	1	1	1	1	1	1	1	1	1	1	1	1	1	1								
70	+	2	2	2	2	2	2	2	2	2	2	2	2	2	2	2	2	2	2	2	2	2	2	2	2	2	2	2	2	2	2	2	2	2	2	2	2	2	2	2	2	2	2								
65	+	2	2	2	2	2	2	2	2	2	2	2	2	2	2	2	2	2	2	2	2	2	2	2	2	2	2	2	2	2	2	2	2	2	2	2	2	2	2	2	2	2	2	2							
60	+	2	2	2	2	2	2	2	2	2	2	2	2	2	2	2	2	2	2	2	2	2	2	2	2	2	2	2	2	2	2	2	2	2	2	2	2	2	2	2	2	2	2	2							
55	+	3	3	3	3	3	3	3	3	3	3	3	3	3	3	3	3	3	3	3	3	3	3	3	3	3	3	3	3	3	3	3	3	3	3	3	3	3	3	3	3	3	3	3							
50	+	2	2	2	2	2	2	2	2	2	2	2	2	2	2	2	2	2	2	2	2	2	2	2	2	2	2	2	2	2	2	2	2	2	2	2	2	2	2	2	2	2	2	2	2						
45	+	3	3	3	3	3	3	3	3	3	3	3	3	3	3	3	3	3	3	3	3	3	3	3	3	3	3	3	3	3	3	3	3	3	3	3	3	3	3	3	3	3	3	3	3	3					
40	+	3	3	3	3	3	3	3	3	3	3	3	3	3	3	3	3	3	3	3	3	3	3	3	3	3	3	3	3	3	3	3	3	3	3	3	3	3	3	3	3	3	3	3	3	3	3				
35	+	3	3	3	3	3	3	3	3	3	3	3	3	3	3	3	3	3	3	3	3	3	3	3	3	3	3	3	3	3	3	3	3	3	3	3	3	3	3	3	3	3	3	3	3	3	3	3			
30	+	3	3	3	3	3	3	3	3	3	3	3	3	3	3	3	3	3	3	3	3	3	3	3	3	3	3	3	3	3	3	3	3	3	3	3	3	3	3	3	3	3	3	3	3	3	3	3	3		
25	+	2	2	2	2	2	2	2	2	2	2	2	2	2	2	2	2	2	2	2	2	2	2	2	2	2	2	2	2	2	2	2	2	2	2	2	2	2	2	2	2	2	2	2	2	2	2	2	2		
20	+	2	2	2	2	2	2	2	2	2	2	2	2	2	2	2	2	2	2	2	2	2	2	2	2	2	2	2	2	2	2	2	2	2	2	2	2	2	2	2	2	2	2	2	2	2	2	2	2		
15	+	1	1	1	1	1	1	1	1	1	1	1	1	1	1	1	1	1	1	1	1	1	1	1	1	1	1	1	1	1	1	1	1	1	1	1	1	1	1	1	1	1	1	1	1	1	1	1	1		
10	+	2	2	2	2	2	2	2	2	2	2	2	2	2	2	2	2	2	2	2	2	2	2	2	2	2	2	2	2	2	2	2	2	2	2	2	2	2	2	2	2	2	2	2	2	2	2	2	2		
5	+	2	2	2	2	2	2	2	2	2	2	2	2	2	2	2	2	2	2	2	2	2	2	2	2	2	2	2	2	2	2	2	2	2	2	2	2	2	2	2	2	2	2	2	2	2	2	2	2	2	
0	+	1	1	1	1	1	1	1	1	1	1	1	1	1	1	1	1	1	1	1	1	1	1	1	1	1	1	1	1	1	1	1	1	1	1	1	1	1	1	1	1	1	1	1	1	1	1	1	1		
-5	+	1	1	1	1	1	1	1	1	1	1	1	1	1	1	1	1	1	1	1	1	1	1	1	1	1	1	1	1	1	1	1	1	1	1	1	1	1	1	1	1	1	1	1	1	1	1	1	1		
-10	+	1	1	1	1	1	1	1	1	1	1	1	1	1	1	1	1	1	1	1	1	1	1	1	1	1	1	1	1	1	1	1	1	1	1	1	1	1	1	1	1	1	1	1	1	1	1	1	1		
-15	+	2	2	2	2	2	2	2	2	2	2	2	2	2	2	2	2	2	2	2	2	2	2	2	2	2	2	2	2	2	2	2	2	2	2	2	2	2	2	2	2	2	2	2	2	2	2	2	2	2	
-20	+	2	2	2	2	2	2	2	2	2	2	2	2	2	2	2	2	2	2	2	2	2	2	2	2	2	2	2	2	2	2	2	2	2	2	2	2	2	2	2	2	2	2	2	2	2	2	2	2	2	2
-25	+	2	2	2	2	2	2	2	2	2	2	2	2	2	2	2	2	2	2	2	2	2	2	2	2	2	2	2	2	2	2	2	2	2	2	2	2	2	2	2	2	2	2	2	2	2	2	2	2	2	2
-30	+	1	1	1	1	1	1	1	1	1	1	1	1	1	1	1	1	1	1	1	1	1	1	1	1	1	1	1	1	1	1	1	1	1	1	1	1	1	1	1	1	1	1	1	1	1	1	1	1	1	
-35	+	1	1	1	1	1	1	1	1	1	1	1	1	1	1	1	1	1	1	1	1	1	1	1	1	1	1	1	1	1	1	1	1	1	1	1	1	1	1	1	1	1	1	1	1	1	1	1	1	1	
-40	+	0	2	2	2	2	2	2	2	2	2	2	2	2	2	2	2	2	2	2	2	2	2	2	2	2	2	2	2	2	2	2	2	2	2	2	2	2	2	2	2	2	2	2	2	2	2	2	2	2	
-45	+	0	2	2	2	2	2	2	2	2	2	2	2	2	2	2	2	2	2	2	2	2	2	2	2	2	2	2	2	2	2	2	2	2	2	2	2	2	2	2	2	2	2	2	2	2	2	2	2	2	2
-50	+	1	2	2	2	2	2	2	2	2	2	2	2	2	2	2	2	2	2	2	2	2	2	2	2	2	2	2	2	2	2	2	2	2	2	2	2	2	2	2	2	2	2	2	2	2	2	2	2	2	2
-55	+	1	2	2	2	2	2	2	2	2	2	2	2	2	2	2	2	2	2	2	2	2	2	2	2	2	2	2	2	2	2	2	2	2	2	2	2	2	2	2	2	2	2	2	2	2	2	2	2	2	2
-60	+	2	2	2	2	2	2	2	2	2	2	2	2	2	2	2	2	2	2	2	2	2	2	2	2	2	2	2	2	2	2	2	2	2	2	2	2	2	2	2	2	2	2	2	2	2	2	2	2	2	2
-65	+	2	2	2	2	2	2	2	2	2	2	2	2	2	2	2	2	2	2	2	2	2	2	2	2	2	2	2	2	2	2	2	2	2	2	2	2	2	2	2	2	2	2	2	2	2	2	2	2	2	2
-70	+	2	2	2	2	2	2	2	2	2	2	2	2	2	2	2	2	2	2	2	2	2	2	2	2	2	2	2	2	2	2	2	2	2	2	2	2	2	2	2	2	2	2	2	2	2	2	2	2	2	2
-75	+	2	2	2	2	2	2	2	2	2	2	2	2	2	2	2	2	2	2	2	2	2	2	2	2	2	2	2	2	2	2	2	2	2	2	2	2	2	2	2	2	2	2	2	2	2	2	2	2	2	2
-80	+	4	4	4	4	4	4	4	4	4	4	4	4	4	4	4	4	4	4	4	4	4	4	4	4	4	4	4	4	4	4	4	4	4	4	4	4	4	4	4	4	4	4	4	4	4	4	4	4	4	
-85	+	3	3	3	3	3	3	3	3	3	3	3	3	3	3	3	3	3	3	3	3	3	3	3	3	3	3	3	3	3	3	3	3	3	3	3	3	3	3	3	3	3	3	3	3	3	3	3	3	3	
-90	+	3	3	3	3	3	3	3	3	3	3	3	3	3	3	3	3	3	3	3	3	3	3	3	3	3	3	3	3	3	3	3	3	3	3	3	3	3	3	3	3	3	3	3	3	3	3	3	3	3	3

Figure 4-17. GEM-9 Formal Uncertainties With Random Signs, 400-Kilometer Altitude

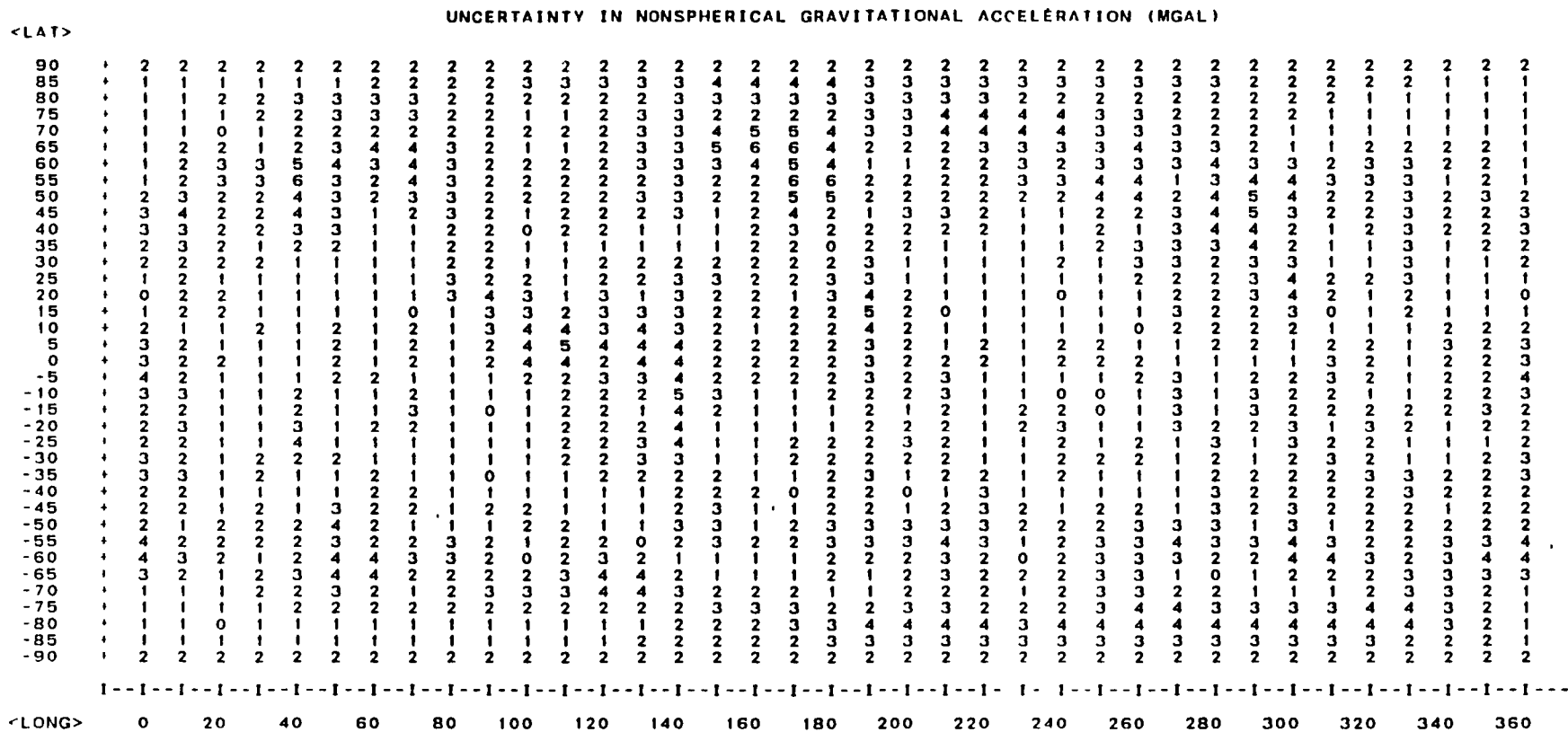
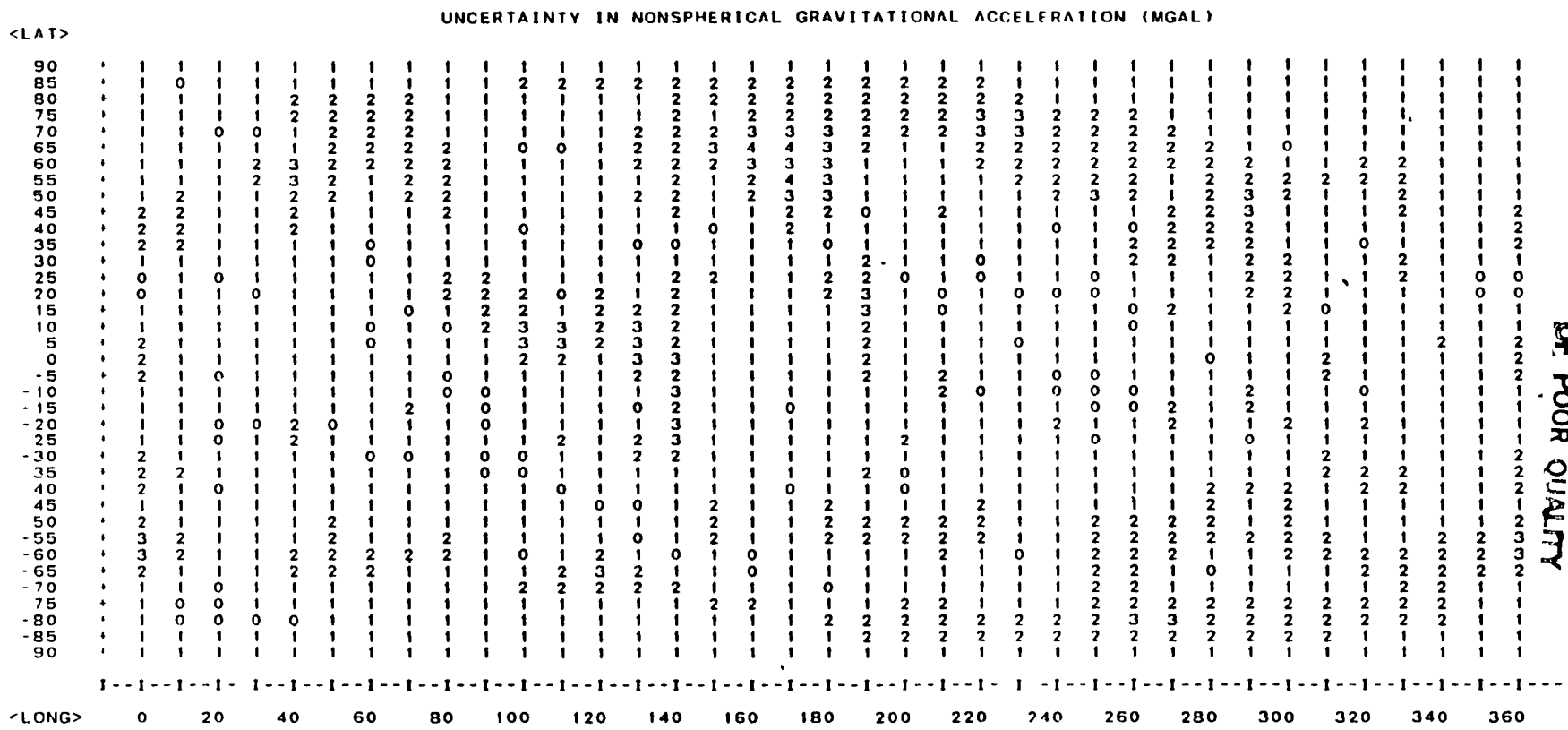


Figure 4-20. GEM-9 Formal Uncertainties With Random Phase, 400-Kilometer Altitude



ORIGINAL PAGE IS OF POOR QUALITY

Figure 4-21. GEM-9 Formal Uncertainties With Random Phase, 600-Kilometer Altitude

ORIGINAL PAGE IS
OF POOR QUALITY

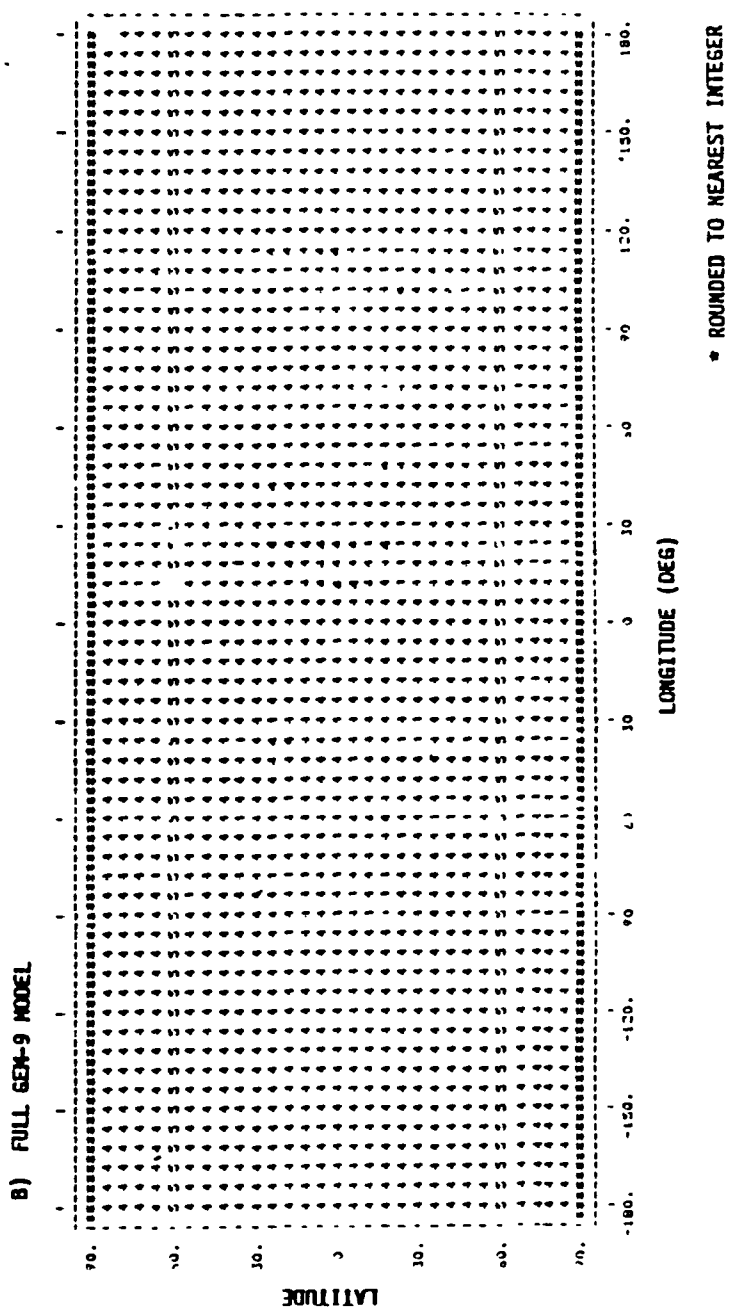


Figure 4-22. GEM-9 Uncorrelated Standard Deviation Model, 200-Kilometer Altitude

C-2

of the GEM-9 spherical harmonic coefficients. The maps depict the following:

- As expected, gravity errors for every model decrease with altitude.

- In addition to the anomalous distribution of gravity errors discussed for the GEM-9 standard deviation model, difference models involving the MD1 and a GEM model show a band of large differences at latitudes near the Equator.

- The GEM-9 uncorrelated model predicts a very uniform distribution of errors with a magnitude around 4 milligals (mgals) (10^{-5} m/sec²) at 200 km. The GEM-9 standard deviation model predicts errors, apart from the anomalous region, at a level considerably smaller than those given by the other models. The other models generally give rise to errors from 1 to 10 mgals and show much greater fluctuations from one location to another.

4.3 NAVIGATION AND ORBIT PREDICTION ERRORS INTRODUCED BY GEOPOTENTIAL UNCERTAINTY

The interest in geopotential error models is not so much in the gravity errors themselves but in their effect on satellite navigation accuracy. Satellite navigation error analyses were thus conducted using the SEA program to evaluate, under postulated navigation scenarios, the expected orbit determination and prediction errors resulting from the geopotential errors given by different error models. The baseline scenario considered was for low-altitude Earth satellite navigation based on a sequential filter using continuous TDAS range and Doppler tracking data sampled at 3-min intervals for 1 day, followed by 5 days of propagation without tracking. Navigation at 200 and 600 km and at 28- and 57-deg inclinations was considered. No process noise was introduced in the filter; thus, the 5-day propagation results should agree with those based on a batch orbit

determination process. The expected navigation errors resulting from geopotential uncertainties are summarized in Table 4-1 for the different geopotential error models.

4.4 COMPARISON WITH LANDSAT-5 ORBIT DETERMINATION RESULTS

Some results on Landsat-5 orbit determination using GSTDN and single-TDRS tracking data are presented in Reference 4-12. Measures of orbit accuracies are provided by

- Overlap ephemeris comparisons of definitive orbit solutions (34-hour data arcs with 10 hours of overlap)
- Ephemeris comparisons of definitive and predictive orbit solutions (1- or 2-day predictions based on 34-hour data arcs)

The overlap comparisons of definitive solutions derived from TDRS data have maximum differences of 82, 71, 35, 74, and 35 m. One-day predictions have maximum differences of 186, 131, 40, 172, and 79 m from definitive solutions. Two-day predictions have maximum differences of 412 and 172 m. Although these differences, or errors, result from a combination of geopotential and atmospheric uncertainties and tracking errors, it is expected that geopotential uncertainties play a major role. These numbers can thus serve as bases for the calibration of geopotential error models. For this purpose, error analyses were set up to evaluate, under the same tracking and batch orbit determination scenario, orbit errors resulting from the GEM-9/SAO one-half difference error model and the GEM-9/MD1 one-half difference model. The GEM-9/SAO error model predicts a maximum position error of 57 m during the tracking period and maximum errors of 184 and 236 m during 1-day and 2-day propagations. These numbers appear quite reasonable compared with actual orbit determination results quoted above. The GEM-9/MD1 error model predicts a maximum position error of 77 m

Table 4-1. Navigation Errors Resulting From Geopotential Uncertainties

ORBIT CHARACTERISTICS	GEOPOTENTIAL ERROR MODEL	ORBIT POSITION ERROR (meters)	
		MAXIMUM DURING 24 HOURS OF TRACKING	MAXIMUM DURING 5-DAY PREDICTION
200-km ALTITUDE, 28-deg INCLINATION	GEM-9 STANDARD DEVIATION	21	205
	½ GEM-9/SAO DIFFERENCE	149	481
	½ GEM-9/MD-1 DIFFERENCE	168	3209
	½ GEM-5/MD-1 DIFFERENCE	186	3495
	RANDOM SIGN	148	496
	RANDOM PHASE	108	575
200-km ALTITUDE, 57-deg INCLINATION	GEM-9 STANDARD DEVIATION	56	1171
	½ GEM-9/SAO DIFFERENCE	126	1271
	½ GEM-9/MD-1 DIFFERENCE	253	44886
	½ GEM-5/MD-1 DIFFERENCE	227	42745
	RANDOM SIGN	105	4562
	RANDOM PHASE	238	2511
600-km ALTITUDE, 28-deg INCLINATION	GEM-9 STANDARD DEVIATION	9	71
	½ GEM-9/SAO DIFFERENCE	60	246
	½ GEM-9/MD-1 DIFFERENCE	73	597
	½ GEM-5/MD-1 DIFFERENCE	71	576
	RANDOM SIGN	68	154
	RANDOM PHASE	44	118
600-km ALTITUDE, 57-deg INCLINATION	GEM-9 STANDARD DEVIATIONS	14	235
	½ GEM-9/SAO DIFFERENCE	58	686
	½ GEM-9/MD-1 DIFFERENCE	81	1537
	½ GEM-5/MD-1 DIFFERENCE	77	2330
	RANDOM SIGN	35	395
	RANDOM PHASE	44	118

0112 (1111)/85

during the tracking period but unrealistic, smaller maximum errors of 58 and 64 m during propagations.

4.5 CONCLUSIONS

The results described in the preceding sections show that the choice of an appropriate model is very difficult. The models studied may be classified into two categories: those dependent on internal accuracy estimates and those dependent on comparisons with other models.

Error models based on internal accuracy estimates run the risk of being unduly optimistic. This weakness can, however, be remedied by a calibration scale factor. The real difficulty is the need to consider correlations between errors in the geopotential coefficients. This is impractical because of the large computational requirements.

Short of actually considering the correlations, the GEM-9 uncorrelated standard deviation model seems to be the most appropriate, although correlations do exist. However, even this model is computationally prohibitive. Comparison of the error map of this model with those of the geopotential difference models shows that the geographical fluctuation of the error as predicted by this model may be too mild. On the other hand, based on the same comparisons, it seems that the predicted gravity error magnitude for GEM-9, approximately 5 mgals at a 200-km altitude, is reasonable.

The random-sign and random-phase models, which are simple to implement, give rise to gravity error maps that seem reasonable, with local error fluctuations possibly somewhat excessive. The orbit determination errors based on these models also appear reasonable, although the error growths during prediction do not clearly exhibit the distinct characteristic of a sinusoidal variation superimposed on a linear growth. The main objection to these models is that they are empirical models without sound theoretical justifications.

The GEM-9 standard deviation model, when compared with other models, shows gravitational errors that are too low in the Southern Hemisphere and near the Equator. Therefore, its prediction of orbit errors for low-inclination satellites is too optimistic. On the other hand, this model has an unrealistic concentration of large errors near 0-deg longitude and 65-deg latitude that may give rise to anomalous orbit error spikes near these regions. This model is definitely faulty and should not be used.

A comparison between different geopotential models provides information about the accuracies of the individual models. The geopotential difference error models use the weighted differences of the spherical harmonic coefficients of two geopotential models as error coefficients. If one of the geopotential models is considerably more accurate than the other, the straight difference of the two models can be considered, with good confidence, as representative of the errors of the less-accurate model. If the two models are derived from independent sources, there is some justification in using their weighted differences as characterizing the accuracies of individual models, although the justification is weak and cannot be rigorously proven.

SAO and MD1 are models independent of GEM-9. GEM-9 was derived several years after SAO and MD1, and there should be no disagreement that GEM-9 is a considerably improved model. Thus, the GEM-9/SAO and GEM-9/MD1 difference models serve as good error models for the SAO and MD1 geopotential models. Doubling the numbers shown in Figure 4-5, which are for one-half the model differences, implies that the gravitational errors for the SAO model at a 200-km altitude vary from 2 to 26 mgals. The error map shows local fluctuations but not any particularly recognizable features. Similarly, it might be said that Figure 4-2, with the errors doubled, describes the accuracy of the MD1 model. It should be noted

that, in Figure 4-2, there is a band of large errors at equatorial latitudes reaching, at a 200-km altitude, as large as 60 mgals (in accuracy), which is comparable in magnitude to the total contribution of the nonaxisymmetric portion of GEM-9. This band and its large magnitude is bothersome, because no ready explanations exist. Away from this band, the error distribution appears reasonable.

Of course, it is not the errors for these older models but the accuracy of GEM-9 that is of interest here. Since, at best, only the level of orbit determination error resulting from geopotential uncertainty can be expected, it may not be unreasonable to take the scaled difference of GEM-9 and a less accurate model as an error model for GEM-9, with the scale factor determined from some means of calibration. For instance, it might be speculated that GEM-9 is twice as accurate as MD1 and that therefore one-half of the GEM-9/MD1 difference would serve as an error model for GEM-9. This is, of course, not completely satisfactory because gravity errors are expected to become more uniformly distributed for higher order and more accurate models. The band of large errors, shown in Figure 4-2, is probably reflective of the nonuniform inaccuracies of MD1, and a simple scaling of the error model that preserves this feature of concentrated error would not be a good error model for GEM-9. The same consideration also applies to the GEM-9/SAO difference model. However, as shown in Figure 4-5, this difference model has a more random error distribution devoid of particular unexplainable features. Thus the GEM-9/SAO difference model, with a proper scaling factor, appears to be a reasonable error model for GEM-9.

The primary interest is not in the global gravity error distribution itself but in the effect of geopotential errors on orbit determination accuracies. Table 4-1 shows the orbit determination and prediction errors according to the

different geopotential error models. The following may be observed from the results presented in the table:

- With the exception of the GEM-9 standard deviation model, the orbit determination errors predicted by the different models do not differ by a factor greater than two during the tracking period. The error of the GEM-9 standard deviation model is too low. Greater differences occur for orbit propagation beyond the tracking period.

- The GEM-9/MD1 and GEM-5/MD1 one-half difference models are similar. Perhaps as a result of the large band of anomalous errors discussed earlier, the orbit determination errors predicted by these models are erratic (The excessive errors for the 200-km-altitude, 57-deg-inclination orbit and the small propagation errors for Landsat-5 as discussed in Section 4.4.)

It may be concluded from this study that the GEM-9 standard deviation model and GEM-9/MD1 and GEM-5/MD1 difference models are all faulty and should not be used. The random-sign and random-phase models are difficult to justify theoretically and do not seem to offer any advantage over the GEM-9/SAO difference model. Although the GEM-9 uncorrelated model has not been extensively studied, it is not expected to be much more accurate than the GEM-9/SAO difference model, yet the computational burden is much greater. It appears, from this limited study, that the scaled GEM-9/SAO difference model is the best error model for GEM-9. A scaling factor of one-half is tentatively suggested before the availability of additional calibration.

4.6 REFERENCES

- 4-1. F. J. Lerch et al., "Gravity Model Improvement Using GEOS-3 Altimetry (GEM 10A and 10B), paper presented at AGU Annual Meeting, Miami Beach, Florida, April 1978

- 4-2. Goddard Space Flight Center, X-552-76-77, Mathematical Theory of the Goddard Trajectory Determination System, J. O. Cappellari, C. E. Velez, and A. J. Fuchs (editors), April 1976
- 4-3. --, X-921-77-246, Gravity Model Improvement Using GEOS-3 (GEM 9 & 10), F. J. Lerch et al., September 1977
- 4-4. C. F. Martin and N. A. Roy, "Error Model for the SAO Standard Earth," The Uses of Artificial Satellite for Geodesy, AGU Monograph 15, Washington, DC, 1970
- 4-5. Computer Sciences Corporation, CSC/TM-81/6033, Feasibility Study on Altimeter Measurements as Supplemental Data for Upper Atmospheric Research Satellite Orbit Determination, B. T. Fang and J. R. Kuhn, January 1981
- 4-6. Stanford Telecommunications, Inc., STI/E-TR-25066, Tracking and Data Acquisition System (TDAS) for the 1990's, Volume VI TDAS Navigation System Architecture, B. D. Elrod et al., May 1983
- 4-7. C. A. Wagner and F. J. Lerch, "The Accuracy of Geopotential Models," Planetary and Space Science, December 1978
- 4-8. EG&G Washington Analytical Services Center, Inc., Applied Systems Department, Report No. 003-78, Gravity Model Improvements and Implications for Operational Orbit Determination, B. T. Fang, October 1978
- 4-9. --, Planetary Sciences Department, Report No. 001-80, Orbital Error Analysis Studies for GRO and Landsat-D Using One-Way and Two-Way Measurements, J. J. McCarthy, May 1980
- 4-10. Smithsonian Astrophysical Observatory, Special Report 315, 1969 Smithsonian Standard Earth (II), E. M. Gaposchkin and K. Lambeck, May 18, 1970
- 4-11. B. T. Fang, "Satellite-to-Satellite Tracking Orbit Determination," Journal of Guidance and Control, January-February 1979
- 4-12. Computer Sciences Corporation, CSC/TM-85/6731, Flight Dynamics Division Single-TDRS S-Band Navigation Certification Plan and Certification Results for Early Tracking and Data Relay Satellite System Users, J. O. Cappellari, Jr., et al., September 1985

SECTION 5 - ORBIT SMOOTHER PROCESS NOISE STUDY

Because the batch method of orbit determination is a subset of an orbit smoother, an improved orbit determination accuracy would be expected with a smoother. As discussed in Appendix A, the SEA program now has the capability of evaluating the performance of orbit smoothers. Limited investigations using this new capability have been performed as an exploratory study of orbit smoothers and also to validate the fading memory process noise option of the SEA smoother capability. Two different orbit determination scenarios are considered:

- The baseline TDAS navigation scenario for a 600-km-altitude, 28-deg inclination satellite considered in Section 3
- The 34-hour arc Landsat-5 orbit determination scenario referred to in Section 4.4 (This investigation is undertaken in part to determine if the degradation of Landsat-5 orbit accuracy discussed in Section 2 results from geopotential errors compounded by the reduction in tracking coverage.)

The TDAS navigation smoother results are summarized in Table 5-1. Two process noise options are considered: the linear growth option and the fading memory option. The linear growth option assumes that, in addition to the modeled evolution of the covariance matrix, there is an additive increase (noise) in the variances of the Cartesian velocity components proportional to the time elapsed since the last measurement. The fading memory option assumes a multiplicative increase of the whole covariance matrix. The orbit smoother does indeed improve the performance over that of a batch orbit determination process for this particular TDAS scenario. The major error sources are geopotential

errors and clock acceleration; the TDAS ephemeris errors are secondary, and other error sources are negligible. Although the fading memory option has not been investigated in as much detail as the linear growth option, the former does not appear to offer any advantage over the latter.

Table 5-1. Orbit Smoother Performance for the TDAS Navigation Scenario

<u>Process Noise Option</u>	<u>Orbit Position Errors (m)</u>	
	<u>Maxima</u>	<u>Root Mean Square</u>
Linear Growth Rate		
10^{-16} (m/sec) ² /sec	104	46
10^{-14} (m/sec) ² /sec	78	41
10^{-12} (m/sec) ² /sec	67	33
10^{-10} (m/sec) ² /sec	40	24
10^{-8} (m/sec) ² /sec	42	23
Fading Memory Multiplicative Factor		
1.1	61	24
1.25	63	36
1.5	98	38

The Landsat-5 results are presented in Table 5-2. Tracking data consist of single TDRS and ground station data. The only error source considered is the one-half the GEM-9/SAO geopotential difference discussed in Section 4. Generally, increasing the process noise tends to decrease dynamic error at the expense of measurement error. Although measurement noise is excluded, Table 5-2 shows that an optimum noise level exists above which the dynamic error also increases. Another interesting result shown in Table 5-2 is that, with the addition of ground tracking data, orbit errors actually increase if process noise is not introduced. This is not a generally valid conclusion but shows that the behavior of

dynamic error is difficult to predict. On the other hand, Table 5-2 shows that, with the use of process noise, orbit errors are decreased when more tracking data are available.

Table 5-2. Landsat-5 Orbit Smoother Error Caused by One-Half GEM-9/SAO Differences

<u>Tracking Data</u>	Process Noise Linear Growth Rate (m/sec) ² /sec	<u>Orbit Position Error (m)</u>	
		<u>Maximum</u>	<u>Root Mean Square</u>
Single TDRS and Lansat-5 ground tracking stations	10 ⁻⁸	69	24
	10 ⁻¹⁰	56	20
	10 ⁻¹²	47	24
	0	57	28
As above with ad- dition of several Landsat-4 ground tracking stations	10 ⁻¹²	42	17
	0	69	30

Other results not shown in Tables 5-1 and 5-2 include the following:

- Maximum errors generally occur near two ends of the data arc where smoothing has smaller effects.
- Orbit solutions propagated beyond the data arc are generally less accurate for smoothed solutions than for batch solutions. This is not unexpected because the process noise introduced in an orbit smoother is artificial rather than physical.

SECTION 6 - CONCLUSIONS

Several topics related to low-altitude satellite orbit determination have been investigated. The topics studied and major conclusions reached are summarized below.

- Landsat-5 Orbit Determination using GPSPAC data-- Landsat-5 orbit solutions computed from GPSPAC delta-pseudorange (Doppler) data are good. Maximum differences between GPSPAC and GSTDN solutions are generally under 70 m. Maximum differences between partially overlapping GPSPAC solutions are even smaller. There is a good possibility that the GPSPAC solutions are superior to the GSTDN solutions in accuracy.

For orbit determination instead of real-time navigation, simultaneous data from four GPS satellites are not necessary. The study results indicate that approximately 3 hours of data from a single GPS satellite are sufficient to resolve Landsat-5 orbit and clock. A study of a randomly selected sample shows that the Landsat-5 orbit solutions based on individual GPS satellites agree to within 80 m, and typically less than 40 m.

As with Landsat-4 GPSPAC data, some inconsistencies exist between the Landsat-5 GPSPAC pseudorange and delta-pseudorange data. Landsat-5 solutions derived from pseudorange data generally differ from the GSTDN solutions by maximas over 100 m. Furthermore, large, GPS-independent range observation residuals of over 100 m are seen in delta-pseudorange Landsat-5 GPSPAC data solutions. Based on these, it may be concluded that the pseudoranges have systematic errors on the order of 100 m in addition to the expected clock errors. The causes of these systematic errors

have not been determined, although bad data from an individual GPS satellite and several easily committed preprocessing errors have been eliminated as possible reasons.

In connection with the GPSPAC study, the computation of Landsat-5 orbits from GSTDN data was undertaken. Unfortunately, there are not as many ground tracking stations for Landsat-5 as for Landsat-4, and the accuracy of the resulting Landsat-5 orbit solutions is not as good as the corresponding Landsat-4 solutions. Investigations show that this degradation cannot be attributed solely to dynamic modeling errors accentuated by the sparsity of tracking coverage.

- TDAS Simulation--Simulated TDAS one-way Doppler data were generated. The data, with errors added, were input to an extended Kalman filter in R&D GTDS for the navigation of low-altitude Earth satellites. Comparisons with truth models yielded information about the navigation performance. The results showed very good agreement with those obtained earlier from error analysis using the SEA program. The agreement provides confidence in the TDAS capabilities of both programs and indicates that TDAS navigation performance can be studied economically using SEA instead of the computationally expensive simulations.

- Error Model for GEM-9--Several candidate error models for GEM-9 were studied. Although the specification of an appropriate model was difficult, the use of the GEM-9/SAO difference model with a proper scaling factor is recommended. A scaling factor of one-half is tentatively suggested before the availability of additional calibration.

- Orbit Smoothers--Some exploratory study of orbit smoothers was conducted using SEA. The fading memory process noise option of SEA was validated. However, this option does not seem to offer particular advantages over the linear growth option. This limited study showed that an orbit

smoother can indeed outperform a batch orbit determination process in accuracy. The following two observations may be made concerning orbit smoothers: (1) If accuracy is of primary concern, a smoothed orbit near the ends of the data arc can be discarded because smoothing action is less at the ends and orbit errors are generally greater. (2) Because process noises are generally artificial rather than physical, orbit propagation beyond the data arc from a smoothed orbit is generally not as accurate as the propagation from a batch solution.

- Validation of the SEA Smoother/TDAS Capability--The SEA Smoother/TDAS capability was fully validated by testing. An inconvenience of the SEA smoother is that it will not output smoother error analysis results at times not coincident with a measurement. It is possible to trick the program into outputting results by introducing dummy measurements with negligible data weights, i.e., large measurement variances.

APPENDIX A - VALIDATION AND VERIFICATION OF THE SEA SMOOTHER/
TDAS CAPABILITY

The Sequential Orbit Determination Error Analysis (SEA) Program has been enhanced to incorporate error analysis capabilities for the following orbit determination scenarios:

- Orbit determination using the smoother method
- Orbit determination using the proposed Tracking and Data Acquisition System (TDAS) data

These enhancements to SEA were designed and implemented in 1984 under Task 42100.

This appendix outlines the results of the validation and verification testing of these enhancements. For the convenience of discussion, the enhanced SEA program will be referred to as SEA Version 4.1 to distinguish it from the unenhanced SEA Version 3.1.

The testing to validate and verify the SEA enhancements was divided into three phases:

- Phase 1 tests ensured that the enhancements have not corrupted the integrity of the original capabilities of SEA Version 3.1.

- Phase 2 tests compared the SEA Version 4.1 error analysis results with those of the independent Orbit Analysis (ORAN) Program. (ORAN is an error analysis program for the batch orbit determination method, which can be considered a subset of an orbit smoother. Thus, ORAN can be used to verify some, but not all, of the SEA smoother capabilities.)

- Phase 3 tests focused on the smoother algorithm's numerical stability and expected behavior under controlled operating conditions.

These three test phases and their results are described in more detail in Sections A.1, A.2, and A.3, respectively.

During the course of testing several software modifications or corrections were required. After they were implemented, the testing sequence was reinitialized. These modifications or corrections are described in the sections describing the testing phases during which they occurred.

Finally, all keyword deck setups and associated job control language (JCL) used in testing have been archived so that they may be used as prototype benchmarks for future modifications to SEA. For reference, the listings of all deck setups are reproduced in Section A.5. References to setups are made in Sections A.1, A.2, and A.3. The convention for labeling a particular setup is as follows: P_iS_jR_k, where i, j, and k are integers associated with the phase, a given scenario, and a given run number, respectively, for which the test was performed. For brevity, the corresponding SEA Version 3.1 control runs used in Phase 1 of the testing are not listed.

A.1 PARALLEL FUNCTIONAL VERIFICATION

A.1.1 TESTING DESCRIPTION

This phase of testing verified the functional integrity between SEA Version 3.1 and SEA Version 4.1 for nonsmoother options. It was undertaken to ensure that the smoother and TDAS enhancements had not corrupted the existing SEA options and processing. Parallel functional verification was performed under four different tracking scenarios:

1. Direct tracking of a low-altitude satellite from 10 ground stations--The satellite orbit is at a 200-km altitude and 28-deg inclination. An effective drag coefficient is alternately a solve-for or a consider parameter in the orbit determination process. Tracking data are available

whenever the satellite is visible to a station (deck setup PLS1T1).

2. Tracking of a user satellite by six Global Positioning System (GPS) satellites. The user orbit is at a 400-km altitude and 57-deg inclination. Tracking data are available during periods of visibility. Several different geopotential error models are considered (deck setup PLS2T1).

3. Scheduled relay tracking of a user satellite through two Tracking and Data Relay Satellite System (TDRSS) relays. The user satellite is at a 600-km altitude and a 98-deg inclination (deck setup PLS3T1).

4. Continuous beacon tracking of a user satellite through three TDAS satellites (one backside, two front-side)--The user satellite is at a 600-km altitude and a 28-deg inclination (deck setup PLS4T1).

Each of these four tracking scenarios constituted more than one test run. In the test runs performed for this phase, most nonsmoother options were tested, although not in all possible combinations.

SEA Version 3.1 does not include either the smoothing or TDAS options; thus, the basis for comparison in this phase of testing was the forward-filtered results and those reports that are smoother/TDAS independent. In testing associated with the TDAS scenario, this comparison was slightly modified: the forward-filtered results of SEA Version 4.1 were compared with a TDAS-only modification of SEA Version 3.1. This was to test for any interference that might be present when the TDAS and smoother updates were combined in SEA Version 4.1. In addition, the SEA Version 4.1 tests were run with and without requesting the smoother option to test for any smoother-introduced inconsistency in the forward-filtered results.

A.1.2 TESTING RESULTS

All tests performed using SEA Version 3.1 agreed with their corresponding SEA Version 4.1 runs. It may be concluded that the smoother/TDAS updates have not corrupted any of the many options preexisting in SEA.

This agreement is demonstrated by the output listings shown in Figures A-1 and A-2, both of which are associated with the GPS tracking scenario. Figure A-1 displays the forward-filtered error budget at 1440 min past epoch resulting from the nonupdated SEA Version 3.1. Figure A-2 displays the corresponding output resulting from SEA Version 4.1 (run PLS3T1). Although only three decimal places of accuracy are output, the length of propagation is long enough (1 day) so that any divergence would be displayed.

A.2 INDEPENDENT VERIFICATION

A.2.1 TESTING DESCRIPTION

For the independent verification phase, the smoother error analysis results of SEA Version 4.1 were compared and contrasted with corresponding results from the batch orbit determination error analysis program ORAN. SEA and ORAN are two independent programs with different capabilities; comparisons were thus made under restricted conditions in which correspondence or near correspondence between the two programs exists. In particular, this means that no TDAS tracking and no process noise were introduced into this phase of testing. Also, clock errors in SEA Version 4.1 were emulated by measurement biases in ORAN.

Under these restrictions, the same geopotential error models, measurement errors, and tracking systems were considered. However, the atmospheric drag models for the two programs are somewhat different. SEA uses the Harris-Priester model, and ORAN uses the Jacchia model.

E R R O R B U D G E T

	SAT-01H METERS	SAT-01C METERS	SAT-01L METERS	RSS-POS METERS	SAT-01HD MET/SEC	SAT-01CD MET/SEC	SAT-01LD MET/SEC	RSS-VEL MET/SEC
SOLRAD 1								
GRAVCJEF	.406D-02	.106D-03	-.124D-01	.130D-01	-.207D-05	.311D-05	.337D-05	.503D-05
LJMPEJ	.709	.217D-01	-.105	.717	.530D-04	-.253D-03	.493D-03	.557D-03
ACCEL 1	.534	.309	-.494	4.98	.524D-02	-.713D-02	.422D-02	.980D-02
MEASBI 1	1.95	.930	-.15.9	16.0	.220D-01	-.214D-04	-.162D-02	.220D-01
MEASBI 2	.0	.0	.0	.0	.0	.0	.0	.0
MEASBI 4	.0	.0	.0	.0	.0	.0	.0	.0
MEASBI 5	.0	.0	.0	.0	.0	.0	.0	.0
RSS	2.15	.980	16.6	16.8	.226D-01	.714D-02	.454D-02	.241D-01

	SAT-02H METERS	SAT-02C METERS	SAT-02L METERS	RSS-POS METERS	SAT-02HD MET/SEC	SAT-02CD MET/SEC	SAT-02LD MET/SEC	RSS-VEL MET/SEC
SOLRAD 1	.0	.0	.0	.0	.0	.0	.0	.0
GRAVCJEF	.553	.285D-01	-.140D-01	.554	-.310D-05	-.583D-04	.649D-03	.652D-03
LJMPEJ	.224	-3.02	64.5	64.6	-.105	-.166D-01	.313D-03	.106
ACCEL 1	.0	.0	.0	.0	.0	.0	.0	.0
MEASBI 1	.0	.0	.0	.0	.0	.0	.0	.0
MEASBI 2	.0	.0	.0	.0	.0	.0	.0	.0
MEASBI 4	-.161D-01	-.424	-.108	.437	.120D-03	-.854D-03	.178D-04	.862D-03
MEASBI 5	.0	.0	.0	.0	.0	.0	.0	.0
RSS	.597	3.05	64.5	64.6	.105	.166D-01	.721D-03	.106

	USERDRAG	CLKBI 1	DRIFT 1	MEASBI 3
SOLRAD 1	.313D-05	.225D-01	-.380D-06	.0
GRAVCJEF	.744D-04	.428	-.446D-05	.0
LJMPEJ	-.258D-02	2.97	-.411D-05	.0
ACCEL 1	-.844D-03	51.1	-.362D-01	.0
MEASBI 1	.127D-09	-.162D-04	.852D-11	.0
MEASBI 2	.0	.0	.0	.0
MEASBI 4	.0	.0	.0	.0
MEASBI 5	.0	.0	.0	.0
RSS	.271D-02	51.2	.362D-01	.0

Figure A-1. SEA Version 3.1 Forward-Filtered Error Budget at 1440 Minutes. User Tracking Through Six GPS Satellites

A-5

ORIGINAL PAGE IS
OF POOR QUALITY

E R R O R B U D G E T

	SAT-01H METERS	SAT-01C METERS	SAT-01L METERS	RSS-POS METERS	SAT-01HD MET/SEC	SAT-01CD MET/SEC	SAT-01LD MET/SEC	RSS+VEL MET/SEC
SJLRAD 1	-.406D-02	.106D-03	-.124D-01	.130D-01	-.207D-05	.311D-05	.337D-05	.503D-05
GRAVCDEF	.709	.217D-01	-.105	.717	.530D-04	-.253D-03	.493D-03	.557D-03
LUMPED	-.534	-.309	4.94	4.98	.524D-02	-.713D-02	.422D-02	.980D-02
ACCEL 1	1.95	.930	-15.9	16.0	.220D-01	-.214D-04	-.162D-02	.220D-01
MEASBI 1	.582D-06	-.271D-06	-.117D-05	.133D-05	.914D-09	-.394D-10	-.603D-09	.110D-08
MEASBI 2	.0	.0	.0	.0	.0	.0	.0	.0
MEASBI 4	.0	.0	.0	.0	.0	.0	.0	.0
MEASBI 5	.0	.0	.0	.0	.0	.0	.0	.0
RSS	2.15	.980	16.6	16.8	.226D-01	.714D-02	.454D-02	.241D-01

	SAT-02H METERS	SAT-02C METERS	SAT-02L METERS	RSS-POS METERS	SAT-02HD MET/SEC	SAT-02CD MET/SEC	SAT-02LD MET/SEC	RSS-VEL MET/SEC
SJLRAD 1	.0	.0	.0	.0	.0	.0	.0	.0
GRAVCDEF	.553	.285D-01	-.140D-01	.554	-.310D-05	-.583D-04	.649D-03	.652D-03
LUMPED	-.224	-3.02	64.5	64.6	-.105	-.166D-01	.313D-03	.106
ACCEL 1	.0	.0	.0	.0	.0	.0	.0	.0
MEASBI 1	.0	.0	.0	.0	.0	.0	.0	.0
MEASBI 2	.0	.0	.0	.0	.0	.0	.0	.0
MEASBI 4	-.161D-01	-.424	-.108	.437	.120D-03	-.854D-03	.178D-04	.862D-03
MEASBI 5	.0	.0	.0	.0	.0	.0	.0	.0
RSS	.597	3.05	64.5	64.6	.105	.166D-01	.721D-03	.106

	USERDRAG	CLKBI 1	DRIFT 1	MEASBI 3
SJLRAD 1	.313D-05	.225D-01	-.380D-06	.0
GRAVCDEF	.744D-04	.428	.446D-05	.0
LUMPED	-.258D-02	2.97	-.411D-05	.0
ACCEL 1	-.344D-03	51.1	-.362D-01	.0
MEASBI 1	.127D-09	-.162D-04	.852D-11	.0
MEASBI 2	.0	.0	.0	.0
MEASBI 4	.0	.0	.0	.0
MEASBI 5	.0	.0	.0	.0
RSS	.271D-02	51.2	.362D-01	.0

A-6

Figure A-2. SEA Version 4.1 Forward-Filtered Error Budget at 1440 Minutes. User Tracking Through Six GPS Satellites

ORIGINAL PAGE IS
OF POOR QUALITY

Because the two programs use different error analysis algorithms, some differences in the results produced were expected even if the initial conditions and input values were the same. Special attention was therefore accorded the degree of disagreement between SEA and ORAN results to ensure that discrepancies were not larger than bounds established by physical considerations.

Independent verification was performed under two different tracking scenarios using corresponding SEA and ORAN setups:

1. Direct tracking of two TDRS-type spacecraft through a single ground tracking station--Dynamic errors considered are lumped geopotential modeling errors (GEM-9 15x15 - GEM-1 8x8) and gravitational constant. Measurement bias errors are considered on both range and range-rate data (deck setups P2S1T1 and P2S1T10 (the 0 indicates the ORAN run)).

2. Relay tracking of a user satellite through two TDRSS-type satellites--The user satellite is at a 400-km altitude and a 28-deg inclination. Dynamic and measurement errors are of the same type as those in the previous scenario. In addition, an effective drag uncertainty is considered (deck setups P2S2T1 through P2S2T20).

In this phase of testing, the smoother results of SEA Version 4.1 were compared with the batch results from ORAN. In addition, corresponding observation measurements and propagated ephemerides between SEA Version 4.1 and ORAN served as additional bases for comparison.

A.2.2 TESTING RESULTS

In the course of testing, it was found that the two programs usually agree quite well: two to three decimal digits were quite common for most numeric results. Close comparison between the two programs was achieved in the direct tracking scenario. Figures A-3 and A-4 display the error budget

TIME FROM EPOCH IN MINUTES = 1080.

F R R O R B U D G E T

	SAT-01H METERS	SAT-01C METERS	SAT-01L METERS	RSS-POS METERS	SAT-01HN MET/SEC	SAT-01CN MET/SEC	SAT-01LD MET/SEC	RSS-VEL MET/SEC
GRAVCOFF	3.43	-.218	-28.3	28.5	.207n-02	.128n-03	.262n-03	.209n-02
LUMPCO	-.278	-.272	2.11	2.15	-.161n-03	.156n-04	.136n-04	.162n-03
MEASPT 1	-.607n-01	-.159	-20.4	20.4	.149n-02	.928n-04	.427n-05	.150n-02
MEASPT 2	0	0	0	0	0	0	0	0
MEASPT 3	7.21	-31.1	-40.4	51.4	.296n-02	.654n-03	-.387n-03	.305n-02
MEASPT 4	0	0	0	0	0	0	0	0
RSS	7.99	31.1	53.4	62.3	.391n-02	.673n-03	.468n-03	.400n-02
	SAT-02H METERS	SAT-02C METERS	SAT-02L METERS	RSS-POS METERS	SAT-02HN MET/SEC	SAT-02CN MET/SEC	SAT-02LD MET/SEC	RSS-VEL MET/SEC
GRAVCOFF	3.54	.821	28.5	28.7	-.208n-02	-.124n-03	.254n-03	.210n-02
LUMPCO	.635	3.31	6.94	7.71	-.515n-03	-.436n-04	-.159n-04	.518n-03
MEASPT 1	0	0	0	0	0	0	0	0
MEASPT 2	.170n-01	.595	30.5	30.5	-.150n-02	-.901n-04	-.166n-05	.150n-02
MEASPT 3	0	0	0	0	0	0	0	0
MEASPT 4	-3.43	1.59	-33.7	34.0	.188n-02	-.192n-02	.782n-04	.269n-02
RSS	4.97	3.01	42.9	43.3	.322n-02	.193n-02	.266n-03	.376n-02

Figure A-3. SEA Version 4.1 Smoothed Error Budget at 1080 Minutes. Direct Tracking on Two TDRS-Type Spacecraft

A-9

ESTIMATED HCI ERROR FOR ARC NO. 1 DUE TO UNMODIFIED PARAMETERS								UNADJUSTED PARAMETER
DELTA H (METERS)	DELTA C (METERS)	DELTA L (METERS)	RSS POS (METERS)	DELTA HDOT (CM/SEC)	DELTA CDOT (CM/SEC)	DELTA LDOT (CM/SEC)	RSS VFL (CM/SEC)	
TIME = 1080.00 MINUTFS								
YYMMDD HHMM SS.S = 800301 1800 0.0								
SATELLITE 1								
3.4244	-.16588	-28.324	28.531	.20736	.13071470-01	.26242980-01	.20948	GRAVCO
-.27861	-.27295	2.1193	2.1539	-.161390-01	.14905120-02	.13646600-02	.162650-01	MD1-MD2 GRAV
-.626160-01	-.12875	-20.376	20.376	.14918	.10004510-01	.43569790-03	.14951	RNGRIAS1
.0	.0	.0	.0	.0	.0	.0	.0	RNGRIAS2
.1973	-.30.992	-40.267	51.320	.29491	.65239360-01	-.38660510-01	.30451	ROOTRIAS1
.0	.0	.0	.0	.0	.0	.0	.0	ROOTRIAS2
SATELLITE 2								
3.5321	.91497	28.476	28.709	-.20853	.13305040-01	.25446300-01	.21050	GRAVCO
.63369	3.3604	6.9516	7.7472	-.516390-01	.45130880-02	-.15628140-02	.518590-01	MD1-MD2 GRAV
.0	.0	.0	.0	.0	.0	.0	.0	RNGRIAS1
.146250-01	.05650	20.486	20.497	-.15002	-.96660680-02	-.13539140-03	.15033	RNGRIAS2
.0	.0	.0	.0	.0	.0	.0	.0	ROOTRIAS1
-.3.4491	0.2164	-23.475	23.830	.18568	-.1860768	.81815640-02	.26300	ROOTRIAS2

Figure A-4. ORAN Batch Error Budget at 1080 Minutes. Direct Tracking on Two TDRS-Type Spacecraft

ORIGINAL PAGE IS
OF POOR QUALITY

output from SEA Version 4.1 and ORAN (setups P2S1T1 and P2S1T10) at 1080 min after epoch.

In the relay tracking scenario, a limitation in ORAN complicated the process of comparison between the two programs. ORAN does not model the TDRSSs directly as relay satellites with given orbits; an artifice has to be used to make ORAN simulate the relay role of the TDRSSs.¹ Naturally, greater disparities should be expected between the results.

An example of the relay tracking scenario results is shown in Figures A-5 and A-6, in which the error budget outputs for 180 min past epoch are shown for SEA and ORAN, respectively (deck setups P2S2T1 and P2S2T10). All error budgets agree quite well except for the errors caused by the gravity coefficient uncertainty and the drag uncertainty. The ORAN result shows considerably greater effect for the gravity coefficient uncertainty. This was expected because, in the artifice of ORAN simulation, this uncertainty also accounts for part of the TDRSS ephemeris errors. In other words, the ORAN result includes both the dynamic effect of gravity coefficient uncertainty and the geometric effect of TDRSS ephemeris error that can be attributed to gravity coefficient uncertainty in deriving the TDRS orbits. The drag uncertainty effects from the two programs are different because, as discussed above, two different atmospheric drag models were used.

A comparison between SEA and ORAN was also performed for the scenario in which all three satellite orbits are solved for simultaneously. Figures A-7 and A-8 demonstrate the results of setups in which both relay and direct tracking of the

¹EG&G Washington Analytical Services Center, Inc., TDRSS Era Orbit Determination System Review Study, B. T. Fang and B. P. Gibbs, December 1975.

TIME FROM EPOCH IN MINUTES = 180.0

F R R O R B U D G E T

	SAT-01H METERS	SAT-01C METERS	SAT-01L METERS	RSS-POS METERS	SAT-01HD MET/SEC	SAT-01CD MET/SEC	SAT-01LD MET/SEC	RSS-VEL MET/SEC
USFRORIG	.17A	2.40	-9.55	9.85	.967E-02	-.273E-02	-.204E-03	.100E-01
GRAVCOFF	.650	.378E-01	-.107	.660	.527E+04	-.900E-03	.545E-03	.105E-02
LAPPOFF	14.4	65.6	-30.4	73.7	.360E+01	.349E-01	.206E-01	.542E-01
MFDASRI 1	-2.33	-3.31	1.59	4.35	-.915E+03	.472E-02	.261E-02	.464E-02
MFDASRI 2	.733	2.27	3.18	7.98	-.157E+02	.687E-02	-.861E-03	.710E-02
MFDASRI 3	1.100E-05	.409E-02	-.396E-02	.570E-02	.422E+05	-.607E+05	.679E-07	.739E-05
MFDASRI 4	-.293E-03	-.366E-02	-.943E-03	.379E-02	.143E+05	.448E+05	.313E-06	.472E-05
RSS	14.6	65.8	32.0	74.6	.373E-01	.358E-01	.208E-01	.558E-01

Figure A-5. SEA Version 4.1 Smoothed Error Budget at 180 Minutes. Relay Tracking of 400-Kilometer-Altitude Spacecraft Through Two TDRSs

A-11

ORIGINAL PAGE IS
OF POOR QUALITY

A-12

ESTIMATED HCI ERROR FOR APC NO. 1 DUE TO UNMODIFIED PARAMETERS

DELTA H (METERS)	DELTA C (METERS)	DELTA I (METERS)	RSS POS (METERS)	DELTA HDOT (CM/SEC)	DELTA PDOT (CM/SEC)	DELTA LDOT (CM/SEC)	RSS VEL (CM/SEC)	UNADJUSTED PARAMETER
TIME = 180.000 MINUTES YYYMMDD HHMM SS.S = 800301 300 0.0								
SATFLITE 1								
-1.3103	5.8107	5.5197	8.1207	-2.3781	-4.337399	.2780898	.56747	GRAVCO
-14.257	68.3339	-27.382	74.987	3.3766	3.450653	2.040667	5.2415	MD1-MD2 GRAV
858640-n1	1.1365	-4.3585	4.5050	.44027	-1274846	-.89893757-02	.45900	NRAG
3.3331	-3.3104	1.5947	4.3526	-.915920-n1	-.3723932	-.2614493-	.46414	RNGRIAS1
7.3331	2.2714	3.1859	3.9805	-.15715-	-.6869283	-.86155613-n1	.70992-	RNGRIAS2
-919270-n5	-409120-n2	-392420-n2	-299700-n2	-.422000-n3	-.60693410-n3	-.67745990-n5	.739250-n3	RDOTRIAS1
-292910-n3	-365990-n2	-.947980-n3	-.379090-n2	-.143360-n3	-.44818790-n3	.31264970-n4	.471600-n3	RDOTRIAS2
SATFLITE 2								
3.6412	1.5951	-28.655	20.930	.20873	-.82832790-n2	-.24690330-n1	.21034	GRAVCO
-13116	-188290-n1	1.0003	1.0041	-.729820-n2	-.24961790-n2	.94132750-n3	.777050-n2	MD1-MD2 GRAV
-917240-n5	-131930-n4	-259800-n5	-134720-n4	-.923900-n8	-.95063680-n7	-.60029390-n8	.957000-n7	NRAG
-249880-n5	-348370-n4	-576720-n6	-349620-n4	-.501350-n8	-.53322060-n7	-.20545080-n7	.573630-n7	RNGRIAS1
-230830-n5	-301680-n4	-195610-n5	-303130-n4	-.365520-n8	-.75319270-n7	-.62774210-n7	.772510-n7	RNGRIAS2
-191960-n3	-601630-n8	-.444850-n8	-.755150-n3	-.257270-n10	-.86538050-n10	-.62764660-n11	.904990-n10	RDOTRIAS1
-229420-n2	-193790-n7	-.570480-n8	-.203320-n7	-.349170-n10	-.10732900-n9	-.15134570-n10	.113880-n9	RDOTRIAS2
SATFLITE 3								
3.4070	-1.9311	28.953	24.227	-.21065	-.36337450-n2	-.26381210-n1	.21233	GRAVCO
1.9010	-2.7022	14.589	14.958	-.10712-	-.14775740-n1	-.74468730-n2	.10841-	MD1-MD2 GRAV
-205880-n5	-158920-n4	-.533490-n5	-168910-n4	-.381840-n7	-.57264400-n7	-.13226000-n7	.690180-n7	NRAG
-266470-n5	-231570-n4	-.118240-n5	-293020-n4	-.469770-n8	-.66064420-n8	-.18767190-n7	.204430-n7	RNGRIAS1
-291440-n5	-289200-n4	-.134950-n5	-.990970-n4	-.121800-n7	-.22345770-n7	-.19927970-n7	.323230-n7	RNGRIAS2
-249350-n3	-123930-n7	-.130230-n7	-.181490-n7	-.886740-n10	-.86358590-n10	-.14421250-n10	.124610-n9	RDOTRIAS1
-220640-n2	-145760-n7	-.842720-n8	-.169810-n7	-.576460-n10	-.27294760-n10	-.13233930-n10	.678090-n10	RDOTRIAS2

Figure A-6. ORAN Batch Error Budget at 180 Minutes. Relay Tracking of 400-Kilometer-Altitude Spacecraft Through Two TDRSs

TIME FROM EPOCH-IN MINUTES = .0

ERROR BUDGET

	SAT-01H METERS	SAT-01C METERS	SAT-01L METERS	RSS-POS METERS	SAT-01HD MET/SEC	SAT-01CD MET/SEC	SAT-01LD MET/SEC	RSS-VEL MET/SEC
MEASBI 1	-1.47	-2.04	-1.03	2.72	.172D-02	.844D-02	.159D-02	.876D-02
MEASBI 2	1.19	2.86	-1.86	3.61	.279D-02	.948D-02	-.143D-02	.998D-02
MEASBI 3	-.414D-02	-.130D-01	-.861D-01	.872D-01	.519D-04	-.441D-04	.597D-05	.683D-04
MEASBI 4	-.889D-02	-.432D-02	.423D-01	.435D-01	-.184D-05	.245D-04	.952D-05	.264D-04
RSS	1.90	3.51	2.12	4.52	.328D-02	.127D-01	.214D-02	.133D-01
	SAT-02H METERS	SAT-02C METERS	SAT-02L METERS	RSS-POS METERS	SAT-02HD MET/SEC	SAT-02CD MET/SEC	SAT-02LD MET/SEC	RSS-VEL MET/SEC
MEASBI 1	-1.42	23.4	-3.62	23.7	.794D-04	.183D-02	.104D-03	.183D-02
MEASBI 2	-.230	12.6	-4.74	13.5	.187D-03	.162D-02	.290D-04	.163D-02
MEASBI 3	-.381D-01	.252	.112	.278	-.592D-05	-.298D-04	.246D-05	.305D-04
MEASBI 4	.542D-01	-.483	-.927D-01	.495	.586D-05	.170D-04	-.361D-05	.183D-04
RSS	1.44	26.6	5.97	27.3	.203D-03	.244D-02	.109D-03	.246D-02
	SAT-03H METERS	SAT-03C METERS	SAT-03L METERS	RSS-POS METERS	SAT-03HD MET/SEC	SAT-03CD MET/SEC	SAT-03LD MET/SEC	RSS-VEL MET/SEC
MEASBI 1	-1.52	19.9	5.92	20.8	-.500D-03	.134D-02	.128D-03	.144D-02
MEASBI 2	-1.95	18.3	-.309	18.4	-.857D-04	.166D-02	.144D-03	.167D-02
MEASBI 3	-.610D-02	-.296	-.358	.465	.232D-04	.250D-04	-.345D-06	.341D-04
MEASBI 4	.482D-02	.170	.236	.291	-.159D-04	-.901D-05	.206D-06	.183D-04
RSS	2.47	27.1	5.95	27.8	.508D-03	.213D-02	.192D-03	.220D-02

A-13

Figure A-7. SEA Version 4.1 Smoothed Error Budget at Epoch. Relay Tracking Scenarios in Which User and Relay Orbits Are Solved for Simultaneously

ORIGINAL PAGE IS
OF POOR QUALITY

A-14

ESTIMATED HCI ERROR FOR ARC NO. 1 DUE TO UNMODIFIED PARAMETERS

DELTA U (CM/SEC)	DELTA C (METERS)	DELTA I (METERS)	PSS POS (METERS)	DELTA HDOT (CM/SEC)	DELTA CDOT (CM/SEC)	DELTA LDOT (CM/SEC)	RSS VEL (CM/SEC)	UNADJUSTED PARAMETER
TIME = 1.0 MINUTES YYYMMDD HHMM SS.S = 800301 0 0.0								
SATFLITE 1								
-1.4754	-2.2414	-1.0274	2.7202	.17206	.8440144	.1592187	.87597	RNGRIAS1
-1.1905	-2.1572	-1.8556	3.6093	.27921	.9475101	-.1427880	.99806	RNGRIAS2
-.416430-02	-.124127-01	-.861770-01	-.372430-01	-.519120-02	-.44042810-02	.59897240-03	.683410-02	ROOTRIAS1
-.176170-02	-.134270-02	-.423940-01	.435120-01	-.190510-03	.24481620-02	.94836760-03	.263230-02	ROOTRIAS2
SATFLITE 2								
-1.4210	2.2402	-3.6353	23.726	.903230-02	.1831492	.10431140-01	.18362	RNGRIAS1
-.22819	12.031	-0.7454	13.502	.187370-01	.1623463	.28903380-02	.16345	RNGRIAS2
-.301200-01	-.25170	.11219	.27824	-.591710-03	-.29873610-02	.24571670-03	.305530-02	ROOTRIAS1
.541630-01	-.43250	-.728890-01	.49426	.584610-03	.17008260-02	-.36090940-03	.183430-02	ROOTRIAS2
SATFLITE 3								
-1.200	10.004	5.9051	20.822	-.498770-01	.1336306	.12779080-01	.14321	RNGRIAS1
-1.9479	1.0533	-1.32583	18.439	-.842360-02	.1656153	.14358780-01	.16645	RNGRIAS2
-.610320-02	-.27550	-.35847	.46498	.231880-02	.25061160-02	-.34412230-04	.341450-02	ROOTRIAS1
.435820-02	.16705	.23616	.29047	-.159150-02	-.90320930-03	.20249220-04	.183000-02	ROOTRIAS2

Figure A-8. ORAN Batch Error Budget at Epoch. Relay Tracking Scenarios in Which User and Relay Orbits Are Solved for Simultaneously

ORIGINAL PAGE IS
OF POOR QUALITY

relays are present (deck setups P2S2T2 and P2S2T20). These figures display the error budgets for all three satellites at the epoch or starting time and show very good agreement.

A.3 FUNCTIONAL PERFORMANCE VALIDATION

A.3.1 TESTING DESCRIPTION

As mentioned in Section A.2.1, the SEA smoother capability cannot be verified in the presence of process noise by examining the agreements between SEA and ORAN. Thus, the final phase of testing concentrated on the effects of process noise on the smoother behavior. (See Section 5 for a related study.)

If the smoother was implemented correctly, the following results should be observed in the tests:

- The smoothed state variances should be smaller than the corresponding filtered state variances. This should be true irrespective of the magnitude of the process noise.

- The smoothed state variances should increase with the increase of the process noise.

- The process noise should introduce a fading memory feature into an estimator. Thus, the effect of dynamic errors is attenuated with the use of process noise whereas the effect of measurement noise is amplified. Furthermore, the filter is a one-sided fading memory estimator whereas the smoother is a two-sided fading memory filter. The fluctuation of errors with time is thus considerably smaller for a smoother than for a filter.

This phase of testing was performed using the following tracking scenarios with controlled process noise parameters:

1. Scheduled relay tracking of a user satellite through two TDRSs--The user satellite was at a 600-km altitude and a 28-deg inclination. A nominal velocity variance process

noise of $1 \times 10^{-9} \text{ m}^2/\text{sec}^3$ and several variations were used (deck setup P3S1T1).

2. Continuous tracking of a user satellite through three TDAS satellites (one backside, two frontside)--The user satellite is at a 600-km altitude and a 28-deg inclination. A nominal velocity variance process noise of $1 \times 10^{-9} \text{ m}^2/\text{sec}^3$ and several variations were used (deck setup P3S2T1).

A.3.2 TESTING RESULTS

During the course of this phase of testing, the following errors relating to the process noise in backward filtering/smoothing were uncovered and corrected:

- The process noise variance had an incorrect sign because the elapsed time was computed based on backward time differences.
- The process noise variance was not propagated using the backward transition matrix. This was a subtle error that was intimately related to the method chosen to model the process noise in forward filtering.
- The backward filter/smoothen executive did not include the backward process noise added since the last measurement, when it computed the smoothed error results.

After these corrections were made, tests performed confirmed that all process noise effects listed in Section A.3.1 were indeed observed, thus providing confidence that the SEA smoother capability was working correctly. Figures A-9 through A-12 show some sample error analysis results at 1140 min of a 1440-min TDAS tracking arc (run corresponding to Scenario 2 of Section A.3.1). The reduction of error from filtering (Figure A-9) to smoothing (Figure A-10) and the decrease in dynamic error (lumped geopotential) and

TIME FROM EPOCH IN MINUTES = 1140.

ERROR BUDGET

	SAT-01H	SAT-01C	SAT-01I	RSS-POS	SAT-01HD	SAT-01CD	SAT-01ID	RSS-VEL
	METERS	METERS	METERS	METERS	MET/SEC	MET/SEC	MET/SEC	MET/SEC
SOLRAD 1	-.419D-02	-.288D-03	-.221D-02	.475D-02	-.439D-05	-.106D-05	.525D-05	.693D-05
GRAVCOEF	.557	.681	-.515D-01	.881	-.945D-04	-.335D-03	.581D-03	.677D-03
LUMPED	-4.47	-16.4	10.2	19.6	-.552D-02	-.186D-01	.428D-02	.198D-01
ACCEL 1	1.13	10.4	-13.7	17.2	.122D-01	-.801D-02	-.206D-02	.147D-01
MEASBI 1	-.432D-01	.103	-.674D-01	.130	-.531D-04	.563D-04	.340D-04	.845D-04
MEASBI 2	.407	-.429D-01	-.881	.971	.798D-03	-.785D-03	-.368D-03	.118D-02
MEASBI 3	-.515D-01	-.167	-.538D-01	.183	.432D-05	-.906D-04	-.325D-04	-.964D-04
MEASBI 4	-.336	1.08	-.541	1.25	.185D-03	-.259D-03	.215D-03	.384D-03
MEASBI 5	-.831D-02	.646D-01	-.121	.138	-.488D-04	-.147D-03	-.142D-05	.155D-03
MEASBI 6	.610D-01	.183D-01	-.363	.369	-.250D-04	.221D-03	-.562D-04	.229D-03
EPHEMERR	.865	3.89	14.0	14.5	-.105D-01	.621D-02	-.103D-02	.122D-01
RSS	4.75	19.8	22.1	30.0	.170D-01	.212D-01	.491D-02	.276D-01

	USERDRAG	CLKBI 1	DRIFT 1
SOLRAD 1	.340D-05	.647D-02	-.260D-06
GRAVCOEF	.737D-04	5.62	-.729D-04
LUMPED	-.686D-04	-45.6	.741D-03
ACCEL 1	.452D-03	28.7	-.401D-01
MEASBI 1	.102D-03	-14.3	-.282D-03
MEASBI 2	-.247D-04	2.48	-.200D-04
MEASBI 3	-.123D-03	3.10	-.512D-04
MEASBI 4	.124D-03	1.69	-.612D-04
MEASBI 5	.211D-04	-15.9	-.231D-03
MEASBI 6	.623D-04	6.32	-.920D-04
EPHEMERR	.518D-03	-71.2	-.339D-03
RSS	.727D-03	92.3	.401D-01

STANDARD DEVIATION - CORRELATION MATRIX

	SAT-01X	SAT-01Y	SAT-01Z	SAT-01XD	SAT-01YD	SAT-01ZD
SAT-01X	.975	.431	.133	-.377	.414	.331
SAT-01Y	.431	.994	.404	.202	.887	.615
SAT-01Z	.133	.404	.916	.255	.640	.494
SAT-01XD	-.377	.202	.255	.552D-03	.156	-.114
SAT-01YD	.414	.887	.640	.156	.126D-02	.487
SAT-01ZD	.331	.615	.494	-.114	.487	.116D-02
USERDRAG	-.312D-02	.332D-02	.351D-02	-.247D-02	.391D-02	.353D-02
CLKBI 1	.137D-01	-.513D-02	.382D-01	.448D-04	.230D-01	-.122D-01
DRIFT 1	-.640D-01	-.326	-.146	-.123	-.288	-.194

	USERDRAG	CLKBI 1	DRIFT 1
SAT-01X	-.312D-02	.137D-01	-.640D-01
SAT-01Y	.332D-02	-.513D-02	-.326
SAT-01Z	.351D-02	.382D-01	-.146
SAT-01XD	-.247D-02	.448D-04	-.123
SAT-01YD	.391D-02	.230D-01	-.288
SAT-01ZD	.353D-02	-.122D-01	-.194
USERDRAG	.250D-01	.352D-02	-.351D-02
CLKBI 1	.352D-02	4.39	-.579
DRIFT 1	-.351D-02	-.579	.110D-03

Figure A-9. SEA Version 4.1 Forward-Filtered Error Budget at 1140 Minutes. Nominal Velocity Variance Rate Process Noise of 1×10^{-9} Meter²/Second³

A-17

ORIGINAL PAGE IS
OF POOR
QUALITY

E R R O R B U D G E T

	SAT-01H	SAT-01C	SAT-01E	RSS-POS	SAT-01HD	SAT-01CD	SAT-01LD	RSS-VEL
	METERS	METERS	METERS	METERS	MET/SEC	MET/SEC	MET/SEC	MET/SEC
SOLRAD 1	-.241D-04	.887D-05	-.812D-04	.851D-04	-.472D-06	-.144D-05	.381D-06	.156D-05
GRAVCOEF	.689	.736	.396D-01	1.01	-.570D-05	-.374D-03	.520D-03	.641D-03
LUMPED	-5.59	-13.2	5.99	15.5	-.285D-02	-.645D-02	.415D-02	.819D-02
ACCEL 1	1.40	14.0	-7.80	16.1	.911D-02	-.976D-02	-.128D-02	.134D-01
MEASBI 1	-.206D-01	.589D-02	.361D-01	.420D-01	-.254D-04	-.236D-04	-.194D-04	.398D-04
MEASBI 2	.198	.591	-.512	.806	.496D-03	-.168D-03	-.192D-03	.557D-03
MEASBI 3	.211D-01	-.807D-01	-.489D-01	-.967D-01	-.425D-04	.137D-04	-.238D-04	.606D-04
MEASBI 4	-.141	.557	-.442	.725	.416D-03	.410D-04	.160D-03	.447D-03
MEASBI 5	-.428D-03	.749D-01	-.850D-01	.113	.679D-04	.991D-05	.432D-05	.687D-04
MEASBI 6	.568D-01	.340D-01	.333	.340	-.186D-03	-.705D-03	-.760D-04	.733D-03
EPHEMERR	1.21	.917	13.8	13.8	-.105D-01	.256D-02	-.116D-02	.108D-01
RSS	5.93	19.3	16.9	26.3	.142D-01	.120D-01	.454D-02	.191D-01

	USERDRAG	CLKBI 1	DRIFT 1
SOLRAD 1	.413D-05	.634D-02	-.932D-07
GRAVCOEF	.576D-04	5.97	-.739D-04
LUMPED	-.101D-02	-45.6	.665D-03
ACCEL 1	-.197D-03	37.5	-.403D-01
MEASBI 1	.102D-03	-14.3	-.279D-03
MEASBI 2	-.489D-04	2.64	-.393D-04
MEASBI 3	-.115D-03	3.15	.483D-04
MEASBI 4	.806D-04	2.14	-.458D-04
MEASBI 5	.123D-04	-15.9	.231D-03
MEASBI 6	.822D-04	6.37	-.939D-04
EPHEMERR	.672D-03	-70.8	-.266D-03
RSS	.125D-02	95.2	.403D-01

S T A N D A R D D E V I A T I O N - C O R R E L A T I O N M A T R I X

	SAT-01X	SAT-01Y	SAT-01Z	SAT-01XD	SAT-01YD	SAT-01ZD
SAT-01X	.720	.509	.202	-.637	.644	.486
SAT-01Y	.509	.449	-.485D-01	.109	.607	.338
SAT-01Z	.202	-.859D-01	.543	.130	.310	.251
SAT-01XD	-.637	.109	.130	.461D-03	-.133	-.283
SAT-01YD	.644	.607	.310	-.133	.511D-03	.910D-01
SAT-01ZD	.486	.338	.251	-.283	.910D-01	.696D-03
USERDRAG	-.174D-03	.158D-03	.212D-03	.514D-03	-.170D-03	.247D-03
CLKBI 1	.107D-01	-.169D-01	.528D-01	-.412D-02	.421D-01	-.174D-01
DRIFT 1	-.119D-02	-.404D-02	-.176D-03	-.154D-02	-.280D-02	-.702D-03

	USERDRAG	CLKBI 1	DRIFT 1
SAT-01X	-.174D-03	.107D-01	-.119D-02
SAT-01Y	.158D-03	-.169D-01	-.404D-02
SAT-01Z	.212D-03	.528D-01	-.176D-03
SAT-01XD	.514D-03	-.412D-02	-.154D-02
SAT-01YD	.170D-03	.421D-01	-.280D-02
SAT-01ZD	.247D-03	-.174D-01	-.702D-03
USERDRAG	.250D-01	.355D-02	-.550D-04
CLKBI 1	.355D-02	4.38	-.151D-01
DRIFT 1	-.550D-04	-.151D-01	.422D-02

Figure A-10. SEA Version 4.1 Smoothed Error Budget at 1140 Minutes. Nominal Velocity Variance Rate Process Noise of 1×10^{-9} Meter²/Second³

TIME FROM EPOCH IN MINUTES = 1140.

ERROR BUDGET

	SAT-01H METERS	SAT-01C METERS	SAT-01L METERS	RSS-POS METERS	SAT-01HD MET/SEC	SAT-01CD MET/SEC	SAT-01LD MET/SEC	RSS-VEL MET/SEC
SOLRAD 1	.412D-04	.117D-03	-.711D-04	.143D-03	-.318D-06	-.651D-06	.129D-06	.736D-06
GRAVCOEF	.557	.619	-.219	.862	-.787D-04	-.299D-03	.643D-03	.713D-03
LUMPED	-3.63	-7.24	-1.02	8.17	.268D-02	.454D-02	.475D-03	.529D-02
ACCEL 1	-1.08	6.61	-18.8	20.0	.734D-02	-.811D-02	.394D-02	.116D-01
MEASBI 1	.680D-01	-.360D-01	-.655D-01	.101	-.252D-04	.164D-03	-.757D-04	.182D-03
MEASBI 2	.670D-01	.271	-.481	.556	.412D-03	-.134D-02	.193D-03	.141D-02
MEASBI 3	-.333D-01	-.169	.179	.248	-.830D-04	-.214D-03	.143D-04	.230D-03
MEASBI 4	-.107	1.14	-1.33	1.75	.506D-03	.135D-02	.250D-03	.146D-02
MEASBI 5	-.347D-01	.205	-.113	.237	.108D-03	.504D-04	.614D-04	.134D-03
MEASBI 6	-.506D-01	-.453	.274	.898	-.320D-03	-.667D-03	-.127D-03	.751D-03
EPHEMERR	-.350	-5.18	15.8	16.6	-.111D-01	.285D-02	-.777D-03	.115D-01
RSS	3.45	11.2	24.6	27.3	.136D-01	.994D-02	.411D-02	.173D-01

	USERDRAG	CLKBI 1	DRIFT 1
SOLRAD 1	-.298D-09	-.275D-03	-.423D-08
GRAVCOEF	-.293D-06	1.56	-.107D-04
LUMPED	-.612D-06	-1.80	.359D-04
ACCEL 1	-.297D-05	16.7	-.399D-01
MEASBI 1	-.175D-06	-15.2	-.260D-03
MEASBI 2	-.162D-06	1.35	-.191D-04
MEASBI 3	-.857D-07	1.12	-.155D-04
MEASBI 4	-.100D-06	1.73	-.452D-04
MEASBI 5	-.260D-06	-19.2	-.275D-03
MEASBI 6	-.203D-06	5.60	-.675D-04
EPHEMERR	-.119D-05	-90.5	.715D-04
RSS	.329D-05	95.5	.393D-01

STANDARD DEVIATION - CORRELATION MATRIX

	SAT-01X	SAT-01Y	SAT-01Z	SAT-01XD	SAT-01YD	SAT-01ZD
SAT-01X	13.7	.360	-.923D-02	-.267	-.444	.412
SAT-01Y	.360	11.3	-.902D-01	.126	-.518D-01	.361
SAT-01Z	-.723D-02	-.902D-01	19.0	.345	.612D-01	.489D-01
SAT-01XD	-.267	.126	.345	.174D-01	.568	-.390D-01
SAT-01YD	-.444	-.518D-01	.612D-01	.568	.606D-02	-.233
SAT-01ZD	.412	.361	.489D-01	-.390D-01	-.233	.289D-01
USERDRAG	-.150D-04	.118D-04	-.824D-05	.107D-04	.114D-04	.285D-05
CLKBI 1	.152D-01	.227D-02	.623D-02	-.415D-02	.165D-01	-.198D-02
DRIFT 1	-.163D-01	-.115	.720D-02	-.246D-01	-.972D-02	-.328D-01

	USERDRAG	CLKBI 1	DRIFT 1
SAT-01X	-.150D-04	.152D-01	-.163D-01
SAT-01Y	.118D-04	.227D-02	-.115
SAT-01Z	-.324D-05	.623D-02	.720D-02
SAT-01XD	.107D-04	-.415D-02	-.246D-01
SAT-01YD	.114D-04	.165D-01	-.972D-02
SAT-01ZD	.285D-05	-.198D-02	-.328D-01
USERDRAG	.257D-01	.152D-04	-.357D-05
CLKBI 1	.152D-04	31.8	-.109
DRIFT 1	-.357D-05	-.109	.427D-02

Figure A-11. SEA Version 4.1 Smoothed Error Budget at 1140 Minutes. Velocity Variance Rate Process Noise of 1×10^{-6} Meter²/Second³

ORIGINAL PAGE IS
OF POOR QUALITY

A-19

TIME FROM EPOCH IN MINUTES = 1140.

ERROR BUDGET

	SAT-01H METERS	SAT-01C METERS	SAT-01L METERS	RSS-PDS METERS	SAT-01HD MET/SEC	SAT-01CD MET/SEC	SAT-01LD MET/SEC	RSS-VEL MET/SEC
SOLRAD 1	-.111D-01	-.243D-03	-.207D-01	.130D-01	.169D-05	-.227D-05	.123D-04	-.126D-04
JRACVCEJ	.619	.601	-.207D-01	.921	.498D-04	-.324D-03	.587D-03	-.672D-03
LUMPED	-9.93	-6.48	17.2	20.4	-.136D-01	-.120D-02	.874D-02	-.162D-01
ACCL 1	.433	8.82	-9.66	13.1	-.108D-01	-.648D-02	-.450D-03	-.126D-01
MEASBI 1	.343D-02	.159	.558D-01	.168	-.471D-04	-.904D-04	-.431D-05	-.102D-03
MEASBI 2	.905D-01	.190	.468	.563	.651D-03	-.871D-04	-.950D-04	-.469D-03
MEASBI 3	.423D-02	-.194	-.340D-01	.197	.414D-04	-.358D-03	-.380D-05	-.364D-03
MEASBI 4	-.711D-01	.517	-.336	.621	.338D-03	-.310D-03	.703D-04	-.464D-03
MEASBI 5	-.766D-02	.336D-01	-.218D-01	.422D-01	.560D-05	-.268D-03	.811D-05	-.268D-03
MEASBI 6	.147D-01	.267	.765D-01	.278	.340D-04	-.372D-03	-.152D-04	-.859D-02
EPHEMER	.237	3.39	10.3	10.8	-.828D-02	-.227D-02	-.231D-03	-.859D-02
RSS	8.96	11.5	22.3	26.6	.192D-01	.701D-02	.877D-02	.223D-01

USERDRAG CLKBI 1 DRIFT 1

SOLRAD 1	.289D-03	-.678D-01	.570D-06
GRAVCEJ	.149D-02	.339	-.376D-04
LUMPED	-.283D-01	-.103	-.571D-04
ACCL 1	-.478D-02	8.35	-.398D-01
MEASBI 1	-.400D-02	-11.0	-.331D-03
MEASBI 2	-.184D-02	1.47	-.209D-04
MEASBI 3	-.144D-02	-1.81	.310D-04
MEASBI 4	.673D-03	1.36	-.313D-04
MEASBI 5	.544D-02	-20.6	.300D-03
MEASBI 6	-.321D-03	3.75	-.605D-04
EPHEMER	-.302D-01	-53.6	-.583D-01
RSS	.104	60.6	.398D-01

STANDARD DEVIATION - CORRELATION MATRIX

	SAT-01X	SAT-01Y	SAT-01Z	SAT-01XD	SAT-01YD	SAT-01ZD
SAT-01X	.421	.568	.291	-.791	.800	.526
SAT-01Y	.564	.246	-.147	-.945D-01	.659	.329
SAT-01Z	.291	-.147	.147	-.945D-01	.319	.320
SAT-01XD	.800	-.945D-01	-.945D-01	.222D-03	-.445	-.445
SAT-01YD	.526	.329	.319	-.445	.335D-03	.159
SAT-01ZD	-.154D-01	-.326D-01	.320	-.445	.159	.380D-03
CLKBI 1	-.229D-02	-.936D-01	.763D-02	-.624D-02	-.162D-01	-.782D-03
DRIFT 1	-.712D-03	-.127D-02	-.176	-.106D-01	-.708D-01	-.838D-01
USERDRAG				-.576D-03	-.190D-02	.452D-03

CLKBI 1 DRIFT 1

SAT-01X	-.154D-01	-.229D-02	-.712D-03
SAT-01Y	-.326D-01	-.936D-01	-.127D-02
SAT-01XD	-.763D-02	.176	-.127D-02
SAT-01YD	-.624D-02	.106D-01	-.576D-03
SAT-01ZD	-.162D-01	.703D-01	-.190D-02
USERDRAG	-.782D-03	-.833D-01	.452D-03
CLKBI 1	.224D-01	.524D-01	-.558D-03
DRIFT 1	-.553D-03	3.09	-.104D-01

Figure A-12. SEA Version 4.1 Smoothed Error Budget at 1140 Minutes. Velocity Variance Rate Process Noise of 1×10^{-12} Meter²/Second³

increase in measurement error (TDAS ephemeris error and others) as the process noise increases (Figure A-10, A-11, and A-12), should be noted.

A.4 CONCLUSIONS

The following conclusions can be drawn from the series of tests performed:

- The SEA smoother/TDAS enhancements were implemented successfully. The only major errors uncovered were those process noise errors described in Section A.3.2.

- The SEA smoother/TDAS capability is now fully validated and ready for use.

- The close agreement between the process-noise-free SEA smoother results and the batch ORAN results verifies that SEA now also has the error analysis capability for a batch orbit determination process. Because SEA is a well-structured, well-documented, and easily enhanced program, it can be easily modified to analyze new tracking systems and data types, whether these are used in a sequential or batch orbit determination mode.

One of the limitations of a smoother (or a smoother error analysis program) is that, for discrete time measurements, smoothed states (or smoother errors) are only available at those measurement times peculiar to the tracking scenario. This means that the smoother results will not be output during data gaps between tracking passes. Smoother output from SEA during data gaps can be obtained by entering fictitious measurements at the desired output times. These artificially introduced, fictitious measurements are given large standard deviations so that they do not affect the error analysis accuracy.

A.5 LISTING OF TEST DECK SETUPS

The following pages contain listings of representative deck setups used in the validation and verification of the SEA smoother/TDAS capabilities.

```

//ZBPAP1T1 JOB (GC002,311H,FFF), 'SEA P1S1T1',MSGLEVEL=(1,1),
// MSGCLASS=A,TIME=30,CLASS=C,NOTIFY=ZBPAP
/*JOBPARM LINES=30
/*ROUTE PRINT PRUSS
/*MEMBER P1S1T1 DATA IN TESTPAN LIBRARY
/*DIRECT TRACKING OF A 200-KM 28 DEG INC S/C, W/DAG A SOLVE-FOR
/*RANGE AND RANGE RATE MEASUREMENTS EVERY 180 0 SECONDS
/*DETERMIN TRACKING SCHEDULE, FOR 13 TRACKING STATIONS, FOR 24 HRS
/*USING SMTHDUSM SEA SMOOTHER/TDAS UPDATES, SEA VER 4 1 KEYWORDS
/*WITH SMOOTHING
//STEP1 EXEC PGM=PAN#1,REGION=300K,COND=(1,LE)
//PANDD1 DD DSN=GCDEV.MVT SEA.PANLIB DATA,UNIT=DISK,DISP=SHR
//PANDD2 DD DSN=&&SEAUPD,UNIT=VIO,SPACE=(CYL,(2,1),RLSE),
// DISP=(NEW,PASS),DCB=(RECFM=FB,LRECL=80,BLKSIZE=3600)
//SYSPRINT DD SYSOUT=*
//SYSPUNCH DD DUMMY
//SYSIN DD DSN=ZBPAP SMTHDUSM DATA,UNIT=DISK,DISP=SHR
// EXEC FORTRANH,PARM='XREF'
//SYSLIN DD SPACE=(CYL,(2,1))
//SOURCE.SYSTERM DD DUMMY
//SOURCE.SYSPRINT DD DUMMY
//SYSIN DD DSN=&&SEAUPD,UNIT=VIO,DISP=(OLD,DELETE)
// EXEC LINK,PARM='LET,LIST,MAP,SIZE=(200K,20K)',REGION=250K
//SYSLIB DD DSN=SYS2 FORTLIB,DISP=SHR
// DD DSN=GCDEV SEAMVS LOAD,DISP=SHR
//SYSPRINT DD SYSOUT=*
//SYSUT1 DD SPACE=(TRK,(55,1,1))
//SYSLIN DD
// DD *
INCLUDE SYSLIB(SEA)
ENTRY MAIN
//GO EXEC PGM=GSFC,REGION=400K
//STEPLIB DD DSN=&&LODMOD,DISP=(OLD,DELETE)
//FT01FOO1 DD UNIT=DISK,DCB=(RECFM=VBS,LRECL=44,BLKSIZE=4404),
// SPACE=(CYL,(5,1)) SORTING FOR TRACKING DATA SCHEDULE
//FT02FOO1 DD UNIT=DISK,DCB=(RECFM=VBS,LRECL=44,BLKSIZE=4404),
// SPACE=(CYL,(1,1)) MERGING FOR TRACKING DATA SCHEDULE
//FT03FOO1 DD UNIT=DISK,DCB=(RECFM=VBS,LRECL=44,BLKSIZE=4404,
// BUFNO=1),DISP=(NEW,PASS),SPACE=(CYL,(1,1)),
// DSN=&&SORTRK SORTED TRACKING DATA SCHEDULE
//FT05FOO1 DD DDNAME=DATAS TRACKING SCHEDULE CARD INPUT
//*FT06FOO1 DD SYSOUT=*,DCB=(RECFM=VBA,LRECL=137,BLKSIZE=3990),
//FT06FOO1 DD SYSOUT=*,DCB=(RECFM=VBA,LRECL=137,BLKSIZE=141),
// SPACE=(CYL,(3,1),RLSE),
// DSN=&&PRTOUT SEA PRINTER OUTPUT
//*FT08FOO1 DD DDNAME=INPCRD SEA KEYWORD CARD INPUT
//*INPCRD DD *
//FT08FOO1 DD * SEA KEYWORD CARD INPUT
EPOCHTIM 0 99 861101 000000 0000
USERSATO 1 11 1 6578140. 0 0001 28.8
USERSATO 1 12 1 0 0
SATELITE 2 11 0 42166750. 0.0004 5 0
SATELITE 2 12 0 358 0 0
SATELITE 3 11 0 42163592 42 0 0004 5.0
SATELITE 3 12 0 228 0 0
STATIONS 1 0 0 323003.857 2532329 162 1441 37
STATIONS 2 0 0 352029.642 2430737 214 0 913310D+03
STATIONS 3 0 0 352029 642 2430735 042 0 918710D+03
STATIONS 5 0 0 283029.905 2791826.183 -0 558200D+02
STATIONS 6 0 0 -075717.371 3454022.570 0 528370D+03
STATIONS 8 0 0 322105 001 2952031 937 -0 337500D+02
STATIONS 11 0 0 220734.461 2002005 439 0 113975D+04
STATIONS 12 0 0 283029.774 2791823 853 -0 544500D+02
STATIONS 13 0 0 352031.937 2430735 561 0 912710D+03
STATIONS 4 0 0 402719.656 3554953.596 0 808990D+03
STATIONS 7 0 0 -330903.596 2892001 065 0 706610D+03
STATIONS 9 0 0 385954 656 2830926 161 -0 250000D+01
STATIONS 10 0 0 131838.265 1444412 524 0 115950D+03
EARTH 15 15 150 0
SPCPARAM 1 0 0 0.00272 2 0
EBOUTPUT -99 2 1440 0 30 0 30 0
CLKBIAS 1 1 1000000
CLKDRIFT 1 1 200 0 0 000001

```

```

USERDRAG 1 1 0 1
GRAVCOEF -1 0.25
/*
// DD UNIT=DISK,DSN=ZBBTF ZBEXS.GEM DATA(RECOEF2),DISP=SHR
// DD *
SATSOLPR 1 -1 1
MEASBIAS 2 -1 2000000010002. 10.0
MEASBIAS 3 -1 13000000010013. 001
MEASBIAS 2 -1 10000000010000. 10 0
MEASBIAS 3 -1 10000000010000 .001
MEASBIAS 2 -1 5000000010000. 10 0
MEASBIAS 3 -1 12000000010000 .001
EPHEMERR 1 25.0 23 0 40 0
EPHERROR 99
CLKACCEL 1 -1 .11574
COVARANC 1
2.5D+05 2.5D+05 2 5D+05 1.0D+00 1 0D+00 1 0D+00
NOISECOV 1 1 0
0 0 0 1 00000D-10 1.00000D-10 1 00000D-10
/*
/**FT09F001 DD SYSOUT=*,DCB=(RECFM=VBA,LRECL=137,BLKSIZE=3990),
//FT09F001 DD SYSOUT=*,DCB=(RECFM=VBA,LRECL=137,BLKSIZE=141),
// SPACE=(CYL,(2,1),RLSE),
// DSN=&&NOMOUT SATELLITE NOMINAL TRAJECTORY OUTPUT
/**FT10F001 DD SYSOUT=*,DCB=(RECFM=VBA,LRECL=137,BLKSIZE=3990),
//FT10F001 DD SYSOUT=*,DCB=(RECFM=VBA,LRECL=137,BLKSIZE=141),
// SPACE=(CYL,(2,1),RLSE),
// DSN=&&MEASOUT PROCESSED MEASUREMENTS PRINTER OUTPUT
//FT20F001 DD DISP=(NEW,PASS),SPACE=(CYL,(1,1)),
// DCB=(RECFM=VBS,LRECL=144,BLKSIZE=2884),UNIT=DISK,
// DSN=&&FESUM SEQUENTIAL ERROR BUDGET SUMMARY
//FT21F001 DD DISP=(NEW,PASS),SPACE=(CYL,(1,1)),
// DCB=(RECFM=VBS,LRECL=144,BLKSIZE=2884),UNIT=DISK,
// DSN=&&SESUM BACKWARD SMOOTHER ERROR BUDGET SUMMARY
//FT27F001 DD UNIT=DISK,DCB=(RECFM=VBS,LRECL=196,BLKSIZE=1964,
// BUFNO=1),DISP=(NEW,PASS),SPACE=(CYL,(1,1)),
// DSN=&&AKKHIN VISIBLE TRACKING DATA SCHEDULE
//FT40F001 DD UNIT=DISK,DCB=(RECFM=FB,LRECL=1688,BLKSIZE=18568),
// DISP=(NEW,DELETE),SPACE=(CYL,(2,1),RLSE),
// DSN=&&SMSTOR SMOOTHER INFORMATION STORAGE FILE
//GO SYSUDUMP DD DUMMY
/**SYSUDUMP DD SYSOUT=*,SPACE=(TRK,1),
//* DCB=(RECFM=VBA,LRECL=137,BLKSIZE=1922)
//GO DATA5 DD *
3 861101000000 0000 -1
100020001 3 1800.0 10000.0
0 00 1440.0
100030001 3 1800.0 10000 0
0 00 1440.0
100000002 2 1800.0 1.5
0 00 1440 0
200000001 2 20 0 1 5
638 0 640 0 732.0 733 0
200000001 3 20 0 0 002
638 0 640 0 732 0 733.0
300000001 2 20.0 1.5
638 0 640 0 732.0 733 0
300000001 3 20 0 0 002
638.0 640 0 732 0 733 0
500000001 2 20 0 1.5
365 0 369 0 459.0 463 0
552.0 556 0 646.0 649 0
500000001 3 20.0 0 002
365 0 369.0 459 0 463 0
552 0 556 0 646 0 649 0
600000001 2 20 0 1 5
665 0 668 0

```

600000001	3	20 0	0 002	
665 0	668 0			
700000001	2	600 0	1 5	
1200 0	1440.0			
700000001	3	600 0	0.002	
0.00	240 0			
800000001	2	20.0	1 5	
369 0	373.0	462 0		466 0
556 0	559 0			
800000001	3	20.0	0 002	
369 0	373.0	462.0		466 0
556 0	559 0			
1100000001	2	20 0	1.5	
627 0	631.0	721.0		724 0
815.0	817 0			
1100000001	3	20 0	0 002	
627.0	631 0	721 0		724 0
815 0	817 0			
1200000001	2	20 0	1 5	
365 0	369 0	459 0		463 0
552 0	556 0	646 0		649 0
1200000001	3	20 0	0 002	
365 0	369 0	459 0		463 0
552.0	556 0	646 0		649 0
1300000001	2	20 0	1.5	
638.0	640 0	732 0		733 0
1300000001	3	20 0	0 002	
638 0	640 0	732 0		733 0

```

/*
//NTSO EXEC PGM=NOTIFY,COND=EVEN
//

```

```

//ZBPAP2T1 JOB (GCO02,311H,FFF), 'SEA P1S2T1', TIME=30,
// MSGCLASS=X, MSGLEVEL=(1,1), NOTIFY=ZBPAP, CLASS=C
/*JOBPARM LINES=30
//*ROUTE PRINT RMT6
//*MEMBER P1S2T1.DATA IN TESTPAN LIBRARY
//*6 GPS'S TRACKING A 400-KM 57 DEG INC S/C,
//*RANGE AND RANGE RATE MEASUREMENTS EVERY 300 0 SECONDS
//*USING SMTHDUSM SEA SMOOTHER/TDAS UPDATES, SEA VER 4 1 KEYWORDS
//*WITH SMOOTHING
//STEP1 EXEC PGM=PAN#1, REGION=300K, COND=(1,LE)
//PANDD1 DD DSN=GCDEV.MVT.SEA PANLIB DATA, UNIT=DISK, DISP=SHR
//PANDD2 DD DSN=&&SEAUPD, UNIT=VIO, SPACE=(CYL,(2,1),RLSE),
// DISP=(NEW,PASS), DCB=(RECFM=FB, LRECL=80, BLKSIZE=3600)
//SYSPRINT DD SYSOUT=*
//SYSPUNCH DD DUMMY
//SYSIN DD DSN=ZBPAP.SMTHDUSM DATA, UNIT=DISK, DISP=SHR
// EXEC FORTRANH, PARM='XREF'
//SYSLIN DD SPACE=(CYL,(2,1))
//SOURCE.SYSTEM DD DUMMY
//SOURCE.SYSPRINT DD DUMMY
//SYSIN DD DSN=&&SEAUPD, UNIT=VIO, DISP=(OLD,DELETE)
// EXEC LINK, PARM='LET,LIST,MAP,SIZE=(200K,20K)', REGION=250K
//SYSLIB DD DSN=SYS2.FORTLIB, DISP=SHR
// DD DSN=GCDEV.SEAMVS.LOAD, DISP=SHR
//SYSPRINT DD DUMMY
//SYSUT1 DD SPACE=(TRK,(55,1,1))
//SYSLIN DD
// DD *
INCLUDE SYSLIB(SEA)
ENTRY MAIN
//GO EXEC PGM=GSFC, REGION=400K
//STEPLIB DD DSN=&&LODMOD, DISP=(OLD,DELETE)
//FTO1FOO1 DD UNIT=DISK, DCB=(RECFM=VBS, LRECL=44, BLKSIZE=4404),
// SPACE=(CYL,(5,1)) SORTING FOR TRACKING DATA SCHEDULE
//FTO2FOO1 DD UNIT=DISK, DCB=(RECFM=VBS, LRECL=44, BLKSIZE=4404),
// SPACE=(CYL,(1,1)) MERGING FOR TRACKING DATA SCHEDULE
//FTO3FOO1 DD UNIT=DISK, DCB=(RECFM=VBS, LRECL=44, BLKSIZE=4404,
// BUFNO=1), DISP=(NEW,PASS), SPACE=(CYL,(1,1)),
// DSN=&&SORTRK SORTED TRACKING DATA SCHEDULE
//FTO5FOO1 DD DDNAME=DATAS TRACKING SCHEDULE CARD INPUT
//*FTO6FOO1 DD SYSOUT=*, DCB=(RECFM=VBA, LRECL=137, BLKSIZE=3990),
//FTO6FOO1 DD SYSOUT=*, DCB=(RECFM=VBA, LRECL=137, BLKSIZE=141),
// SPACE=(CYL,(3,1),RLSE),
// DSN=&&PRTOUT SEA PRINTER OUTPUT
//*FTO8FOO1 DD DDNAME=INPCRD SEA KEYWORD CARD INPUT
//*INPCRD DD *
//FTO8FOO1 DD * SEA KEYWORD CARD INPUT
EPOCHTIM 2 1 -9 860101. 000000.0000
USERSATO 1 11 1 8978140. 0.0005 57.0
USERSATO 1 12 1 0. 0. 0
SATELITE 2 11 28560123.0 .001 63.0
SATELITE 2 12 120.0 0.0 100.0
SATELITE 3 11 26560123.0 .001 63.0
SATELITE 3 12 120.0 0 0 140.0
SATELITE 4 11 26560123.0 .001 63.0
SATELITE 4 12 120.0 0 0 180.0
SATELITE 5 11 26560123.0 .001 63.0
SATELITE 5 12 240.0 0 0 60.0
SATELITE 6 11 26560123.0 .001 63.0
SATELITE 6 12 240.0 0 0 100.0
SATELITE 7 11 26560123.0 .001 63.0
SATELITE 7 12 240.0 0.0 140.0
EARTH 4 4 0 .0
SPCPARAM 1 0 0 .0117618 .0 2.0
GRAVCOEF 0 0 -1 1.0 .0 0
/*
// DD DSN=ZBBTF.ZBEXS.GEM.DATA(RECOEF4), DISP=SHR, UNIT=DISK
// DD *
USERDRAG 1 0 -1 0.25
CLKBIAS 1 0 1 10000.
CLKDRIFT 1 0 1 10000
CLKACCEL 1 0 -1 .0001
MEASBIAS 2 -1 200010000. 5.0

```

```

MEASBIAS 2 -1 300010000. 5 0
MEASBIAS 2 -1 400010000. 5 0
MEASBIAS 2 -1 500010000 5 0
MEASBIAS 2 -1 600010000 5.0
MEASBIAS 2 -1 700010000 5 0
MEASBIAS 3 -1 200010000 0 .001
MEASBIAS 3 -1 300010000 0 .001
MEASBIAS 3 -1 400010000 0 .001
MEASBIAS 3 -1 500010000.0 .001
MEASBIAS 3 -1 600010000.0 .001
MEASBIAS 3 -1 700010000.0 .001
EPHEMERR 1 0 0 10 0 10.0 20 0
EPHERROR 0 0 0 99.0 .0 0
EBOUTPUT 0 99 2 1440.0 30 0 30 0
COVARANC 1 0 0
100000.0 100000 0 100000 0 1.0 1 0 1 0
NOISECOV 1 1 0
0 0 0 1 00000D-10 1.00000D-10 1.00000D-10

```

```

/*
/*
/*FT09F001 DD SYSOUT=*,DCB=(RECFM=VBA,LRECL=137,BLKSIZE=3990),
/*FT09F001 DD SYSOUT=*,DCB=(RECFM=VBA,LRECL=137,BLKSIZE=141),
// SPACE=(CYL,(2,1),RLSE),
// DSN=&&NOMOUT SATELLITE NOMINAL TRAJECTORY OUTPUT
/*FT10F001 DD SYSOUT=*,DCB=(RECFM=VBA,LRECL=137,BLKSIZE=3990),
/*FT10F001 DD SYSOUT=*,DCB=(RECFM=VBA,LRECL=137,BLKSIZE=141),
// SPACE=(CYL,(2,1),RLSE),
// DSN=&&MEASOUT PROCESSED MEASUREMENTS PRINTER OUTPUT
/*FT20F001 DD DISP=(NEW,PASS),SPACE=(CYL,(1,1)),
// DCB=(RECFM=VBS,LRECL=144,BLKSIZE=2884),UNIT=DISK,
// DSN=&&FESUM SEQUENTIAL ERROR BUDGET SUMMARY
/*FT21F001 DD DISP=(NEW,PASS),SPACE=(CYL,(1,1)),
// DCB=(RECFM=VBS,LRECL=144,BLKSIZE=2884),UNIT=DISK,
// DSN=&&SESUM BACKWARD SMOOTHER ERROR BUDGET SUMMARY
/*FT27F001 DD UNIT=DISK,DCB=(RECFM=VBS,LRECL=196,BLKSIZE=1964,
// BUFNO=1),DISP=(NEW,PASS),SPACE=(CYL,(1,1)),
// DSN=&&AKKHIN VISIBLE TRACKING DATA SCHEDULE
/*FT40F001 DD UNIT=DISK,DCB=(RECFM=FB,LRECL=1688,BLKSIZE=18568),
// DISP=(NEW,DELETE),SPACE=(CYL,(2,1),RLSE),
// DSN=&&SMSTOR SMOOTHER INFORMATION STORAGE FILE
//GO SYSUDUMP DD DUMMY
/*SYSUDUMP DD SYSOUT=*,SPACE=(TRK,1),
/* DCB=(RECFM=VBA,LRECL=137,BLKSIZE=1922)
//GO.DATAS DD *

```

```

3 850101000000.0000 -1
20001 2 300.0 1.0
0 00 1440.0
20001 3 300 0 0.001
0.00 1440 0
30001 2 300.0 1.0
0.00 1440.0
30001 3 300.0 0.001
0.00 1440.0
40001 2 300.0 1.0
0.00 1440.0
40001 3 300 0 0.001
0.00 1440 0
50001 2 300.0 1 0
0.00 1440.0
50001 3 300.0 0.001
0.00 1440.0
60001 2 300 0 1 0
0.00 1440.0
60001 3 300.0 0 001
0 00 1440.0
70001 2 300.0 1.0
0 00 1440 0
70001 3 300.0 0.001
0.00 1440.0

```

```
/*
```

//NTSO EXEC PGM=NOTIFY,COND=EVEN
//


```

//ZBPAP3T1 JOB (GCO02 311H,FFF), 'SEA P1S3T1',MSGLEVEL=(1,1),
// MSGCLASS=X,TIME=30,CLASS=C,NOTIFY=ZBPAP
/*JOBPARM LINES=40
//*ROUTE PRINT PRUSS
//*MEMBER P1S3T1.DATA IN TESTPAN LIBRARY
//*TDRSS TRACKING OF A 600-KM 98 DEG INC S/C
//*RANGE AND RANGE RATE MEASUREMENTS EVERY 180 0 SECONDS
//*USING SMTHOUM SEA SMOOTHER/TDAS UPDATES, SEA VER 4.1 KEYWORDS
//*WITH SMOOTHING
//STEP1 EXEC PGM=PAN#1,REGION=300K,COND=(1,LE)
//PANDD1 DD DSN=GCDEV MVT SEA PANLIB DATA,UNIT=DISK,DISP=SHR
//PANDD2 DD DSN=&&SEAUPD,UNIT=VIO,SPACE=(CYL,(2,1),RLSE),
// DISP=(NEW,PASS),DCB=(RECFM=FB,LRECL=80,BLKSIZE=3600)
//SYSPRINT DD SYSOUT=*
//SYSPUNCH DD DUMMY
//SYSIN DD DSN=ZBPAP SMTHOUM DATA,UNIT=DISK,DISP=SHR
// EXEC FORTRANH,PARM='XREF'
//SYSLIN DD SPACE=(CYL,(2,1))
//SOURCE.SYSTERM DD DUMMY
//SOURCE.SYSPRINT DD DUMMY
//SYSIN DD DSN=&&SEAUPD,UNIT=VIO,DISP=(OLD,DELETE)
// EXEC LINK,PARM='LET,LIST,MAP,SIZE=(200K,20K)',REGION=250K
//SYSLIB DD DSN=SYS2 FORTLIB,DISP=SHR
// DD DSN=GCDEV.SEAMVS.LOAD,DISP=SHR
//SYSPRINT DD SYSOUT=*
//SYSUT1 DD SPACE=(TRK,(55,1,1))
//SYSLIN DD
// DD *
INCLUDE SYSLIB(SEA)
ENTRY MAIN
//GO EXEC PGM=GSFC,REGION=400K
//STEPLIB DD DSN=&&LODMOD,DISP=(OLD,DELETE)
//FTO1FOO1 DD UNIT=DISK,DCB=(RECFM=VBS,LRECL=44,BLKSIZE=4404),
// SPACE=(CYL,(5,1)) SORTING FOR TRACKING DATA SCHEDULE
//FTO2FOO1 DD UNIT=DISK,DCB=(RECFM=VBS,LRECL=44,BLKSIZE=4404),
// SPACE=(CYL,(1,1)) MERGING FOR TRACKING DATA SCHEDULE
//FTO3FOO1 DD UNIT=DISK,DCB=(RECFM=VBS,LRECL=44,BLKSIZE=4404,
// BUFNO=1),DISP=(NEW,PASS),SPACE=(CYL,(1,1)),
// DSN=&&SORTRK SORTED TRACKING DATA SCHEDULE
//FTO5FOO1 DD DDNAME=DATA5 TRACKING SCHEDULE CARD INPUT
//*FTO6FOO1 DD SYSOUT=*,DCB=(RECFM=VBA,LRECL=137,BLKSIZE=3990),
//FTO6FOO1 DD SYSOUT=*,DCB=(RECFM=VBA,LRECL=137,BLKSIZE=141),
// SPACE=(CYL,(3,1),RLSE),
// DSN=&&PRTOUT SEA PRINTER OUTPUT
//*FTO8FOO1 DD DDNAME=INPCRD SEA KEYWORD CARD INPUT
//*INPCRD DD *
//FTO8FOO1 DD * SEA KEYWORD CARD INPUT
EPOCHTIM 1 99 851101. 000000.0000
USERSATO 1 11 1 6978140. 0.0001 98 8
USERSATO 1 12 1 0. 0. 0
SATELITE 2 11 1 6778140. 0.0017 28
SATELITE 2 12 1 160 0 0
SATELITE 3 11 0 42166750. 0 0004 5.0
SATELITE 3 12 0 358 0. 0
SATELITE 4 11 0 42163592.42 0 0004 5 0
SATELITE 4 12 0 228 0 0
SATELITE 5 11 0 42163592 42 0 0004 5 0
SATELITE 5 12 0 113 0. 0
STATIONS 1 0 0 323003 857 2532329.162 1441 37
STATIONS 3 0 0 385953.936 2830929 141 0 400000D+01
STATIONS 4 0 0 402719 656 3554953.596 0 808990D+03
STATIONS 6 0 0 -075717 371 3454022.570 0 528370D+03
STATIONS 7 0 0 -330903.596 2892001.065 0 706610D+03
STATIONS 8 0 0 322105 001 2952031 937 -0.337500D+02
STATIONS 10 0 0 131838 265 1444412 524 0 115950D+03
STATIONS 11 0 0 220734 461 2002005 439 0 113975D+04
STATIONS 12 0 0 283029.774 2791823 853 -0 544500D+02
STATIONS 13 0 0 352031 937 2430735 561 0.912710D+03
EARTH 150 0
SPCPARAM 1 0 0 0 0011765 2 0 2.0
EBOUTPUT -99 2 1020 0 30 0 30.0
MEASRMNT 1020
CLKBIAS 1 1 1000000

```

```

CLKDRIFT 1 1 200 0 0 00001
USERDRAG 1 1 0 1
GRAVCOEF -1 0 25
/*
// DD UNIT=DISK,DSN=ZBBTF.ZBEXS.GEM DATA(RECOEF2),DISP=SHR
// DD *
SATSOLPR 1 -1 .1
MEASBIAS 2 -1 1000300010000. 0 00001
MEASBIAS 2 -1 6000000010000 10.0
MEASBIAS 3 1 10000000010000. 001
MEASBIAS 2 -1 70000000020000. 10 0
MEASBIAS 3 -1 30000000020000. 001
EPHEMERR 1 25.0 23.0 40.0
EPHERROR 99.
CLKACCEL 1 -1 .11574
COVARANC 1
1.0D+05 1 0D+05 1.0D+05 1 0D+00 1 0D+00 1 0D+00
COVARANC 2 1
1 0D+06 0 0 0. 0 1 0D-06
0. 1 0D+06 0. 0. 5 0D-01 1 0D-06
0. 0 1.0D+06 1.0D-06 0 1 0D-06
0 0 1 0D-06 5.0D+00 0 5 0D-09
0. 5 0D-01 0. 0. 5 0D+00 5 0D-09
1 0D-06 1 0D-06 1 0D-06 5 0D-09 5 0D-09 5 0D+00
NOISECOV 1 1 0
0 0 0 1 00000D-10 1 00000D-10 1.00000D-10
NOISECOV 2 1 0
1 00000D-12 1.00000D-12 1.00000D-12 0 0 0
/*
//FT09FOO1 DD SYSOUT=*,DCB=(RECFM=VBA,LRECL=137,BLKSIZE=3990),
//FT09FOO1 DD SYSOUT=*,DCB=(RECFM=VBA,LRECL=137,BLKSIZE=141),
// SPACE=(CYL,(2,1),RLSE),
// - DSN=&&NOMOUT SATELLITE NOMINAL TRAJECTORY OUTPUT
//FT10FOO1 DD SYSOUT=*,DCB=(RECFM=VBA,LRECL=137,BLKSIZE=3990),
//FT10FOO1 DD SYSOUT=*,DCB=(RECFM=VBA,LRECL=137,BLKSIZE=141),
// SPACE=(CYL,(2,1),RLSE),
// DSN=&&MEASOUT PROCESSED MEASUREMENTS PRINTER OUTPUT
//FT20FOO1 DD DISP=(NEW,PASS),SPACE=(CYL,(1,1)),
// DCB=(RECFM=VBS,LRECL=144,BLKSIZE=2884),UNIT=DISK,
// DSN=&&FESUM SEQUENTIAL ERROR BUDGET SUMMARY
//FT21FOO1 DD DISP=(NEW,PASS),SPACE=(CYL,(1,1)),
// DCB=(RECFM=VBS,LRECL=144,BLKSIZE=2884),UNIT=DISK,
// DSN=&&SESUM BACKWARD SMOOTHER ERROR BUDGET SUMMARY
//FT27FOO1 DD UNIT=DISK,DCB=(RECFM=VBS,LRECL=196,BLKSIZE=1964,
// BUFNO=1),DISP=(NEW,PASS),SPACE=(CYL,(1,1)),
// DSN=&&AKKHIN VISIBLE TRACKING DATA SCHEDULE
//FT40FOO1 DD UNIT=DISK,DCB=(RECFM=FB,LRECL=1688,BLKSIZE=18568),
// DISP=(NEW,DELETE),SPACE=(CYL,(2,1),RLSE),
// DSN=&&SMSTOR SMOOTHER INFORMATION STORAGE FILE
//GO SYSUDUMP DD DUMMY
//*SYSUDUMP DD SYSOUT=*,SPACE=(TRK,1),
//* DCB=(RECFM=VBA,LRECL=137,BLKSIZE=1922)
//GO.DATAS DD *
3 861101000000.0000 -1
100030001 2 180.0 30.0
0 00 1440 0
100030001 3 180 0 0.01
0 00 1440 0
100040001 2 180 0 30 0
0.00 1440 0
100040001 3 180 0 0.01
0 00 1440 0
1000400050002 2 180.0 30 0
0.00 120.0
100000002 2 60.0 1.5
30 0 39.0 1122.0 1128 0
1218.0 1227.0 1317 0 1323 0
100000002 3 60.0 0 002
30 0 39.0 1122 0 1128 0
1218 0 1227 0 1317 0 1323 0
300000002 2 60 0 1 5

```

1128 0	1134.0		1032.0	1038 0
300000002	3	60 0	0 002	
1032.0	1038.0		1128.0	1134 0
400000002	2	60 0	1.5	
852.0	861.0			
400000002	3	60.0	0 002	
852 0	861 0			
600000002	2	60 0	1 5	
354.0	363.0		453 0	462 0
552.0	558 0		1245 0	1254.0
1344.0	1350 0			
600000002	3	60.0	0 002	
354 0	363 0		453.0	462 0
552 0	558.0		1245 0	1254 0
1344 0	1350.0			
700000002	2	60.0	1.5	
237.0	255 0		339 0	348.0
435.0	447 0		534 0	543 0
700000002	3	60 0	0 002	
237.0	255 0		339 0	348 0
435.0	447 0		534 0	543 0
800000002	2	60 0	1 5	
936.0	942 0		1032 0	1041 0
1131 0	1140.0		1230 0	1236 0
800000002	3	60.0	0.002	
936 0	942 0		1032 0	1041 0
1131.0	1140.0		1230 0	1236 0
900000002	2	180.0	1 5	
60.0	30.0			
1000000002	2	60.0	1.5	
3 00	12 0		102 0	111 0
201 0	207 0		300.0	306 0
399.0	405 0		495.0	504 0
594 0	603.0		1389 0	1395 0
1000000002	3	60.0	0 002	
3.00	12 0		102 0	111 0
201.0	207.0		300.0	306.0
399 0	405.0		495 0	504 0
594.0	603.0		1389 0	1395.0
1100000002	2	60.0	1.5	
18 0	27.0		114 0	126 0
213 0	225.0		312 0	321 0
1206.0	1212.0		1305 0	1311 0
1401 0	1410 0			
1100000002	3	60.0	0.002	
18.0	27 0		114 0	126 0
213 0	225 0		312 0	321 0
1206 0	1212 0		1305 0	1311 0
1401 0	1410.0			
1200000002	2	60.0	1 5	
933 0	939 0		1029 0	1038 0
1028.0	1034.0		1224 0	1233 0
1323 0	1329 0			
1200000002	3	60.0	0.002	
933 0	939.0		1029.0	1038 0
1028.0	1034.0		1224 0	1233 0
1323 0	1329.0			
1300000002	2	60 0	1 5	
27 0	36 0		1218.0	1224 0
1314 0	1320.0		1413 0	1419 0
1300000002	3	60 0	0 002	
27 0	36 0		1218 0	1224 0
1314 0	1320.0		1413 0	1419 0

```
/*  
//NTSO EXEC PGM=NOTIFY,COND=EVEN  
//
```

```

//ZBPAP4T1 JOB (GCOO2,311H,FFF),'SEA P1S4T1',
//      MSGCLASS=X,TIME=30,MSGLEVEL=(1,1),NOTIFY=ZBPAP,CLASS=C
/*JOBPARM LINES=30
/*ROUTE PRINT RMT6
/*MEMBER P1S4T1 DATA IN TESTPAN LIBRARY
/*USING SMTHDUSM SMOOTHER/TDAS UPDATES, SEA VER 4 1 KEYWORDS
/*TDAS TRACKING SCENARIO, CONTINUOUS BEACON TRACKING
//STEP1 EXEC PGM=PAN#1,REGION=300K,COND=(1,LE)
//PANDD1 DD DSN=GCDEV MVT SEA PANLIB DATA,UNIT=DISK,DISP=SHR
//PANDD2 DD DSN=&&SEAUPD,UNIT=VIO,SPACE=(CYL,(2,1),RLSE),
//      DISP=(NEW,PASS),DCB=(RECFM=FB,LRECL=80,BLKSIZE=3600)
//SYSPRINT DD SYSOUT=*
//SYSPUNCH DD DUMMY
//SYSIN DD DSN=ZBPAP SMTHDUSM DATA,UNIT=DISK,DISP=SHR
//      EXEC FORTRANH,PARM='XREF'
//SYSLIN DD SPACE=(CYL,(2,1))
//SOURCE SYSTEM DD DUMMY
//SOURCE SYSPRINT DD DUMMY
//SYSIN DD DSN=&&SEAUPD,UNIT=VIO,DISP=(OLD,DELETE)
//      EXEC LINK,PARM='LET,LIST,MAP,SIZE=(200K,20K)',REGION=250K
//SYSLIB DD DSN=SYS2 FORTLIB,DISP=SHR
//      DD DSN=GCDEV SEAMVS LOAD,DISP=SHR
//SYSPRINT DD SYSOUT=*
//SYSUT1 DD SPACE=(TRK,(55,1,1))
//SYSLIN DD
//      DD *
      INCLUDE SYSLIB(SEA)
      ENTRY MAIN
//GO EXEC PGM=GSFC,REGION=400K
//STEPLIB DD DSN=&&LODMOD,DISP=(OLD,DELETE)
//FT01FOO1 DD UNIT=DISK,DCB=(RECFM=VBS,LRECL=44,BLKSIZE=4404),
//      SPACE=(CYL,(5,1)) SORTING FOR TRACKING DATA SCHEDULE
//FT02FOO1 DD UNIT=DISK,DCB=(RECFM=VBS,LRECL=44,BLKSIZE=4404),
//      SPACE=(CYL,(1,1)) MERGING FOR TRACKING DATA SCHEDULE
//FT03FOO1 DD UNIT=DISK,DCB=(RECFM=VBS,LRECL=44,BLKSIZE=4404),
//      BUFNO=1,DISP=(NEW,PASS),SPACE=(CYL,(1,1)),
//      DSN=&&SORTRK SORTED TRACKING DATA SCHEDULE
//FT05FOO1 DD DDNAME=DATA5 TRACKING SCHEDULE CARD INPUT
//*FT06FOO1 DD SYSOUT=*,DCB=(RECFM=VBA,LRECL=137,BLKSIZE=3990),
//FT06FOO1 DD SYSOUT=*,DCB=(RECFM=VBA,LRECL=137,BLKSIZE=141),
//      SPACE=(CYL,(3,1),RLSE),
//      DSN=&&PRTOUT SEA PRINTER OUTPUT
//*FT08FOO1 DD DDNAME=INPCRD SEA KEYWORD CARD INPUT
//*INPCRD DD *
//FT08FOO1 DD * SEA KEYWORD CARD INPUT
EPOCHTIM 3 1 840805 12000 0000
USERSATO 1 11 1 6681144 0 00078765 57 01940796
USERSATO 1 12 1 96 4218 360 0
SATELITE 2 11 0 42166750 0 0004 5 0
SATELITE 2 12 0 360 160 292
SATELITE 3 11 0 42163592 42 0 0004 5 0
SATELITE 3 12 0 240 60 22
SATELITE 4 11 0 42163592 42 0 0004 5 0
SATELITE 4 12 0 240 60 292
EARTH 15 15 150 0
SPCPARAM 1 0 0 0 00214 2 2
STATIONS 1 0 0 323003 857 2532329 162 1441 37
GRAVCOEF -1 1
// DD UNIT=DISK,DSN=ZBBTF ZBEXS GEM DATA(RECOEF),DISP=SHR
// DD *
USERDRAG 1 1 1.
CLKDRIFT 1 1 1000
CLKACCEL 1 -1 0 12
SATSOLPR 1 -1 1.
EPHEMERR 1 10 0 20 0 50 0
EPHERROR 99
EBOUTPUT 1 2 1320 10 10
COVARANC 1
1 0D+06 1 0D+06 1 0D+06 1 0D+00 1 0D+00 1 0D+00
NOISECOV 1 1 0
0 0 0 1 00000D-10 1 00000D-10 1 00000D-10
/*
//*FT09FOO1 DD SYSOUT=*,DCB=(RECFM=VBA,LRECL=137,BLKSIZE=3990),

```

```

//FT09FO01 DD SYSOUT=*,DCB=(RECFM=VBA,LRECL=137,BLKSIZE=141),
//          SPACE=(CYL,(2,1),RLSE),
//          DSN=&&NOMOUT          SATELLITE NOMINAL TRAJECTORY OUTPUT
//*FT10FO01 DD SYSOUT=*,DCB=(RECFM=VBA,LRECL=137,BLKSIZE=3990),
//FT10FO01 DD SYSOUT=*,DCB=(RECFM=VBA,LRECL=137,BLKSIZE=141),
//          SPACE=(CYL,(2,1),RLSE),
//          DSN=&&MEASOUT          PROCESSED MEASUREMENTS PRINTER OUTPUT
//FT20FO01 DD DISP=(NEW,PASS),SPACE=(CYL,(1,1)),
//          DCB=(RECFM=VBS,LRECL=144,BLKSIZE=2884),UNIT=DISK,
//          DSN=&&FESUM          SEQUENTIAL ERROR BUDGET SUMMARY
//FT21FO01 DD DISP=(NEW,PASS),SPACE=(CYL,(1,1)),
//          DCB=(RECFM=VBS,LRECL=144,BLKSIZE=2884),UNIT=DISK,
//          DSN=&&SESUM          BACKWARD SMOOTHER ERROR BUDGET SUMMARY
//FT27FO01 DD UNIT=DISK,DCB=(RECFM=VBS,LRECL=196,BLKSIZE=1964,
//          BUFND=1),DISP=(NEW,PASS),SPACE=(CYL,(1,1)),
//          DSN=&&AKKHIN          VISIBLE TRACKING DATA SCHEDULE
//FT40FO01 DD UNIT=DISK,DCB=(RECFM=FB,LRECL=1688,BLKSIZE=18568),
//          DISP=(NEW,DELETE),SPACE=(CYL,(2,1),RLSE),
//          DSN=&&SMSTOR          SMOOTHER INFORMATION STORAGE FILE
//GO SYSUDUMP DD DUMMY
//*SYSUDUMP DD SYSOUT=*,SPACE=(TRK,1),
//*          DCB=(RECFM=VBA,LRECL=137,BLKSIZE=1922)
//GO DATA5 DD *

```

```

          3          840805120000 0000
000100020001      3 180          0 01
0          25          80          120
185          215          285          310
380          415          475          515
570          610          665          700
760          795          860          890
960          985          1055          1090
1160          1190          1265          1285

000100030001      3 180          0 01
30          80          130          185
230          285          335          380
430          475          525          565
625          660          720          755
820          860          925          960
1030          1055          1125          1150
1225          1245

0001000300040001  3 180          0 01
25          30          120          130
215          230          310          335
415          430          515          525
610          625          705          720
805          820          900          925
995          1030          1090          1120
1190          1220          1300          1320

```

```

/*
//NTSO EXEC PGM=NOTIFY,COND=EVEN
//

```

ORIGINAL PAGE IS
OF POOR QUALITY

```
//ZBPAPSOR JOB (GCO02,311H,FFF), 'SEA P2S1T1',MSGLEVEL=(1,1),
// MSGCLASS=A,TIME=30,CLASS=C,NOTIFY=ZBPAP
/*JOBPARM LINES=30
/*ROUTE PRINT RMT6
/* MEMBER P2S1T1 IN TESTPAN
/* SOLVE FOR ONLY TWO SATELLITES, PROPOGATE FOR 1 DAY
/* WITH 15X15 GEM9 - 8X8 GEM1 MISMATCH, GM (DATA CUT-OFF AT 1440MIN)
/* USE ZBPAP SMTHDUSM.DATA TO UPDATE THE SEA SOURCE
//STEP1 EXEC PGM=PAN#1,REGION=300K,COND=(1,LE)
//PANDD1 DD DSN=GCDEV.MVT.SEA.PANLIB.DATA,UNIT=DISK,DISP=SHR
//PANDD2 DD DSN=&&SEAUPD,UNIT=VIO,SPACE=(CYL,(2,1),RLSE),
// DISP=(NEW,PASS),DCB=(RECFM=FB,LRECL=80,BLKSIZE=3600)
//SYSPRINT DD SYSOUT=*
//SYSPUNCH DD DUMMY
//SYSIN DD DSN=ZBPAP.SMTHDUSM.DATA,UNIT=DISK,DISP=SHR
// EXEC FORTRANH,PARM='XREF',TERM='*'
//SYSLIN DD SPACE=(CYL,(2,1))
//SYSPRINT DD DUMMY
//SYSIN DD DSN=&&SEAUPD,UNIT=VIO,DISP=(OLD,DELETE)
// EXEC LINK,PARM='LET,LIST,MAP,SIZE=(200K,20K)',REGION=250K,
// NBLK=100
//SYSLIB DD DSN=SYS2.FORTLIB,DISP=SHR
// DD DSN=GCDEV.SEAMVS.LOAD,DISP=SHR
//SYSPRINT DD SYSOUT=*
//SYSUT1 DD SPACE=(TRK,(55,1,1))
//SYSLIN DD
// DD *
INCLUDE SYSLIB(SEA)
ENTRY MAIN
//GO EXEC PGM=GSFC,REGION=500K
//GO.STEPLIB DD DSN=&&LODMOD,DISP=(OLD,DELETE)
//FTO1FOO1 DD UNIT=DISK,DCB=(RECFM=VBS,LRECL=44,BLKSIZE=4404),
// SPACE=(CYL,(5,1)) SORTING FOR TRACKING DATA SCHEDULE
//FTO2FOO1 DD UNIT=DISK,DCB=(RECFM=VBS,LRECL=44,BLKSIZE=4404),
// SPACE=(CYL,(1,1)) MERGING FOR TRACKING DATA SCHEDULE
//FTO3FOO1 DD UNIT=DISK,DCB=(RECFM=VBS,LRECL=44,BLKSIZE=4404,
// BUFNO=1),DISP=(NEW,PASS),SPACE=(CYL,(1,1)),
// DSN=&&SORTRK SORTED TRACKING DATA SCHEDULE
//FTO5FOO1 DD DDNAME=DATA5 TRACKING SCHEDULE CARD INPUT
//FTO6FOO1 DD SYSOUT=*,DCB=(RECFM=VBA,LRECL=137,BLKSIZE=1922),
//FTO6FOO1 DD SYSOUT=*,DCB=(RECFM=VBA,LRECL=137,BLKSIZE=141),
// SPACE=(CYL,(1,1),RLSE),
// DSN=&&PRTOU SEA PRINTER OUTPUT
/*INPCRD DD *
/*FTO8FOO1 DD DDNAME=INPCRD SEA KEYWORD CARD INPUT
//FTO8FOO1 DD * SEA KEYWORD CARD INPUT
EPOCHTIM 1 1 800301. 000000 0000
USERSATO 1 11 1 42166663.0 0.2499 D-7 7.0
USERSATO 1 12 1 319. 0. 158.92521261
SATELITE 2 11 1 42166663.0 0.17865865 D-7 7.
SATELITE 2 12 1 189. 0. 158.9521261
EARTH 8 8 40.0
GRAVCOEF -1 0.25
/*
// DD UNIT=DISK,DSN=ZBBTF.ZBEXS.GEM.DATA(RECOEF),DISP=SHR
// DD *
SPCPARAM 1 0 0 0.036 1 5
SPCPARAM 2 0 0 0.036 1.5
MEASBIAS 2 -1 00010001000000001. 5.0
MEASBIAS 2 -1 00010002000000001 5 0
MEASBIAS 3 -1 00010001000000001. 0.0005
MEASBIAS 3 -1 00010002000000001 0.0005
STATIONS 1 0 0 323003.857 2532329.162 1441 37
EBOUTPUT 1 2 1440. 180. 30.0
COVARANC 1
1.0D+06 1.0D+06 1.0D+06 1 0D+00 1.0D+00 1.0D+00
/*
/*FTO9FOO1 DD SYSOUT=*,DCB=(RECFM=VBA,LRECL=137,BLKSIZE=1922),
//FTO9FOO1 DD SYSOUT=*,DCB=(RECFM=VBA,LRECL=137,BLKSIZE=141),
// SPACE=(CYL,(1,1),RLSE),
// DSN=&&NOMOUT SATELLITE NOMINAL TRAJECTORY OUTPUT
/*FT10FOO1 DD SYSOUT=*,DCB=(RECFM=VBA,LRECL=137,BLKSIZE=1922),
//FT10FOO1 DD SYSOUT=*,DCB=(RECFM=VBA,LRECL=137,BLKSIZE=141),
```

```

//          SPACE=(CYL,(1,1),RLSE),
//          DSN=&&MEASOUT      PROCESSED MEASUREMENTS PRINTER OUTPUT
//FT20F001 DD DISP=(NEW,PASS),SPACE=(CYL,(1,1)),
//          DCB=(RECFM=VBS,LRECL=144,BLKSIZE=2884),UNIT=DISK,
//          DSN=&&FESUM        SEQUENTIAL ERROR BUDGET SUMMARY
//FT21F001 DD DISP=(NEW,PASS),SPACE=(CYL,(1,1)),
//          DCB=(RECFM=VBS,LRECL=144,BLKSIZE=2884),UNIT=DISK,
//          DSN=&&SESUM        BACKWARD SMOOTHER ERROR BUDGET SUMMARY
//FT27F001 DD UNIT=DISK,DCB=(RECFM=VBS,LRECL=196,BLKSIZE=1964,
//          BUFNO=1),DISP=(NEW,PASS),SPACE=(CYL,(1,1)),
//          DSN=&&AKKHIN      VISIBLE TRACKING DATA SCHEDULE
//FT40F001 DD UNIT=DISK,DCB=(RECFM=FB,LRECL=1688,BLKSIZE=18568),
//          DISP=(NEW,DELETE),SPACE=(CYL,(2,1),RLSE),
//          DSN=&&SMSTOR      SMOOTHER INFORMATION STORAGE FILE
//GO SYSUDUMP DD DUMMY
//*SYSUDUMP DD SYSOUT=*,SPACE=(TRK,1),
//*          DCB=(RECFM=VBA,LRECL=137,BLKSIZE=1922)
//GO DATA5 DD *

```

```

          3          800301000000.0000          0
00010001      0001  2  10          30.0
0 0          1 0          120 0          121.0
240.0          241.0          360.0          361.0
480.0          481 0          600 0          601.0
720.0          721.0          840.0          841.0
960.0          961.0          1080          1081.
1200.          1201          1320.          1321
1440.          1440.
00010001      0001  3  10.          0.003
0.0          1.0          120 0          121.0
240 0          241.0          360 0          361.0
480.0          481.0          600.0          601.0
720.0          721 0          840.0          841.0
960.0          961 0          1080.          1081.
1200          1201.          1320.          1321.
1440          1440.
00010002      0001  2  10.          30.0
1.0          2.0          121.0          122.0
241 0          242 0          361.0          362.0
481.0          482.0          601.0          602.0
721.0          722.0          841.0          842.0
961 0          962.0          1081.          1082.
1201.          1202          1321.          1322.

00010002      0001  3  10          0.003
1 0          2.0          121.0          122.0
241.0          242.0          361.0          362.0
481.0          482.0          601 0          602.0
721.0          722.0          841.0          842.0
961.0          962.0          1081.          1082.
1201.          1202.          1321.          1322

```

```

/*
//NTSD EXEC PGM=NOTIFY,COND=EVEN
//

```



```

//ZBPAP2S2 JOB (GCO02,311H,FFF),'SEA P2S2T1',MSGLEVEL=(1,1),
// MSGCLASS=X,TIME=30,CLASS=C,NOTIFY=ZBPAP
/*JOBPARM LINES=30
/*ROUTE PRINT RMT6
/* MEMBER P2S2T1 IN TESTPAN
/* SOLVE FOR ONLY ONE OF 3 SATELLITES, PROPOGATE FOR 1 DAY
/* USE ZBPAP.SMTHDU5M.DATA TO UPDATE THE SEA SOURCE
//STEP1 EXEC PGM=PAN#1,REGION=300K,COND=(1,LE)
//PANDD1 DD DSN=GCDEV.MVT.SEA.PANLIB.DATA,UNIT=DISK,DISP=SHR
//PANDD2 DD DSN=&&SEAUPT,UNIT=VIO,SPACE=(CYL,(2,1),RLSE),
// DISP=(NEW,PASS),DCB=(RECFM=FB,LRECL=80,BLKSIZE=3800)
//SYSPRINT DD SYSOUT=*
//SYSPUNCH DD DUMMY
//SYSIN DD DSN=ZBPAP.SMTHDU5M.DATA,UNIT=DISK,DISP=SHR
// EXEC FORTRANH,PARM='XREF',TERM='*'
//SYSLIN DD SPACE=(CYL,(2,1))
//SYSPRINT DD DUMMY
//SYSIN DD DSN=&&SEAUPT,UNIT=VIO,DISP=(OLD,DELETE)
// EXEC LINK,PARM='LET,LIST,MAP,SIZE=(200K,20K)',REGION=250K,
// NBLK=100
//SYSLIB DD DSN=SYS2.FORTLIB,DISP=SHR
// DD DSN=GCDEV.SEAMVS.LOAD,DISP=SHR
//SYSPRINT DD SYSOUT=*
//SYSUT1 DD SPACE=(TRK,(55,1,1))
//SYSLIN DD
// DD *
INCLUDE SYSLIB(SEA)
ENTRY MAIN
//GO EXEC PGM=GSFC,REGION=500K
//GO.STEPLIB DD DSN=&&LDMOD,DISP=(OLD,DELETE)
//FT01FOO1 DD UNIT=DISK,DCB=(RECFM=VBS,LRECL=44,BLKSIZE=4404),
// SPACE=(CYL,(5,1)) SORTING FOR TRACKING DATA SCHEDULE
//FT02FOO1 DD UNIT=DISK,DCB=(RECFM=VBS,LRECL=44,BLKSIZE=4404),
// SPACE=(CYL,(1,1)) MERGING FOR TRACKING DATA SCHEDULE
//FT03FOO1 DD UNIT=DISK,DCB=(RECFM=VBS,LRECL=44,BLKSIZE=4404,
// BUFNO=1),DISP=(NEW,PASS),SPACE=(CYL,(1,1)),
// DSN=&&SORTRK SORTED TRACKING DATA SCHEDULE
//FT05FOO1 DD DDNAME=DATA5 TRACKING SCHEDULE CARD INPUT
//*FT06FOO1 DD SYSOUT=*,DCB=(RECFM=VBA,LRECL=137,BLKSIZE=1922),
//FT06FOO1 DD SYSOUT=*,DCB=(RECFM=VBA,LRECL=137,BLKSIZE=141),
// SPACE=(CYL,(1,1),RLSE),
// DSN=&&PRTOU SEA PRINTER OUTPUT
//*FT08FOO1 DD DDNAME=INPCRD SEA KEYWORD CARD INPUT
//*INPCRD DD *
//FT08FOO1 DD * SEA KEYWORD CARD INPUT
EPOCHTIM 1 1 800301. 000000.0000
USERSATO 1 11 1 6778140. 0.0017 28.
USERSATO 1 12 1 0. 0. 0
SATELITE 2 11 42188883.0 0.2499 D-7 7.0
SATELITE 2 12 319 0. 158.92521261
SATELITE 3 11 42188883.0 0.17885865 D-7 7.
SATELITE 3 12 189. 0. 158 9521261
EARTH 8 8
SPCPARAM 1 0 0 0.0011785 1.5 2 0
SPCPARAM 2 0 0 0.036 0.00000000000000000001 0.0000000000000001
SPCPARAM 3 0 0 0.036 0.00000000000000000001 0.0000000000000001
STATIONS 1 0 0 323003.857 2532329.162 1441.37
USERDRAG -1 0.25
GRAVCOEF -1 0.25
/*
// DD UNIT=DISK,DSN=ZBBTF.ZBEXS.GEM.DATA(RECOEF),DISP=SHR
// DD *
MEASBIAS 2 -1 0001000200010000. 5 0
MEASBIAS 2 -1 0001000300010000. 5.0
MEASBIAS 3 -1 0001000200010000. 0.0005
MEASBIAS 3 -1 0001000300010000. 0.0005
EBOUPTUT 1 2 1440.0 180.0 30.0
COVARANC 1
1.0D+05 1.0D+05 1.0D+05 1.0D+00 1.0D+00 1.0D+00
/*
//*FT09FOO1 DD SYSOUT=*,DCB=(RECFM=VBA,LRECL=137,BLKSIZE=1922),
//FT09FOO1 DD SYSOUT=*,DCB=(RECFM=VBA,LRECL=137,BLKSIZE=141),
// SPACE=(CYL,(1,1),RLSE),

```

```

//          DSN=&&NOMOUT          SATELLITE NOMINAL TRAJECTORY OUTPUT
// *FT10F001 DD SYSOUT=*, DCB=(RECFM=VBA, LRECL=137, BLKSIZE=1922),
// FT10F001 DD SYSOUT=*, DCB=(RECFM=VBA, LRECL=137, BLKSIZE=141),
//          SPACE=(CYL, (1, 1), RLSE),
//          DSN=&&MEASOUT          PROCESSED MEASUREMENTS PRINTER OUTPUT
// FT20F001 DD DISP=(NEW, PASS), SPACE=(CYL, (1, 1)),
//          DCB=(RECFM=VBS, LRECL=144, BLKSIZE=2884), UNIT=DISK,
//          DSN=&&FESUM          SEQUENTIAL ERROR BUDGET SUMMARY
// FT21F001 DD DISP=(NEW, PASS), SPACE=(CYL, (1, 1)),
//          DCB=(RECFM=VBS, LRECL=144, BLKSIZE=2884), UNIT=DISK,
//          DSN=&&SESUM          BACKWARD SMOOTHER ERROR BUDGET SUMMARY
// FT27F001 DD UNIT=DISK, DCB=(RECFM=VBS, LRECL=196, BLKSIZE=1964,
//          BUFNO=1), DISP=(NEW, PASS), SPACE=(CYL, (1, 1)),
//          DSN=&&AKKHIN          VISIBLE TRACKING DATA SCHEDULE
// FT40F001 DD UNIT=DISK, DCB=(RECFM=FB, LRECL=1688, BLKSIZE=18588),
//          DISP=(NEW, DELETE), SPACE=(CYL, (2, 1), RLSE),
//          DSN=&&SMSTOR          SMOOTHER INFORMATION STORAGE FILE
// GO.SYSUDUMP DD DUMMY
// *SYSUDUMP DD SYSOUT=*, SPACE=(TRK, 1),
// *          DCB=(RECFM=VBA, LRECL=137, BLKSIZE=1922)
// GO.DATAS DD *
//          3          800301000000.0000          0
000100020001          2          600.          30.
10.          380.
000100020001          3          600.          0.3
10          360.
000100030001          2          600.          30.
10.          360.
000100030001          3          600.          0.3
10.          380.

/*
//NTSO EXEC PGM=NOTIFY, COND=EVEN
//

```

```

//ZBCPYST JOB (GJ002,311H,FFF), 'SEA P2S2T2',MSGLEVEL=(1,1),
// MSGCLASS=X,TIME=30,CLASS=C,NOTIFY=ZBCPY
/*JOBPARM LINES=30
/*ROUTE PRINT PRUSS
/* MEMBER P2S2T2 IN TESTPAN
/* SOLVE FOR ALL THREE SATELLITES, PROPOGATE FOR 1 DAY
/* **** USING EQUAL WEITHTS FOR A DATA TYPE- REGARDLESS OF S/C
/* USE ZBCPY.SMTHDUSM DATA TO UPDATE THE SEA SOURCE
//STEP1 EXEC PGM=PAN#1,REGION=300K,COND=(1,LE)
//PANDD1 DD DSN=GCDEV.MVT.SEA.PANLIB.DATA,UNIT=DISK,DISP=SHR
//PANDD2 DD DSN=&&SEAUPD,UNIT=VIO,SPACE=(CYL,(2,1),RLSE),
// DISP=(NEW,PASS),DCB=(RECFM=FB,LRECL=80,BLKSIZE=3600)
//SYSPRINT DD SYSOUT=*
//SYSPUNCH DD DUMMY
//SYSIN DD DSN=ZBCPY SMTHDUSM.DATA,UNIT=DISK,DISP=SHR
// EXEC FORTRANH,PARM='XREF',TERM='*'
//SYSLIN DD SPACE=(CYL,(2,1))
//SYSPRINT DD SYSOUT=*
//SYSIN DD DSN=&&SEAUPD,UNIT=VIO,DISP=(OLD,DELETE)
// EXEC LINK,PARM='LET,LIST,MAP,SIZE=(200K,20K)',REGION=250K,
// NBLK=100
//SYSLIB DD DSN=SYS2.FORTLIB,DISP=SHR
// DD DSN=GCDEV.SEAMVS.LOAD,DISP=SHR
//SYSPRINT DD SYSOUT=*
//SYSUT1 DD SPACE=(TRK,(55,1,1))
//SYSLIN DD
// DD *
INCLUDE SYSLIB(SEA)
ENTRY MAIN
//GO EXEC PGM=GSFC,REGION=500K
//GO STEPLIB DD DSN=&&LODMOD,DISP=(OLD,DELETE)
//FT01FO01 DD UNIT=DISK,DCB=(RECFM=VBS,LRECL=44,BLKSIZE=4404),
// SPACE=(CYL,(5,1)) SORTING FOR TRACKING DATA SCHEDULE
//FT02FO01 DD UNIT=DISK,DCB=(RECFM=VBS,LRECL=44,BLKSIZE=4404),
// SPACE=(CYL,(1,1)) MERGING FOR TRACKING DATA SCHEDULE
//FT03FO01 DD UNIT=DISK,DCB=(RECFM=VBS,LRECL=44,BLKSIZE=4404,
// BUFNO=1),DISP=(NEW,PASS),SPACE=(CYL,(1,1)),
// DSN=&&SORTRK SORTED TRACKING DATA SCHEDULE
//FT05FO01 DD DDNAME=DATA5 TRACKING SCHEDULE CARD INPUT
/*FT06FO01 DD SYSOUT=*,DCB=(RECFM=VBA,LRECL=137,BLKSIZE=1922),
//FT06FO01 DD SYSOUT=*,DCB=(RECFM=VBA,LRECL=137,BLKSIZE=141),
// SPACE=(CYL,(1,1),RLSE),
// DSN=&&PRTOUT SEA PRINTER OUTPUT
//FT08FO01 DD DDNAME=INPCRD SEA KEYWORD CARD INPUT
/*FT09FO01 DD SYSOUT=*,DCB=(RECFM=VBA,LRECL=137,BLKSIZE=1922),
//FT09FO01 DD SYSOUT=*,DCB=(RECFM=VBA,LRECL=137,BLKSIZE=141),
// SPACE=(CYL,(1,1),RLSE),
// DSN=&&NOMOUT SATELLITE NOMINAL TRAJECTORY OUTPUT
/*FT10FO01 DD SYSOUT=*,DCB=(RECFM=VBA,LRECL=137,BLKSIZE=1922),
//FT10FO01 DD SYSOUT=*,DCB=(RECFM=VBA,LRECL=137,BLKSIZE=141),
// SPACE=(CYL,(1,1),RLSE),
// DSN=&&MEASOUT PROCESSED MEASUREMENTS PRINTER OUTPUT
//FT20FO01 DD DISP=(NEW,PASS),SPACE=(CYL,(1,1)),
// DCB=(RECFM=VBS,LRECL=144,BLKSIZE=2884),UNIT=DISK,
// DSN=&&FESUM SEQUENTIAL ERROR BUDGET SUMMARY
//FT21FO01 DD DISP=(NEW,PASS),SPACE=(CYL,(1,1)),
// DCB=(RECFM=VBS,LRECL=144,BLKSIZE=2884),UNIT=DISK,
// DSN=&&SESUM BACKWARD SMOOTHER ERROR BUDGET SUMMARY
//FT27FO01 DD UNIT=DISK,DCB=(RECFM=VBS,LRECL=196,BLKSIZE=1964,
// BUFNO=1),DISP=(NEW,PASS),SPACE=(CYL,(1,1)),
// DSN=&&AKKHIN VISIBLE TRACKING DATA SCHEDULE
//FT40FO01 DD UNIT=DISK,DCB=(RECFM=FB,LRECL=1688,BLKSIZE=18568),
// DISP=(NEW,DELETE),SPACE=(CYL,(2,1),RLSE),
// DSN=&&SMSTOR SMOOTHER INFORMATION STORAGE FILE
//GO.SYSUDUMP DD DUMMY
/*SYSUDUMP DD SYSOUT=*,SPACE=(TRK,1),
//* DCB=(RECFM=VBA,LRECL=137,BLKSIZE=1922)
//INPCRD DD *
EPOCHTIM 1 1 800301. 000000.0000
USERSATO 1 11 1 6778140. 0.0017 28.
USERSATO 1 12 1 0 0 0.
SATELITE 2 11 1 42166663.0 0 2499 D-7 7 0
SATELITE 2 12 1 319, 0. 158.92521261

```

```

SATELITE 3 11 1 42166663.0 - 0 17865885 D-7 7
SATELITE 3 12 1 189. 0. 158 9521261
EARTH 8 8 40 0
SPCPARAM 1 0 0 0.0011765 2.0 2.0
SPCPARAM 2 0 0 0.036 1.5
SPCPARAM 3 0 0 0.036 1.5
STATIONS 1 0 0 323003 857 2532329.162 1441 37
MEASBIAS 2 -1 0001000200010000. 5.0
MEASBIAS 2 -1 0001000300010000. 5 0
MEASBIAS 3 -1 0001000200010000 0.005
MEASBIAS 3 -1 0001000300010000 0.005
EBDOUTPUT 0 2 1440. 180. 30.0
CDVARANC 1
1.0D+05 1.0D+05 1.0D+05 1 0D+00 1.0D+00 1 0D+00

```

```

/*
//GD.DATAS DD *
3 800301000000.0000 1
000100020001 2 600 30
10. 360.
000100020001 3 600. 0 3
10. 360.
000100030001 2 600. 30.
10. 360.
000100030001 3 600. 0.3
10. 360.
00010002 0001 2 10. 30.0
0.0 1.0 120 0 121 0
240.0 241.0 360.0 361 0
480.0 481.0 600.0 601.0
720.0 721.0 840.0 841.0
960.0 961 0 1080. 1081.
1200. 1201. 1320. 1321.
1440. 1440.
00010002 0001 3 10. 0.3
0.0 1.0 120.0 121.0
240.0 241.0 360.0 361.0
480.0 481.0 600.0 601.0
720.0 721.0 840.0 841.0
960 0 961.0 1080. 1081.
1200. 1201. 1320. 1321.
1440. 1440.
00010003 0001 2 10. 30.0
1.0 2.0 121.0 122.0
241.0 242.0 361.0 362.0
481.0 482.0 601.0 602 0
721.0 722.0 841.0 842 0
961.0 962.0 1081. 1082.
1201. 1202. 1321. 1322.

00010003 0001 3 10. 0.3
1.0 2.0 121.0 122.0
241.0 242.0 361.0 362.0
481.0 482.0 601.0 602 0
721.0 722.0 841.0 842 0
961 0 962 0 1081 1082.
1201 1202 1321. 1322.

```

```

/*
//NTSO EXEC PGM=NOTIFY,COND=EVEN
//

```

```

//ZBPAPSWN JOB (GCOO2,311H,FFF), 'SEA P3S1T1',MSGLEVEL=(1,1),
// MSGCLASS=A,TIME=30,CLASS=C,NOTIFY=ZBPAP
/*JOBPARM LINES=30
/*ROUTE PRINT PRTSS
/* MEMBER P3S1T1 IN TESTPAN
/* SOLVE FOR ONLY ONE OF 3 SATELLITES, PROPOGATE FOR 1 DAY
/* WITH VELOCITY PROCESS NOISE OF 1 OD-09 ON STATE VELOCITIES
/* USE ZBPAP.SMTHDUSM.DATA TO UPDATE THE SEA SOURCE
/* SMTHDUP3 MODIFIED TO SET VAR DELTAT WITH THE OPPOSITE SIGN
//STEP1 EXEC PGM=PAN#1,REGION=300K,COND=(1,LE)
//PANDD1 DD DSN=GCDEV.MVT.SEA.PANLIB.DATA,UNIT=DISK,DISP=SHR
//PANDD2 DD DSN=&&SEAUPD,UNIT=VIO,SPACE=(CYL,(2,1),RLSE),
// DISP=(NEW,PASS),DCB=(RECFM=FB,LRECL=80,BLKSIZE=3600)
//SYSPRINT DD SYSOUT=*
//SYSPUNCH DD DUMMY
//SYSIN DD DSN=ZBPAP.SMTHDUSM DATA,UNIT=DISK,DISP=SHR
// EXEC FORTRANH,PARM='XREF',TERM='*'
//SYSLIN DD SPACE=(CYL,(2,1))
//SYSPRINT DD DUMMY
//SYSIN DD DSN=&&SEAUPD,UNIT=VIO,DISP=(OLD,DELETE)
// EXEC LINK,PARM='LET,LIST,MAP,SIZE=(200K,20K)',REGION=250K,
// NBLK=100
//SYSLIB DD DSN=SYS2.FORTLIB,DISP=SHR
// DD DSN=GCDEV.SEAMVS.LOAD,DISP=SHR
//SYSPRINT DD SYSOUT=*
//SYSUT1 DD SPACE=(TRK,(55,1,1))
//SYSLIN DD
// DD *
INCLUDE SYSLIB(SEA)
ENTRY MAIN
//GO EXEC PGM=GSFC,REGION=500K
//GO.STEPLIB DD DSN=&&LODMOD,DISP=(OLD,DELETE)
//FT01F001 DD UNIT=DISK,DCB=(RECFM=VBS,LRECL=44,BLKSIZE=4404),
// SPACE=(CYL,(5,1)) SORTING FOR TRACKING DATA SCHEDULE
//FT02F001 DD UNIT=DISK,DCB=(RECFM=VBS,LRECL=44,BLKSIZE=4404),
// SPACE=(CYL,(1,1)) MERGING FOR TRACKING DATA SCHEDULE
//FT03F001 DD UNIT=DISK,DCB=(RECFM=VBS,LRECL=44,BLKSIZE=4404,
// BUFNO=1),DISP=(NEW,PASS),SPACE=(CYL,(1,1)),
// DSN=&&SORTRK SORTED TRACKING DATA SCHEDULE
//FT05F001 DD DDNAME=DATAS TRACKING SCHEDULE CARD INPUT
//*FT08F001 DD SYSOUT=*,DCB=(RECFM=VBA,LRECL=137,BLKSIZE=1922),
//FT08F001 DD SYSOUT=*,DCB=(RECFM=VBA,LRECL=137,BLKSIZE=141),
// SPACE=(CYL,(1,1),RLSE),
// DSN=&&PRTOUT SEA PRINTER OUTPUT
//*FT08F001 DD DDNAME=INPCRD SEA KEYWORD CARD INPUT
//*INPCRD DD *
//FT08F001 DD * SEA KEYWORD CARD INPUT
EPOCHTIM 1 1 800301. 000000.0000
USERSATO 1 11 1 6778140. 0.0017 28
USERSATO 1 12 1 0. 0. 0
SATELITE 2 11 42166683.0 0.2499 D-7 7 0
SATELITE 2 12 319. 0. 158.92521261
SATELITE 3 11 42166683.0 0.17865865 D-7 7
SATELITE 3 12 189 0 158 9521261
EARTH 8 8
SPCPARAM 1 0 0 0 0011765 0 00000000001
SPCPARAM 2 0 0 0.036 1 5
SPCPARAM 3 0 0 0.036 1.5
STATIONS 1 0 0 323003.857 2532329 162 1441 37
GRAVCOEF -1 0.25
/*
// DD UNIT=DISK,DSN=ZBBTF.ZBEXS.GEM.DATA(RECOEF),DISP=SHR
// DD *
MEASBIAS 2 -1 0001000200010000. 5.0
MEASBIAS 2 -1 0001000300010000. 5.0
MEASBIAS 3 -1 0001000200010000. 0.0005
MEASBIAS 3 -1 0001000300010000. 0.0005
EBOUTPUT 1 2 360. 30. 30.0
COVARANC 1
1 0D+05 1.0D+05 1 0D+05 1.0D+00 1 0D+00 1.0D+00
NOISECOV 1 1 0
0.0D+00 0.0D+00 0.0D+00 1.0D-09 1 0D-09 1 0D-09
/*

```



```

//ZBCPYSTS JOB (GJ002,311H,FFF), 'SEA P3S2T1', TIME=30,
//      MSGCLASS=X, MSGLEVEL=(1,1), NOTIFY=ZBCPY, CLASS=C
/*JOBPARM LINES=100
/*ROUTE PRINT PRSS
/*MEMBER P3S2T1 IN TESTPAN
/**BEAKON TRACKING (FLBT) FOR A SPACE TELESCOPE MISSION MODEL
/**RANGE AND RANGE RATE MEASUREMENTS EVERY 180 0 SECONDS
/**USING SMTHDUSM SEA SMOOTHER/TDAS UPDATES, SEA VER 4 1 KEYWORDS
/**WITH SMOOTHING
/**WITH LOW ACCURACY TRACKING EVERY 30 MINUTES TO INCREASE THE
/**NUMBER OF SMOOTHED ERROR BUDGETS
//STEP1 EXEC PGM=PAN#1, REGION=300K, COND=(1, LE)
//PANDD1 DD DSN=GCDEV.MVT.SEA.PANLIB.DATA, UNIT=DISK, DISP=SHR
//PANDD2 DD DSN=&&SEAUPD, UNIT=VIO, SPACE=(CYL, (2, 1), RLSE),
//      DISP=(NEW, PASS), DCB=(RECFM=FB, LRECL=80, BLKSIZE=3600)
//SYSPRINT DD SYSOUT=*
//SYSPUNCH DD DUMMY
//SYSIN DD DSN=ZBCPY.SMTHDUSM.DATA, UNIT=DISK, DISP=SHR
//      EXEC FORTRANH, PARM='XREF', TERM='*', OUT='*'
//SYSLIN DD SPACE=(CYL, (2, 1))
//SOURCE.SYSTEM DD SYSOUT=*
//SOURCE.SYSPRINT DD DUMMY
//SYSIN DD DSN=&&SEAUPD, UNIT=VIO, DISP=(OLD, DELETE)
//      EXEC LINK, PARM='LET, LIST, MAP, SIZE=(200K, 20K)', REGION=250K
//SYSLIB DD DSN=SYS2.FORTLIB, DISP=SHR
//      DD DSN=GCDEV.SEAMVS LOAD, DISP=SHR
//SYSPRINT DD SYSOUT=*
//SYSUT1 DD SPACE=(TRK, (55, 1, 1))
//SYSLIN DD
//      DD *
INCLUDE SYSLIB(SEA)
ENTRY MAIN
// EXEC PGM=GSFC, REGION=400K
//STEPLIB DD DSN=&&LODMOD, DISP=(OLD, DELETE)
//FT01FOO1 DD UNIT=DISK, DCB=(RECFM=VBS, LRECL=44, BLKSIZE=4404),
//      SPACE=(CYL, (5, 1)) SORTING FOR TRACKING DATA SCHEDULE
//FT02FOO1 DD UNIT=DISK, DCB=(RECFM=VBS, LRECL=44, BLKSIZE=4404),
//      SPACE=(CYL, (1, 1)) MERGING FOR TRACKING DATA SCHEDULE
//FT03FOO1 DD UNIT=DISK, DCB=(RECFM=VBS, LRECL=44, BLKSIZE=4404,
//      BUFNO=1), DISP=(NEW, PASS), SPACE=(CYL, (1, 1)),
//      DSN=&&SORTRK SORTED TRACKING DATA SCHEDULE
//FT05FOO1 DD DDNAME=DATA5 TRACKING SCHEDULE CARD INPUT
/**FT06FOO1 DD SYSOUT=*, DCB=(RECFM=VBA, LRECL=137, BLKSIZE=3990),
/**      DSN=&&PRTOUT SEA PRINTER OUTPUT
//FT06FOO1 DD SYSOUT=*,
//      DCB=(RECFM=VBA, LRECL=137, BLKSIZE=141),
//      SPACE=(CYL, (3, 1), RLSE)
/**FT08FOO1 DD DDNAME=INPCRD SEA KEYWORD CARD INPUT
/**INPCRD DD *
//FT08FOO1 DD * SEA KEYWORD CARD INPUT
EPOCHTIM 3 -1 861101. 000000.0000
USERSATO 1 11 1 6978140. 0.0001 28 8
USERSATO 1 12 1 0. 0. 0.
SATELITE 2 11 0 42166750 0.0004 5.0
SATELITE 2 12 0 358 0 0
SATELITE 3 11 0 42163592.42 0 0004 5 0
SATELITE 3 12 0 228. 0 0
SATELITE 4 11 0 42163592 42 0.0004 5 0
SATELITE 4 12 0 113. 0. 0.
STATIONS 1 0 0 323002.867 2532329.163 1441 37
EARTH 15 15 150.0
SPCPARAM 1 0 0 0.00272 2.0
EBOUTPUT -1 2 1440.0 30.0 30.0
CLKBIAS 1 1 1000000.
CLKDRIFT 1 1 200.0 0.000001
USERDRAG 1 1 .025
GRAVCOEF -1 0.25
/*
// DD UNIT=DISK, DSN=ZBBTF.ZBEXS.GEM.DATA(RECOEF2), DISP=SHR
// DD *
SATSOLPR 1 -1 1
MEASBIAS 2 -1 1000200010000. 10.0
MEASBIAS 3 -1 1000200010000. .001

```

```

MEASBIAS  2  -1  1000300010000  10 0
MEASBIAS  3  -1  1000300010000.  .001
MEASBIAS  2  -1  1000200040001.  10.0
MEASBIAS  3  -1  1000200040001.  .001
EPHEMERR  1           25.0           23 0           40.0
EPHERROR           99
CLKACCEL  1  -1  .11574
COVARANC  1
      2.5D+05      2.5D+05      2.5D+05      1 0D+00      1 0D+00      1 0D+00
NOISECOV  1  1  0
      0           0.           0.           1 00000D-10  1.00000D-10  1.00000D-10

```

```

/*
**FT09FOO1 DD SYSOUT=*,DCB=(RECFM=VBA,LRECL=137,BLKSIZE=3990),
**          DSN=&&NOMOUT          SATELLITE NOMINAL TRAJECTORY OUTPUT
**FT09FOO1 DD SYSOUT=*,
**          DCB=(RECFM=VBA,LRECL=137,BLKSIZE=141),
**          SPACE=(CYL,(2,1),RLSE)
**FT10FOO1 DD SYSOUT=*,DCB=(RECFM=VBA,LRECL=137,BLKSIZE=3990),
**          DSN=&&MEASOUT          PROCESSED MEASUREMENTS PRINTER OUTPUT
**FT10FOO1 DD SYSOUT=*,
**          DCB=(RECFM=VBA,LRECL=137,BLKSIZE=141),
**          SPACE=(CYL,(2,1),RLSE)
**FT20FOO1 DD DISP=(NEW,PASS),SPACE=(CYL,(1,1)),
**          DCB=(RECFM=VBS,LRECL=144,BLKSIZE=2884),UNIT=DISK,
**          DSN=&&FESUM          SEQUENTIAL ERROR BUDGET SUMMARY
**FT21FOO1 DD DISP=(NEW,PASS),SPACE=(CYL,(1,1)),
**          DCB=(RECFM=VBS,LRECL=144,BLKSIZE=2884),UNIT=DISK,
**          DSN=&&SESUM          BACKWARD SMOOTHER ERROR BUDGET SUMMARY
**FT27FOO1 DD UNIT=DISK,DCB=(RECFM=VBS,LRECL=196,BLKSIZE=1964,
**          BUFNO=1),DISP=(NEW,PASS),SPACE=(CYL,(1,1)),
**          DSN=&&AKKHIN          VISIBLE TRACKING DATA SCHEDULE
**FT40FOO1 DD UNIT=DISK,DCB=(RECFM=FB,LRECL=1888,BLKSIZE=18568),
**          DISP=(NEW,DELETE),SPACE=(CYL,(2,1),RLSE),
**          DSN=&&SMSTOR          SMOOTHER INFORMATION STORAGE FILE
**GO.SYSUDUMP DD DUMMY
**SYSUDUMP DD SYSOUT=*,SPACE=(TRK,1),
**          DCB=(RECFM=VBA,LRECL=137,BLKSIZE=1922)
**GO.DATAS DD *

```

```

      3      861101000000.0000      -1
      100020001      2  180.0      1.66667
0.00      2.7      95.3333      132.0
200.3333      235.7      304.6666      339.7
407.6666      443.7      510.0      547.0
612.3333      650.0      715.3333      753.0
819.6666      856.0      924.3333      959.7
1028.3333      1064.0      1131.3333      1167.7
1233.6666      1271.0      1336.3333      1374.4
1439.6666      1440.0
      100020001      3  180.0      0.00166667
0.00      2.7      95.3333      132.0
200.3333      235.7      304.6666      339.7
407.6666      443.7      510.0      547.0
612.3333      650.0      715.3333      753.0
819.6666      856.0      924.3333      959.7
1028.3333      1064.0      1131.3333      1167.7
1233.6666      1271.0      1336.3333      1374.4
1439.6666      1440.0
      100030001      2  180.0      1.66667
63.6666      95.0      166.3333      200.0
268.6666      304.4      371.6666      407.4
475.3333      509.7      580.0      612.0
684.3333      715.0      787.6666      819.4
890.3333      924.0      992.6666      1028.0
1095.6666      1131.0      1199.6666      1233.4
1304.0      1336.0      1408.6666      1439.4
      100030001      3  180.0      0.00166667
63.6666      95.0      166.3333      200.0
268.6666      304.4      371.6666      407.4
475.3333      509.7      580.0      612.0
684.3333      715.0      787.6666      819.4
890.3333      924.0      992.6666      1028.0
1095.6666      1131.0      1199.6666      1233.4

```


1304.0	1336.0	1408 6666	1439.4
1000200040001	2 180.0	1 66667	
3 00	63.4	132 3333	166.0
236.0	268.4	340.0	371.4
444 0	475.0	547.3333	579.7
650.3333	684.0	753 3333	787.4
856.3333	890.0	960 0	992.4
1064.3333	1095.4	1168.0	1199.4
1271.3333	1303.7	1374.6666	1408.4
1000200040001	3 180 0	0.00166667	
3.00	63.4	132.3333	166.0
236.0	268.4	340 0	371.4
444.0	475 0	547 3333	579.7
650.3333	684 0	753.3333	787.4
856.3333	890.0	960.0	992.4
1064.3333	1095.4	1168 0	1199.4
1271.3333	1303.7	1374.6666	1408.4
100020001	3 1800.0	10000.0	
0.00	1440.0		
100030001	3 1800.0	10000 0	
0.00	1440 0		
1000200040001	3 1800.0	10000.0	
0.00	1440.0		

```

/*
//NTSO EXEC PGM=NOTIFY,COND=EVEN
//

```

APPENDIX B - UTILITIES FOR GEOPOTENTIAL ERROR MODEL STUDIES

This appendix describes two utilities adapted from the Sequential Error Analysis (SEA) program for geopotential error model studies. Both utilities compute the gravitational acceleration errors that result from a given geopotential error model. The first utility outputs the magnitudes of the acceleration errors as a function of geocentric latitude and longitude at a fixed altitude. The second utility outputs the magnitudes as well as the acceleration components in the radial, alongtrack, and crosstrack directions as the satellite travels in its orbit. These two utilities are described in more detail in Sections B.1 and B.2.

B.1 GEOPOTENTIAL ACCELERATION ERROR WORLD-MAP UTILITY

This SEA utility computes the uncertainty in the gravitational acceleration due to nonspherical effects of the Earth at a specified altitude for a given geopotential error model. The utility computes and prints out the global distribution of gravitational acceleration uncertainties in meters per second squared for latitudes between -89 deg and +89 deg¹ with 5-deg increments and longitudes varying between 0 deg and 360 deg with 10-deg increments.

The utility also generates a global distribution plot of the gravitational acceleration uncertainties in milligals ($10^{-5}\text{m}/\text{sec}^2$) rounded to the nearest integer, with longitude as abscissa and latitude as ordinate.

¹The geopotential computation subroutine is adapted from the corresponding GTDS subroutine, which has a singularity at the poles (+90 deg). The use of +89 deg avoids this program deficiency.

B.1.1 INPUT DATA SETUP

This utility can be executed using the SEA keyword cards setup, and no special keyword cards are required. The geopotential error model is provided by the LUMPGEOP keyword card followed by the corresponding set of RECOEF cards if other than the default model--GEM-9 formal uncertainties--is desired. The coefficients of any geopotential error model, except the default model, can be scaled using the first real field of the LUMPGEOP keyword card. The altitude for which geopotential acceleration uncertainties are computed is based on the orbital elements provided on the USERSATO card.

B.1.2 MODIFICATIONS TO SEA PROGRAM

Modifications are made in subroutines RDKEYS and SPART to adapt SEA to function as described in Section B.1. In subroutine RDKEYS, which reads in keyword cards, modifications are made so that the first real field (R1) on the LUMPGEOP keyword card can be used as a scaling factor (multiplication factor) to the sine and cosine coefficients uncertainties of an input geopotential error model. This provides a convenient means to scale down or scale up the coefficients to study the effects of an error model.

Subroutine SPART, which normally computes the gravitational accelerations due to a geopotential model, is modified to compute the acceleration uncertainties resulting from a geopotential error model instead. A nested DO-loop for latitudes and longitudes is added so that the subroutine computes and outputs the global distribution of gravitational acceleration uncertainties. These uncertainties are calculated based on the orbital radius of the user satellite as provided by the orbital elements in the USERSATO card. The subroutine also converts the acceleration uncertainties from meters per second squared to milligals (rounded to the nearest integer) and generates a global distribution plot of

gravitational acceleration uncertainties. After printing out the above results, the program execution is allowed to terminate instead of executing the rest of the normal SEA program.

B.1.3 REQUIRED CODING UPDATES TO SEA PROGRAM

The following is the listing of Panvalet updates to the Panvalet SEA source program stored in the data set GCDEV.MVT.SEA.PANLIB.DATA. To create an updated SEA program load module, the updates that follow must be compiled and linked to the existing SEA load module GCDEV.SEAMVS.LOAD.

```

++UPDATE RDKEYS,1,TEMP
++C 229,229
      DPMAP(ILUMP) = 1 ODO
      IF ( R1 NE. O.ODO ) DPMAP(ILUMP) = R1
++C 251,252
      CSIG(I1, I2+1 ) = R1 * DPMAP(ILUMP)
      CSIG(31-I1, 33-I2 ) = R2 * DPMAP(ILUMP)
++WRITE WORK,RDKEYS
++UPDATE SPART,1,TEMP
++C 69,69
      COMMON/CONST / AE, GM, DUM(3), THETG, DTR
++C 73,73
      COMMON/FMODEL/CSIG(30,33),C(30,33),MAXDEG,MAXORD,NMAX,MMAX
++C 76
      LOGICAL*1 HORZ(115),VERT,SLASH
      INTEGER*2 PLOT(40,40),A1(40),A2(40)
      DATA DLAT/5 DO/, DLON/10 DO/, FACTOR/1.DS/
      DATA HORZ/115*'-'/, VERT/'+'/, SLASH/'I'/
C
      DO 50 ICOL = 1,112,3
      HORZ(ICOL) = SLASH
      50 CONTINUE
++D 93,94
      WRITE(6,10)R
      10 FORMAT('1' ///,' *** ENTER SPART TO GENERATE WORLD MAP ',
* '- USE GEOP UNCE'R'S TO CALC ACCELERATIONS ***',///,
* ' THE SIZE OF THE GEOPOTENTIAL UNCERTAINTY IS SPECIFIED BY ',
* 'THE "EARTH" KEYWORD'///,
* ' THE ORBITAL RADIUS FOR WHICH THIS WORLD MAP IS BEING ',
* 'CALCULATED IS R=' D25 15,//////,
* ' THE C ARRAY CONTAINING THE GEOPOTENTIAL UNCE'R'S IS.')
```

```

C
C      PRINT OUT THE C ARRAY CONTAINING THE GEOPOTENTIAL UNCE'R'S
C
C      CALL OUTCOF(C,MAXDEG,MAXORD,1)
C
C      INDO = 180 DO/DLAT + 1
C      IND1 = 360.D0/DLON + 1
C
C      ENTER LATITUDE LOOP
C
C      WRITE(6,390)
      390 FORMAT('1          NON-SPHERICAL ACCELERATION AS A FUNCTION',
* ' OF LATITUDE AND LONGITUDE')
```

```

C
      ALAT = (DLAT + 90 DO)
      DO 1000 I=1,INDO
      IF ( MOD(I,2) .NE. 0 AND. I GT 1 ) WRITE(6,401)
      401 FORMAT('1')
      WRITE(6,400)
      400 FORMAT(/
      ALAT = ALAT - DLAT
      A,(I) = ALAT
      ALAT1 = ALAT
      IF ( ALAT GE. 90.DO ) ALAT1 = ALAT - 1 O
      IF ( ALAT LE -90 DO ) ALAT1 = ALAT + 1 O
      SINP = DSIN(DTR*ALAT1)
      COSP = DCOS(DTR*ALAT1)
++C 112,112
C
C      ENTER LONGITUDE LOOP
C
C      ALON = -(DLON + 0 DO)
      DO 2000 J = 1,IND1
      ALON = ALON + DLON
      A2(J) = ALON
      ALAM = DTR*ALON
--C 205
      PLAMDA = PLAMDA / ( R * COSP)
++C 209
      PPSI = PPSI/R
C
C      COMPUTE ACCELERATION
```

```

C      ACC = DSQRT(PS*PS + PLAMDA*PLAMDA + PPSI*PPSI)
C      WRITE(6,500) ALAT1,ALON,ACC
500  FORMAT(' ALAT=',G14 8,' ALON=',G14 8,' ACC=',G14 8)
C      LOAD PLOT ARRAY
C      PLOT(I,J) = ACC*FACTOR + 0.5
C      2000 CONTINUE
C      1000 CONTINUE
C      ***** GENERATE PLOT *****
C      WRITE(6,700)
700  FORMAT('1',//,T36,' UNCERTAINTY IN NONSPHERICAL GRAVITATIONAL',
*      ' ACCELERATION (MGAL)',/,2X,'<LAT>' 3X,/)
C      DO 800 I=1,INDO
      WRITE(6,750) A1(I),VERT,(PLOT(I,J),J=1,IND1)
750  FORMAT(3X,I3,3X,A1,40I3)
800  CONTINUE
C      WRITE(6,770) HORZ,(A2(I),I=1,IND1,2)
770  FORMAT(/,T10,115A1,/,2X,'<LONG>',2X,I3,19I6)
C      *****
      IF ( 5 NE 0 )STOP
++WRITE WORK,SPART

```

B.2 UTILITY FOR COMPUTING GRAVITATIONAL ACCELERATION UNCERTAINTIES ALONG THE TRAJECTORY OF A USER SATELLITE

This SEA utility computes the gravitational acceleration uncertainties that result from a given geopotential error model as a user satellite travels in its orbit. The utility computes and prints out a table of radial, crosstrack, and alongtrack components; the magnitudes of the gravitational acceleration uncertainties; and the latitude and longitude of the ground trace of the satellite, for each error budget time requested.

The data are then presented in five separate plots. The first four plots show the radial (height), crosstrack, and alongtrack components and the magnitudes of the gravitational acceleration uncertainties, respectively, as a function of time from epoch. The last plot shows the magnitudes of the gravitational acceleration uncertainties as the satellite moves in its orbit as a function of latitude and longitude.

B.2.1 INPUT DATA SETUP

This utility can be executed using the SEA keyword cards setup, and no special keyword cards are required. The geopotential error model can be set up the same way as described in Section B.1.1.

B.2.2 MODIFICATIONS TO SEA PROGRAM

In subroutine RDKEYS, which reads in keyword cards, modifications are made so that the first real field (R1) on the LUMPGEOP keyword card can be used as a scaling factor (multiplication factor) to the sine and cosine coefficients uncertainties of an input geopotential error model. This provides a convenient means to scale down or scale up the coefficients to study the effect of an error model.

In subroutine FORCE, which calculates force per unit mass acting on the satellite for the integration of the nominal trajectory, additional codings are added to print out a table of time from epoch; latitude; longitude; radial, crosstrack, and alongtrack components; and the magnitudes of the gravitational acceleration uncertainties whenever current time equals error budget time. This subroutine is modified so that, for each error budget time, SPART is called twice: the first time for computing the geopotential acceleration uncertainties due to the geopotential error model; the second time to help in computing the nominal trajectory of the user satellite. The acceleration uncertainties computed are stored in separate arrays for later plotting purpose. To be able to recognize the error-budget time, the calling sequence of FORCE is also modified to include the input of the variable EBTIME.

Subroutine FORCE is called from subroutine INTAG for each of the integration steps for the propagation of the satellite trajectory. Coding modification is therefore required in INTAG whenever FORCE is invoked using the modified calling sequence. The calling sequence (argument list) of INTAG is also modified with the addition of the variable EBTIME, to be able to transfer the error-budget time to FORCE.

Subroutine SEQUEN, which controls the forward sequential filter computation, specifies the variable EBTIME, which is passed to subroutine INTAG through its calling sequence.

Modifications are made to suppress the error-budget and standard deviation correlation output reports. In addition, a new subroutine, GTPLOT, is added at the end of the filter computation to generate five separate plots (Section B.2). GTPLOT uses the arrays previously loaded in subroutine FORCE to generate the required plots.

Minor modifications are also made in subroutine SEA01 to suppress the error summary reports and error plots. In addition to the nonspherical gravitational accelerations or acceleration uncertainties, the calling sequence of subroutine SPART is modified to pass the latitude and longitude of the user satellite to the calling subroutine, FORCE.

Subroutine THCL is also modified to output the 3 by 3 transformation matrix for transforming the gravitational acceleration uncertainties from inertial coordinates to height, crosstrack, and alongtrack coordinates.

B.2.3 REQUIRED CODING UPDATES TO SEA PROGRAM

The following is the listing of Panvalet updates to the Panvalet SEA source program stored in the data set GCDEV.MVT.SEA.PANLIB.DATA. To create an updated SEA program load module, the updates that follow must be compiled and linked to the existing SEA load module GCDEV.SEAMVS.LOAD.

```

--UPDATE FORCE,1,TEMP
++C 1,1
  SUBROUTINE FORCE ( T , ISAT , D2Y , ACCEL , EBTIME)
++C 40
  LOGICAL*1 LTOOUT
++C 45,45
  COMMON/CONST / AE, GM, DUMMY(5), RTD
  COMMON/FMODEL/C(30,33),CSIG(30,33)
  COMMON/GTRACK/GTMIN(96),GALAT(96),GALAM(96),GGRAV(96,3),GG(96),
  * IGCNT
  DIMENSION CTEMP(30,33)
  DATA OEBTIM / -1 ODO /
++C 50
  DIMENSION GRAV(3),TR(3,3)
C   LTOOUT - TRACKING ORIENTED OUTPUT FLAG
  LTOOUT = .FALSE
C   IS EBTIME A NEW ERROR BUDGET TIME
  IF ( EBTIME NE. OEBTIM ) LTOOUT = TRUE
++D 72
C
C   GENERATE THE TRACKING ORIENTED OUTPUT ONLY DURING ERROR
C   BUDGET REQUEST TIMES
C
  IF ( T .NE. EBTIME ) GO TO 550
  IF ( NOT. LTOOUT ) GO TO 550
C
C   FIND THE ACCELERATION DUE TO GEM UNCERTAINTIES CONTAINES IN CSIG
C   - BUT FIRST STORE THEM IN ARRAY C BECAUSE THIS IS THE ARRAY ACTED
C   UPON BY SUBROUTINE SPART
C
  DO 510 IROW = 1,30
    DO 515 ICOL =1,33
      CTEMP(IROW,ICOL) = C(IROW,ICOL)
      C(IROW,ICOL) = CSIG(IROW,ICOL)
  515 CONTINUE
  510 CONTINUE
  CALL SPART(X,XDD,ALAT,ALAM)
  DO 530 IROW = 1,30
    DO 535 ICOL =1,33
      C(IROW,ICOL) = CTEMP(IROW,ICOL)
  535 CONTINUE
  530 CONTINUE
  CALL THCL1(STATE(1,ISAT),TR)
  CALL MATMUL(TR,XDD,GRAV,3,3,1)
  G = DSQRT(GRAV(1)*GRAV(1)+GRAV(2)*GRAV(2)+GRAV(3)*GRAV(3))
  ALAT = RTD * ALAT
  ALAM = RTD * ALAM
  IF ( ALAM GE 0 ODO ) GO TO 537
  IMULT = 1.ODO + DABS(ALAM / 360 DO)
  ALAM = ALAM + DFLOAT(IMULT) * 360 ODO
  537 TMIN = T / 60 ODO
C
C   LOAD ARRAYS USED LATER FOR PLOTTING
C
  IGCNT = IGCNT + 1
  GTMIN(IGCNT) = TMIN
  GALAT(IGCNT) = ALAT
  GALAM(IGCNT) = ALAM
  GGRAV(IGCNT,1) = GRAV(1)
  GGRAV(IGCNT,2) = GRAV(2)
  GGRAV(IGCNT,3) = GRAV(3)
  GG(IGCNT) = G
C
  WRITE(6,500) TMIN,ALAT,ALAM,GRAV,G
  500 FORMAT(' TMIN=',G17.10,' ALAT=',G14.8,' ALAM=',G14.8,
  + ' GRAV= ',3(G14.8,1X),' G=',G14.8)
  OEBTIM = EBTIME
  550 CALL SPART(X,XDD,ALAT,ALAM)
++WRITE WORK,FORCE
++UPDATE INTAG,1,TEMP
++C 1,1
  SUBROUTINE INTAG(T1,T2,PXX,TXU,PXZ,D2Y,YDY,YDY1,RK,ACCEL,EBTIME)
++C 244,244

```

```

      CALL FORCE(T, ISAT, D2Y, ACCEL, EBTIME)
++C 299,299
      CALL FORCE(T, ISAT, D2Y, ACCEL, EBTIME)
++WRITE WORK,INTAG
++UPDATE RDKEYS,1,TEMP
++C 229,229
      DPMAP(ILUMP) = 1 ODO
      IF ( R1 NE O ODO ) DPMAP(ILUMP) = R1
++C 251,252
      CSIG(I1, I2+1) = R1 * DPMAP(ILUMP)
      CSIG(31-I1, 33-I2) = R2 * DPMAP(ILUMP)
++WRITE WORK,RDKEYS
++UPDATE SEQUEN,1,TEMP
++C 167
      COMMON/GTRACK/GTMIN(96), GALAT(96), GALAM(96), GGRAV(96,3), GG(96),
      * IGCNT
++C 176,177
++C 207
      IGCNT = 0
++C 292,292
      95 CALL INTAG(TIME, TTO, PXX, TXU, PXZ, D2Y, YDY, YDY1, RK, ACCEL, EBTIME)
++D 343,346
++D 412,413
++C 458,459
C
C      GENERATE GEOPOTENTIAL TRACK ERROR PLOTS
C
      800 CALL GTPLOT(EBSTOP)
++WRITE WORK,SEQUEN
++UPDATE SEAO1,1,TEMP
++C 216,216
C      SUPPRESS ERROR SUMMARY REPORT AND PLOT, BECAUSE THIER EXECUTION
C      IN COMBINATION WITH THESE UPDATED, RESULTS IN A SOC1 ABEND
C
C      CALL OUTRSS
++C 220,220
C      CALL PLTHLC
++WRITE WORK,SEAO1
++UPDATE SPART,1,TEMP
++C 1,1
      SUBROUTINE SPART ( X, XDD, ALAT, ALAM )
++C 93
      ALAT = DARSIN(SINP)
++WRITE WORK,SPART
++UPDATE THCL,1,TEMP
++C 4,4
      SUBROUTINE THCL1 ( X, T )
++R 17,.,/6,6/3,3/
++D 35,37
++D 55,61
++WRITE WORK,THCL
++INSERT WORK
      SUBROUTINE GTPLOT(EBSTOP)
C
      IMPLICIT REAL*8(A-H,O-Z)
C
      COMMON/GTRACK/GTMIN(96), GALAT(96), GALAM(96), GGRAV(96,3), GG(96),
      * IGCNT
C
      DIMENSION TPLOT(53,103),XLINE(101),YLINE(53)
      DIMENSION XLAB(11),SYM(4)
      DIMENSION PLOT(40,111),DIGITS(36)
      LOGICAL*1 HORZ(113),VERT,SLASH
      INTEGER*2 A1(40),A2(40)
      DATA DLAT/5 DO/, DLON/10 DO/, FACTOR/1 D5/
      DATA HORZ/113*'-'//, VERT/'I'//, SLASH/' '/'
C
      DATA SYM /'H',
      *          'C',
      *          'L',
      *          'R'//
      DATA DOT /' '/'//,
      *          DASH /'-'//,

```

```

* ANILET /'I' /,
* BLANK /' ' /,
* OVERFL /'Z' /,
DATA DIGITS/'0','1','2','3','4',
*          '5','6','7','8','9',
*          'A','B','C','D','E',
*          'F','G','H','I','J',
*          'K','L','M','N','O',
*          'P','Q','R','S','T',
*          'U','V','W','X','Y',
*          'Z' /,
C
DO 5 ICOL = 4,112,6
HORZ(ICOL) = SLASH
5 CONTINUE
HORZ( 1) = VERT
HORZ(113) = VERT
C
DO 7 I=1,40
DO 8 J=1,111
PLOT(I,J) = BLANK
8 CONTINUE
7 CONTINUE
C
C BUILD XLINE AND YLINE
C
DO 10 I=1,101
10 XLINE(I) = DASH
DO 20 I=1,101,10
20 XLINE(I) = DOT
DO 30 I=1,53
30 YLINE(I) = ANILET
DO 40 I=2,52,5
40 YLINE(I) = DOT
C
C INITIALIZE ARRAY TPLLOT AND LOAD AXIES
C
DO 50 ICOL=2,102
DO 60 IROW=2,52
TPLLOT(IROW,ICOL) = BLANK
60 CONTINUE
50 CONTINUE
DO 80 I=2,102
TPLLOT(1 ,I) = XLINE(I-1)
TPLLOT(53,I) = XLINE(I-1)
80 CONTINUE
DO 90 I=1,53
TPLLOT(I,1 ) = YLINE(I)
TPLLOT(I,103) = YLINE(I)
90 CONTINUE
C
C FIND MAX AND MIN OF THE GEOPOTENTIAL ACCELERATIONS
C
AMAX = -1 OD-50
AMIN = 1 OD+50
DO 200 I=1,IGCNT
IF ( GG(I) GT. AMAX ) AMAX = GG(I)
DO 210 ISET=1,3
IF ( GGRAV(I,ISET) LT AMIN ) AMIN = GGRAV(I,ISET)
210 CONTINUE
200 CONTINUE
WRITE(6,4000)AMAX,AMIN
4000 FORMAT('O**** AMAX = ',D25 15,' AMIN = ',D25 15,/)
C
C FIND SCALING FOR THE X AXIES
C
IEBED = EBSTOP/60 ODO + 5D0
IEBST = 0 0
IXSCAL = ( ( DFLOAT(IEBED) - DFLOAT(IEBST))/100 ODO ) + 99999D0
XSCAL = IXSCAL
IXMIN = IEBST
WRITE(6,4010)EBSTOP,IEBED,IEBST,XSCAL,IXMIN
4010 FORMAT('O**** EBSTOP = ',D14 7,' IEBED = ',I6,' IEBST = ',I6,

```

```

      *' XSCAL =',D14 7,' IXMIN =',I6,/)
C
C   FIND SCALING FOR THE Y AXIES
C
      YRANGE = ( AMAX - AMIN ) * 1.0D5
      YSCAL = YRANGE / 50.0D0
      YTEMP = YSCAL * 5.0D0
C   ROUND YTEMP UP TO NEAREST 1 MG
      IYTEMP = ( YTEMP * 10.0D0 ) + 99999D0
      YTEMP = DFLOAT(IYTEMP) / 10.0D0
      YSCAL = YTEMP / 5.0D0
      YMIN = ( ( AMIN * 1.0D5 ) / YRANGE ) * ( YSCAL * 50.0D0 )
C   ROUND YMIN DOWN TO NEAREST .1 MG
      IYTEMP = YMIN * 10.0D0
      IF ( YMIN LT 0.0D0 ) IYTEMP = ( YMIN * 10.0D0 ) - 99999D0
      YMIN = DFLOAT(IYTEMP) / 10.0D0
      YMAX = YMIN + 50.0D0 * YSCAL
      WRITE(6,4020)YRANGE,YSCAL,YMIN,YMAX
4020  FORMAT('O**** YRANGE =',D14 7,' YSCAL =',D14 7,' YMIN =',D14 7,
      *' YMAX =',D14 7,/)
C
C   LOOP OVER ALL FOUR PLOTS
      WHERE. ISET = 1, HEIGHT PLOT (H)
      *          2, CROSS TRACK PLOT (C)
      *          3, ALONG TRACK PLOT (L)
      *          4, RSS PLOT (R)
C
C   DO 500 ISET = 1,4
C
C   LOAD INDIVIDUAL POINTS IN TO ARRAY TPL0T
C
      YCOR = YMIN / YSCAL
      WRITE(6,4040) ISET,YCOR
4040  FORMAT('O**** ISET =',I3,' YCOR =',D14 7,/)
      DO 600 I = 1,IGCNT
          IXCOL = ( GTMIN(I) / XSCAL ) + 5D0
          IF ( ISET LT 4 )
      *       IYROW = ( (GGRV(I,ISET) * 1.0D5 ) / YSCAL ) - YCOR + 5
      *       IF ( ISET EQ. 4 )
      *       IYROW = ( (GG(I) * 1.0D5) / YSCAL ) - YCOR + 5
          WRITE(6,4050)IYROW,IXCOL,SYM(ISET)
4050  FORMAT(' **** IYROW =',I5,' IXCOL =',I5,' USING SYMBOL->',A1)
          TPL0T(52-IYROW,IXCOL+2) = SYM(ISET)
600   CONTINUE
C
C   PRINT OUT ARRAY TPL0T ONE ROW AT A TIME
C
      WRITE(6,2000)
2000  FORMAT(' ',T10,'PLOT OF TRACK ACCELERATIONS FROM THE ',
      *'GEOPOTENTIAL UNCERTAINTY, IN MGAL',/)
      YVAL = YMAX + 5.0 * YSCAL
      DO 700 IROW = 1,53
          WRITE(6,2010) (TPL0T(IROW,ICOL),ICOL=1,103)
2010  FORMAT(' ',T14,103A1)
          IF ( MOD(IROW-2,5) NE 0 ) GO TO 800
          YVAL = YVAL - 5.0 * YSCAL
          WRITE(6,2050)YVAL
2050  FORMAT('+',T3,F10.2)
800   CONTINUE
C   LATER ON ONE MAY WISH PLACE HERE THE CODE TO GIVE
C   Y-AXIS LABELS
700   CONTINUE
      IXVAL = IXMIN - 10 * IXSCAL
      DO 900 I=1,11
          IXVAL = IXVAL + 10 * IXSCAL
          XLAB(I) = IXVAL
900   CONTINUE
      WRITE(6,2100)XLAB
2100  FORMAT(' ',T8,11F10.2,/,T47,
      * 'TIMES FROM EPOCH IN MINUTES')
C
C   BEFORE PRINTING NEXT PLOT, BLANK OUT TPL0T ARRAY
C

```

```

        IF ( ISET EQ 4 ) GO TO 500
        DO 1000 ICOL=2,102
            DO 1010 IROW=2,52
                TPLOT(IROW,ICOL) = BLANK
1010     CONTINUE
1000     CONTINUE
500     CONTINUE
C
C     LOAD PLOT ARRAY TO GENERATE LONGITUDE LATITUDE PLOT
C
        DO 1020 II=1,IGCNT
            I = 19 5DO - ( GALAT(II) / DLAT )
            ALAMT = GALAM(II)
            JCOL = ( ALAMT / 3 3333DO ) + 3.5DO
            AMGAL = GG(II) * FACTOR + 0 5
            IMGAL = AMGAL
            IF ( IMGAL LE 36 ) GO TO 1018
            PLOT(I,JCOL) = OVERFL
            GO TO 1020
1018     CONTINUE
        WRITE(6,4060)II,GTMIN(II),II,GALAT(II),ALAMT,AMGAL,I,JCOL
4060     FORMAT(' **** GTMIN(',I2,')=',F7.2,' GALAT(',I2,')=',
* D14.7,' ALAMT=',D14.7,' AMGAL=',F6.2,' I=',I3,' JCOL=',I3)
C
        PLOT(I,JCOL) = DIGITS ( IMGAL + 1 )
C
1020     CONTINUE
C
C     GENERATE LATITUDE/LONGITUDE PLOT
C
        INDO = 180 ODO / DLAT + 1
        IND1 = 360 ODO / DLON + 1
        ILONGV = 0
        ILATV = 90
        DO 1025 I=1,40
            A1(I) = ILATV
            ILATV = ILATV - 5
            A2(I) = ILONGV
            ILONGV = ILONGV + 20
1025     CONTINUE
        WRITE(6,1030) HORZ
1030     FORMAT(' 1',//,T36,' UNCERTAINTY IN NONSPHERICAL GRAVITATIONAL',
* ' ACCELERATION (MGAL)',/,2X,'<LAT>',3X,/,
* 9X,115A1)
C
        DO 1040 I=1,INDO
            WRITE(6,1050) A1(I),VERT,(PLOT(I,J),J=1,111),VERT
1050     FORMAT(3X,I3,3X,A1,111A1,A1)
1040     CONTINUE
C
        WRITE(6,1060) HORZ,(A2(I),I=1,19)
1060     FORMAT(' ',T10,113A1,/,10X,I3,18I6,/,60X,
* '<LONG>')
        RETURN
        END

```

End of Document